INVESTIGATION OF DIESEL AND BIODIESEL PROPERTIES AND THEIR EFFECTS ON SOOT OXIDATION KINETICS AND DPF FILTRATION AND REGENERATION BEHAVIOR

Morteza Borhanipour

A THESIS SUBMITTED IN PARTIAL FULFILLMENT
OF THE REQUIREMENT FOR THE DEGREE OF
MASTER OF ENGINEERING IN AUTOMOTIVE ENGINEERING
(INTERNATIONAL PROGRAM)
INTERNATIONAL COLLEGE
KING MONGKUT'S INSTITUTE OF TECHNOLOGY
LADKRABANG
2014

KMITL-2014-IC-M-004-009

INVESTIGATION OF DIESEL AND BIODIESEL PROPERTIES AND THEIR EFFECTS ON SOOT OXIDATION KINETICS AND DPF FILTRATION AND REGENERATION BEHAVIOR

Morteza Borhanipour

A THESIS SUBMITTED IN PARTIAL FULFILLMENT
OF THE REQUIREMENT FOR THE DEGREE OF
MASTER OF ENGINEERING IN AUTOMOTIVE ENGINEERING
(INTERNATIONAL PROGRAM)
INTERNATIONAL COLLEGE
KING MONGKUT'S INSTITUTE OF TECHNOLOGY
LADKRABANG
2014

KMITL-2014-IC-M-004-009

Thesis title: INVESTIGATION OF DIESEL AND BIODIESEL PROPERTIES AND THEIR EFFECTS ON SOOT OXIDATION KINETICS AND DPF FILTRATION AND REGENERATION BEHAVIOR

Student Mr. Morteza Borhanipour

Student ID. 55600909

Degree Master of Engineering

Program Automotive Engineering

Thesis Advisor Dr. Preechar Karin

Co advisors Dr. Nuwong Chollacoop

Prof. Dr. Katsunori Hanamura

Year 2015

Abstract

Increase of air pollution, global warming, petroleum price and tougher emission standards and regulations has obliged countries and companies to seek for alternative sources of fuels and betterment of after treatment systems. Among the alternate fuels, biodiesels have been considered as a promising, non-toxic, CO_2 free and renewable source for substitution with petroleum based diesel fuel. Diesel engines are widely used all over the globe in transportation and industries due to its high efficiency but the higher soot or PM production in their emission and filtration of this PM is the main challenge. The common method for filtration is application of diesel particulate filter (DPF) and investigations of effect of fuel properties on PM physical and chemical features can improve

designing of DPF and study of its filtration trend. At this study, at first step the chemical and physical properties of Thai commercial diesel fuel and Palm biodiesel fuel is examined. At the next step the fuels were applied at a single cylinder engine and exhaust PM were collected. At this study , the PM oxidation kinetics of palm biodiesel PM, diesel and carbon black is investigated in the presence of pure oxygen and air with isothermal TGA , under five different temperatures including (400 , 450, 500, 550 , 600^{o} (C)) . Mass-conversion, apparent activation energy and reaction order of carbon, *n*, for each sample is calculated and discussed. Hence the composition of the PM of diesel and biodiesel is different the CHN analyze is done in order to find out the composition of PM for each sample. At the third level of the project, PM micro and nanostructure were analyzed by image processing of SEM(Scan electron microscope) and TEM (Transmission electron microscope), obtained from PM samples and the diameter of single particles and size distributions of single and agglomerated particles were measured. At the final step, the same engine was used for PM filtration and regeneration monitoring by means of engine pressure drop and the filtration and regeneration trends were explained based on chemical and physical characteristics of fuels and their produced PM. The results of this study can provide a good insight about the role of physical and chemical features of diesel and biodiesel fuel and the filtration of their PM, which can be applied in further investigations regard to after treatment studies of alternative fuels.

Keywords: Soot oxidation, biodiesel, TGA, soot image processing, nanostructure.

ACKNOWLEDGEMENTS

I would like to represent my gratitude to Dr.Preechar Karin, my thesis advisor for his kind supports and efforts for this project and during this project, technically and financially and this project wouldn't be done without his great responsibility and his helpful attitude. His scientific point of view is a unique and rare case among professors and researchers in KMITL.

I would also thank Dr. Nuwong Chollacoop,Dr.Manida Tongroon, MTEC REN LAB staffs and Prof. Dr.Katsunori Hanamura for their assistances and supports during the experiments and study.

I also thank all KMITL automotive workshop students and my under graduate assistances for corporation during the tests. Especial thanks to Mr.Pratan Srichai and other senior students for their support and advices.

And finally I would thank my family for their emotional and financial support throughout my life and all I have attained in my life is due to their kindness and responsibility.

Contents

CHAPTER 1

INTRODUCTION

1. Background

The global economic growth is mainly dependent on secure, reliable, affordable, clean and renewable source of energy. Increase of industrial development and world population growth have resulted into increase of fuel demands and thus air pollution and thus global warming. The fossil fuel sources are still main source of energy and therefore many countries are dependent to foreign petroleum suppliers. Besides, increase of the fossil fuel consumption causes severe environmental hazards and health related problems. According to World Energy Council, WEC, at least by 2050, the world will need to double today's level of energy supply to meet increased demand. More primary energy will be needed initially in 2020, although some regions will moderate this need by more energy efficient technologies and to double energy supplies, policymakers must consider all energy options [1]. Such factors has made countries and companies to find different remedies in order to use the fuels and energy sources more efficiently with higher performance and alternative energy sources to deal with the environmental and financial obstacles. Among the power producer sources, diesel engines have higher performance in comparison with other types of engines and it's been widely in use in different areas of transport and industries. However the soot particle or PM and NOx emission from diesel engine is much higher in comparison

with other types of engines and therefore betterment is needed at this area.

	Security	*Economy*			*Social*		*Environment*	
	Energy security	Trade balance	Price of petroleum	Improve economy	Increase jobs in agricultural sector	Improve farmers' income	Climate change	Air quality
(the) PRC	✓	✓			✓	✓		✓
India	✓	✓	✓	✓	✓	✓		✓
Malaysia		✓	✓	✓			✓	
Indonesia	✓			✓	✓	✓		
Philippines	✓	✓		✓				✓
Thailand	✓	✓		✓	✓	✓		
Number of Countries	5	5	2	5	4	4	1	3

Figure 1. Summary of the main drivers of biofuel policies in Asia.

Energy from renewable sources, especially biofuels, will have an important impact on markets during the time period especially in South East Asian countries and supply demand tensions rise as demand outstrips supply especially for alternative fuels from edible sources. Summary of the main drivers of biofuel policies is presented in figure 1. The energy sectors of Southeast Asian countries have developed significantly over the past two decades. Energy demand became more than doubled between 1990 and 2007, while power generation increased nearly fourfold over the same period [2]. With Thailand's expected diesel consumption at 85 million liter per day in 2012, the Government of Thailand has planned for an installed capacity of 8.5 million liter per day of biodiesel production in order to meet the B10 requirements. A key element is the plantation development of palm oil and Jatropha. Thailand plans to develop plantations totaling 0.7 million ha. In addition, there are plans to invest and develop an additional 0.175 million ha in neighboring Malaysia. Biodiesel production still lags far behind ethanol in Thai and due to limited feedstock and a lack of

clearly defined incentives for biodiesel investment [3]. Large-scale commercial production of biodiesel has not yet begun. On the community scale, there are biodiesel plants with capacities ranging from 5000 to 20,000 liter per day that serve communities in 11 provinces. These plants use used frying oil and crude palm oil as feedstock to produce about 60,000 liter per day [3]. A dual policy which is a good solution for reduction of dependency to fossil fuel and pollution reduction is utilization of biofuels such as biodiesel and application of diesel particulate filters (DPF) in order to improve fuel and emission. Improvement in application and production of biodiesel can modify the dependency of energy demand to fossil fuels and also improve the exhaust emission. Biodiesel is cleaner, renewable and domestic which can reduce the dependency to importing the fossil fuels. The first application of biodiesel dates back to 1900, when Rudolf Diesel, inventor of diesel engine, in his first demonstration of first diesel engine at World Exhibition at Paris used peanut oil as a fuel. But due to abundance of fossil fuels at that time the researches about biodiesel were not persuaded seriously. Biodiesels, defined as mono-alkyl esters of long chain fatty acids derived from renewable feedstock such as vegetable oils and animal fats, for using in Compression Ignition (CI) engines. They are commonly composed of fatty acid methyl esters that can be prepared from triglycerides, by transesterifcation with methanol. The biodiesels are more environmental friendly due to cleaner combustion, biodegradability, being non-toxic and lower emission profile as compared to petroleum based diesels [4]. Since the biodiesel fuel (especially from vegetables) is a renewable fuel, so it is non-toxic and does not increase the level of CO2 at all in the

atmosphere at global level hence CO2 can be absorbed by photosynthesis process by planets.

Diesel particulate matter or PM is part of a complex mixture of combustion of diesel engines product which is consists of carbonaceous, unburnt hydrocarbons and other impurities. The composition of PMs from a diesel engine may vary widely depending on the operating conditions and fuel composition. PM is traditionally divided into three main fractions: solid fraction (SOL), soluble organic fraction (SOF), and sulfate particulates (SO_4) that consist of sulfuric acid and water. The SOL of diesel PMs is composed primarily of elemental carbon, sometimes referred to as inorganic carbon. This carbon, which does not chemically bound with other elements, is the finely dispersed carbon black or soot substance responsible for black smoke emission. Hydrocarbons (HCs) adsorbed on the surface of the carbon particles are present in the form of fine droplets from the SOF of diesel particulates. In some researches, this fraction is also referred to as the volatile organic fraction (VOF) [5-9]. Many diseases can be related to the PM and other products of diesel engine exhaust. Increases in ambient airborne particulate matter (PM) have been reported to be associated with increased human morbidity and mortality in many geographical locations over the past and the mortality associated with increases in PM has been attributed to exacerbation of preexisting lung diseases in primarily older individuals [10].

While the morbidity has been reported to be increased due to hospitalizations for lung infections and asthmatic symptoms. PM is

present with many other air pollutants, and the effects induced by PM may be possibly influenced by pollutants. The interaction between PM and other pollutants in the induction of cardiopulmonary responses could occur by atmospheric reactions and/or by alteration of cell and organ system hemostasis via common biological pathways [10]. The US EPA initiated diesel emissions research in 1977 to evaluate the human health impact of an increase in diesel vehicle emissions [11]. The first diesel characterization research led to the discovery that diesel particles contained relatively large quantities of mutagenic organic compounds and mutagenesis and carcinogenesis studies of a range of diesel particles was published in the early 1980s as well as inhalation cancer and toxicology studies [11]. In utilization of biodiesels, differences in the toxicity induced by biodiesel could be due to several factors including the chemical composition of biodiesel, different additives used in engines, age and operating conditions. These parameters could in turn facilitate a number of varied health outcomes found in occupational settings of the engine [12].

For several decades in after treatment systems, the most common method to cope with the engine PM has been the application of Diesel Particulate filter (DPF). There are a variety of DPFs available, such as the wall-flow monolith, wire mesh, and foams. Of these, the wall-flow monolith DPF exhibits the highest filtration efficiency (>95 percent by mass) for the least pressure drop. The wall-flow monolith comprises a honeycomb of square channels, typically 1–2 mm in square cross-section, with each end of each channel plugged alternately. The mechanism of DPF is based on entrapment of

exhaust PM by the porous material of DPF. After compiling the PM inside DPF, the filter will be regenerated in two main method, active and passive method. In active method, the heat of engine exhaust is responsible for DPF regeneration and the trapped PM will be oxidized by engine exhaust while in passive form, the DPF will be regenerated by the heating up the DPF with a high temperature system separately after removal from the vehicle. The goal of studies on this field is to study the factors which can affect the soot oxidation inside the DPF and finding the methods which can enable us to oxidize the PMs in a lower temperature. The soot oxidation kinetics is the crux of investigations and many researches and studies have done on this field. The main goal for all these efforts is to improve the DPF filtration ability and reduction of oxidation temperature. At this study at first stage the chemical and physical characteristics of diesel and Palm biodiesel fuels were investigated. In second stage of the study, both of the fuels were used in a single cylinder engine at 80% load and the PM were collected by metallic filters and TGA isothermal test in presence of air and pure oxygen was performed on the soot samples and soot oxidation kinetics were analyzed. At the final stage, a sample of DPF was used for soot trapping and pressure drop was monitored by data acquisition system and then the system was regenerated by high temperature tube furnace with application of air, oxygenated air and mixture of air and nitrogen.

Literature review

Physical and chemical characteristics of fuels such as viscosity, density, calorific value, flash point and so on, can affect the engine functionality and thus PM composition directly and indirectly. Studies in the field of PM also consists of a variety of topics for investigation including soot oxidation kinetics and TGA isothermal and non-isothermal studies. Studies about soot nanostructures with TEM, HRTEM and SEM images is another prevalent area of research. Here the summery of literature reviews of previous studies are mentioned as below:

Preechar Karin et al [9] have investigated the nanostructure Investigation of Particle Emission by Using TEM Image Processing Method. The primary size distributions as well as PM structures were presented by TEM images. The average primary sizes of biodiesel and diesel fuels PMs are approximately 30-40 nm and 50-60 nm, respectively. The average carbon platelet sizes of both PMs are in the range of 0.1-7.0 nm. Moreover, approximately 830 carbon atoms per cubic nanometer of PMs also could be estimated and presented in the present report. Biodiesel combustion produces PM about two times lower than that of diesel combustion. Therefore, the conventional DPF also can be used for about two times of trapping duration. The carbon atom density and mass of PM could be estimated by using TEM image processing method. The length and density of carbon platelet might be strongly depended on the fuel properties and soot generation method. The bio-oxygenated fuel plays an important role for agglomerate particle and single particle size due to oxygen atom inside fuel molecule. Moreover, the impact of oxygenated fuel in the length of platelet also

needed to investigate for better understanding. This is an interesting result of bio-oxygenated fuel combustion behavior and particles emission nanostructure which should be researched in more details to discover the useful information for better understanding and future designs of modern ICE and DPF configurations.

Khalid Al-Qurashi and André L. Boehman [13] have studied the effect of EGR on PM nanostructure and oxidative reactivity. They use a 4 cylinder direct injection (DI) common rail engine with 0% and 20% EGR to produce the soot. Earlier studies showed that soot derived from oxygenated fuels such as biodiesel carries some surface oxygen functionality and thereby possesses higher reactivity than soot from conventional diesel fuel. In this work, results show that EGR exerts a strong influence on the physical properties of the soot which leads to enhanced oxidation rate. HRTEM images showed a dramatic difference between the burning modes of the soot generated under 0 and 20% EGR. The soot produced under 0% EGR strictly followed an external burning mode with no evidence of internal burning. In contrast, soot generated under 20%EGR exhibited dual burning modes: slow external burning and rapid internal burning. The results demonstrate clearly that highly reactive soot can be achieved by manipulating the physical properties of the soot via EGR. The 0% EGR soot underwent a slow surface oxidation process due to its less disordered fraction compared to the 20% EGR soot. Presumably, the grapheme layers of the 0% EGR soot are more ordered so that they resist oxidation at 450 °C. The 0% EGR soot exhibits strictly external burning by the dissociation of the carbon atoms from the edges of the layer planes of the crystallites and does not show any

change in the interior of the primary particles, following solely a surface burning process. On the other hand, the 20% EGR soot exhibited dual simultaneous burning modes: fast internal burning and slow external burning. The interior of the primary particles of the 20% EGR soot are oxidized in preference to the peripheral carbon.

Magín Lapuerta et al [14] investigated the effect of fuel on the soot nanostructure and consequences on loading and regeneration of diesel particulate filters. In their study an automotive diesel engine was tested in three representative modes of soot accumulation, active regeneration and spontaneous regeneration of its catalyzed diesel particulate filter (DPF), among the typical driving operation modes. During the engine tests, pressure and temperature along the DPF were measured, and soot samples were taken from the exhaust manifold upstream of the DPF for their thermal, structural and morphological characterization. In order to study the morphological analyze, the soot samples were subjected to TEM analyze. Thermal heating under oxidant atmosphere for studying the oxidation kinetics, Raman spectroscopy for describing their nanostructure and X-ray diffraction spectroscopy (XRD) for studying their internal lattice parameters. When the engine was operated in a typical accumulation mode, the pressure drop across the DPF increased up to 80 hPa with diesel fuel, while pressure drop stopped increasing after 4000 s of engine testing with biodiesel. In the regeneration mode, the DPF regenerated more slowly in the biodiesel case as a consequence of lower post-injected fuel energy and thus lower exhaust temperature. In the self-regenerating mode, the DPF was charged more slowly with biodiesel than with diesel fuel and its break even temperature was 40 ^{o}C lower with biodiesel

fuel. These results showed that biodiesel PM is more reactive to oxidation. Although thermo gravimetric results confirmed this tendency based on the differences on the pre-exponential factor, Raman spectra showed that biodiesel soot reached more ordered graphite-like structures and lower amorphous carbon concentration and XRD analysis showed that biodiesel soot displayed a higher degree of graphitization. The TEM analysis of the agglomerates showed that PM primary particles from biodiesel fuel were significantly smaller and had higher specific active surface than those of diesel soot. From these results, an interpretation of the differences in soot oxidation between both soot samples was made based on the different length scales, from the carbon fringes to the particulate filter.

Dongke Zhang et al [15] has investigated the effect of an iron-based catalyst homogeneous combustion catalyst on the oxidative behavior and nanostructure characteristics of soot emitted from a single cylinder CI engine. The results showed that smoke opacity 7.3–39.5% lesser soot emissions when the catalyst was applied, depending on the catalyst dosage ratio. Also the results of TGA that soot from the catalyst treated fuels possessed higher oxidative reactivity as indicated by ignition at lower temperatures and faster oxidation rates than those of soot from the reference diesel and this trend increases by increasing the dosage ratio of catalyst. Further kinetic analysis revealed an increase in the oxidation rate constant k and pre-exponential factor A for the soot from the catalyst treated fuels. Smaller and more narrowly-distributed primary soot particles with the catalyst treated fuels than those of the reference diesel were evident. High-resolution TEM

imaging revealed graphitic crystallite structures of the soot samples from both catalyst-treated and -untreated fuels with no obvious variations in the nuclei core areas, suggesting that the internal structure of the soot was not affected by the catalyst. It was evident that iron ions from the catalyst were more involved in the soot oxidation process, rather than in the early soot formation stage, and eventually resulted in smaller and narrowly-distributed primary soot particles.

Aleksey Yezerets et al [16] investigated the differential kinetic analysis of diesel PM oxidation by oxygen, using a step–response technique. This technique was applied to soot oxidation by O_2 and showed that, after decoupling effects due to the sample history, carbon oxidation by O_2 in the absence of H_2O can be well-described by an unmodified Arrhenius equation, with similar activation energy values for diesel and model soot samples (137 $\pm$ 8.7 and 132 ± 5.1 kJ/mol, respectively). The reaction order in O_2 for these samples was found to be 0.61 ± 0.03 and 0.71 ±0.03, respectively, and was remarkably independent of the temperature, suggesting that the fractional order is not due to mixed kinetic control. The reaction mechanism was also found to be independent of carbon conversion. The density of the reaction sites, however, appeared to increase with oxidation. This increase could not be accounted for by the changes in the specific surface area, either directly measured or derived from such simplified models as the shrinking-core formalism. The entire set of obtained experimental results can be described using a kinetically uncomplicated model in a broad range of temperatures, partial pressures of oxygen and degrees of soot oxidation.

J. Jung et al [17] have focused on understanding the mechanism of carbon oxidation in their study. They investigated carbon black (Printex-U) soot oxidation by designing a simulation system which represented as DPF. A flow reactor system that could simulate the condition of a diesel particulate filter and diesel exhaust gas was designed. In the constant temperature oxidation experiments, the reaction order of carbon was 0.75±0.01 in the steady oxidation condition and that of NO_2 was unity after 15% carbon was converted. In the temperature programmed oxidation experiments, the reaction rate increased proportionally to NO_2 but it increased with O_2 or H_2O concentration nonlinearly. From the experiments, the apparent activation energy for carbon oxidation with NO_2- O_2 - H_2O was determined to be 40±2 kJ/mole, with the first order of carbon in the range of 10~90% oxidation and a temperature range of 250~500^oC. This value was exceedingly lower than the activation energy of NO_2- O_2 oxidation, which was 60±3 kJ/mol. When NO2 exists with O_2 and H_2O, the reaction rate increases in proportion to NO_2. It increases nonlinearly with O_2 or H_2O concentration when the other two oxidants are fixed.

Kuen Yehliu et al [18] studied the impact of fuel formulation on PM nanostructure and reactivity. They utilized three types of diesel fuels including an ultra-low sulfur diesel fuel (BP15), a pure soybean methyl-ester (B100), and a synthetic Fischer-Tropsch fuel (FT) produced in a gas-to-liquid process. The collected soot samples were characterized using thermogravimetric analyzer (TGA), X-ray photoelectron spectroscopy (XPS), X-ray diffraction (XRD), and high resolution transmission electron microscopy (HRTEM). According to TGA, B100 soot exhibits the fastest oxidation on a

mass basis followed by BP15 and FT derived soot in order of apparent rate constant. XPS analysis indicates no relation between the surface oxygen content and the soot reactivity and fuel formulation such as oxygen content and aromatics has an influence on soot reactivity. B100 soot exhibits the fastest oxidation on a mass basis followed by BP15 and FT soot in order of apparent rate constant. When using single injection, B100 soot has twice the apparent rate constant compared to FT soot. The basal plane diameter obtained from XRD is inversely related to the apparent rate constants for soot oxidation. Quantitative analysis of HRTEM images also suggests soot nanostructure disorder correlates with a faster oxidation rate. XRD and HRTEM analysis results are compared, and they both show excellent correlation of soot nanostructure and reactivity.

C.J. Tighe et al [19] investigated the effect of NO_2 on kinetics of diesel soot oxidation. Diesel engine fuelled by either Ultra-Low Sulphur Diesel (ULSD) or biodiesel, by NO_2 have been measured in a packed bed at various temperatures (300–550 ^oC) and NO_2 (20–880 ppm) relevant to regenerating a Diesel Particulate Filter. Adsorbed hydrocarbons and oxygen accounted for a significant fraction (~20% by mass) of the otherwise carbonaceous material. After pre-treatment (heating up to 550 C in a flow of pure Ar and holding the temperature at 550 ^oC for 1 h) to ensure consistency between samples, they were subsequently burned at a fixed temperature in a flow of NO2 + Ar. For this, a balance on oxygen atoms entering and leaving the packed bed showed that during oxidation in NO_2 any oxygen remaining in a soot after pre-treatment was not rapidly liberated as CO or CO_2. A mass balance on the

element nitrogen demonstrated that no N_2 or NO_2 was formed below 550 ^oC; mass balances on carbon and oxygen demonstrated that all the carbon ended up as CO or CO_2 and below 550 ^oC the nitrogen yielded only NO. The oxidation of soot in NO_2 was found to be first-order with respect to NO_2. Also, the soot derived from biodiesel was more reactive than soot from ULSD; nevertheless, the apparent activation energies for oxidation by NO_2 were the same (70 ± 18 kJ $mole^{-1}$) for each carbon. When the distribution of diameters of the individual spherules of soot was taken into account, it was not possible to tell whether there was internal burning of porous spherules or, on the other hand, non-porous, solid spherules were burning on their exteriors.

Robert L. McCormick et al [20], have studied the impact of biodiesel feed stock and its chemical structure on engine exhaust pollution. In their study biodiesels produced from a variety of real world feedstock as well as pure (technical grade) fatty acid methyl and ethyl esters were examined for emissions performance in a heavy-duty truck engine. The objective was to understand the impact of biodiesel chemical structure, specifically fatty acid chain length and number of double bonds, on emissions of NOx and PM. A group of seven biodiesels produced from real-world feed stocks and 14 produced from pure fatty acids were tested in a heavy-duty truck engine using the U.S. heavy-duty federal test procedure (transient test). It was found that the molecular structure of biodiesel can have a substantial impact on emissions. The properties of density, cetane number, and iodine number were found to be highly correlated with one another. For neat biodiesels, PM emissions were essentially constant at about 0.07 g/bhp-h for all biodiesels as

long as density was less than 0.89 g/cm3 or cetane number was greater than about 45. NOx emissions increased with increasing fuel density or decreasing fuel cetane number. Increasing the number of double bonds, quantified as iodine number, and correlated with increasing emissions of NOx. Thus the increased NOx observed for some fuels cannot be explained by the NOx/Tradeoff and is therefore not driven by thermal NO formation. For fully saturated fatty acid chains then NOx emission increased with decreasing chain length for tests using 18, 16, and 12 carbon chain molecules. Additionally, there was no significant difference in NOx or PM emissions for the methyl and ethyl esters of identical fatty acids.

John P. A. Neeft et al [21], they have investigated the Kinetics of the oxidation of diesel soot. This study was and still is a valuable reference for soot oxidation kinetics and reaction order. The kinetics of the unanalyzed oxidation of a flame soot and diesel soot were studied. Oxidation of the flame soot could be described by an *n*th-order model, with an order in carbon of 0.7. The order in molecular oxygen concentration was found to be 1 for the flame soot and slightly lower than 1 for the diesel soot. This order in oxygen concentration was also found to be a function of conversion. Water caused a significant increase in oxidation rate of the flame soot, which was accompanied by an increase in reaction order in carbon and a much higher CO_2/CO ratio, whereas the activation energy did not change. The oxidation rate of the diesel soot was not significantly influenced by the addition of water. Experimental results were more reproducible for the oxidation of the flame soot than for the oxidation of diesel soot, and the flame soot appeared to be a good model for diesel soot in oxidation studies. Therefore it is

recommended to use a model soot in (kinetic) studies of soot oxidation.

B.R. Stanmore [22], have provided a resourceful review study on soot oxidation. In this review, the experimental techniques which have been used to study the gasification of soot are described and the methods and results obtained by analysis of the data from them are considered. Firstly, the mechanism of soot formation and its structure are briefly discussed. The various scales of particulate which comprise it, i.e. spherule, particle and aggregate, influence its properties and behavior. Next, the experimental equipment used in the study of its gasification is briefly described. Gasification kinetics at low temperatures are measured either in fixed beds or by thermogravimetry. The apparatus may be operated as a thermally programmed desorption system to identify the species involved. High temperature investigations have been carried out in entrainment burners and shock tubes. The chemistry of soot oxidation is discussed for both non-catalytic and catalytic conditions. The oxidation pathway involves interaction between adsorption and desorption processes, which determine the primary products, the order of reaction and the activation energy. The consensus is that two types of adsorbed surface species are present in unanalyzed combustion. The combustion mechanism of individual spherules is considered in terms of basic property changes. During thermogravimetry, the influence of the competition between reaction and oxygen diffusion in soot beds is analyzed. The reaction of catalyzed soot displays a different mechanism, as the primary products, the order of reaction and the activation energy all change. The lower activation energy and higher reactivity lead to lower

ignition temperatures. Catalysts may be incorporated into the soot spherules by addition to the fuel, or may be added after formation. Two types of contact between the carbon and added catalyst have been identified, ‘loose’ and ‘tight’. Tight catalyst, which has been mechanically ground with the soot, produces more pronounced effects. Finally, the behavior of soot during gasification by other oxidants, namely H_2O, CO_2 and NO_2 is summarized.

Pierre Darcy et al [23] also investigated the Kinetics of catalyzed and non-catalyzed oxidation of soot from a diesel engine. This study deals with catalyzed and non-catalyzed oxidation, respectively (CSO and NCSO) of diesel soot in laboratory conditions, using a ceria–zirconia based catalyst. The soot oxidation study is done via temperature programmed oxidations (TPO), temperature programmed desorption (TPD) and isothermal reactions at ambient pressure in a fixed bed reactor. NCSO of diesel soot leads to CO and CO2 formation, in a molar ratio of roughly 0.4. Isothermal runs have shown that soot particulates are composed of two parts with different reactivity towards O2: oxygenated species (VOF) are very reactive. They spontaneously decompose under inert atmosphere when they are heated up. Their oxidation in oxygen containing gases occurs at low temperature (300 ^{o}C in our experimental conditions). Carbonaceous core of diesel soot is less reactive and is oxidized only above 450 ^{o}C. Based on this observation, a simple kinetic model has been proposed for non-catalytic soot oxidation. This model has been successfully used to model our TPO results. CSO with a $Pt/CeZrO_2$ catalyst has also been studied. The oxidation leads to CO_2 production only. Our experiments showed that three mechanisms occur in soot

consumption: first, a VOF oxidation, which is catalyzed by our $Pt/CeZrO_2$ catalyst. The proportion of catalyzed soot mass increases with the catalyst: soot ratio. Kinetic parameters of this oxidation have been determined. Partial order versus oxygen (0.3) and activation energy (114 kJ/mole) are both lower than for the non-catalyzed oxidation process, whose kinetic parameters are respectively 0.9 and 164 kJ/mol. Finally, the whole soot mass reacts via slow oxidation, which looks like a non-catalytic oxidation (partial order versus oxygen: 0.7, activation energy: 161 kJ/mole). VOF are oxidized first, well below 450 °C. Catalyzed part of soot reacts from 400 °C, with a maximum activity between 520 and 550 °C, while slow oxidation occurs when temperature is 30–40 °C higher and reaches a maximum for temperatures between 570 and 600 °C. Kinetics of these three steps have been determined and successfully applied to our TPO results.

Objectives

The objectives of this study is to investigate the impact of fuel properties on engine soot oxidation kinetics, DPF filtration and regeneration behavior for betterment of DPF design and future application in Thailand. At this study, the fuel physical and chemical characteristics of diesel and palm biodiesel fuel is investigated and the results were collected and key features.

For soot preparation, diesel and biodiesel fuels were burnt inside the single cylinder engine and the collected soot samples were sent for TGA isothermal investigation in presence of pure oxygen and air. At final phase, a sample of DPF was used to investigate the filtration mechanism of DPF while applying diesel and biodiesel on pressure drop. For DPF regeneration trend, the DPF were heated up to 600 ^{o} C in presence of air and pure oxygen.

The scopes of research

- Investigation of oxidation kinetics of soot from biodiesel and diesel in presence of pure oxygen and air in isothermal condition.
- Investigation of PM morphology and nanostructure with image processing
- Study of effect of diesel and biodiesel fuel on DPF filtration and regeneration trend with regard to fuel physical and chemical features.

CHAPTER 2

BACKGROUND THEORY

2.1. Diesel engine

Diesel engines have an excellent reputation for their low fuel consumption, reliability, and durability characteristics. They are also known for their extremely low hydrocarbon and carbon monoxide emissions. No other internal-combustion engine is as widely used as the diesel engine. This is due primarily to its high degree of efficiency and resulting fuel economy. The chief areas of use for diesel engines are:

- fixed-installation engines
- cars and light commercial vehicles
- heavy goods vehicles
- construction and agricultural machinery
- Railway locomotives and Ships

The diesel engine is the internal-combustion engine that offers the greatest overall efficiency more than 50% in the case of large, slow-running types. The associated low fuel consumption, its low-emission exhaust and quieter running characteristics assisted, for example, by pre-injection have combined to give the diesel engine its present significance. However, they have also been rejected by many for their odorous and sooty exhaust that is also characterized with high nitric oxide and particulate matter emissions. Combustion in diesel engines is very complex and until recently, its detailed mechanisms were not well understood. In diesel engines, only air is send into the combustion chamber during induction. This air is

compressed during the compression stroke and towards the end of compression stroke, fuel is injected by the fuel injection system into the cylinder just before the desired start of combustion. Liquid fuel is injected at high velocities as one or more jets through small orifices or nozzles in the injector tip. The fuel atomizes into small droplets and penetrates into the combustion chamber the droplets vaporize and mix with high-temperature and high-pressure cylinder air.

Since the air temperature and pressure are above the fuel's ignition point, spontaneous ignition of portions of already mixed fuel and air occurs after a delay period of a few crank angle degrees. The cylinder pressure increases as combustion of fuel-air mixture occurs. As the piston continues to move closer to top dead center (TDC), the mixture's (mostly air) temperature reaches the fuel's ignition temperature. Instantaneous ignition of some premixed fuel and air occurs after the ignition delay period. This instantaneous ignition is considered the start of combustion (also the end of the ignition delay period) and is marked by a sharp cylinder pressure increase as combustion of the fuel-air mixture takes place. Increased pressure resulting from the premixed combustion, compresses and heats the unburned portion of the charge and shortens the delay before its ignition. It also increases the evaporation rate of the remaining fuel. Atomization, vaporization, fuel vapor-air mixing, and combustion continue until all the injected fuel has combusted.

Combustion in Diesel Engines has 4 main stages:

- Ignition delay period
- Premixed combustion phase
- Mixing-controlled combustion phase
- Late combustion phase

The period between the start of fuel injection into the combustion chamber and the start of combustion is termed as ignition delay period. The start of combustion is determined from the change in slope on the p ~ α diagram, in figure 2, or from heat release analysis of the p (α) data, or from luminosity detector in experimental conditions and Start of injection can be determined by a needle-lift indicator to record the time when injector needle lifts off its seat. Start of combustion is more difficult to determine precisely.

It is best identified from the change in slope of heat release rate, determined from cylinder pressure data. In DI engines ignition is well defined, in IDI engines ignition point is harder to identify. Both physical and chemical processes must take place before a significant fraction of the chemical energy of the injected liquid fuel is released. The physical processes are; atomization of the liquid fuel jet, vaporization of the fuel droplets, mixing of the fuel vapor with air. The chemical processes are the pre-combustion reactions of the fuel, air and residual gas mixture which lead to auto ignition. Chemical delay is more effective for the duration of the ignition delay period.

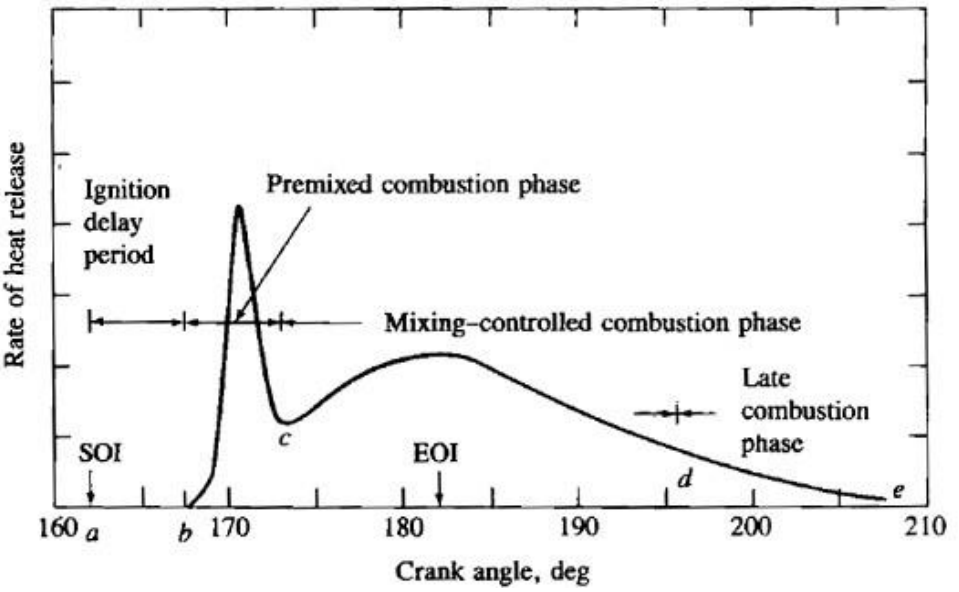

Figure 2. Four stages of combustion and heat release [24].

Combustion of the fuel which has mixed with air within flammability limits during ignition delay period, occurs rapidly in a few crank angle degrees high heat release characteristics in this phase. If the amount of fuel collected in the combustion chamber during the ignition delay is much, high heat release rate results in a rapid pressure rise which causes the diesel knock. For fuels with low cetane number, with long ignition delay, ignition occurs late in the expansion stroke results in incomplete combustion, reduced power output, poor fuel conversion efficiency. If the pressure gradient is in the range 0.4 - 0.5 (MPa/o CA), engine operation is not smooth and diesel knock starts. This value should be in the range 0.2 to 0.3 (MPa/o CA) for smooth operation (max allowable value is 1.0 (MPa/o CA)). Once the fuel and air which is premixed during the ignition delay is consumed, the burning rate (heat release rate) is controlled by the rate at which mixture becomes available for burning. The rate of burning in this phase is mainly controlled by the

mixing process of fuel vapor and air. Liquid fuel atomization, vaporization, pre-flame chemical reactions also effect the rate of heat release. Heat release rate sometimes reaches a second peak (which is lower in magnitude) and then decreases as the phase progresses. Generally it is desirable to have the combustion process near the TDC for low particulate (soot) emissions and high performance (and efficiency). Heat release rate continues at a lower rate into the expansion stroke there are several reasons for this: a small fraction of the fuel may not yet burnt, a fraction of the energy is present in soot and fuel-rich combustion products and can be released. The cylinder charge is no uniform and mixing during this phase promotes more complete combustion and less dissociated product gases Kinetics is slower.

2.2. Diesel and Biodiesel Fuels:

Diesel

Diesel fuel is a mixture of hydrocarbons with boiling points in the range of 150 to 380°C which are obtained from petroleum. The term “diesel fuel” is generic; it refers to any fuel for a compression ignition engine. In common use, however, it refers to the fuels made commercially for diesel-powered vehicles. It is composed of a blend of different types of hydrocarbons, including paraffin’s, naphthenic, olefins, and aromatics. Different types of diesel fuel have different blend ratios, depending on what the fuel will be used for, the temperature of the area in which it will be used, and regional governmental regulations. Diesel is usually produced by distillation in oil refineries. Different hydrocarbons of crude oil vaporize at different temperatures which are used in making diesel usually

vaporize at between 250 and 350°C. When the oil is heated to that temperature in a device called a fractional distillate column, the specific hydrocarbon chains are vaporized and are pulled out for use. This can also be done with the use of chemicals instead of a fractional distillate column. After the components are isolated, they're blended together in specific ratios to make different types of diesel fuel.

Biodiesel

In the United States, biodiesel fuel production has grown from approximately one half-million gallons (just under 2 million liters) in 1999 to an estimated 75 million gallons (284 million liters) in 2005 [25]. This was approximately 0.2 percent of total diesel production in 2005. The main reason for the interest is that biodiesel is a renewable source of energy. In general usage, the term biodiesel covers a variety of materials made from vegetable oils, recycled cooking greases or oils, or animal fats. The definition of the term “biodiesel” is being debated, but for the purposes of the publication the following ASTM International definition applies: “a fuel comprised of mono-alkyl esters of long chain fatty acids derived from vegetable oils or animal fats, designated B100”. Vegetable oils and animal fats consist of three fatty acids hydrocarbon chains of varying lengths, bonded to a glycerol molecule. This structure is commonly known as a triglyceride. Figure 3 lists a variety of fatty acids, indicating hydrocarbon chain length and the number of carbon-carbon double bonds. In a process known as transesterification, triglycerides react in the presence of a base chemical (sodium or potassium hydroxide) with an alcohol, usually

methanol, resulting in three fatty acids bonded to the methyl group from methanol. These chemicals are referred to as fatty acid methyl esters (FAME) with alkyl chain lengths of 12 to 22 carbons. Water, base chemical, unreacted triglycerides and alcohol, and glycerin are byproducts of the transesterification reaction and must be removed from biodiesel fuel. The glycerin (also called glycerol) is purified and has uses in the cosmetic, food and other industries, and as an animal feed stock. Biodiesel has chemical and physical properties similar to those of conventional diesel fuel. In the United States, soybean oil is the largest source of biodiesel, although oil from other plants is used as well. Canola oil (canola is a hybrid of rapeseed) is the source for most of the biodiesel produced in Europe. In countries where winters are warm, palm and coconut methyl esters are commonly used. Jatropha nut oil esters are becoming important in India and Africa, where the jatropha plant tolerates poor soil and is disease resistant.

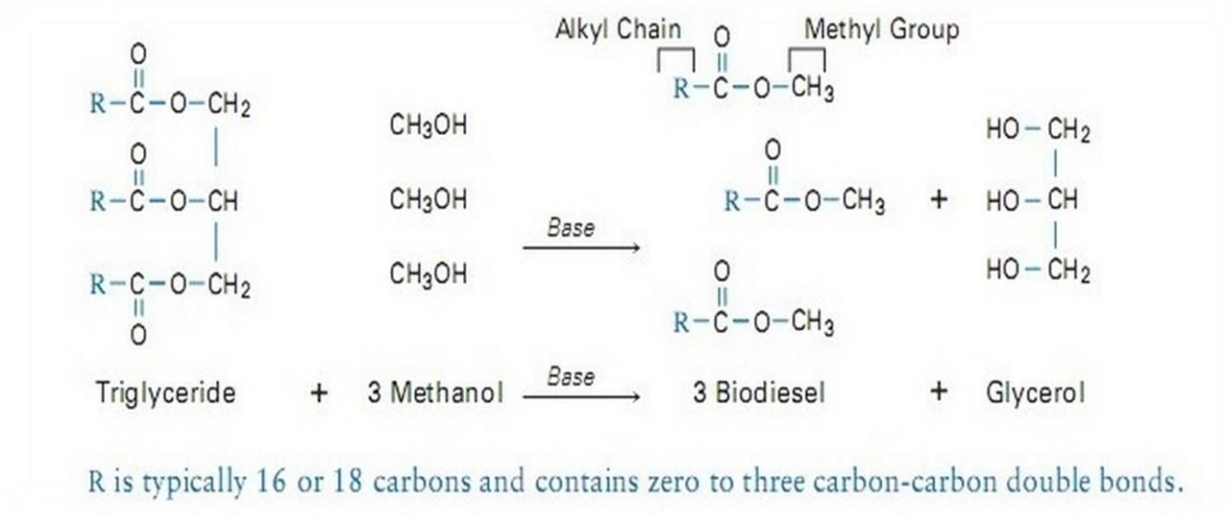

Figure 3. Transesterification of Vegetable Oil to Biodiesel [25].

2.3. Particulate matter

Particulate matter also known as particle pollution or PM, is a complex mixture of extremely small particles and liquid droplets. Particle matter is made up of several components, including acids, organic chemicals, metals, and soil or dust particles. Carbon is the main important part of PM and is found in three distinct forms including (a) carbonate (b) myriad organic compounds, referred to collectively as organic carbon (OC); and (c) carbonaceous or quasi-graphitic material dubbed elemental carbon (EC). The first type is a minor component associated with rocks and (lime) stone and is mineral based. The other two forms of carbon are mostly generated in the combustion of carbonaceous materials, chiefly fossil fuels and biomass. The carbonaceous part, which is considered as solid part of PM, is an agglomeration of much smaller particles. This agglomeration is referred as spherules, and the sizes range are ~20−50 nm. The microstructures of which are partly amorphous and partly graphitic or quasi-graphitic. The morphology of the whole particle, or agglomerate, is characteristic of the combustion process, e.g. globular for biomass, fractal for diesel and compacted for coal. The agglomerate forms a kind of skeleton, onto which organic compounds, emitted as gases, condense as the exhaust gas cools. The relative proportions of carbonaceous and organic particulate are characteristic of the source. Figure 4 shows some characteristic particles which are likely to be present in the exhaust stream of a motor vehicle. Although this diagram is schematic and conceptual, it contains many of the features that would be observed, if the exhaust gas were to be passed through a filter and the particles

collected thereon were to be examined in an electron microscope. The most immediately striking aspect of figure 4 is the presence of three distinct types of particle, labelled *nucleation mode*, *accumulation mode* and *coarse mode*. Particles in the atmospheric aerosol invariably exhibit this trimodality, and particulate emissions from motor vehicles are no exception.Coarse mode particles from different compositions are mainly made by attaching the predecessors lodge within exhaust system. These particles join each other and make a much larger particle which will go out by exhaust stream. This trend has a random manner and is unpredictable. As shown in figure 4, they may consist of solid core and a volatile organic fraction (VOF) layer on the surface.

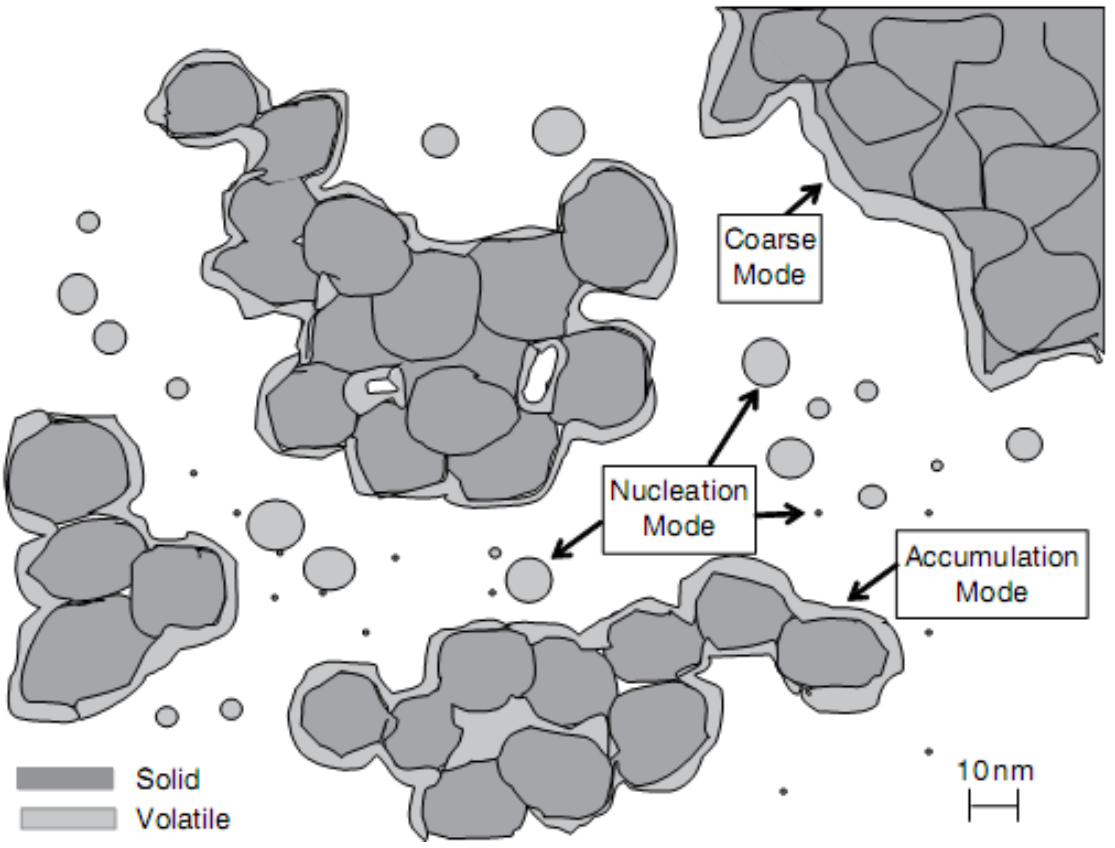

Figure 4. Coarse mode (largest, shown in part), nucleation mode (smallest); accumulation mode (middling) [26].

Most researchers suggest that nucleation-mode particles consist of volatile material and that's the reason of showing the particles as spherical in figure 4. Other research suggests that some nucleation-mode particles are in fact solid, or at least possess minute solid kernels. These questions are being avidly researched in many research laboratories at the moment. The most immediately obvious feature of accumulation-mode particles is that they consist of a collection of much smaller primary particles. These primary particles are referred to as spherules, meaning that while not exactly spherical, they nonetheless quite closely approximate sphericity. The size range for spherules is typically ~20–50 nm. The agglomerate surface is coated by a layer of liquid or semi-liquid material which is adhesive and penetrates into the pores and internal voids of the agglomerate. This leads to a significant difference between surface composition and the core composition. The adherence of this volatile or semi volatile layer leads to the expression *wet particulate* which will vaporize by heating, on the contrary, the solid core that remains after a heating process, which is the *dry* particulate.

The factors which affect the chemical composition of PM is presented in figure 5. At the first level, everything is included that might be captured when exhaust gas is passed through a filter except condensed water. Water droplets contain minute solid particles, and also absorb soluble combustion products such as aldehydes and ketones. As already mentioned before upon heating, some material evaporates and some does not. Alternatively, some material dissolves in certain solvents, and some does not. This

divides the particulate into that which is volatile or soluble, and that which is nonvolatile or insoluble.

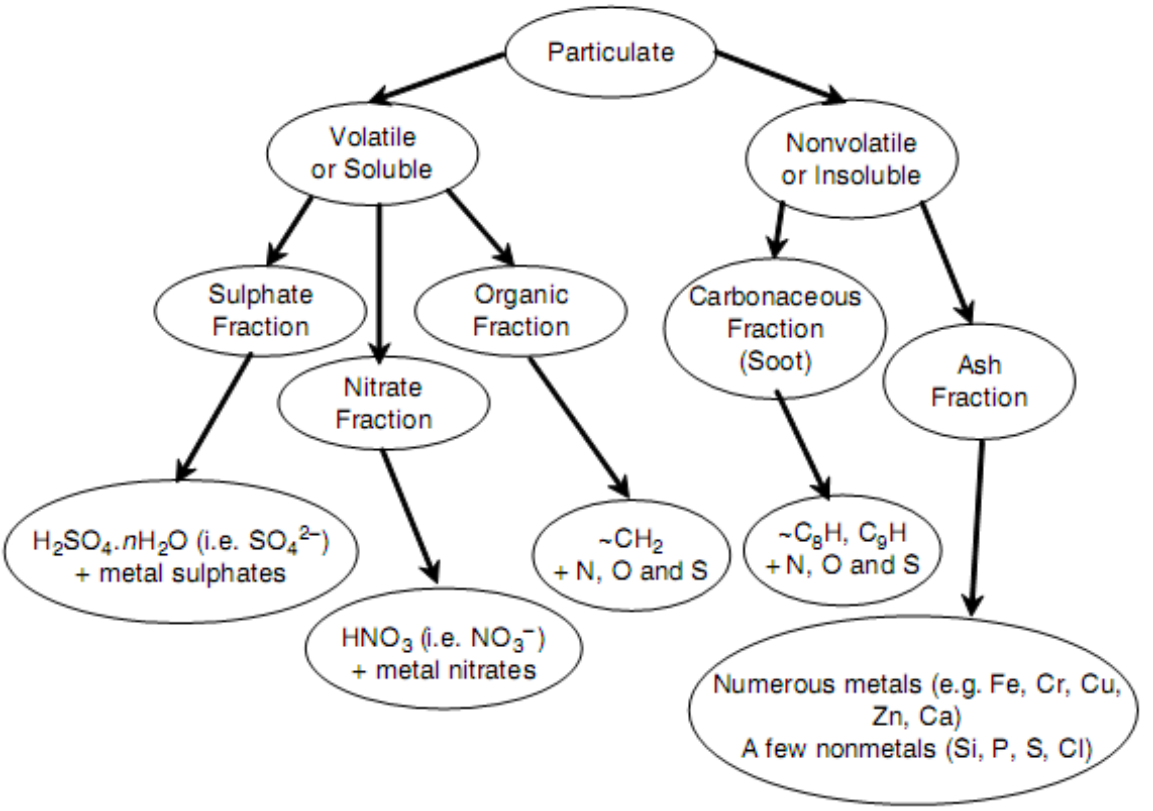

Figure 5. Shows a conceptual model of particulate composition, categorized in five distinct groups or fractions: sulphates, nitrates, organics, carbonaceous and ash [26].

So in general there are five clear subgroups, or fractions: sulphates, nitrates, carbonaceous, organics and ash. The chemical composition (Figure 5) corresponds, in a large degree, to the physical representation (Figure 4).

Organic Fraction

If the composition is dissolve in an organic solvent, then it's considered as a soluble organic fraction (SOF) and if it vaporize by heating up, it will be considered as volatile organic fraction (VOF). The methods for separation of these two parts are varied thus there is no unique method for determination of it, however based on most of the researches these two fractions have nearly close percentages. The SOL and VOF are made up of many components. Most of the major chemical families are represented, although their proportions vary widely: alkenes, alkanes, alcohols, esters, ketones, acids, esters and aromatics.

Sulphate Fraction

This fraction consists of water-soluble sulphates, or the $SO2^{-4}$ ion, but the chief component is sulphuric acid, H_2SO_4. Sulphuric acid has high tendency to react with water. In fact, the water content of the particulate often varies only with the sulphate content, because the particulate-bound water is found predominantly with the sulphuric acid. So, what sulphates really means is the acid and the water. The water content is an important case of consideration hence the amount of water usually is not negligible and environmental elements can also affect it.

Nitrate Fraction

In Nitrate fraction, NO^{-3} and nitric acid, HNO3, are the key players. Normally the HNO_3 is formed via reaction between water NO_2 and overall process is related to NOx chemistry.

The typical reaction is:

$2NO_2 + H_2O \rightarrow HNO_2 + HNO_3$

$3HNO_2 \rightarrow HNO_3 + 2NO + 2H_2O$

Existence of small portions of HNO_2 and HNO_3 in exhaust gas is reported. Water acts as an assistant in catalytic oxidation of carbon by NO_2. On the other hand, an opposite trend is seen between sulphates and nitrates in absorptions of oxygen molecules of engine exhaust gas. It should be considered that nitrates have more volatility in comparison with sulphates and nitric acid has lower boiling point than sulphuric acid.

Carbonaceous Fraction

The carbonaceous fraction is mainly consists of carbon as can be understood by its name. In this thesis, *soot* and *carbonaceous fraction* are synonyms. The inky blackness of smoke arises from this fraction therefore, emissions regulations framed in terms of smoke overlook the other fractions, although measures that reduce smoke may also, for example, fortuitously reduce the organic fraction.

Ash Fraction

The ash fraction contains inorganic compounds, mainly metals and some very small portions of complex compositions which cannot be defined easily and clearly. A common method for the ash measurement is burning all the particles and examine the remaining mass. These five fractions correspond in a large measure to the features delineated in Figure 5: the sulphate, nitrate and organic fractions form the volatile coatings, and the carbonaceous fraction

is largely represented by the spherules. With this regard, the accumulation-mode particles are sometimes called an ‘aciniform’ type of carbon, or clustered like grapes but the location of the ash fraction is less certain it may be atomically dispersed.

2.3.1. Combustion process and effect on PM formation

Inside the engine

Among the five fractions which was mentioned before, ash and carbonaceous parts of particulate matters are generated within the engine and the rest of the fractions are produced within exhaust process. Fuel, lubricant, air and material breakdown are the four main source of particles from engine. Figure 6 depicts shows the schematic of PM fraction source and its level of importance. There are two main modes of combustion in diesel engine functional process. If, before combustion, the fuel droplets vaporize, and the vapor has ample opportunity to mix with the air, this is a *premixed flame*; and if fuel and air are insufficiently mixed before combustion is initiated, this is a *diffusion flame*. In a premixed flame, the rate of combustion is controlled by chemical kinetics, whereas in a diffusion flame, it is the physical processes of mixing, i.e. mass transport that are rate-determining premixed and diffusion flames are both found in diesel engines: the first gives way to the second as the combustion proceeds.

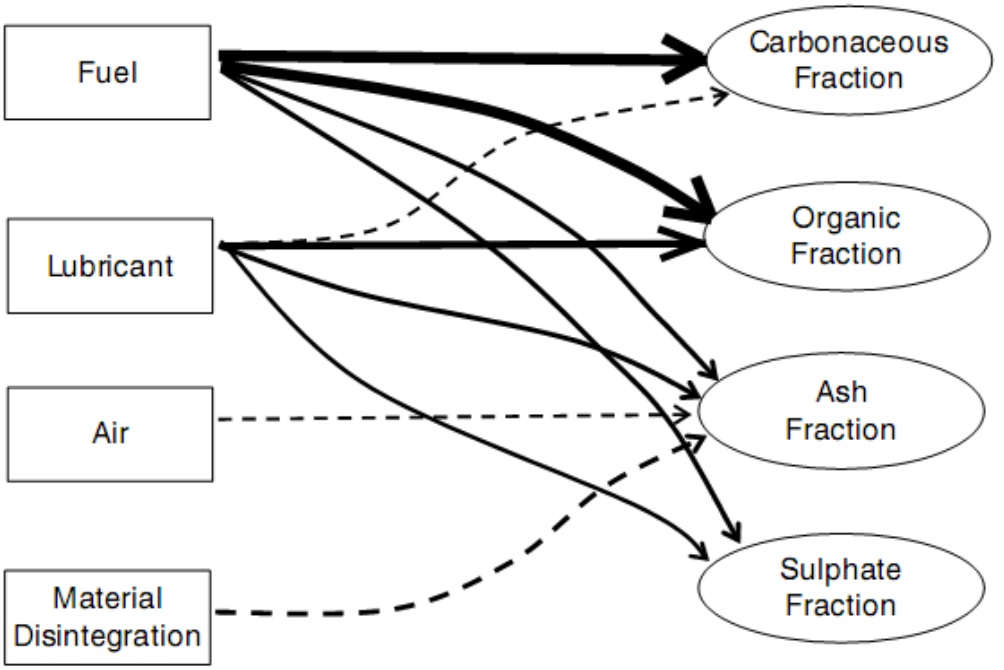

Figure 6. What happens within the engine: conversion of fuel, lubricant, air and engineering materials into carbonaceous, organic, ash and sulphate particulate purely subjectively, the line widths suggest relative importance; dashed lines suggest poorly explored possibilities a less obvious scenario is the entry of foreign material (i.e. ash) into the fuel tank during refueling [26].

The premixed flame occurs due to ignition delay, the interval between start of injection and the start of combustion, during which preparatory pre-combustion reactions occur. Therefor a premixed of a fraction of injected fuel will reach to a combustible condition. However, due to faster burning rate of this premixed fraction than the rate of fuel injection replenish, so the flame boosts. After this point, flame proceeds slower than the rate of availability of combustible mixture and reaches to a condition which is called diffusion flame. Another factor for consideration is to know that some portion of injected fuel will experience oxygen privation inside diesel

engine, even though the global air/fuel ratio is lean, the charge is heterogeneous. Heating up the hydrocarbons without sufficient oxygen, the reaction undergoes to an endothermic reaction which is called pyrolysis. The combustion chemistry then sets out in the direction of soot. Pyrolysis includes the reactions between hydrocarbons, dehydrogenation to form hydrocarbons of greater unsaturation, and cracking of hydrocarbons into fragments. This type of reaction is also used in crude oil refinery systems. As the amount of oxygen decreases, the tendency for more pyrolytic reactions increases. At different ranges of temperatures various pyrolytic reactions occurs. When a complex material is subjected to pyrolysis, at higher temperatures bond rupture and dehydrogenation are the key reactions. This results in generation of species with lower molecular weight. At lower temperatures, polymerization and condensation are the prevalent reactions which create species of higher molecular weight. In case of hydrocarbons, pyrolysis converts the high amount of carbon atoms of fuel molecules to soot particles. The original fuel molecules are broken down and rebuilt as structures of ever-greater molecular weight. These reactions makes the components lesser organic and more carbonaceous by reducing the carbon–hydrogen ratio.

The organic fraction arises from fuel in two ways: direct and indirect. The direct path is when fuel escapes combustion and simply passes unburned through the engine. For example if some fuel portion is over mixed with air some regions of the charge can’t support the flame and fuel goes out unburned. Ignition delay can promote over mixing. The indirect path is when pyrolysis reactions are for some reason interrupted in their conversion of fuel to soot. For example,

if they are quenched by continued mixing. In this case the organic fraction will contain species not present in the fuel, i.e. those synthesized in the combustion. Lubricants are an important none-fuel source of particulate matter and they also can be a part of PM composition.

Through exhaust

Particle's formation process continues after combustion and alteration on its composition continues when exhaust valve is opened. The exhaust temperature is sufficient enough for ongoing reactions among gases and particles. At this phase, particles grow by agglomeration and other particles settle in internal surfaces. Among the volatile fractions, sulphates, nitrates and organics attach to existing particles. The only solid parts of particles are ash and carbonaceous fractions hence the exhaust temperature is still high. But when the temperature decreases, more volatile fractions join the particles. Water is the main condensable component and its condensation starts as the temperature goes down. Sulphates are the other principal volatile component in exhaust gas but hence they are in gas phase and emitted as SO_2, without catalytic converters they can't be filtered but oxidation catalyst can convert SO_2 to SO_3 which is rapidly hydrolyzed into sulphuric acid, H_2SO_4.This acid, in turn undergoes gas-to-particle conversion. Ash fraction usually exists as metal oxides or salts. Wear particles can originate from different parts of engine and rust due to the combined action of oxidation, thermal cycling, vibration and corrosion by sulphuric acid, exfoliate from the walls of the exhaust system. Various wear

particles are also released from catalytic converters or other after treatment devices, and from mufflers.

2.3.2. Particle size distribution and number

The particles are mainly categorized in three groups or modes. This division is based on the size of the PM. These three modes are nucleation, accumulation and course mode and this order is based on increase of size. These modes are presented in figure 7.

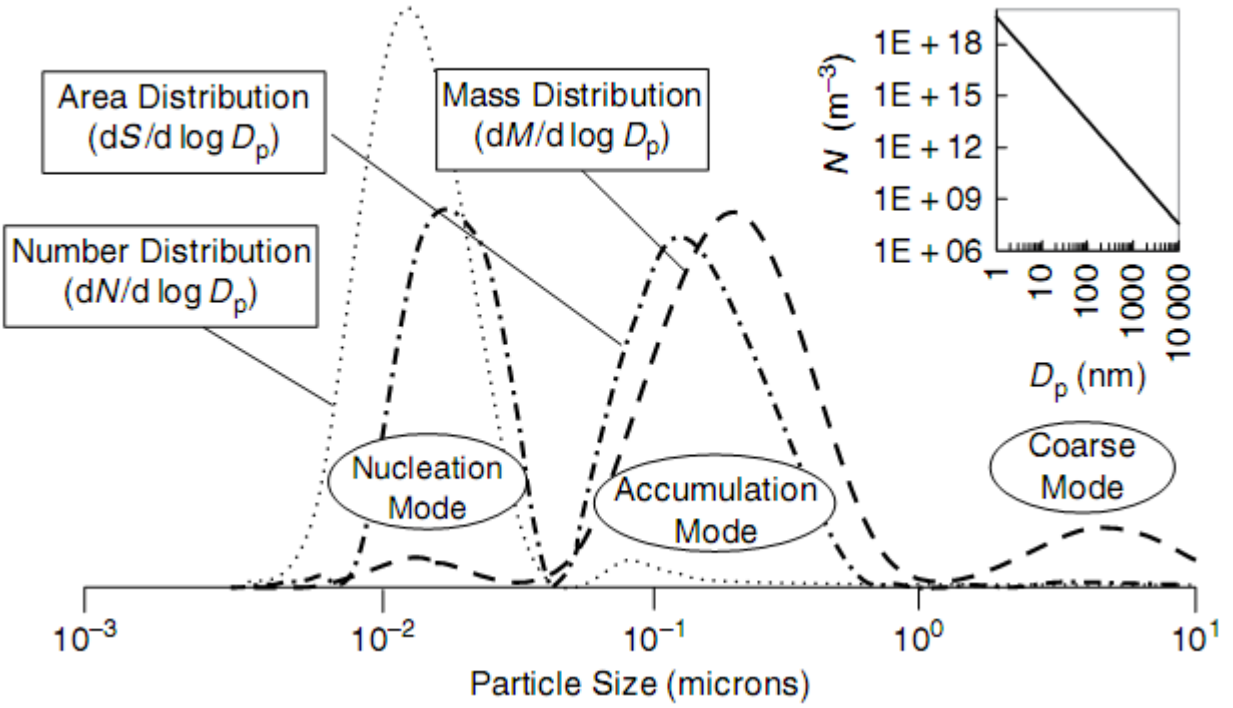

Figure 7. Generalized size distributions for typical particles emitted by internal combustion engines, taking spheres and constant density as a first approximation: by number N, surface area S and mass M (after Kittelson, 1998). The inset shows, as a function of size, and assuming unit density, the required N, in particles per cubic meter, in order to realize M = 20 µg/m3 [26].

With regard to number of particles, most of the particles are in the range of nucleation mode while with regard to mass most of particles are within the range of accumulation mode. This difference in size can also be related to difference of PM's composition. The size distribution is lognormal. Most particulate, by mass, resides in the accumulation mode (100–900 nm), and most particulate, by number, resides in the nucleation mode (<100 nm). The coarse mode (>900 nm) is not usually significant [26]. Accumulation mode particles are made of a solid core of carbonaceous building blocks called spherules, which join each other and form agglomerates. Spherules are uniform in size, i.e. mostly 20–50 nm, and the agglomerates they form contain no defined number. It ranges from a very low numbers to several thousand [26]. An outer layer of volatile compounds is attached to the agglomerates. The nucleation-mode particles are more unclear and most are probably formed from nucleated volatiles, but some research suggests that a few of them are solid, or contain minute solid cores [26]. The coarse-mode particles are solid and are formed from the other two modes through a process of storage and release in the exhaust system, or through material disintegration. There are five distinct fractions as mentioned before: *ash*, *carbonaceous*, *organic*, *sulphate* and *nitrate* which are on a competition condition with each other. The first two are nonvolatile and the others volatile. This classification scheme is not perfect and separation between the fractions are often difficult. The organic fraction contains hundreds or thousands of compounds and it's the most complex part with most of the major chemical families such as esters, aromatics, alcohols, etc. The sulphate fraction is predominantly sulphuric acid and its associated water, but

there can also be metal sulphates. The carbonaceous fraction is chiefly carbon. The nitrate fraction denotes nitric acid. The ash fraction consists of what is incombustible, and contains mostly metals, but also a few nonmetals.

2.3.3. PM formation and growth

The compression ratio of diesel engine is higher than other engines and rapid combustion of injected fuel inside the chamber occurs. Soot is an unavoidable by product of diesel combustion and the heterogeneity of charge, rich burning regimes during mixed control combustion phase are considered as the chief reasons for soot production [26]. The soot formation initiates with fuel molecules containing 12 to 22 carbon atoms. This molecules also have hydrogen atoms, twice number of carbon atoms and it terminates after a few milliseconds with particles or spherules, containing thousands of carbon atoms and about one tenth of H atoms. The schematics of soot formation is shown in figure 8. The soot precursors are made by breaking down of fuel molecules by pyrolytic reactions. These precursors go through out a nucleation process to make the first noticeable particles which are called *Nuclei* and it's size is about 3 nm. The nuclei particles are processed through out another phenomenon which is called surface growth. At this stage carbon is added and hydrogen is removed until spherules size reaches to 20 ~ 50 nm of size range. At the surface growth process the spherules themselves start agglomeration and the smaller particles join each other and make bigger particles.

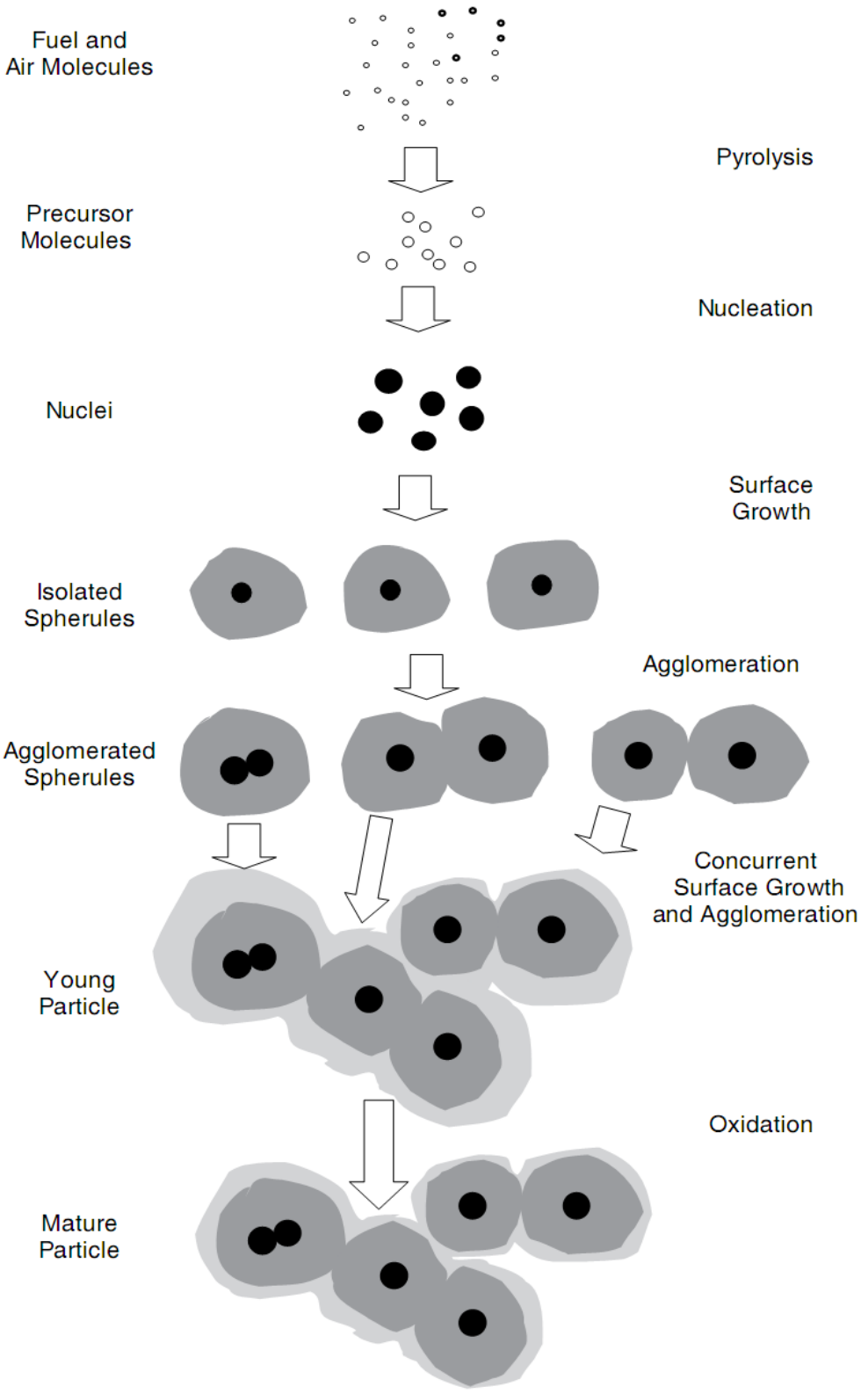

Figure 8. Conceptual scheme for the formation of soot [26].

The soot is generated at a critical air/fuel (A/F) rations and the starting point of this critical point is governed by global reaction formula of hydrocarbons combustion reaction which is show as formula (2.1) and (2.2). α ,β and γ are the number of C,H and the C/O ratio.

$$C_\alpha H_\beta + xO_2 \rightarrow \alpha CO + \left(\frac{\beta}{2} - \frac{\alpha(1-\gamma)}{\gamma}\right) H_2 + \left(\frac{\alpha(1-\gamma)}{\gamma}\right) H_2O + \left(x - \frac{\alpha}{2\gamma}\right) O_2 \quad [(\alpha/2x) \leq \gamma], \tag{2.1}$$

$$C_\alpha H_\beta + xO_2 \rightarrow 2x\gamma CO + \left(\frac{\beta}{2} - 2x(1-\gamma)\right) H_2 + 2x(1-\gamma) H_2O + (\alpha - 2x\gamma) C(s) \quad [(\alpha/2x) \geq \gamma]. \tag{2.2}$$

Based on this model a supposed critical point is for the ratio of C/O when it is unity. This means there is one oxygen for each carbon atom thus the CO is formed. If this ratio is more than unity some carbon atoms appears as soot. In real condition, this value is often lesser than unity and sometimes reaches 0.5 so all of the existing oxygen atoms are not used. Practically, the critical A/F ratio required for soot generation is depended on several elements such as nature of fuel to air (F/A) ratio mixing, structure of the flame and molecular structure of hydrocarbons. The nuclei particles begin absorption of hydrocarbon fragments and thus grow and the spherules grow into a certain range of size, 20–50 nm, and then stop. This growth increases the mass of nuclei while keeping the numbers of nuclei particles constant. The primary unite of the carbonaceous agglomerate is spherules, which is generated by *surface growth* and

is responsible for layered microstructure of outlaying regions where the crystallite structures are arranged. This structure of layering is different from the microstructure of central regions, which are more disordered and amorphous and lesser crystallite. Spherules stick together due to collision and make bigger particles. These bigger particles also collide with each other and grow. This growth is known as agglomeration. Agglomerative growth is physical, rather than chemical, and it decreases the particle number without affecting the particle mass. At this stage it can be said that the soot is formed. Some agglomeration occurs when the spherules are still very young, and may be consist of tarry materials or fluid, so that original identities are unclear and many nuclei are found within one spherule. But even in the absence of fusing, surface growth continues concurrently, so that an overlying shared lattice structure develops, by which original boundaries are obscured. Clustered or chained morphologies are displayed, according to the nature of the collisions that generated the agglomerates.

The last stage which is shown in figure 8 is *oxidation*. This stage reverses the soot production. This is a parallel reaction with soot oxidation and makes it harder to distinguish the soot formation. Inhibited production and promoted oxidation can result in engine-out soot production. In engine modelling instantaneous soot concentration inside cylinder, which is related to crank angle, is computed by subtracting the oxidation model from production model. These studies show that soot production is the dominant trend in early stages of combustion, while oxidation mainly occurs at later phases. The oxidation and formation trend are the important factors for determination of emitted products of engine. About 90%

of produced soot is destroyed by the combustion and the remaining 10 % only escape the oxidation. The late combustion stage or burn out stage, is the main responsible for oxidation prevention of this 10 %. Not only O_2, but other oxidants such as O, OH, H, CO_2 can affect the soot oxidation. In flames, O_2 is not the only active oxidative element. It's said that OH is a more active oxidant [26]. The fluid mechanics which dominates the combustion chamber, controls the mixing of air and soot and movement of the soot cloud plays an important rule. The oxidation of spherules is generally supposed to be kinetically limited and to take place on the surface, as expressed by surface recession. Evidence exists, though, that some oxidation takes place inside spherules. So overall it can be said the nuclei particle gains mass through surface growth and then by agglomeration joins other nuclei particles which results in increase of the size and decrease of the particles number, while mass gain and surface growth still continue, and a mature particle will be created. Most of these particles will be oxidize by engine combustion and a small portion goes out via exhaust.

PM structure geometry

sThe structure of PM is the result of adherence of carbon atoms to each other in a bonding hexagonal shape. Each edge of these hexagonal shape is known as carbon platelet or fringe. These platelets make a crystallite structure by bonding with two to three layers. These formations proceed further and creates a spherical shape which forms the particle. The schematic of this structure is depicted in figure 9.

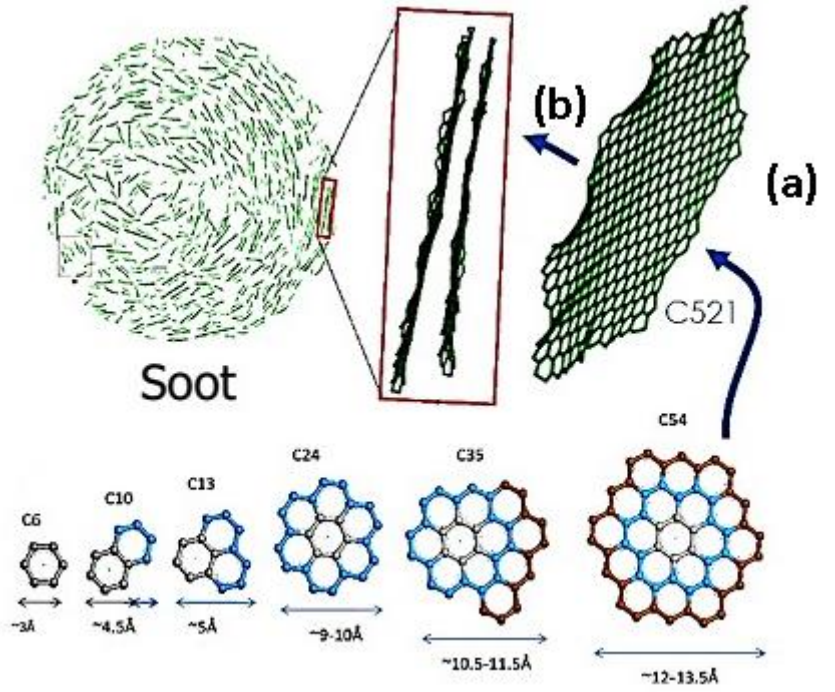

Figure 9. The structure of soot PM (a) a carbon hexagonal layer (b) carbon platelet (fringe) [27].

2.3.4. PM formation and different combustion phases

From commence of combustion, the portion of soot inside the cylinder rises rapidly and reaches a peak. After reaching to the peak, this amount decreases with a diminishing trend and reaches to an asymptote. This trend shows the equal importance of soot formation and oxidation. The soot formation is favored at early stage of

combustion while the oxidation is dominant at the later phase. These two parameters are affected by engine functions and working condition such as injection pressure, injection timing and EGR, thus the net effect is not clear. It can be said that the formation of more soot in higher peak, can be balanced by higher rate of oxidation which ends in lesser engine exhaust soot. So it's necessary to have an eye on the different stages of combustion on soot formation.

Premixed Burn

At the premixed burning phase, the first soot particles are formed in a well-mixed section of air and fuel vapor, toward the combusting plume. This soot is seen in multiple zones, which the whole region is immediately overspread. The soot which is formed at premixed phase has significant contribution to exhaust soot. The conceptual model of ignition, premixed combustion and the emergence of soot is shown in figure 10. At the beginning of injection, a jet of liquid fuel grows inside the combustion chamber with extreme velocity but then slows down due to collision with hot air, which results to vaporization of injected fuel and increases the air-vapor segment. Before ignition there are two types of contiguous zones which are an unmixed segment of liquid fuel and a mixed segment of air and vaporized fuel. The air-vapor segment continues to expand immediately inside the chamber before the ignition and at that moment it has a mixed ratio of 1/4< ʎ <1/2. Ignition occurs at the air-vapor segment under stoichiometric condition. At this segment the break down and pyrolysis of fuel occurs and this results in production of PAH. These PAH rapidly covers the whole segment of air-vapor. The first soot particles appear within pockets of combustion plume varies in size and shape and location of formation in each cycle from another.

These soot particles multiply and cover the whole air-vapor segment. The concentration of soot arises temporarily within the combusting plume and spatially toward the leading edge. An Important change in plume structure takes place and various particles emerges around the periphery. This variety is due to the larger size of particles and faster growth rate in comparison with their kind inside the combusting plume. The zone of peripheral soot becomes thicker due to localized turbulence mixing. This can be an indication of some relations between peripheral and diffusion flame envelope that is established around the combustion plume. At this condition peripheral soot and enveloping diffusion flame are generated just prior to peak in premixed burn heat release. The process of soot formation in premixed phase is extremely fast. For example the interval between commence and ending the combustion plume is 70μs or 0.5^0CA, reported by Dec and Epsy [26]. So simultaneous formation of soot at multiple points has become possible due to this rapid trend.

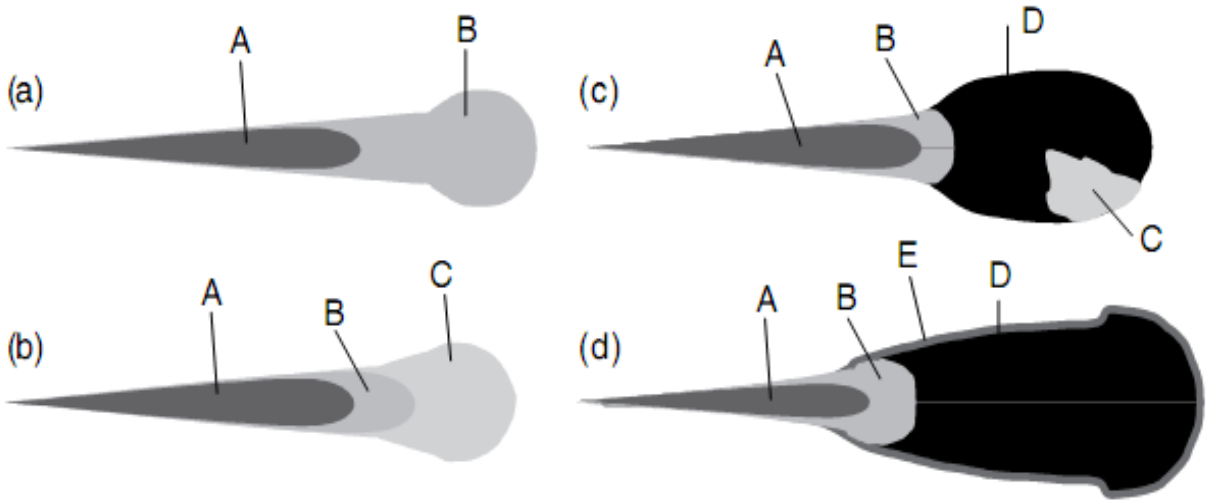

Figure 10. Conceptual model of plume development: (a) immediately prior to ignition; (b) just after ignition ;(c) early phase of premixed burn; (d) late phase of premixed burn. A, liquid fuel; B, fuel vapor; C, PAH; D, low concentration of soot; E, diffusion-flame envelope (Dec, 1997) [26].

Mixing-Controlled Burn

An ideal mixed control combustion is illustrated in figure 11. The majority of emitted soot originates from inside the combusting plume. The conceptual models of diesel engine combustion confirms that during a mixed control phase soot generation occurs in a rich premixed flame which stands off from injector nozzle. Those particles then grow while moving down the combusting plume alone the plume stem toward the head of vortex. In the vortex then, the particles are burned by an enveloping diffusion flame. The concentration of soot particles and their size increases with distance along the plume, but, at any particular cross-section, both appear to be roughly constant. The laser imaging investigations also show that peak of particle concentration is in the vortex .These particles are

agglomerates and their features vary with distance from the nozzle .The spherules size range is 20 ~ 50 nm.

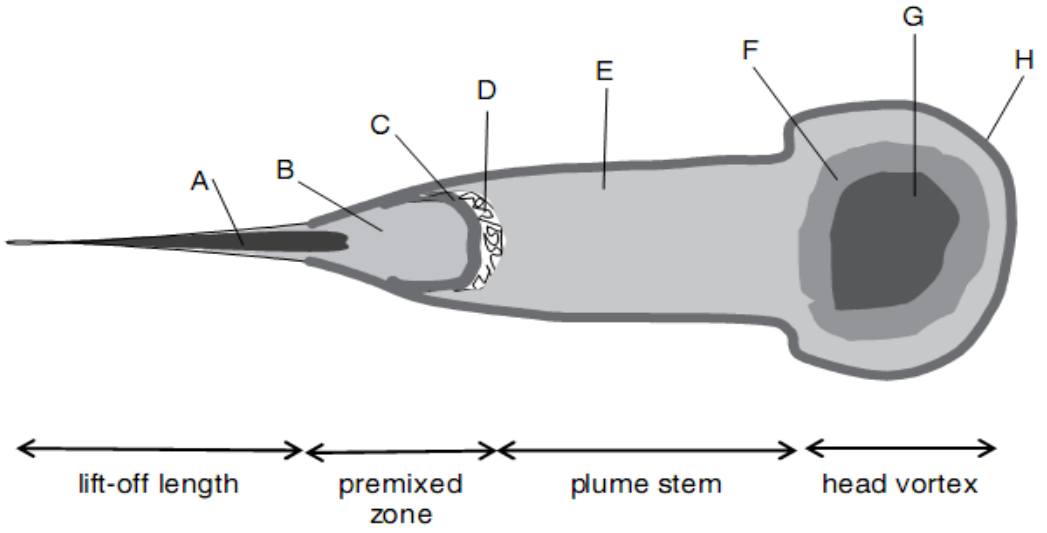

Figure 11. Conceptual model of combustion during the mixing-controlled phase: A, liquid fuel; B, mixture of fuel vapor and air; C, fuel-rich premixed flame; D, initial soot formation; E, F, G, in order of increasing soot concentration; H, diffusion-flame envelope (Dec, 1997, and subsequent papers) [26].

Late Burn

All the soot inside combusting plume cannot be burned and thus this soot particles forms engine exhaust PM. At the end of injection the combusting plume vanishes and the head of vortex is taken apart into many soot filled pockets which are quenched too early before complete oxidization. At this condition the temperature is too low to handle oxidation, therefore soot particles last until exhaust valve opening. Figure 12 (a) shows a schematic of folding up and collapse of combusting plume. The plume stem moves into the head of vortex, then a collision occurs between cylinder wall and head vortex

which spreads out the stem circumferentially. This is a terminating trend and divides the head vortex into many segments, which ends up in the elimination of combusting plume by soot pockets. It shall be considered that the location of these pockets varies in each cycle. In figure 12 (b) the residing soot particles in pockets are depicted.

Those pockets may be still burning by diffusion flame, however, as mentioned before, this diffusion flame is quenched earlier than the required time for complete oxidation which leads to failure of burning all the soot particles and thus emitting the soot out to atmosphere.

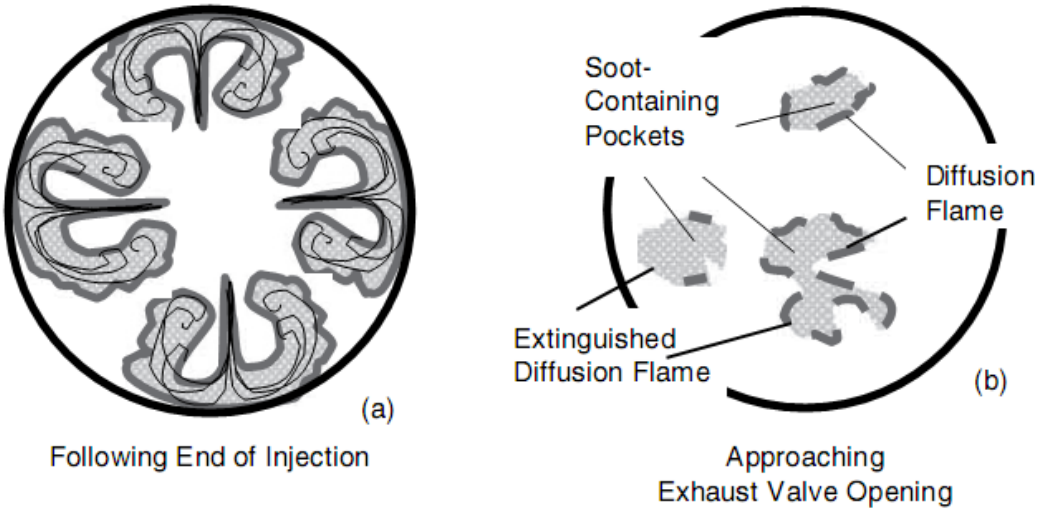

Figure 12.folding up and collapse of combusting plume: (a) immediately following end of injection; (b) late burn-up of soot-containing pockets, partially surrounded by diffusion flames. Sketched from ideas developed by Dec and Kelly-Zion (2000)[26].

4. Diesel Particle Filter (DPF)

Diesel particulate traps are devices that physically capture diesel particulates to prevent their Release to the atmosphere. Although they are not a new technology, they are most effective control technology for the reduction of particulate emissions with high efficiencies. Particle traps are effective in controlling the SOL fractions of diesel particulates, including elemental carbon (soot) and the related black smoke emission precisely, due to the particle deposition mechanisms which is applied in these devices. Lower bulk density of diesel PM, which is depended on the degree of compactness, enables the DPF to filter diesel PM quickly, which results in higher accumulation volume of trapped PM inside the DPF. Several liters of soot per day may be collected from a heavy-duty truck or bus engine. The compiled soot can cause high exhaust gas pressure drop and thus impact the engine negatively and to cope with this bad trend a method for soot removal is required. This removal of particulates, known as the filter regeneration, can be done actively or passively. In active method the regeneration occurs while the engine is still functional while in passive form it is done after a pre-determined quantity of soot has been accumulated.

In both conditions, the operator/driver has no hand in the process and the regeneration phase won't intervene the engine function. In most cases, thermal regeneration of diesel filters is employed, where the collected particulates are removed from the trap by oxidation to gaseous products, primarily to carbon dioxide (CO2) [28]. The thermal regeneration, schematically represented in Figure 13, is undoubtedly the cleanest and most attractive method of operating diesel filters.

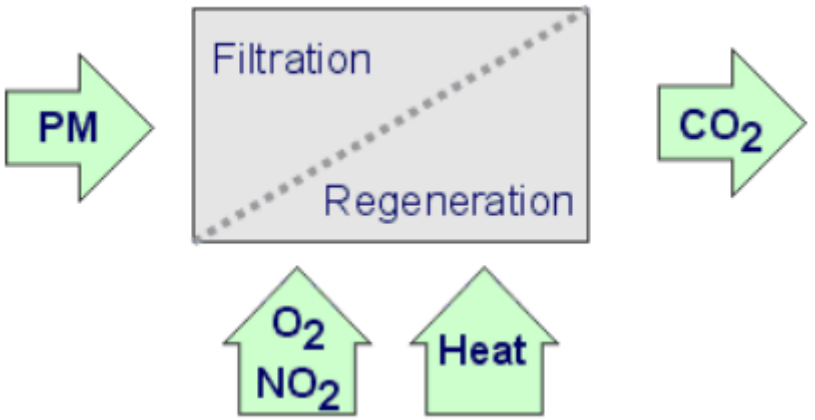

Figure 13. Schematic of Particulate Filter with Thermal Regeneration.

In order to provide a suitable condition for oxidation, the enough temperature and oxidative materials such as oxygen or nitrogen dioxide (or its precursors) are required. In passive regeneration, the heat source is the engine exhaust temperature and the filter is regenerated continuously during engine working time. Application of catalyst in filters, in order to decrease the oxidation temperature of trapped soot, is prevalent. In Active form of regeneration of DPF, the filter is dismantled from the system periodically and is heated up in order to burn the trapped particles.

4.1. Principle of Operation

The wall-flow monolith is the most common design of diesel particulate filter. It is an extruded, usually cylindrical ceramic structure with many small, parallel channels running in the axial direction. Indeed, the design of diesel filter monoliths has been derived from automotive, “flow-through” catalyst substrates [28].

There are, however, two important differences between these structures: (1) the wall-flow monoliths are made of ceramics of higher and more precisely controlled porosity, and (2) adjacent channels in the wall-flow filters are alternatively plugged at each end, thus forcing the gas to flow through the porous walls which act as a filter medium. The flow pattern difference between the flow-through and the wall-flow substrate is illustrated in figure 14.

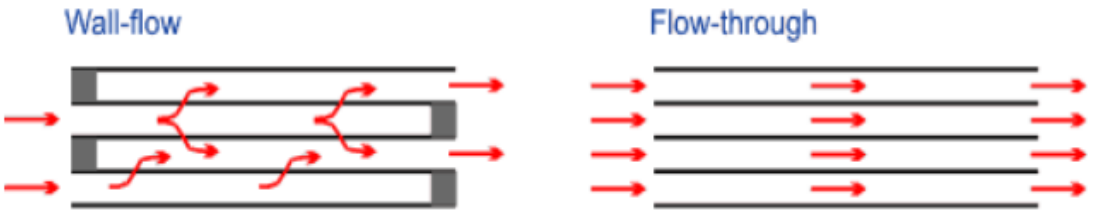

Figure 14. Wall-Flow and Flow-Through Substrates: Flow Pattern [28].

The wall-flow filter substrates are easily distinguished from catalyst substrates by the Characteristic checkerboard pattern created by the open and plugged cells at their inlet (as well as outlet) face, Figure 15. Regardless of the type of material or design, the filter media is ultimately packaged into steel container which is installed in the exhaust system of the vehicle. The DPF can be packaged as a stand-alone unit resembling a catalytic converter but usually of bigger size. In an alternative design, the DPF is placed inside a muffler. However, due to the good noise attenuation properties of many filter media, the filter unit can frequently replace the muffler without any additional provisions for noise attenuation. An example design of a diesel particulate filter is shown in figure16.

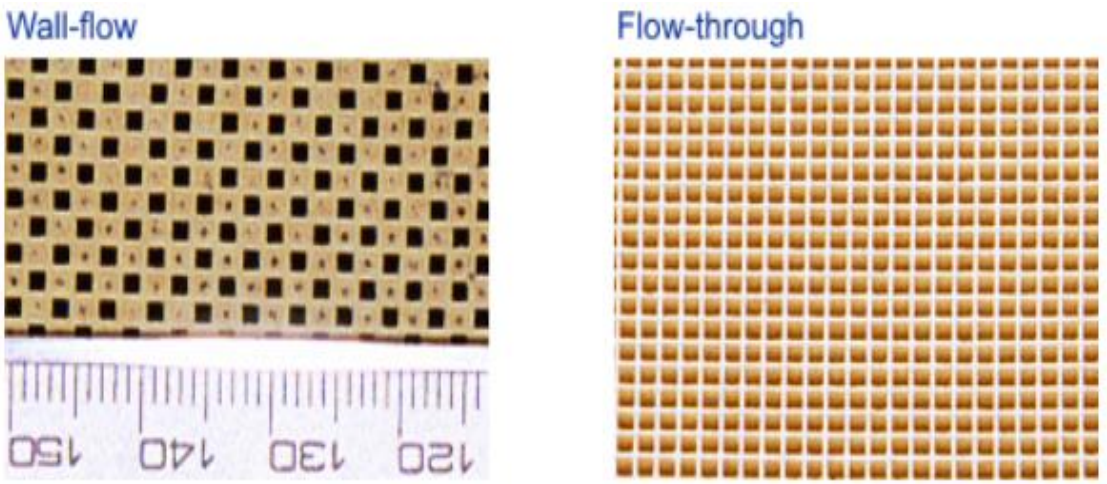

Figure 15. Wall-Flow and Flow-Through Substrates: Inlet Cell Pattern [28].

Figure16. Cutout of Catalyzed DPF for Urban Bus and Non-road Applications [28].

4.2. Filtration Mechanisms

The general mechanism of filtration is depicted in Figure17, from engine to exhaust, with schematic and real microscopic image.

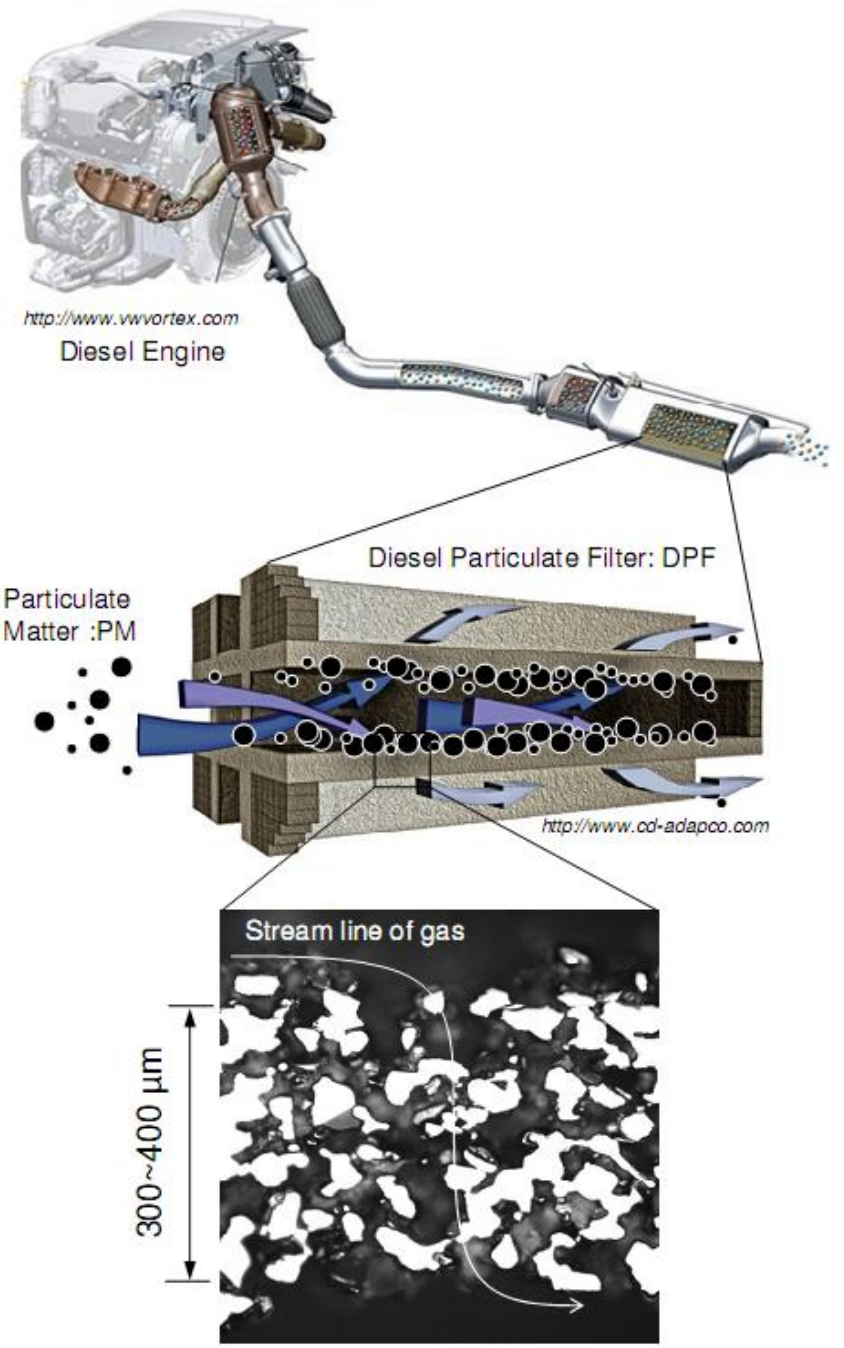

Figure17. Schematic diagram of Diesel Particulate Filter (DPF) [29].

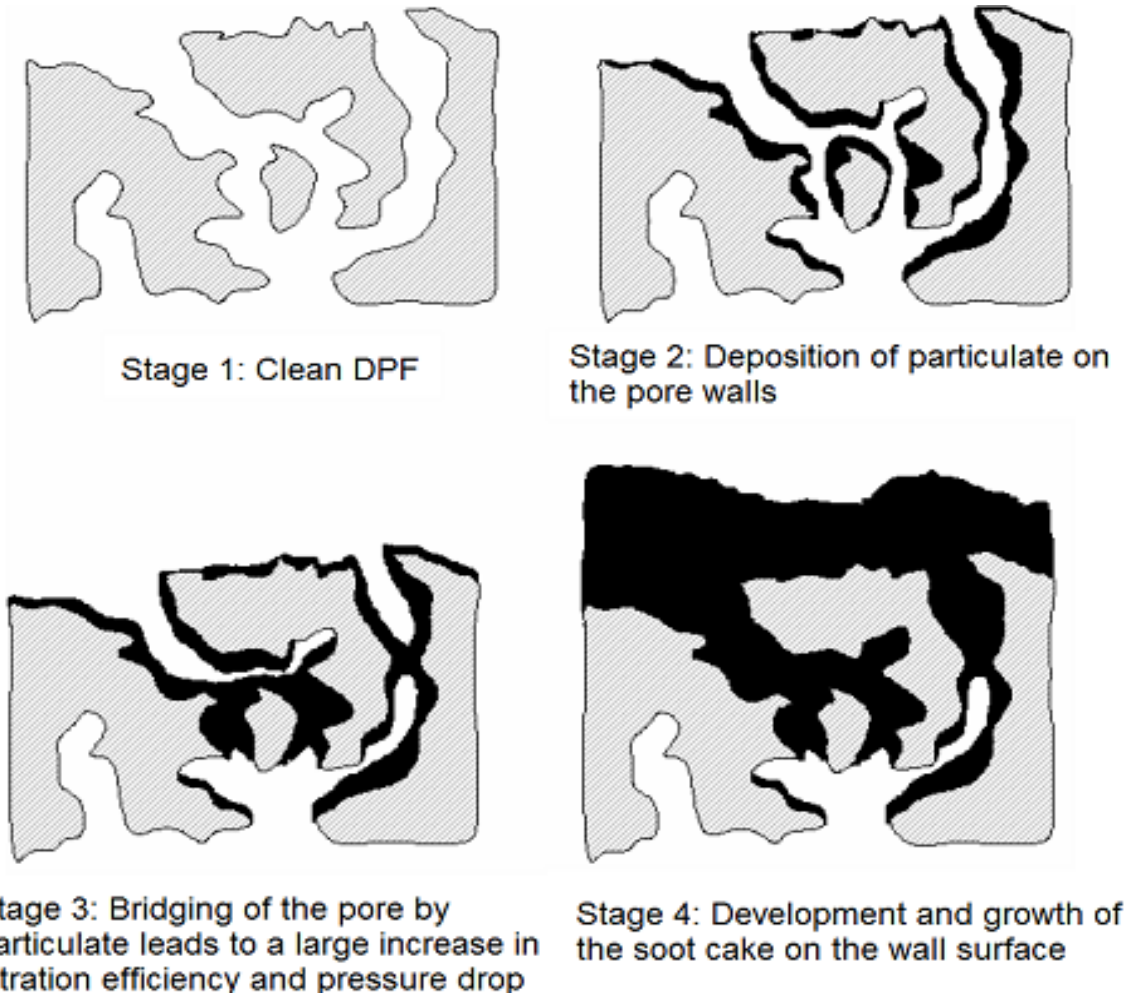

Figure 18. Conceptual model of PM trapping on the DPF wall [30].

As seen in picture, exhaust flow passes throw out the DPF and the soot particles are trapped inside the DPF pores and a cleaner flow goes out. For better illustration of the soot trapping stages inside the pores wall, a schematic of the four filtrations stages are presented in figure 18.

As explained in the picture, at first step the DPF is clean and all the pores are free to capture the PM. In second stage, the exhaust flow is passing throw the filter. As the flow passes the soot particles are trapped inside the pores and first pores are filled. The third phase is the result of continuing of the second stage. At third stages the soot

particles cover and block the pores so the incoming PM are trapped on the PM which are captured at an earlier time and soot cake formation begins at this stage and filtration efficiency is promoted. At the final stage, the soot cake starts to grow and expand on the wall surface and covers the filter. In order to connect this concept to pressure drop its better to refer to figure 19. As seen in figure 19, the pressure drop starts to boost from 1-2 stage. The larger pores of filter will host the PM at this stage. From stage 2-3 the pressure drop increase with large scope and the necking occurs on the surface pores. Further trapping in stage 3-4 shows that the pressure drop increase with constant slope and this trend indicates the soot cake layer forming and the filter wall is completely covered by soot.

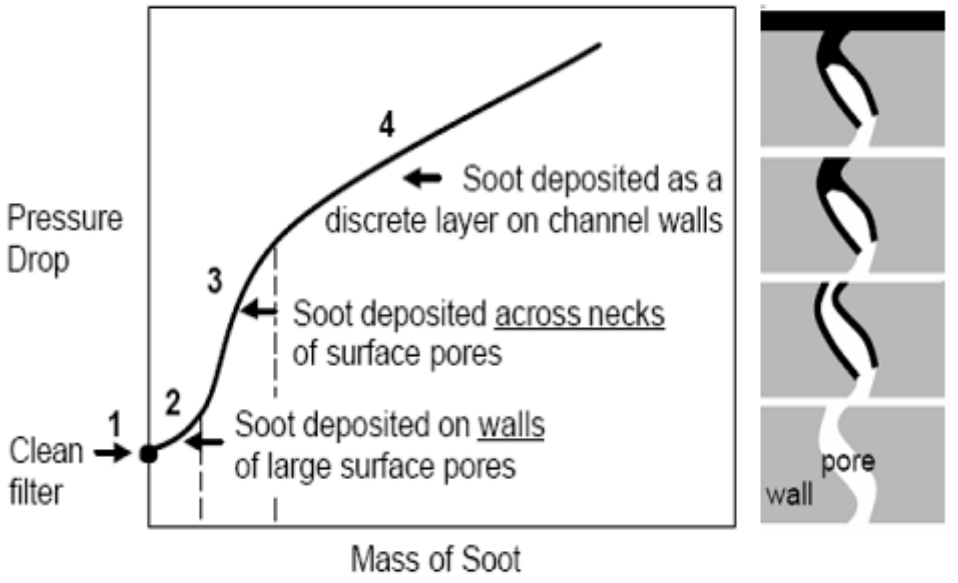

Figure 19. Conceptual model of pressure drop during particulate trapping [30].

The governing mechanism of filtration in any kind of DPF is based on based on separation of the gas-borne particles from the gas stream by deposition on a collecting surface [28]. This process

includes passing the gas flow within a porous barrier which blocks the PM particles [28]. DPFs are usually categorized by type of filtering barrier in two main groups: (1) deep-bed filters and (2) surface-type filters. In the first group the average pore size of DPF is larger than the average size of trapped PM and these trapped particles are affected by different force fields. These force can be related to velocity or concentration gradients in the gas. In second group the PM diameter is larger than the pore size of DPF. At this type of DPF, the PM are trapped by sieving. A schematic of these two types of DPF is shown in figure 20[28].

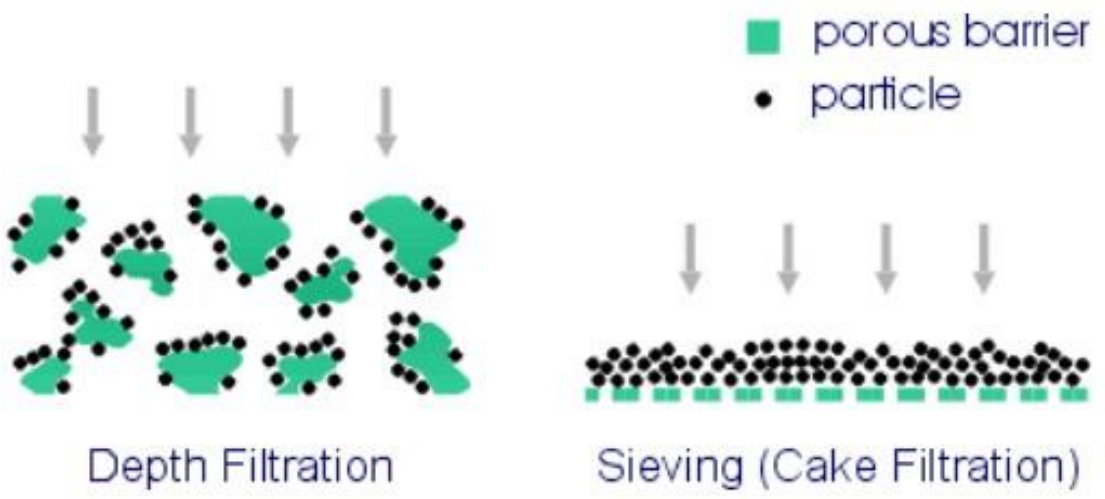

Figure 20. The two types of filtration mechanism [28].

The main filtration method is depth filtration which is applied in most of dust collection devices such as engine intake-air cleaners and DPF. The trapped PM on the surface of DPF, which is called soot cake layer or filtration cake, can act as a surface-type filter and this process is known as cake filtration. Although pure cake filtration is not seen among DPF in general, ceramic wall-flow monolith type DPFs may work through a combination of depth and surface

filtration [28]. At higher soot load, a filtration cake or a soot cake layer is formed on the surface of filter and then after the filtration capacity is reaches to its limit, a particulate layer starts covering the filtration surface. Diffusional deposition, inertial deposition and Flow-line interception are three controlling mechanisms of aerosol deposition. All these three mechanism are pictured in figure 21.

e big gray circle in the middle represents a collecting body in the filter media. The lines around the circle indicates the exhaust gas flow and the small black-red dots indicate PM traveling the gas

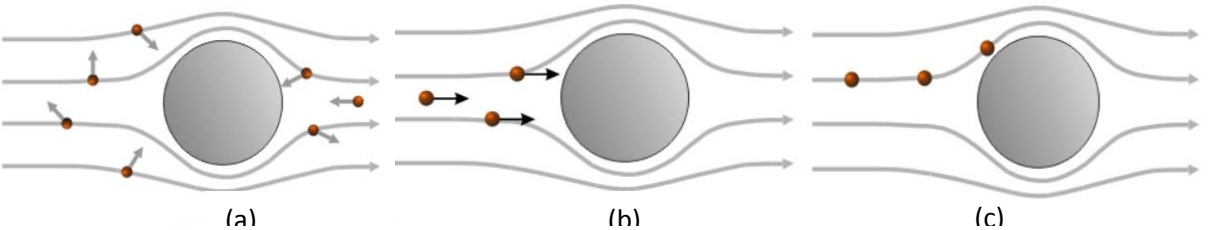

Figure 21. (a) Diffusional Deposition (b) Inertial Deposition(c) Flow-line

stream.

Diffusional deposition

As depicted in figure 21 (a), the Brownian movement governs the particulates especially those with size lower than 0.3 μm in diameter. The movement of particles along the stream is not uniform and they diffuse from the gas toward the surface of collecting body.

Inertial Deposition

In figure 21 (b), the inertial deposition is depicted. This mechanism turns more significant as the PM size increases. On approaching the collecting body, particles carried along by the gas stream tend

to follow the stream but may strike the obstruction because of their inertia.

Flow-line interception

This mechanism, as pictured in figure 21 (c), may occur as a flow stream crosses through one particle radius of the collecting body and after that ,the particle moves along the streamline and collides the body and may be trapped without being affected by Brownian diffusion or inertia.

Another term related to DPF is expressed as the filtration efficiency (E). It's defined as is the mass ratio of the particulate matter collected on the filter to the particulate matter entering the filter. Another term is penetration which is the mass ratio of the particulates escaping to the particulates entering the filter. Both of these mentioned terms are expressed as percentages. The depth filtration is characterized by somewhat lower filtration efficiency and lower pressure drop than the cake filtration. The trapped PM on deep-bed filter may be also re-entrained by the gas causing a decrease in the observed filtration efficiency. This process is known as blow-*off* of trapped PM. This trend occurs at high exhaust flow rates. The cake filtration is characterized by higher filtration efficiency and relatively high pressure drop. The pressure drop steadily increases with the increase of filtration cake thickness as mentioned before.

CHAPTER 3

EXPERIMENTAL SYSTEMS AND METHODOLOGY

3.1. Technical data

3.1. 1. Fuel samples

Fuel properties has significant effect on engine function and emission and they can alter the PM of diesel engine directly, by changing the chemical composition of PM, and indirectly, by changing the engine function. In order to know the chemical and physical characteristics of the applied fuels in the study the samples of commercial diesel, Palm biodiesel (PB100) and 10% and 20 % blends of these fuels (PB10, PB20) were tested. Features such as viscosity, density, calorific value, acid value, cloud point, flash point, pour point, Iodine value and other features were tested and the results were calculated and compared. The results are discussed in later chapters.

3.1.2. Engine

The engine which is used in this project is a single cylinder agricultural diesel engine, four stroke 638 cm3 displacements, and direct injection with a rated output of 8.8 kW at 2400 rpm. The compression ratio of engine cylinder is 16.1 per 1. The fuel injection pressure was approximately 19.6 MPa. More technical data is shown in figure 22.

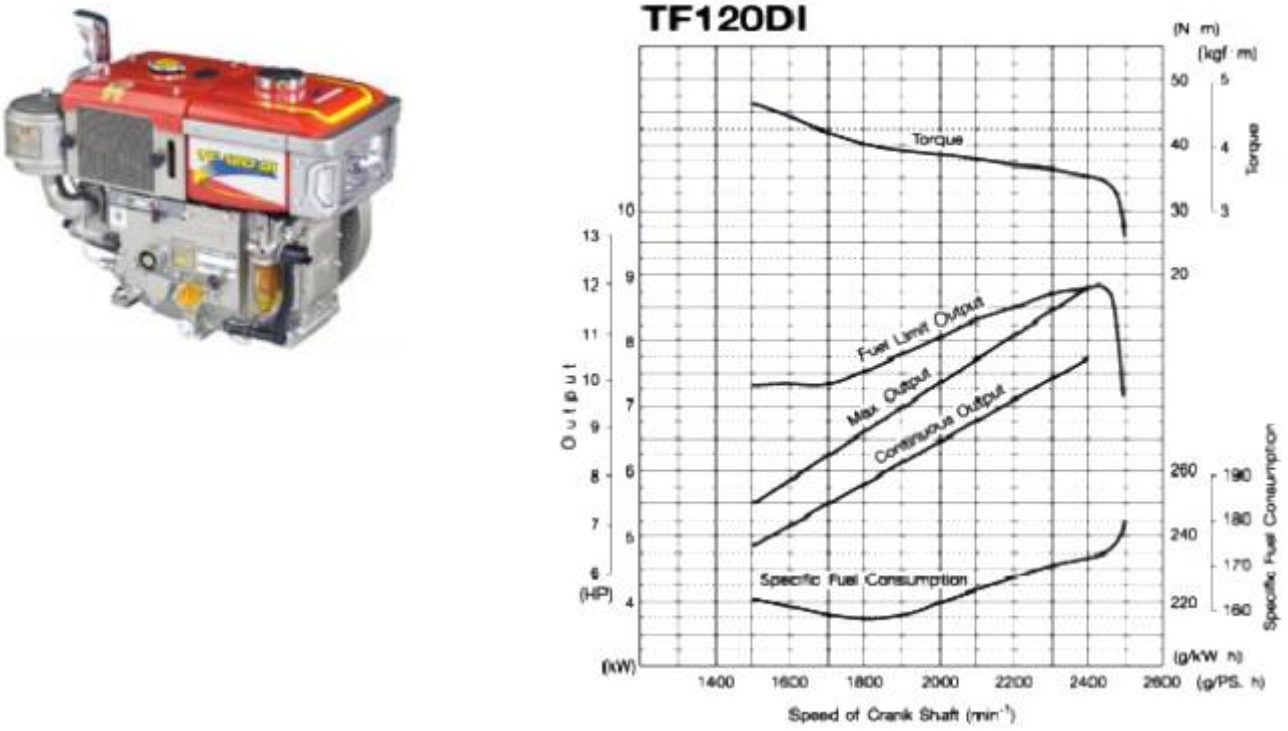

Figure 22. Yanmar single cylinder Diesel engine and specification.

3.1.3. Dynamometer

The dynamometer which is used is Tokyo Planet 60 KW. This is an Eddy current type dynamometer which is cooled by water recirculation. The mechanism of dynamometer is depicted in figure 23. When electric current flows in a ring-type coil which is fixed to the casing, an electromagnetic path shown in red is generated. And, a brake force is obtained by the eddy current created when the electromagnetic path is cut by a gear teeth shaped rotor. The heat generated in this process is carried away by cooling water flowing in the casing. The torque which acts to rotate the casing by the brake force is detected by a load cell.

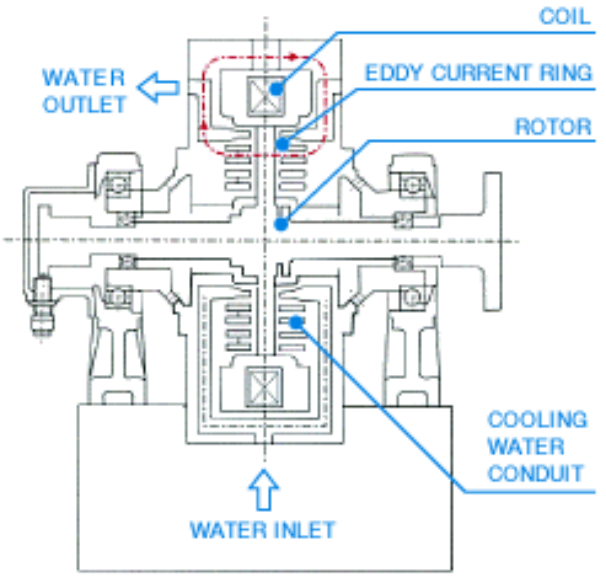

Figure 23. The schematic picture of ED current dynamometer.

3. 1. 4. Thermo gravimeter analyze

Thermo gravimetric analysis or thermal gravimetric analysis (TGA) is a method of thermal analysis in which changes in physical and chemical properties of materials are measured as a function of increasing temperature (with constant heating rate), or as a function of time (with constant temperature and/or constant mass loss). TGA can provide information about physical phenomena, such as second-order phase transitions, including vaporization, sublimation, absorption, adsorption, and desorption. Likewise, TGA can provide information about chemical phenomena including chemisorption's, desolvation (especially dehydration), decomposition, and solid-gas reactions (e.g., oxidation or reduction). One of the common use of TGA is the study of oxidation of different materials in various temperatures and soot oxidation studies are prevalent among the studies. The test can be done in inert environment with application of inert gases such Helium and Argon or in active condition with

utilization of air or pure oxygen. Also analyze can be done isothermal, in which the temperature remains constant, and non-isothermal, which temperature changes as time passes. A picture of the TGA device is shown in figure 24. The TGA device which is used is TGA /SDTA 85 METLLER TOLEDO.

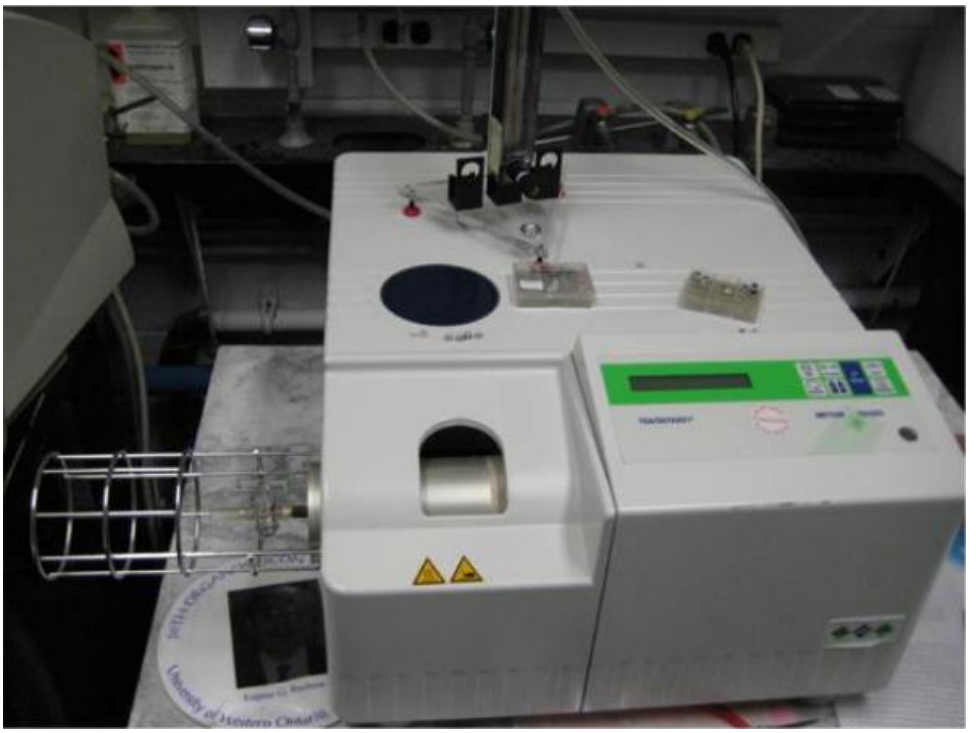

Figure 24. Thermo gravimetric analyses device.

At this phase, the soot samples from diesel and biodiesel were collected and tested under isothermal condition. The samples were tested at 5 different temperatures including 400,450,500,550 and 600 ^{o}C. The nitrogen gas is used as an inert gas and then after reaching to the desired temperature, the oxygen is introduced into the system. Same procedure is repeated in second time but this time air was applied instead of oxygen.

3. 1. 5. Diesel Particulate Filter (DPF) and

A sample of conventional DPF used as the filtration device .The technical data and the picture of the DPF is shown in table 1 and figure 25.

Table 1. The specification of conventional diesel particulate filter

Type Ceramics cordierite	Type Ceramics cordierite
Wall thickness 300 micrometer	Wall thickness 300 micrometer
Porosity (%) 52%	Porosity (%) 52%
Average pore size 10 - 50 micrometer	Average pore size 10 - 50 micrometer
Cell density (cpsi) 300	Cell density (cpsi) 300

(a)

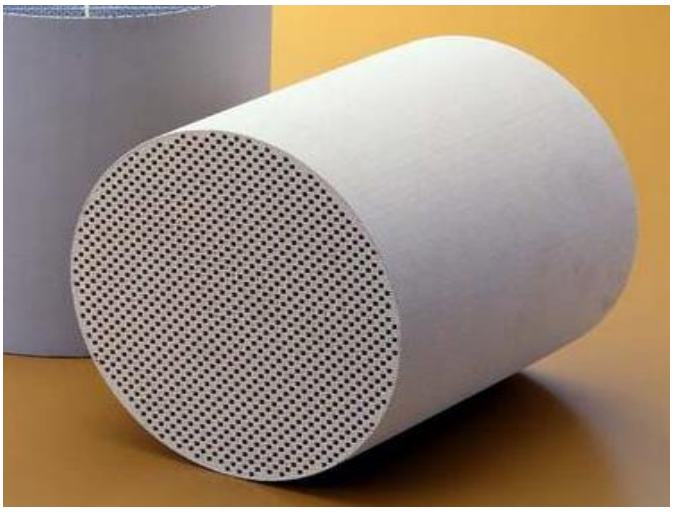

(b)

Figure 25. (a). A cut of DPF sample which is used in this project.(b) the conventional DPF .

A sample of DPF with 10 cm diameter and 1cm thickness is cut form the DPF filter and attached to a ceramic container in order to be used for trapping and regeneration.

3. 1. 6. High temperature furnace

In order to provide enough temperature for soot oxidation inside the DPF, a high temperature furnace is applied at this study. The picture and the technical data of the furnace is shown in figure 26 and in appendix.

Figure 26. The high temperature furnace.

3. 1.7. Differential pressure sensor

In order to measure the pressure drop ,which is cused by soot filtraion mechanism of DPF, its requiered to use Differential pressure sensor, to measure the pressure before and after DPF. The picture of pressure sensor and its technical data is illustrated in figure 27. As the pressure drop increases in trapping phase, it can be indication of soot compiling on the DPF and as it decreases in

regeneration phase, its indication soot oxidation and thus PM reduction, which leads to an easier air flow passage.

Characteristic	Symbol	Min	Typ	Max	Unit
Pressure Range	P_{cp}	0	-	50	kPa
Supply Voltage	V_s	4.75	5	5.25	V_{dc}
Supply Current	I_0	-	7	10	mA_{dc}
Minimum Pressure Offset @ V_s = 5.0 Volts (0 - 85 °C)	V_{off}	0.088	0.2	0.313	V_{dc}
Full Scale Output @ V_s = 5.0 Volts (0 - 85 °C)	V_{FSO}	4.587	4.7	4.813	V_{dc}
Full Scale Span @ V_s = 5.0 Volts (0 - 85 °C)	V_{FSS}	-	0.5	-	V_{dc}
Accuracy (0 - 85 °C)	-	-	-	± 2.5	$\%V_{FSS}$
Sensitivity	V/P	-	90	-	mV/kPa
Response Time	t_R	-	1	-	ms
Output Source Current at Full Scale Output	I_{0+}	-	0.1	-	mA_{dc}
Warm - Up Time	-	-	20	-	ms
Offset Stability	-	-	± 0.5	-	$\%V_{FSS}$

Figure 27. Technical data of pressure sensor.

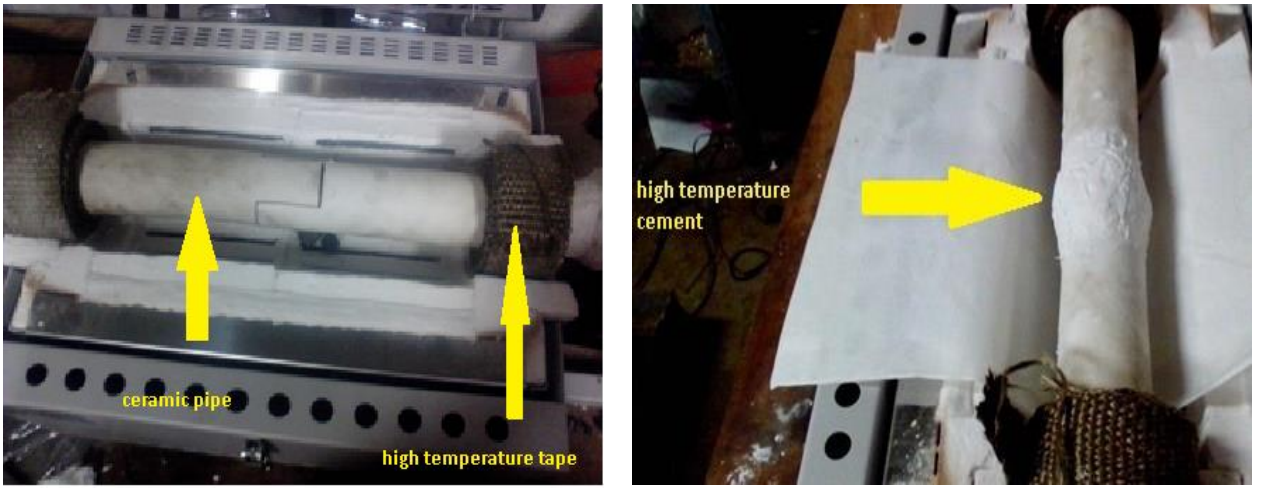

Figure 28. The ceramic inside the tube furnace.

3.1.8. The ceramic pipe

Figure 28 shows the ceramic pipes which is held inside the high temperature tube furnace. The two ceramic pipes are joined each other by high temperature cement. The DPF holder also is made by same Ceramic and is attached at one end of one of the pipes. Both ends of the pipes which are located at both ends of furnace are sealed by high temperature tapes in order to seal them from thermal loss.

3.1.9. Data acquisition system

In order to monitor the collected data from thermocouple and pressure sensors and plot them with time, a Data acquisition system (DAQ) National instrument 6009 is used .This system operates with national instruments Lab VIEW program. The picture of the DQ card is shown in figure 29 and the technical data of program and DAQ card is presented in the appendix. The pressure signal from

differential pressure sensor is 0 - 5V and pressure drop range is 0-45kPa and signal from thermocouple is 0 -10 V.

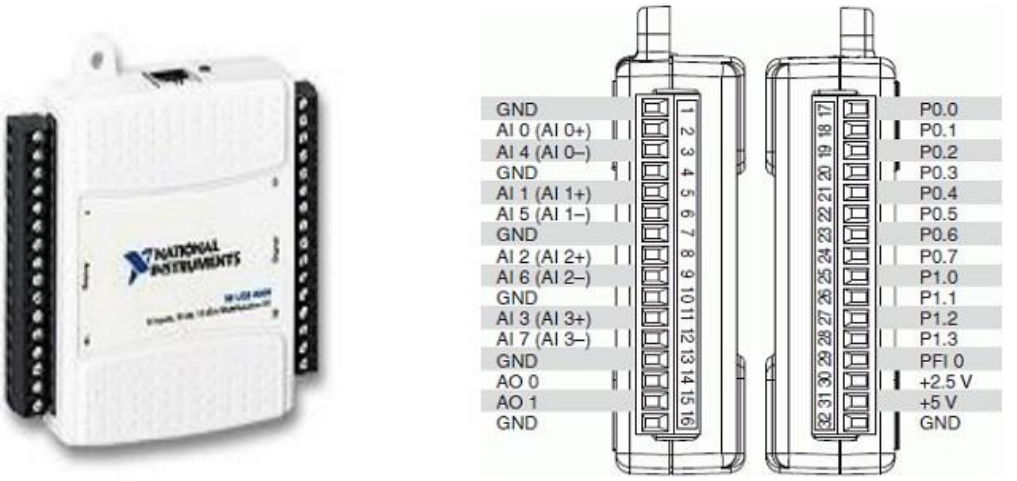

Figure29. Data acquisition system (DAQ) National instrument 6009.

3.1.10. Thermocouple

A type K thermocouple, which is tuned 0-10 V to DAQ with a transmitter TM – 004 controller is used. The head of thermocouple is put as close as possible to DPF, in order to measure the temperature DPF surrounding inside the ceramic pipe. A picture of thermocouple and its controller is shown in figure 30. The technical data of controller is presented in appendix.

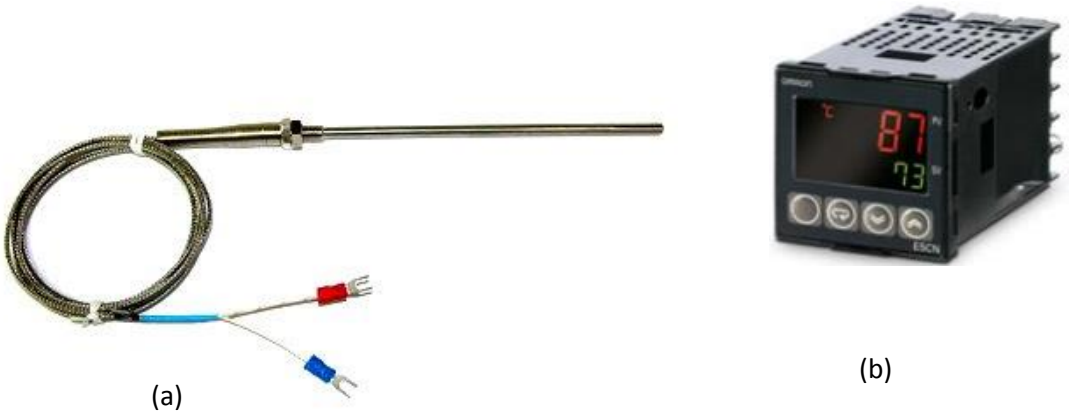

(a) (b)

Figure 30. (a) K type thermocouple. (b) Temperature controller.

3.2. Methodology

3.2.1. Soot collection

In order to know the oxidation reactivity and other chemical features of the exhaust soot, it's required to collect the soot from the engine exhaust. To do so, the engine and dynamometer was set at 80 % load and 2400 RPM. A metallic filter is used to trap the exhaust PM. after running the engine for a while, the collected soot were moved to a sealed container and sent to the lab for TGA and CHN test. This process is done for both diesel and biodiesel fuel, and for biodiesel the exhaust filter was changed in order to prevent the mixing up the diesel and biodiesel PM. The schematic of the soot collection apparatuses is illustrated in figure 31.

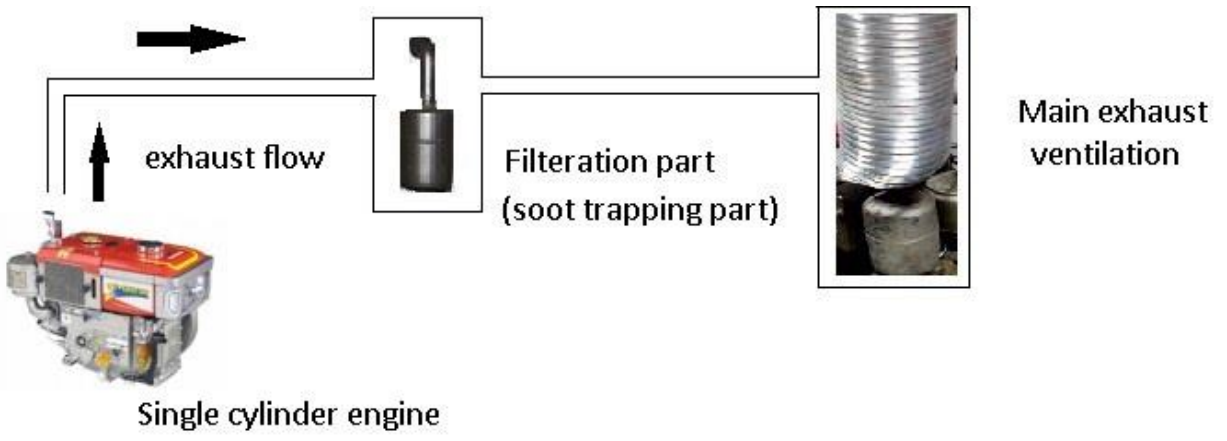

Figure 31. The soot collection apparatus.

3.2.2. Soot filtration and regeneration test

To measure the filtration of the DPF and effect of diesel and biodiesel fuel it, the engine and dynamometer was set on similar condition of soot collection test and then the filtration was commenced. A vacuum pump was used to suck the exhaust from

the engine and guide it through the ceramic pipe and DPF. At first step, the furnace was set to 200 ◦C and the pump was started. Then the temperature was increased up to 600 ◦C while the pump was working in order to know the permeability of the DPF. Then this process was repeated for diesel and biodiesel fuel and trapping was measured by pressure drop. A picture of the real system and a schematic of the apparatuses is depicted in figure 32.

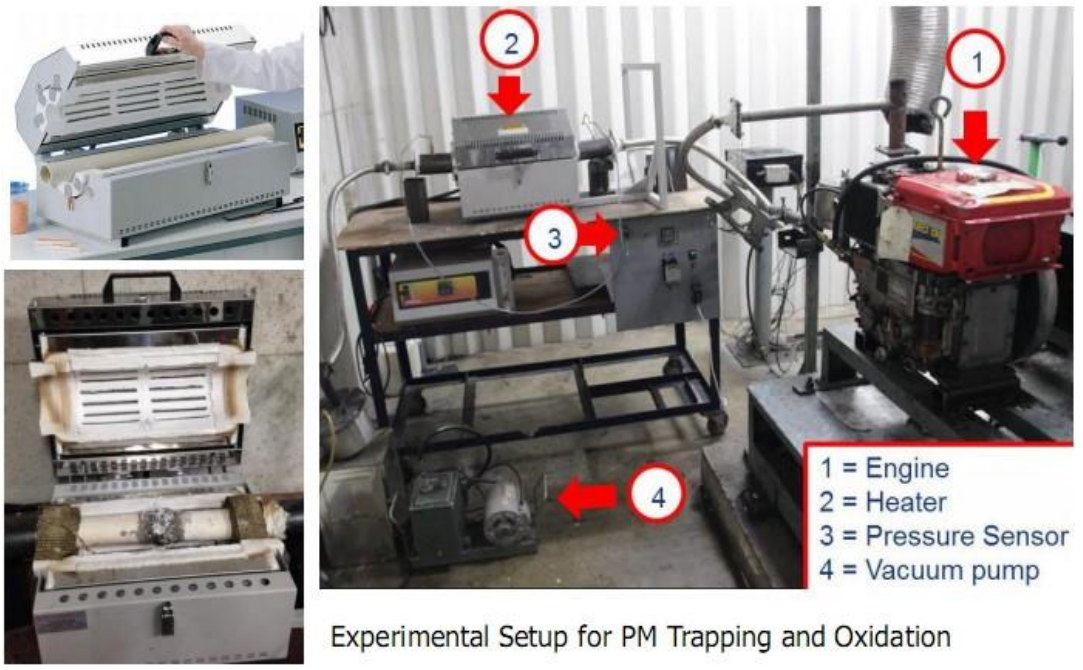

(a)

Figure 32.(b)the schematic of testing.

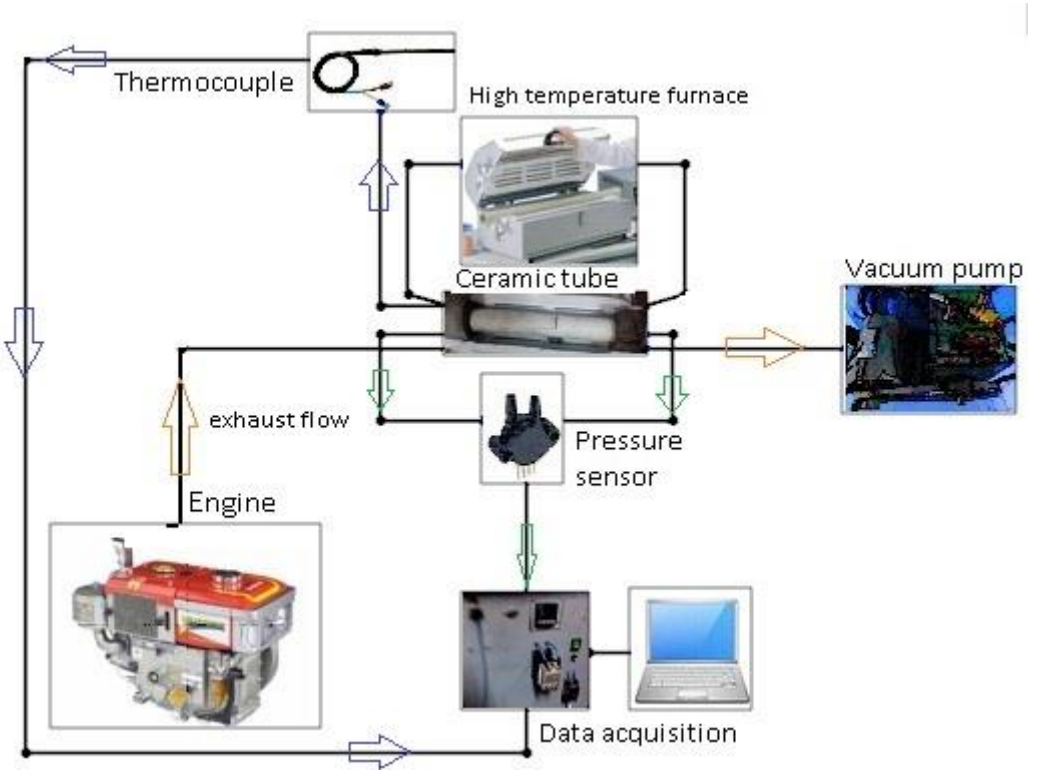

(b)

Figure 32. (a) , (1) The engine (2) high temperature tube furnace (3) Pressure and temperature sensor (DAQ system) (4) vacuum pump.

CHAPTER 4

RESULTS AND DISCUSSION

4.1. Fuel chemical and physical properties

The physical and chemical features of fuel play key role in engine function. These features can alter injection, ignition delay, engine wear and emission. Such changes can alter PM composition and morphology directly, by changing the PM composition, or indirectly, with changes in combustion behavior. At this chapter several physical and chemical characteristics of diesel and palm biodiesel and blends of 10 and 20 % of it was tested. The viscosity, density, pour point, cloud point, flash point, oxidation stability, acid value, and water content and calorific value of all samples were tested. Gas chromatography test and iodine value test for biodiesel and CHN test for all pure samples is done in order to make the relation between physical and chemical properties of fuel more clear. At this chapter, each tested feature is discussed and its effects on PM formation and composition is explained.

4.1.2. Chemical Properties

Fatty Acid Composition

It's said that the most important element, which alters the chemical and also chemical features of biodiesel is the fatty acid composition. The performance of an ester (biodiesel) as diesel fuel depends on the chemical composition of the ester, particularly on the length of carbon chain and the degree of saturation (and unsaturation) of fatty acid molecules. Properties such as cetane number, cold flow

characteristics and oxidation stability are affected by the composition according to earlier researches [4]. There are three main types of fatty acids including saturated, unsaturated and polyunsaturated. Vegetable oils with higher degree of unsaturation tend to have higher freezing point, poor flow characteristic and can become solid. The composition of palm biodiesel was analyzed by gas chromatography, Shimadzu GC-2010. The results of PB100 are shown in the table 2. For the PB100 the results show that Palmitic acid, which is a saturated acid, is dominant (38.77%) and Oleic acid percentage is (37.612%).

Table 2. Fatty acid composition of palm biodiesel.

Lauric acid methyl ester C12:0	0.8735
Myristic acid methyl ester C14:0	0.036
Palmitic acid methyl ester C16:0	38.7725
Stearic acid methyl ester C18:0	3.158
Oleic acid methyl ester C18:1	37.612
Linoleic acid methyl ester C18:2	8.783
Linoleic acid methyl ester C18:3	0.1625
Arachidic acid methyl ester C20:0	0.2125
Eicosenoic acide methyl ester C20:1	0.092
Molecular weight	240

Oxidation Stability

One of the key features of fuels is the oxidation stability which can help to determine the quality of fuel. It can also affect some of fuel physical and chemical properties such as density, viscosity and water content. Biodiesel s usually have 10% more oxygen in their

structure which can result in poor oxidation stability. The fuel composition can also affect the oxidation stability. Studies show the vegetable oils which are rich in poly unsaturated acids can weaken oxidation stability [4]. Oxidation occurs in the forms of aldehydes, alcohols, carboxylic acids, insoluble gum and sediments in biodiesel [4]. Another affecting factor is temperature, which controls oxidation rate. The thermal oxidation is determined by the rate of oxidation reaction at high temperature when the fuel is exposed to air and as the temperature increase the rate of oxidation increases [4].The fuel samples were tested by Ranciment instrument method by heating up to 110 °C and a schematic of Ranciment and picture of device is shown in figure 33. The results of the test are shown in figure 34. The results show the induction period (IP) of PB100 is (22.86 h) and for commercial diesel is (158.21h) which is significantly higher than the rest of fuel samples. This can be due to various percentages of saturated fatty acids in biodiesel [4]. The induction period decreases by increase of unsaturated fatty acids [4] so stability improves by blending. This can be due to reduction of unsaturated components and amount of oxygen. Storage time and condition, pressure of the air, heat, trace of metal and exposure of light also can affect oxidation of biofuels [4]. Oxidation cannot be avoided completely but can be postponed by applying antioxidant [4].

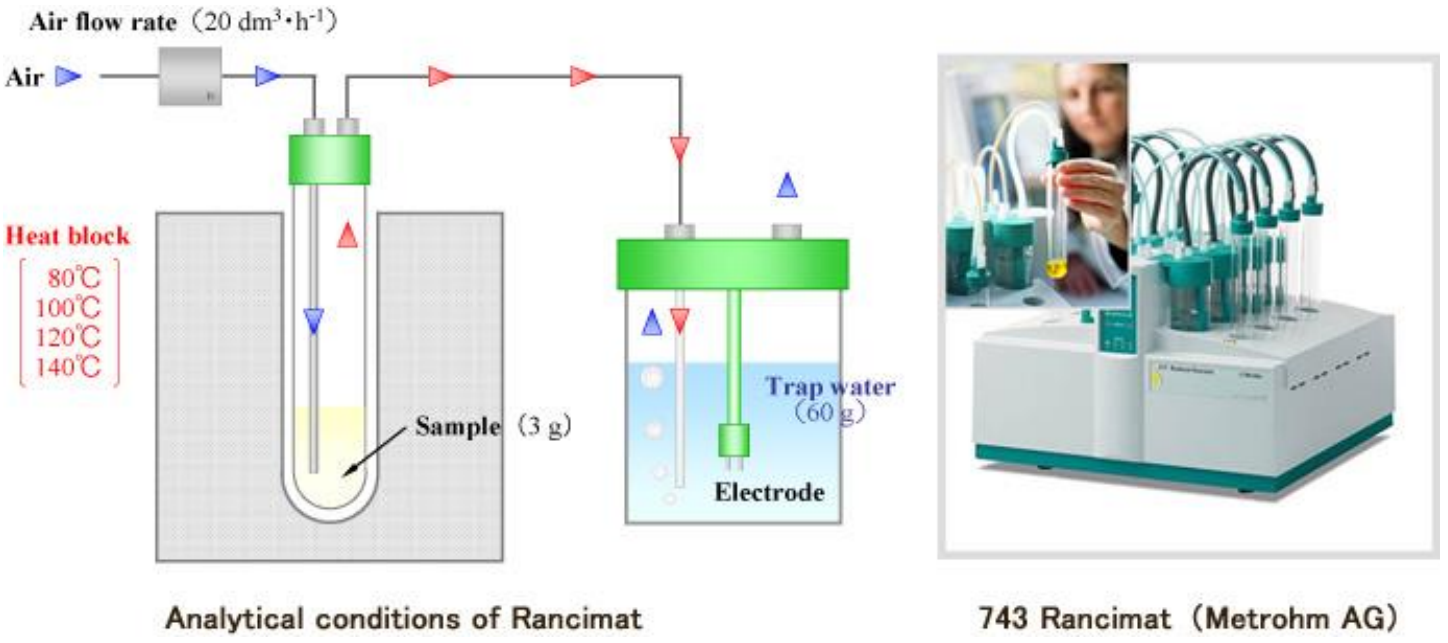

Figure 33. Schematic of Ranciment mechanism and the device.

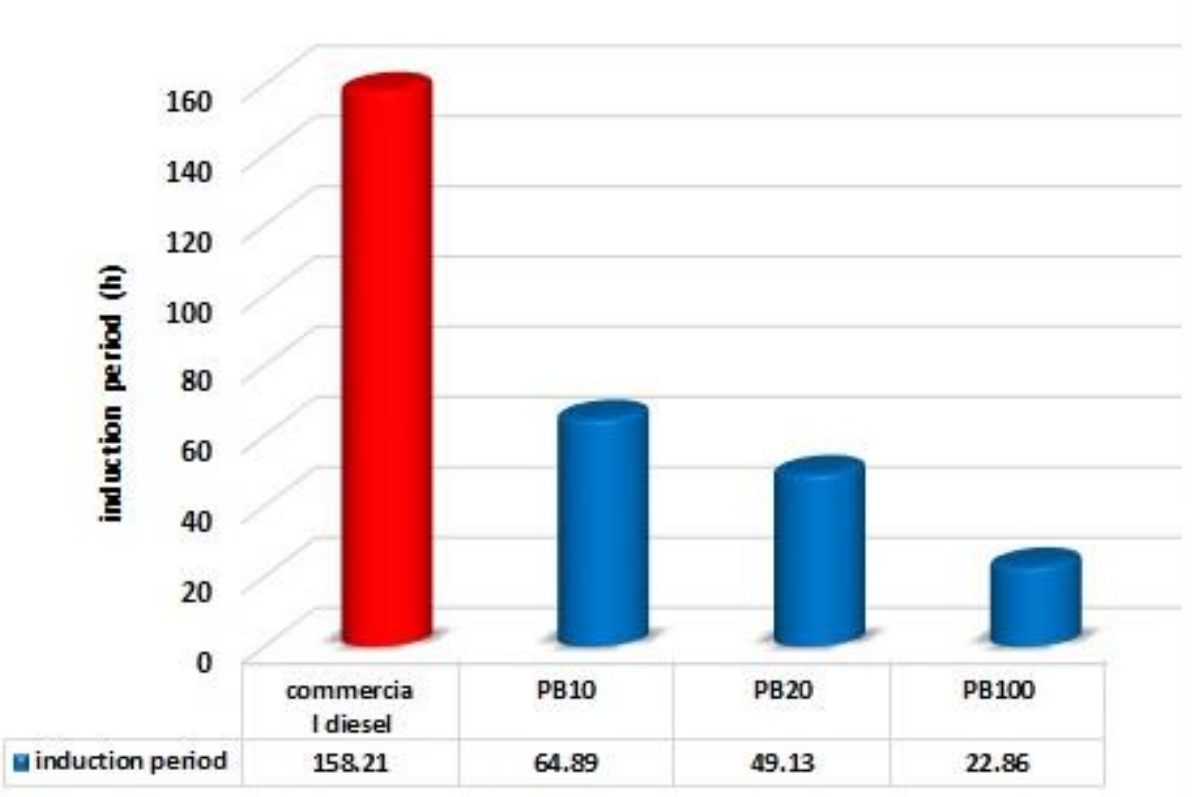

Figure 34. Comparison of induction period of different fuel samples.

Iodine Value

The iodine value is a measure of unsaturation of fats and oils. Iodine value is expressed in terms of number of centigrams of iodine absorbed per gram sample of biodiesel. The iodine is introduced in biodiesel reacts with the double bonds within the fatty acid structure. Therefore, higher the percentage of unsaturation, the larger will be the iodine value. The iodine numbers can influence oxidation stability and the polymerization of glycerides. This can lead to the formation of deposits formed in diesel engines injectors [8]. The results shows that the Iodine value for palm biodiesel 51.5 (g I_2/100 g). Studies shows Increase of Iodine value can be related to increase of PM and NOx emission [20].

Elemental analyze

Elemental analysis on carbon, hydrogen and nitrogen is the most essential - and in many cases the only investigation performed to characterize and prove the elemental composition of an organic sample. Numerous compounds include no additional elements besides C, H and N. Both diesel and palm biodiesel samples were subjected to CHN analyze and the results are presented in table 3.

Table 3. Results of elemental analyze of PB100 and Commercial diesel.

Fuel sample mass	C%	H%	O%	Molecular formula
PB100	78.322	13.281	8.3749	$C_{15.2635}H_{29.479}O_{1.706}$
Commercial diesel	85.177	14.047	0.776	$C_{16.165}H_{32.006}$

As seen in table, the diesel fuel has higher amount of carbon in comparison with the palm biodiesel. This can affect the calorific value of fuel and thus fuel consumption and thus PM formation. The A/F ratio of biodiesel is A/F=5.75 and for diesel A/F=7.2 for one unite of the each fuel sample.

Calorific Value

Heat released in a chemical reaction can be determined experimentally by using an adiabatic calorimeter. Thereaction must proceed without any side reactions and sufficiently fast that the heat exchange with the surroundings is negligible. The heat of combustion can be most conveniently measured using an adiabatic bomb calorimeter. In such calorimeter, the combustion reaction occurs in a closed container under constant volume (“bomb”). The bomb is immersed in a weighted quantity of water and surrounded by an adiabatic shield that serves as a heat insulator. Continuous stirring ensures that heat is distributed evenly in the calorimeter. The bomb and the water bath, which are in direct thermal contact,

constitute an adiabatic bomb calorimeter. In this experiment the heat of combustion of an organic compound is determined using a commercial Parr adiabatic bomb calorimeter. The heat of combustion is directly related to important quantities such as the internal energy and enthalpy of a chemical reaction.A schematic of bomb calorimeter is depicted in figure 35 and the results are plotted in figure 36. As seen in figure 34, the highest calorific value belongs to the commercial diesel (45.8 MJ/kg).

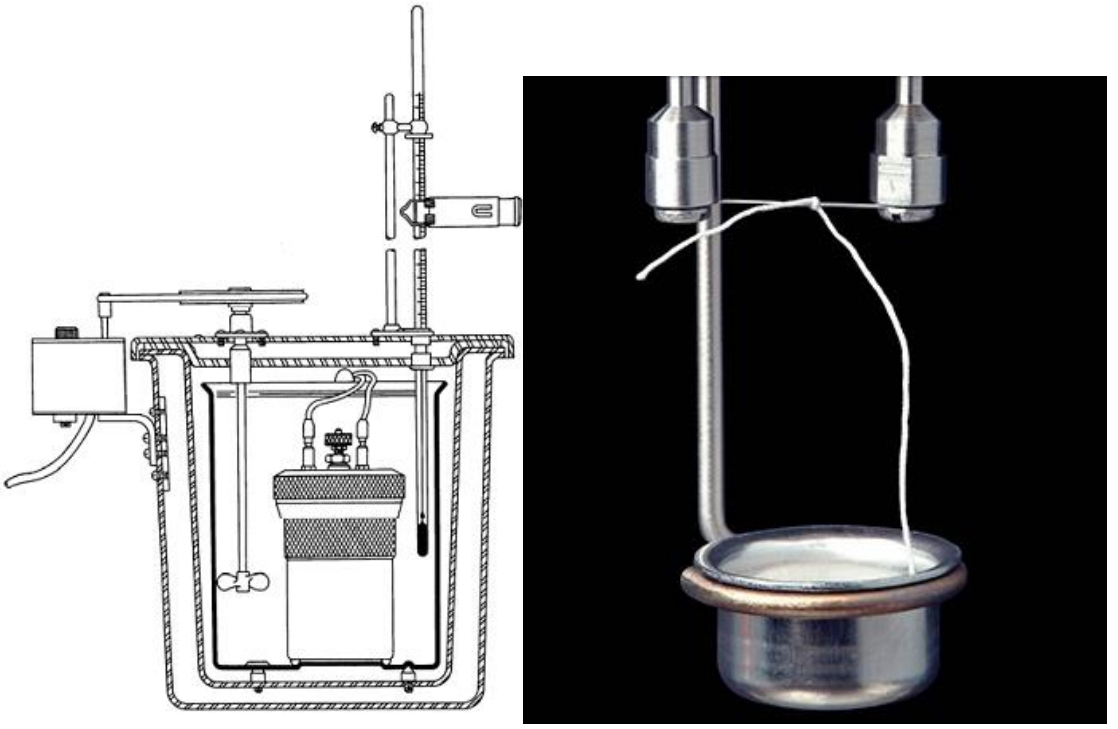

Figure 35.schematic of bomb calorimeter and a test sample container with wire.

As percentage of biofuel in the blends increases the calorific value decreases. The calorific value of pure biofuels PB100, is the lowest among the rest. The calorific value of PB100 is 39.900 (MJ/kg). Such trend is also seen among the blend of palm. The main reason for these phenomena is related to the elemental composition of the

fuels. The lower calorific value of biofuels in comparison with commercial diesel is due to the higher oxygen content of the biofuels [4]. The diesel fuel is made up a mixture of various hydrocarbon molecules and contains very little oxygen percentage (0.3%) but for the biofuels the amount of oxygen is about 10% of the fuel composition. The increase of oxygen in fuel structure results in reduction of carbon and hydrogen in the fuel and this will result in lower energy content. Oxygen is ballast in fuel and carbon and hydrogen are source of thermal energy. It can also verify this explanation that biofuels have higher concentration of oxygen and lower Concentration of carbon in comparison with commercial diesel. Presence of more oxygen can also cause lower stoichiometric air/fuel ratio. This can ensure improvement of combustion.

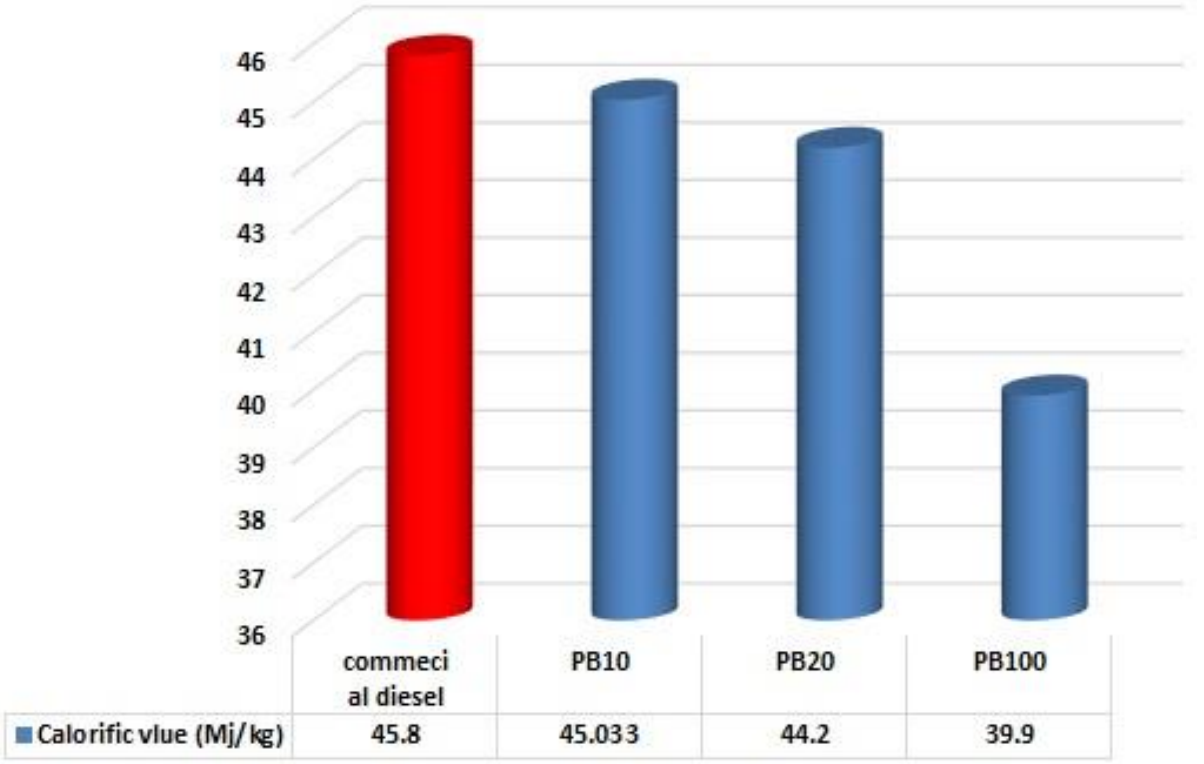

Figure 36. Results of calorific value of each fuel sample from calorimeter bomb.

Acid Value

Acid value is defined as the number of milligrams of potassium hydroxide required to neutralize the free fatty acid presents in 1 gram of the sample. The main acid component could possibly be found in biodiesel are: 1-residual mineral acids from production process. 2-residual free fatty acids from hydrolysis process or post-hydrolysis process of esters. 3-oxidation byproducts in forms of other organic acids [4]. Acid value can also be an indication of lubricity degradation and higher acid value can cause fuel system deposits and reduces the lifelong of fuel pump [4]. Acid value test is done by typical titration method with KOH solvent and Metro-ohm acid value meter device was used to determine the acid value and each test is done thrice for each sample. The test was done in

typical titration method with a potassium hydroxide (KOH) solvent with known concentration. Phenolphthalein is used as a color indicator. The results are shown in figure 37and the device is shown in figure 38. As the concentration of biodiesel increases in the fuel samples the acid value increases. The acid value of PB100 is (0.115 mg of KOH). The lowest value is for commercial diesel. The main reason for this trend can be due to unsaturation level of the biofuels, the fuels containing unsaturated fatty acid with double bonded long chain hydrocarbons have more susceptibility to oxidation and oxidation has an inverse relation with acid value [4]. Increase of acid value can be considered as a result of oxidation of the fuel which may lead to gum and sludge formation besides corrosion. Temperature can also affect the acid value. If fuel is exposed to high temperature oxidation

Figure 38. The acid value measurement device.

occurs due to higher rate of reaction of fuel molecules with oxygen in the air, resulting in increase of acid value [4].

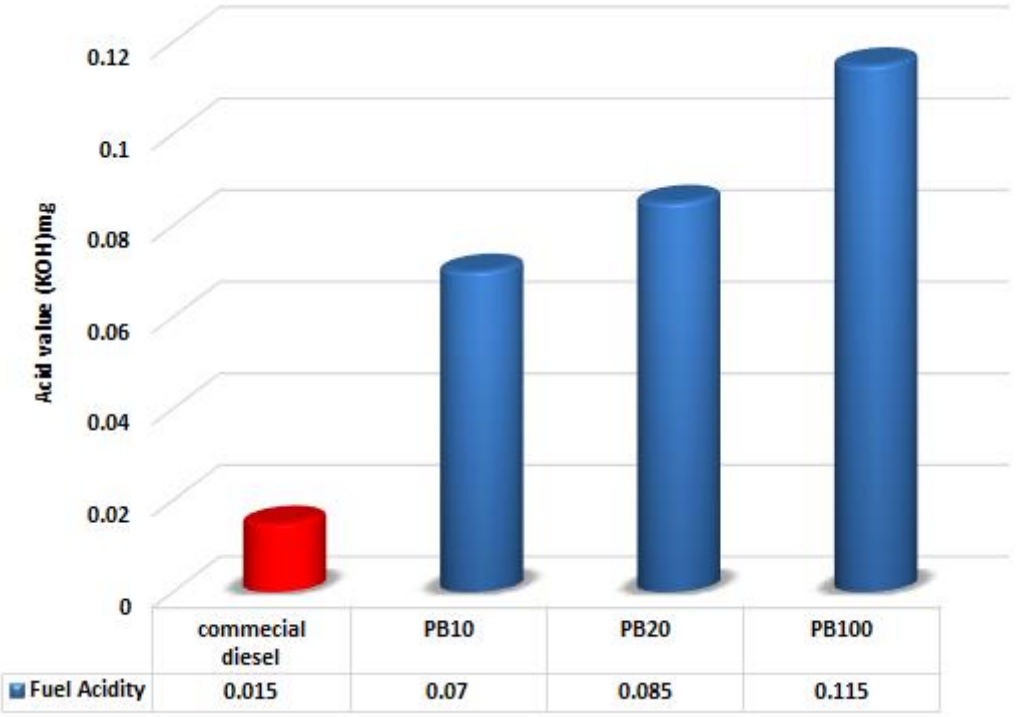

Figure 37. Results of acid value test of the biodiesel fuels, blends of biodiesel fuel and commercial diesel.

Water Content

Water content is an indication of purity of fuel. The absorbed moisture in biodiesel increases the free fatty acid concentration which can cause corrosion of metallic parts of engine and fuel system [4]. Biodiesel fuels are much more hygroscopic than diesel oil fuels which absorbs moister .This can also cause troubles in handling the fuel and storage. Water in biodiesel can also facilitate the growth of microbiological components and formation of sediments [4]. Water and sediments can shorten the fuel filter life or plug fuel filter, which lead to engine fuel starvation. The results of water content test are shown in figure 39. By decreasing of biodiesel in blends reduces level of water content. Storage time and condition and oxidation stability can be one of the affecting factors for this trend. The water content generally increases with storage time and initiation of oxidation instability which is governed by peroxide chain mechanism [4]. Another reason can be related to the fatty acid composition of biodiesel s. Decomposition of unsaturated fatty acids can extend formation of primary oxidation products such as hydro-peroxide which results in increase of water content [4]. The production process and feed stock of biodiesel s also can be considered as an affecting factor. Studies shows biodiesel samples

with lower M/H (methanol/hydrogen) ratio have higher water content [4].

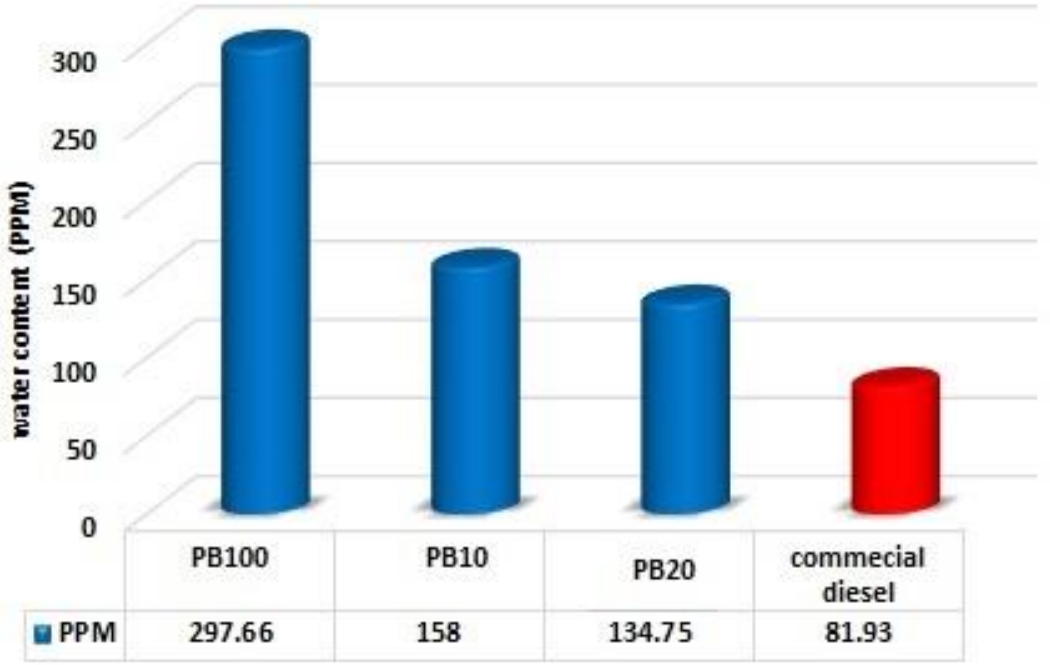

Figure 39. Results of water content analyze of fuel samples.

4.1.3. Physical Properties

Density

The density of biofuels is one of the main concerns in widely utilization of them. Density is defined as the ratio of mass per unit of volume of an object. The higher density, the tighter particles are packed in the substance. Fuel injection devices work on a volumetric system, hence a higher density for biodiesel s results in delivery of slightly greater mass of fuel into combustion chamber higher density of biodiesel can also cause more PM production due to deterioration of fuel atomization [4]. The results of density test are shown in the figure 40. The highest value is for PB100 (0.8748 g/cm3). This trend

can be connected to saturation level of fatty acids. Saturation of fatty acids can increase the density. Since the fuels containing shorter chain length of hydrocarbon and more saturated fatty acid have more prone to be crystalized, therefore cause of reduction of its volume and consequently increase of density [4]. Palm biodiesel is saturated and this can be a reason of having higher density. As the amount of biodiesel decrease in fuel samples by blending with commercial diesel, the density decreases. The density of vegetable oil based methyl esters from different source, reported in many studies is very close to each other [4]. The density also is affected by oxidation of fuel. The density has direct relation with fuels molecular weight, thus oxidation of fuels can increase the mass of fuel by producing by products and sediment, and therefore it results in increase of density [4]. The higher density can cause more fuel consumption due to advance of injection [4]. In comparison between PB100 and commercial diesel we can refer to molecular weight of the fuels. As molecular weight of biodiesel s is higher in comparison with commercial diesel and therefore their density should be higher.

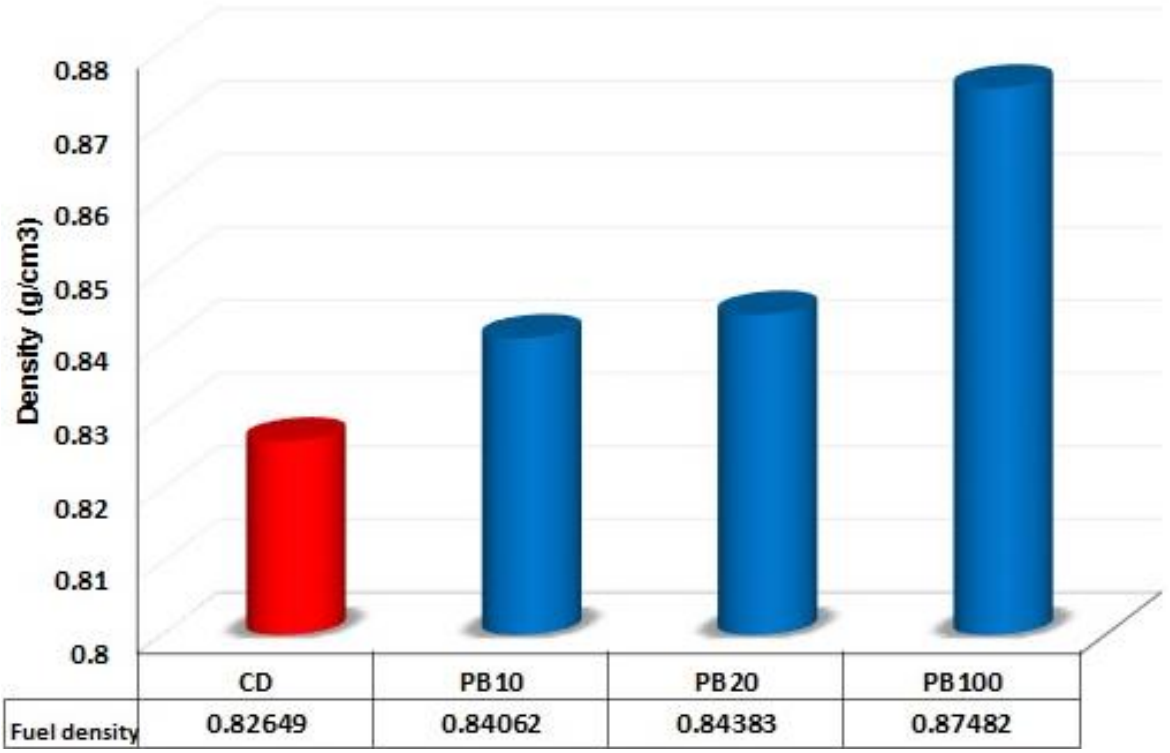

Figure 40. Density of biodiesel fuel, blends of biodiesel fuel samples and commercial diesel.

Viscosity

Viscosity is defined as the resistance of a liquid to flow. Viscosity is one of the main obstacles in widely usages of biodiesel fuels hence fuels with higher viscosity, impact engine durability negatively. Soot deposit formation on injectors (injector clogging), certain components of piston (rings), inlet and outlet valves and fuel filter plugging are common problems caused by high viscos fuels [4]. The higher amount of biodiesel concentration partly dissolves the lubricant, resulting in increased friction of engine moving parts. Fuel atomization and volatility is also affected by viscosity. Higher viscosity results in poorer fuel atomization which leads to combustion deterioration [4]. Low temperature flow problems, cold engine start up and ignition delay are caused by higher viscosity [4].

The results of viscosity test are shown in figure 41. The viscosity values of pure biodiesel is higher than the blends and commercial diesel. By blending with the commercial diesel and decrease of biodiesel percentage the viscosity value decreases. As the proportion of saturated fatty acids with longer carbon chain increases, it can increase the viscosity [4]. Viscosity is reduced by blending with commercial diesel due to decrease of unsaturation level. Oxidation stability of fuels is another important parameter. Oxidation of fuel leads to formation of free fatty acids, double bounds isomerization, saturation and production of higher molecular weight and thus can increase the viscosity [4].Hence biofuels are more oxygenated; blending can reduce the amount of oxygen and consequently improvement of oxidation stability and viscosity.

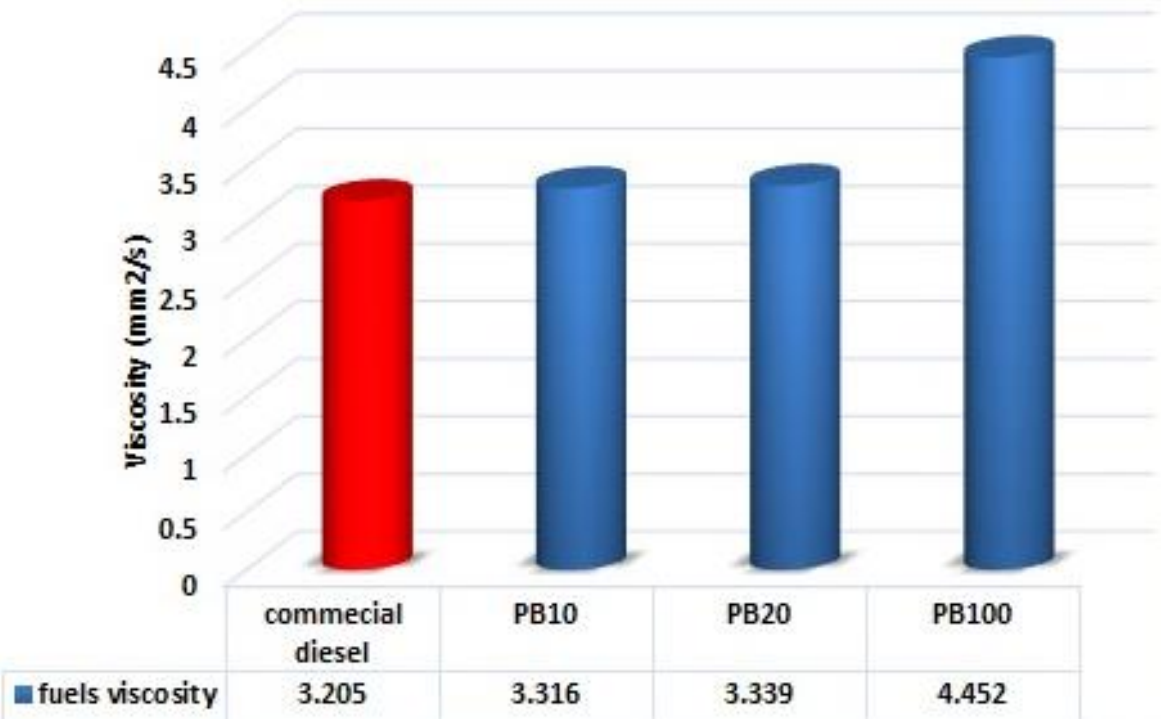

Figure 41. Results of viscosity test at 40 °C biodiesel fuels, blends of biodiesel samples and commercial diesel.

Flash Point

Flash point is another important property of any fuel. It is defined as the temperature at which a fuel can provide a combustible mixture with air while exposed to fame or spark. The results of flash point test are shown in figure 42. The lowest flash point is for commercial diesel (65.5 °C) and highest belong PB100 (198 °C) which are more than 3 times .Flash point has an inverse relation with fuel's volatility [4]. Flash point is an important factor to consider in handling, storage and safety of fuels [4]. As amount of biofuel increase in the blends the flash point increase too. This ensures the safety of biofuels. The reason for this trend can be related to fuel composition of the samples. Diesel consists of hundreds of different hydro carbon components but biofuels are usually consisting of 4 to 5 major

components that will boil at the same temperature [4]. Flash point can also decrease by oxidation and storage time [4].

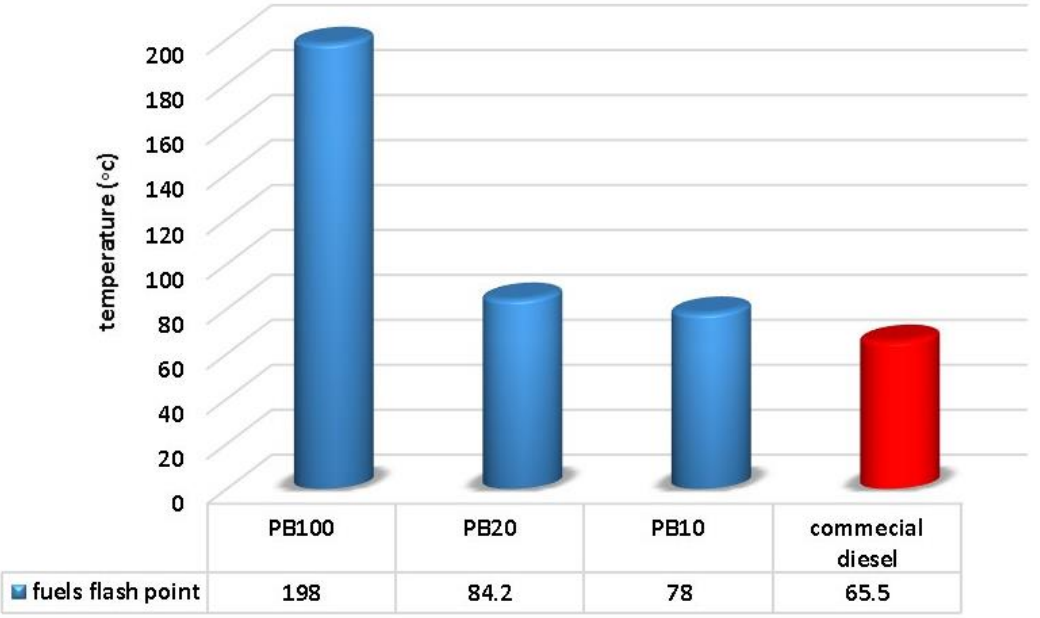

Figure 42. Flash point of biodiesel fuels, blends of biodiesel fuels and commercial diesel.

Cloud Point

The cloud point is an important feature of fuels in winter application and it is defined as the temperature at which first crystals starts to form in the fuel. The results of cloud point test are shown in figure 43. Among the samples, PB100 has the highest cloud point (15.2 °C).The saturation of fatty acids increases the cloud point [4]. The cloud point is most commonly used as a measure of low-

temperature operability of the fuels. Typically the cloud point of biofuels is higher than the cloud point of conventional diesel due to more saturated compositions. As amount of biofuel decreases in the samples the cloud point becomes lower and closer to the commercial diesel which make the application of the biodiesel blends easier especially in cold climates.

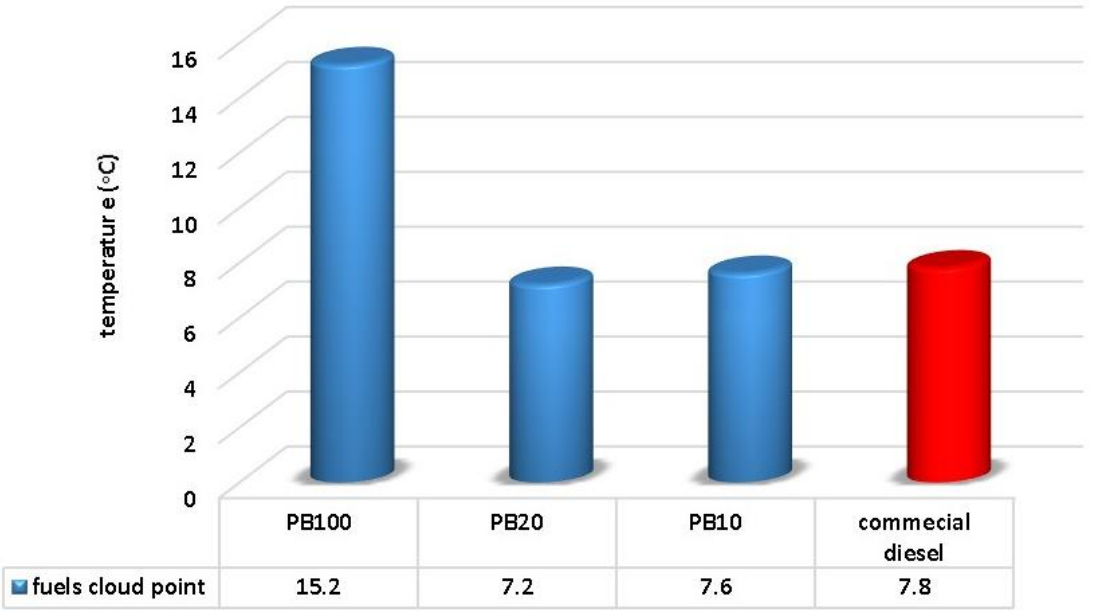

Figure 43. Results of cloud point test biodiesel fuels, blends of biodiesel fuels and commercial diesel.

Pour Point

Pour point is the lowest temperature that the fuel is observed to flow and it's an important property in winter use and cold climate application. The results of the pour point test are shown in figure 44. The highest pour point belongs to PB100 (12.1 °C). By blending with commercial diesel pour point falls drastically. The lowest value (−11.2 °C) belongs to commercial diesel which can cope with cold climate flow problems. Biodiesel has poor flow trend at low temperature. The structural properties of biodiesel that can affect the pour point are degree of unsaturation, chain length and degree of branching [4]. The blends also show improve in pour point. Fuels with higher pour point will face difficulty in cold climates [4]. The higher level of saturation increases the pour point. As palm biodiesel has higher level of saturation it shows higher pour point.

Figure 44. Results of pour point test for biodiesel fuels, blends of biodiesel fuels and commercial diesel.

Distillation

The distillation test of both fuels were done in an earlier study at our lab. The results are shown in figure 45. It was clearly observed that diesel fuel could be distilled in wide range of temperature due to complexity of molecules whereas biodiesel is quite pure molecule which results in its distillation at almost a constant temperature. The vaporize temperature of biodiesel is higher than that of diesel. Therefore, the high temperature inside the biodiesel engine combustion chamber will be reduced. Although biodiesel has a higher distillation temperature, the lower boiling point of biodiesel enhances the probability of the lower soot or tar formed from the heavy HC compounds. The standards of fuels in Thailand for diesel and biodiesel is mentioned in the appendix.

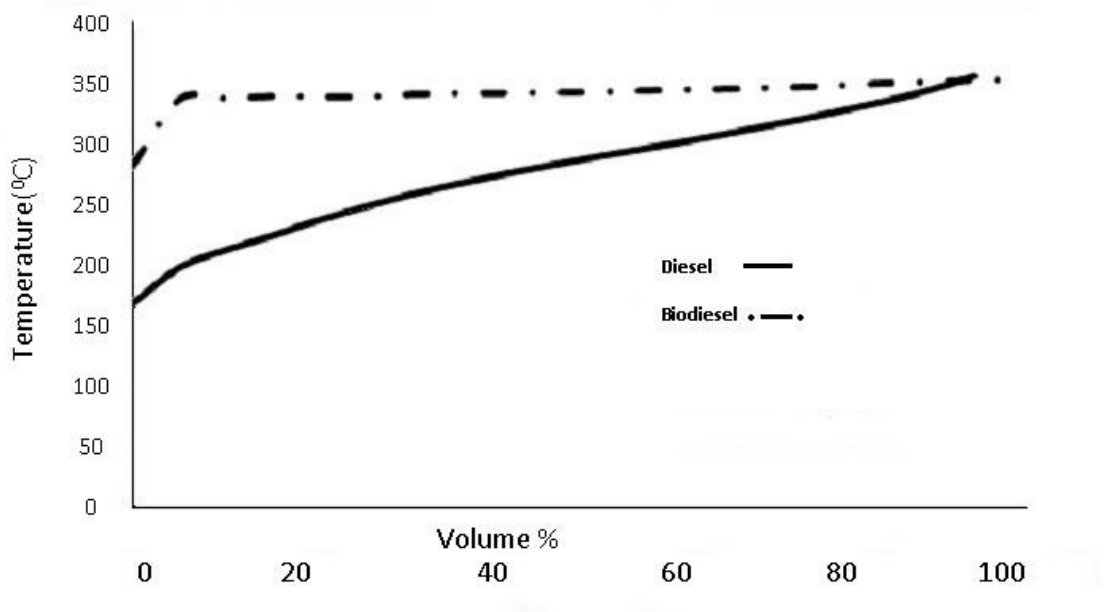

Figure 45. Distillation of conventional and biodiesel test fuel.

The overall summary of test and the effect of each feature is presented in table 4.

Table 4. The summary of fuel analyze

Feature	Diesel	Biodiesel	effect
Oxidation Stability	158.21 hr	22.86 hr	Altering the fuel composition Fuel life reduction Affecting viscosity and density in negative way
Calorific Value	45.8 (MJ)	39.9 (Mj)	Fuel generated power Fuel consumption
Acid Value	0.015 (mg of KOH)	0.115 (mg of KOH)	lubricity degradation and wear
Water Content	81.93 PPM	297.66 PPM	Affects the purity of fuel Reduces the calorific value Increases the acidity in biodiesel Increases corrosion Negative impact of fuel filtration
Density	0.82649 (g/cm3)	0.87482(g/cm3)	More fuel injection Deterioration of fuel atomization
Viscosity	3.205	4.452	Injector clogging Advance of injection Poor atomization Ignition delay
Flash Point	65.5 (°C)	198(°C)	Fuel safety Poor atomization
Cloud Point	7.8 (°C)	15.2 °C	Engine winter work and cold start
Pour Point	−11.2(°C)	12.1 (°C)	Engine winter work and cold start

4.2. Oxidation kinetics and chemical features

TGA with pure oxygen and Air

Thermo gravimetric analyze (TGA), as mentioned before, is the most prevalent method to determine samples reactivity trend, especially oxidation sensitivity. This gives a more transparent picture about the soot oxidation kinetics in presence of different oxidants. In order to have reference, the carbon black N330 is also tested to compare with soot samples.

The overall results of the TGA test of diesel and biodiesel soot samples, mass conversion and with oxygen in figure 46 and 47 and air in figure 48 and 49 is depicted for diesel and biodiesel soot. For both fuel samples, with both air and oxygen, increase of temperature results in increase of mass conversion due to presence of more thermal energy for oxidation process. In comparison between the soot samples, biodiesel shows faster and higher percentage of conversion in comparison with diesel in all temperatures and in presence of air and pure oxidation. The graphs can be divided into two main parts, isothermal and non-isothermal. The non-isothermal part starts from the initiation of the experiment until reaching the desired temperature. At this phase, only nitrogen is used and there is not any oxidant, so the only change in mass of the PM sample is due to vaporization of VOF and humidity. The differences in conversion percentage and amount of it is affected by the heating time and the elemental compositions of the soot samples from diesel and biodiesel. As isothermal stage begins, the

oxygen at first TGA test and air at second TGA test is introduced the mass conversion changes to mass oxidation and the mass percentage reduces as time passes. The oxidation becomes more complete for both soot samples as temperature increases and at 550 and 600 ^{0}C all soot samples are burnt. In all temperatures, as seen in figure 47 and 48 biodiesel shows better and faster conversion trend in comparison with diesel. In comparison between air and oxygen, the mass conversion and oxidation is much faster in presence of pure oxygen due to abundance of oxygen.

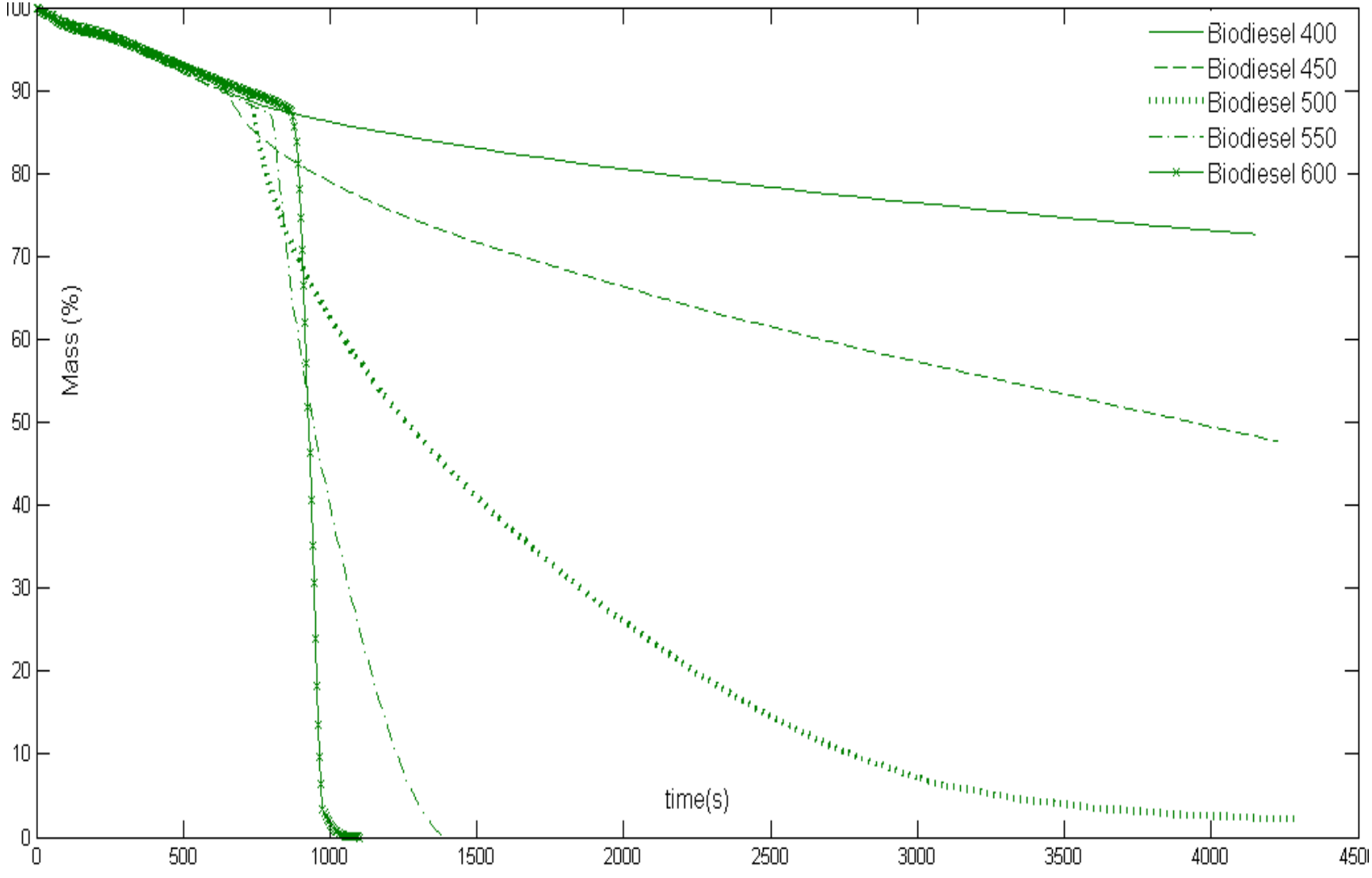

Figure 46. The isothermal TGA test of biodiesel samples with pure oxygen.

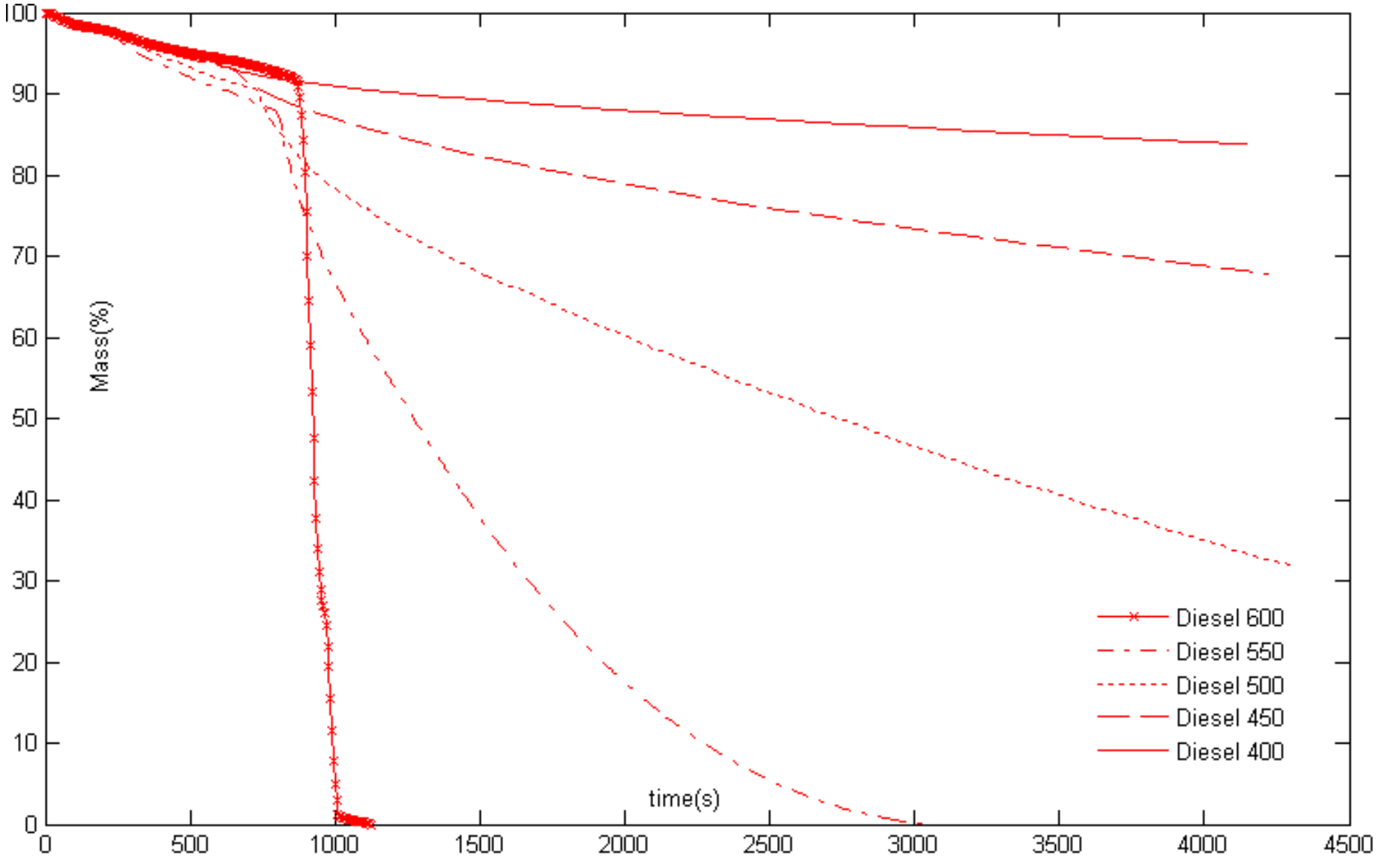

Figure 47. The isothermal TGA test of diesel samples with pure oxygen.

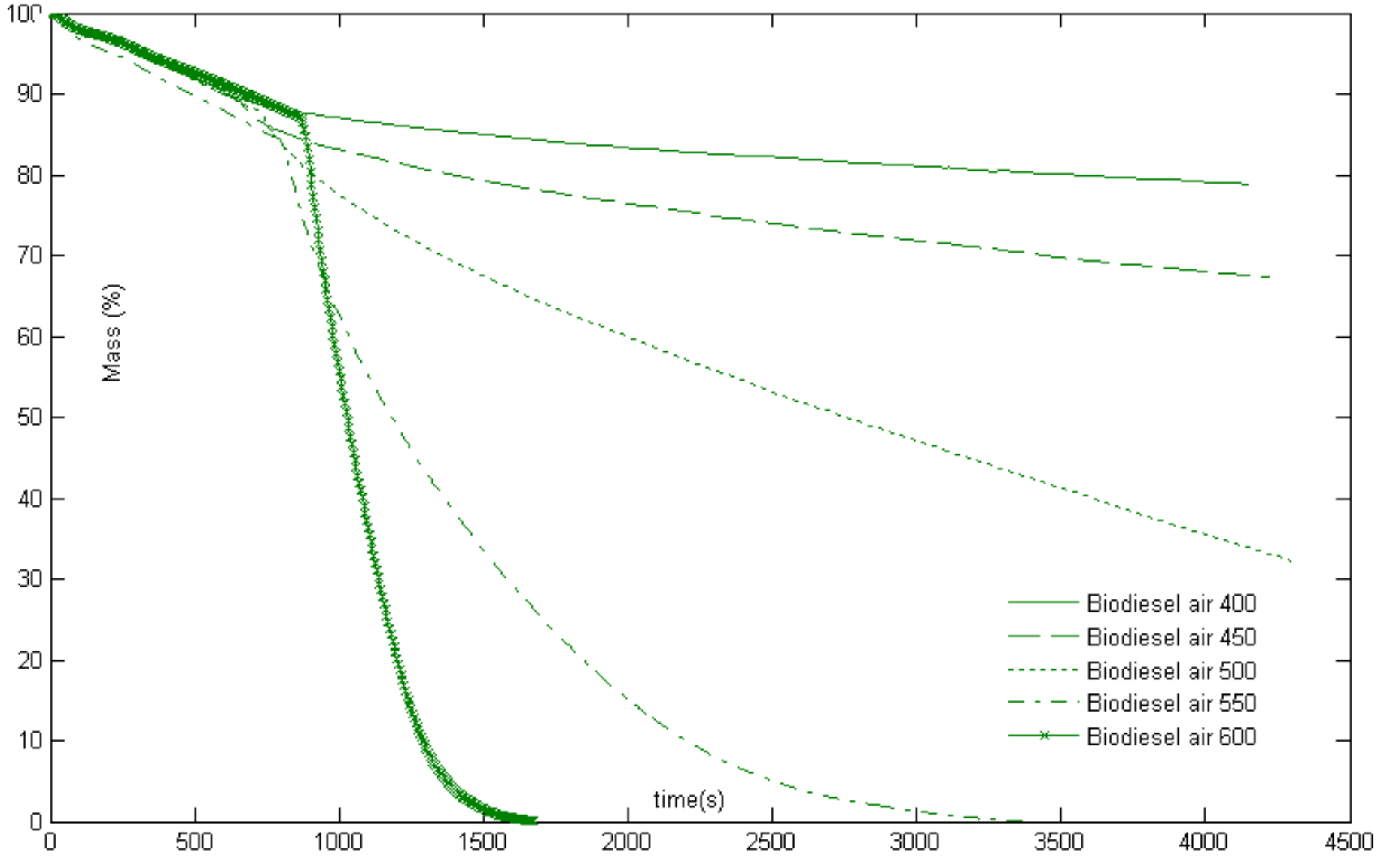

Figure 48. The isothermal TGA test of biodiesel samples with air.

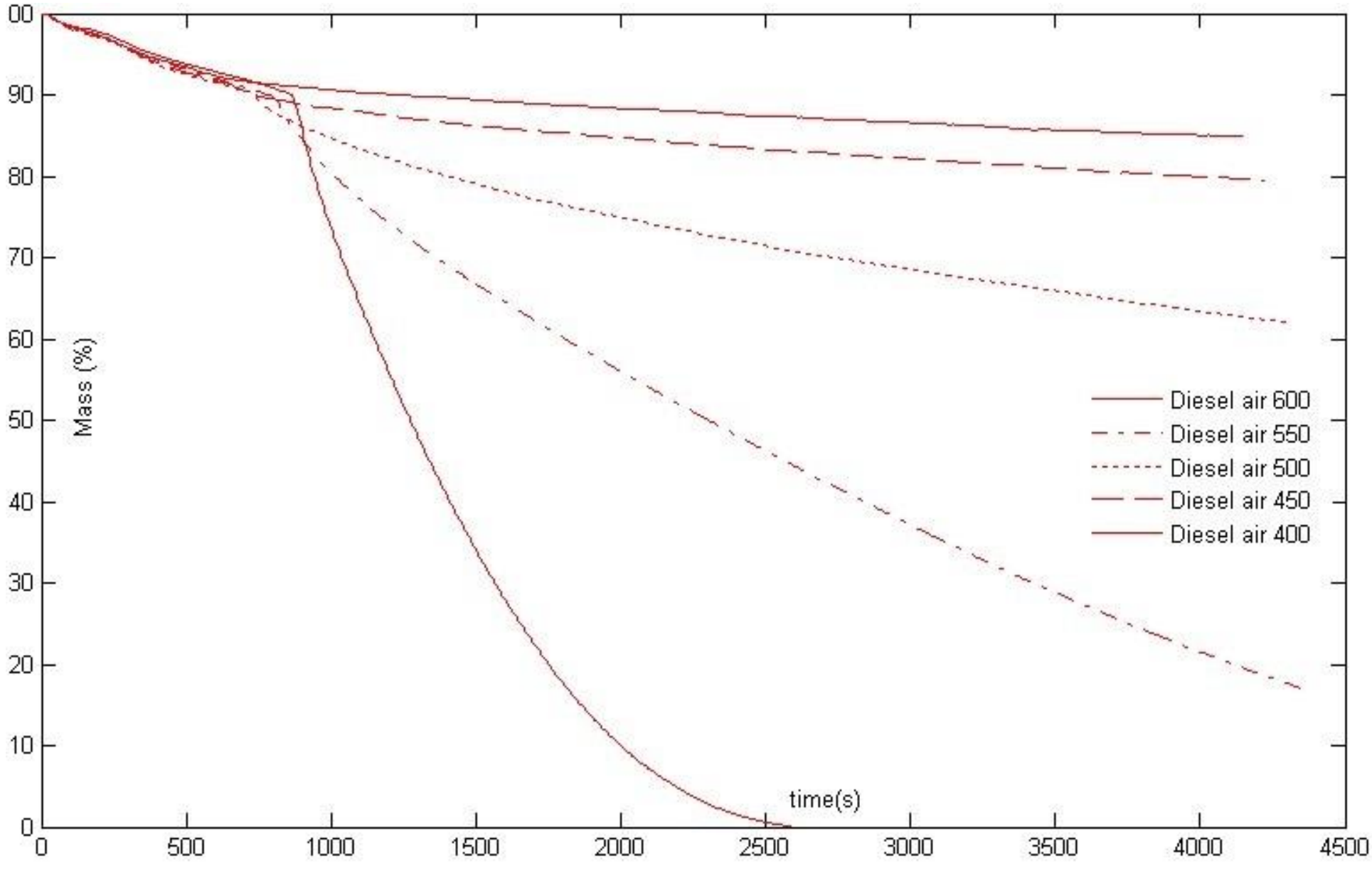

Figure 49. The isothermal TGA test of diesel samples with air.

For better clarification, it's required to refer to rate of conversion and elemental analyze of PM samples, in order to know the chemical composition. The rate of conversion of each soot sample at any temperature is plotted in figure 50. The first small peak in the rates belongs to the non-isothermal phase, where there is no oxidant. The second, larger, peak is indication of isothermal condition with presence of oxygen. Advent of oxidant into the system boosts the reaction and thus the crest of the peak goes up higher and faster. As temperature increase the rate graph becomes smoother and lesser fluctuates, which is due to faster conversion and mass consumption. For all conditions biodiesel soot has better reactivity and thus smoother graphs are seen.

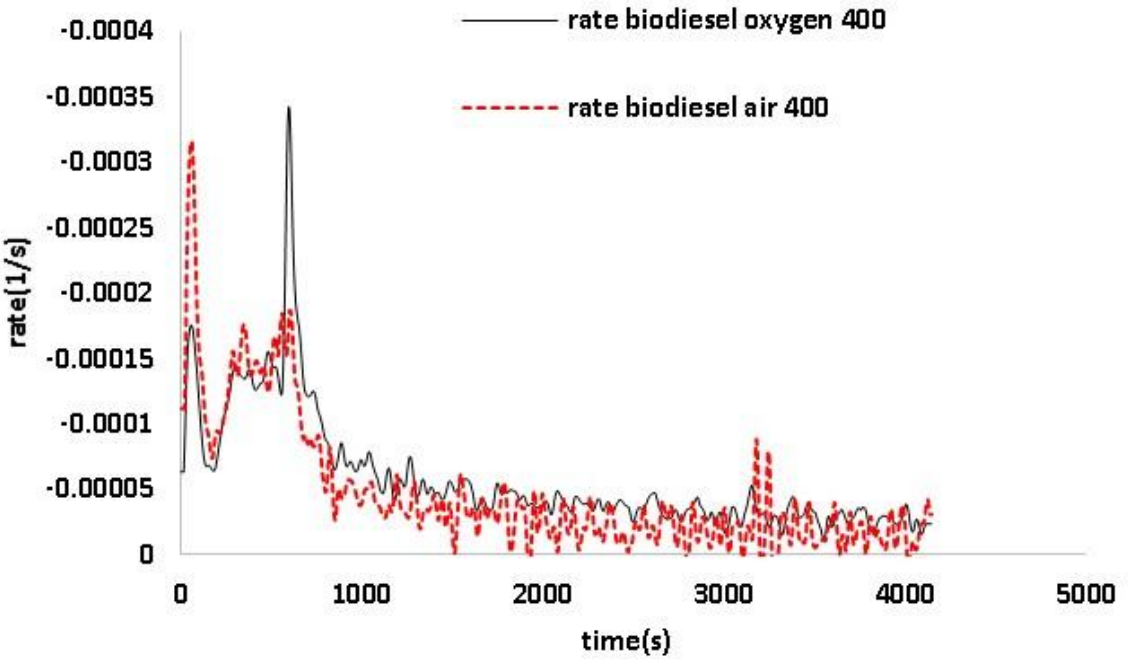

(a)

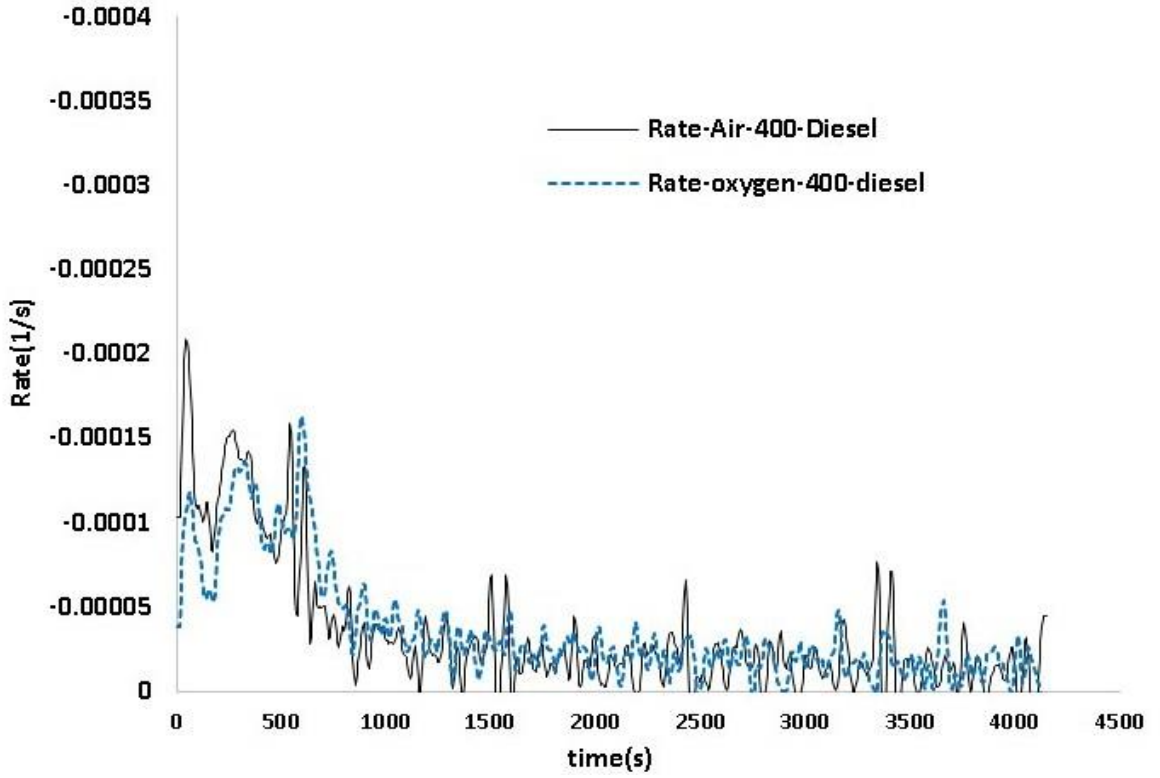
-0.0004
-0.00035
-0.0003
-0.00025
-0.0002
-0.00015
-0.0001
-0.00005
0
Rate(1/s)
Rate-Air-400-Diesel
Rate-oxygen-400-diesel
0
500
1000
1500
2000
2500
3000
3500
4000
4500
time(s)

(b)

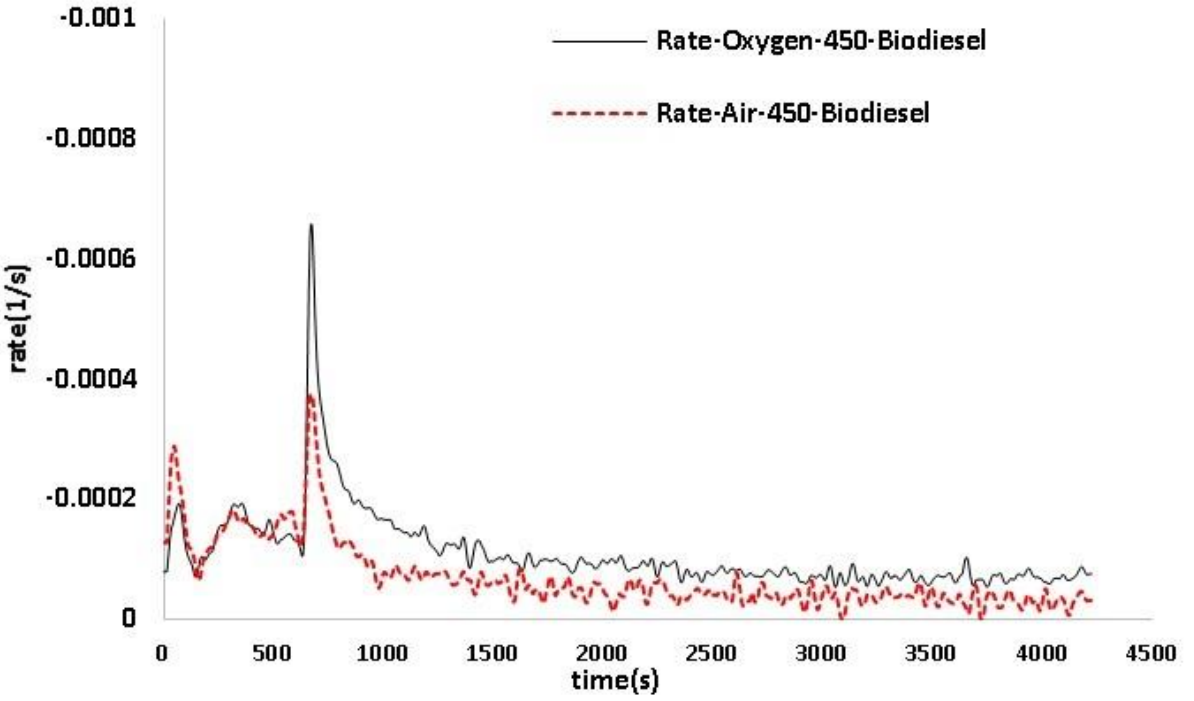
-0.001
-0.0008
-0.0006
-0.0004
-0.0002
0
rate(1/s)
Rate-Oxygen-450-Biodiesel
Rate-Air-450-Biodiesel
0
500
1000
1500
2000
2500
3000
3500
4000
4500
time(s)

(c)

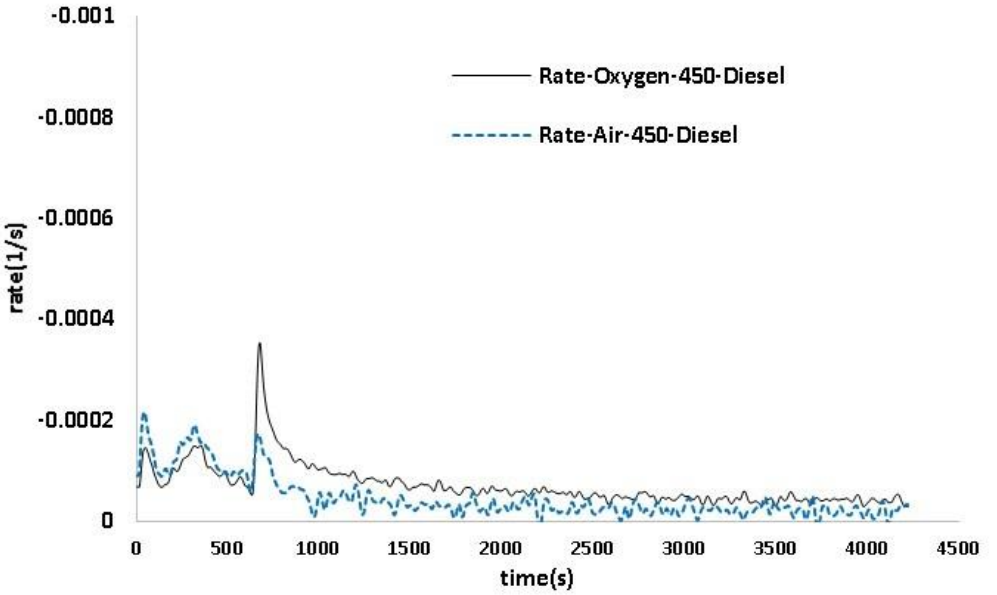
-0.001
-0.0008
-0.0006
-0.0004
-0.0002
0
rate(1/s)
Rate-Oxygen-450-Diesel
Rate-Air-450-Diesel
0
500
1000
1500
2000
2500
3000
3500
4000
4500
time(s)

(d)

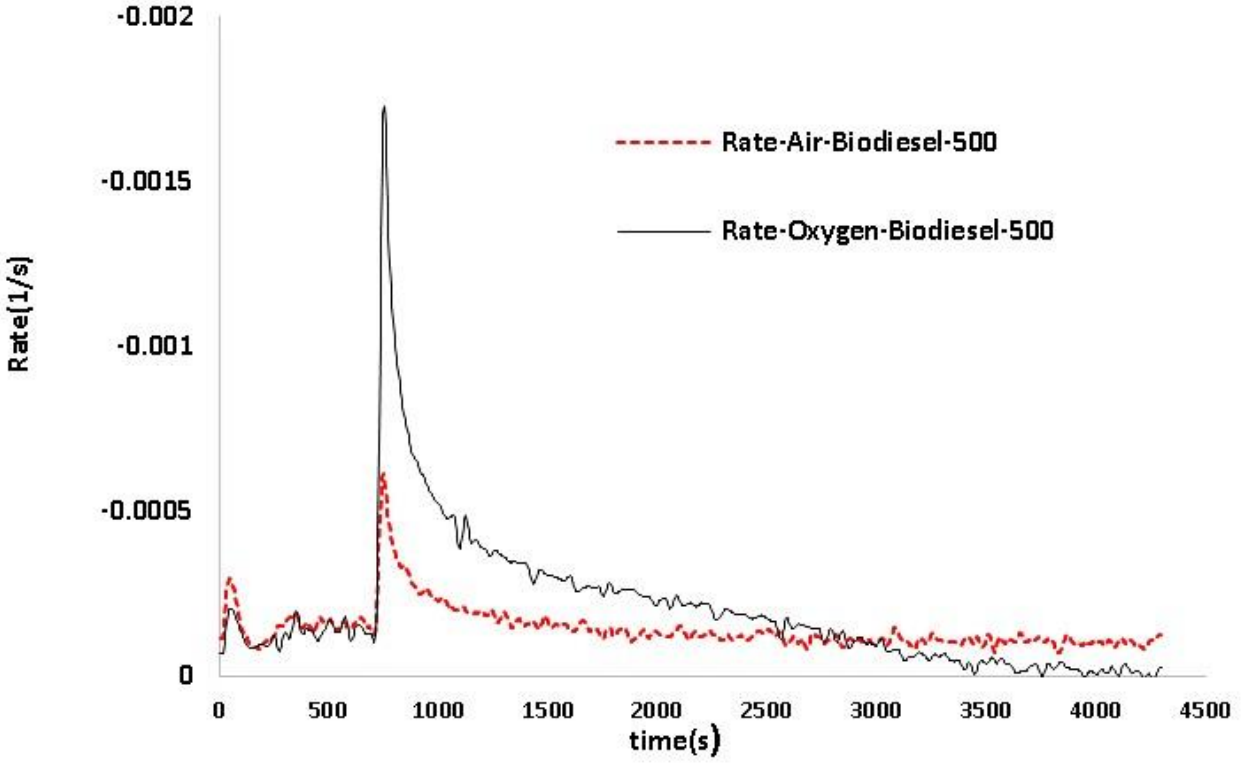
-0.002
-0.0015
-0.001
-0.0005
0
Rate(1/s)
Rate-Air-Biodiesel-500
Rate-Oxygen-Biodiesel-500
0
500
1000
1500
2000
2500
3000
3500
4000
4500
time(s)

(e)

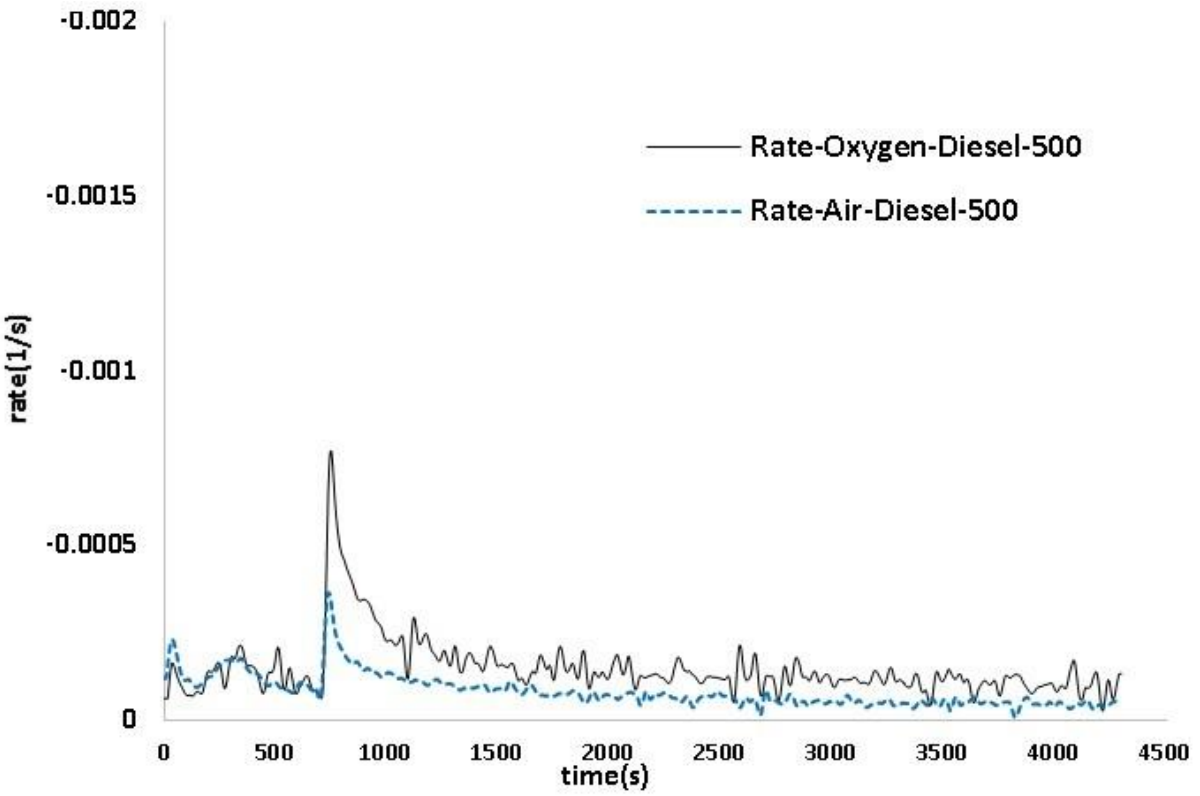
-0.002
-0.0015
-0.001
-0.0005
0
rate(1/s)
Rate-Oxygen-Diesel-500
Rate-Air-Diesel-500
0
500
1000
1500
2000
2500
3000
3500
4000
4500
time(s)

(f)

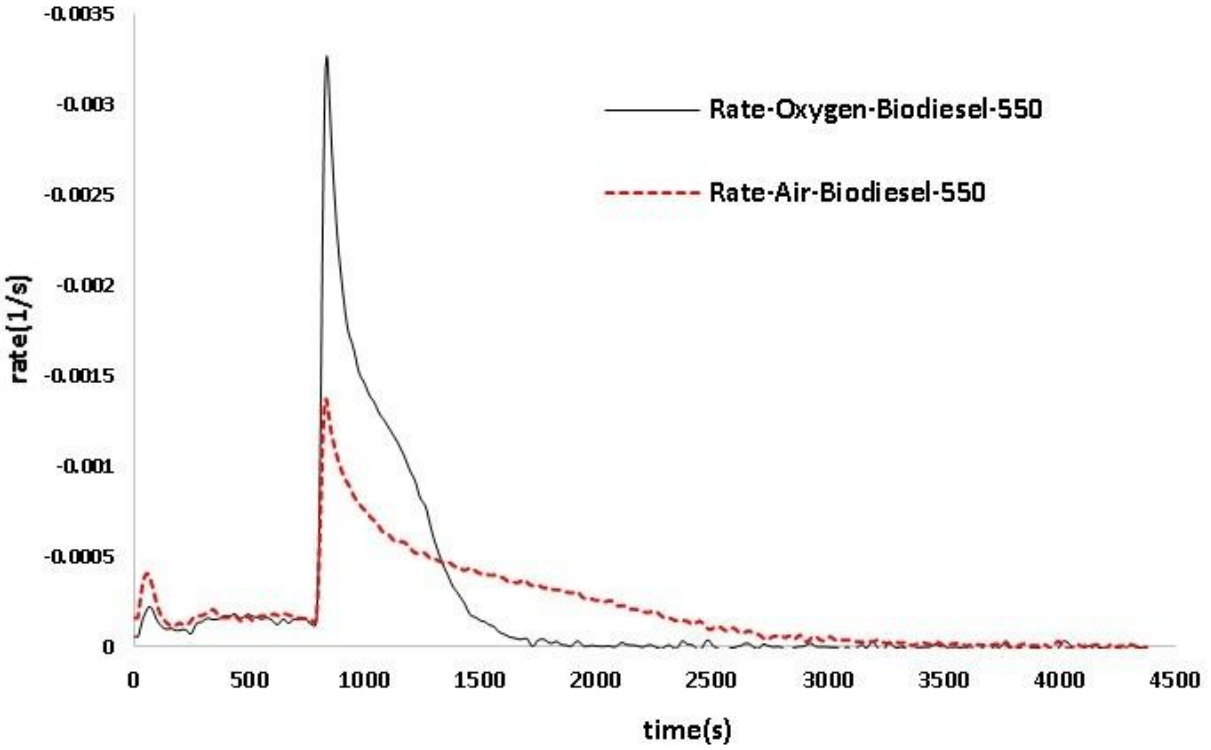
-0.0035
-0.003
-0.0025
-0.002
-0.0015
-0.001
-0.0005
0
rate(1/s)
Rate-Oxygen-Biodiesel-550
Rate-Air-Biodiesel-550
0
500
1000
1500
2000
2500
3000
3500
4000
4500
time(s)

(g)

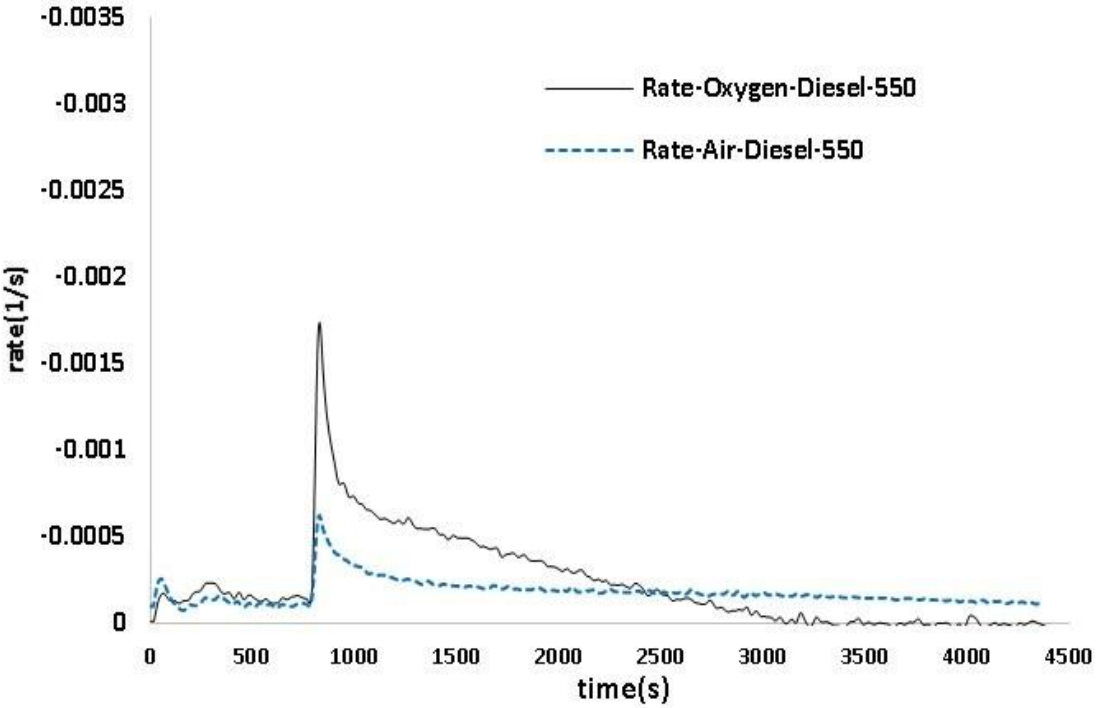
-0.0035
-0.003
-0.0025
-0.002
-0.0015
-0.001
-0.0005
0
rate(1/s)
0
500
1000
1500
2000
2500
3000
3500
4000
4500
time(s)
Rate-Oxygen-Diesel-550
Rate-Air-Diesel-550

(h)

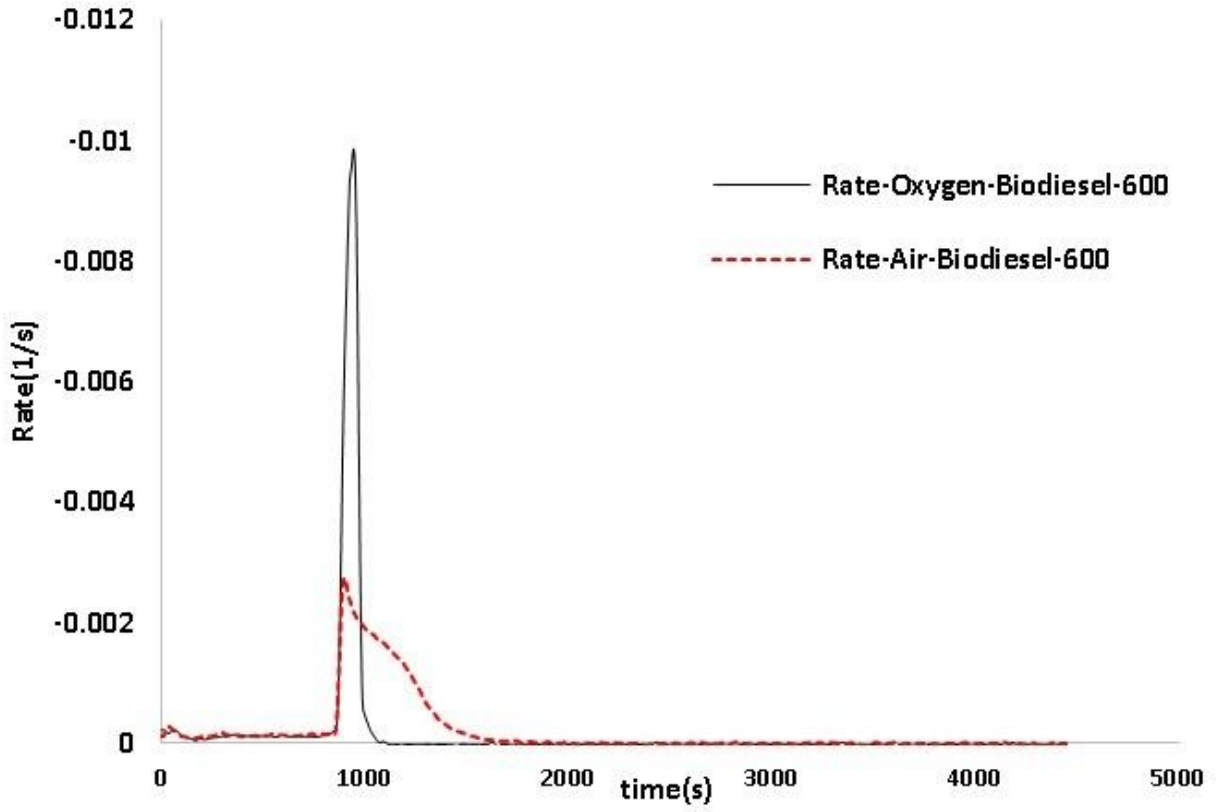
-0.012
-0.01
-0.008
-0.006
-0.004
-0.002
0
Rate(1/s)
0
1000
2000
3000
4000
5000
time(s)
Rate-Oxygen-Biodiesel-600
Rate-Air-Biodiesel-600

(i)

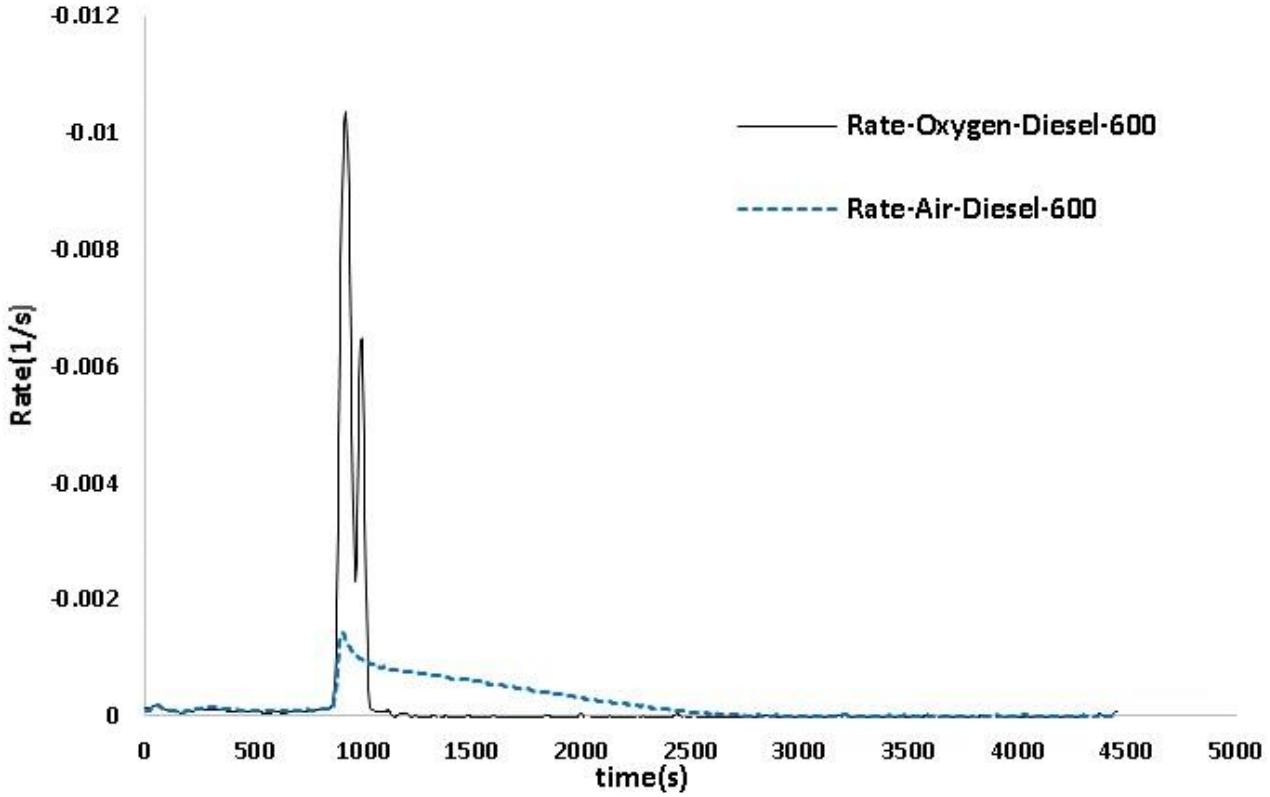

(j)

Figure 50. The rate of mass conversion (a) biodiesel at 400 ^{0}C (b) diesel at 400 ^{0}C (c) biodiesel at 450 ^{0}C (d) diesel at 450 ^{0}C (e) biodiesel 500 ^{0}C (f)diesel at 500 ^{0}C (g)biodiesel at 550 ^{0}C (h) diesel at 550 ^{0}C (i) biodiesel at 600 ^{0}C (j) diesel at 600 ^{0}C.

Comparing between air and oxygen, the rates of oxidation with pure oxygen is smoother due to better oxidation trend, which is result of abundance of oxygen in comparison with air. As seen in figure 50, in all conditions the biodiesel has higher oxidation rate in comparison with diesel and in all conditions also, the reactivity with pure oxygen is much more than air, especially at higher temperatures .Presence of oxygenated functional groups to the soot surface of soot particles enhances their oxidation rate by desorption of CO and CO2 on the application of heat [31]. It's not possible to

estimate the VOF, SOF and SOL fraction part of soot samples with Isothermal condition test. In an earlier study at our lab, soot samples, produced at same condition, were analyzed by the non-isothermal TGA test [5]. The PM of biodiesel consists of 4% moisture, 40% HC and 56% C while composition of diesel PM is made of 4 % moisture, 29% HC and 67 % C at 80% load from non-isothermal TGA rate curves [5].It's hard to differentiate between VOF and SOF, however most of the VOF is made of moisture and unburnt hydrocarbon and majority of it vaporizes during non-isothermal phase. As amount of VOF and SOF becomes higher, the oxidation and evaporation becomes easier in comparison with higher SOL condition, which is mostly solid carbon and needs high temperature for complete oxidation.

The percentage of VOF inside the PM from diesel engine is affected by several factors such as engine design character (DI, IDI, turbocharged) ,fuel injection system (injection principle, injection pressure and timing, nozzles characteristics).EGR, engine load and speed and exhaust temperature [32]. At higher loads and speeds, more incomplete combustion is seen due to higher rate of combustion and lack of time for complete combustion. At this condition also, fuel injection rate is higher and thus much more unburnt hydrocarbon or fuel will go out by exhaust flow. This trend becomes worse when biodiesel is applied. As discussed in earlier section, biodiesel has lower calorific value in comparison with diesel fuel, thus in order to compensate the energy loss more fuel shall be consumed. Higher viscosity and density of biodiesel also results in longer evaporation time and ignition delay, therefore more unburnt HC will be seen in the exhaust PM of biodiesel in comparison with

diesel. As biofuels are oxygenated fuels, they may have more oxygen content in the PM and this can boost oxidation and thus biodiesel shows faster oxidation rate in comparison with diesel [5].The conversion range of moistures and VOF is from 25-100 ^{o}(C), soluble fraction (SOF) parts which mainly consists of HC oxidizes from 100-500 ^{o}(C) and carbonaceous part of PM or solid (SOL) oxidizes at higher peak of temperature between 500-600 ^{o}(C) [5] .So at 600^{o} C for both of soot samples the oxidation trend is much more similar hence at this point the main composition is SOL ,which is carbon black and thus the difference is composition has not significant rule while in lower temperatures the importance of the composition difference is much more apparent. In order to show the impact of non-carbonaceous compositions on the PM oxidation, all soot samples were compared with carbon black N330 and the results are plotted in figure 51 and 52.

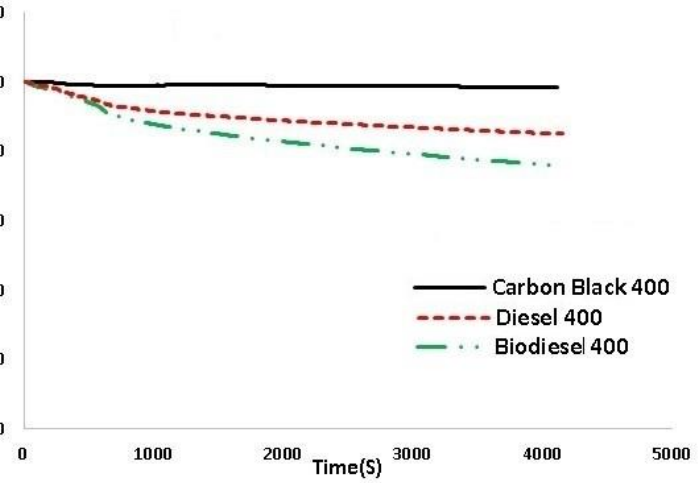

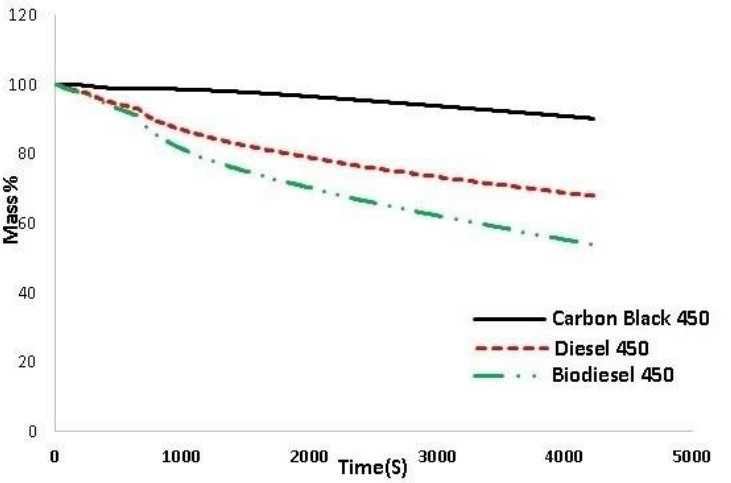

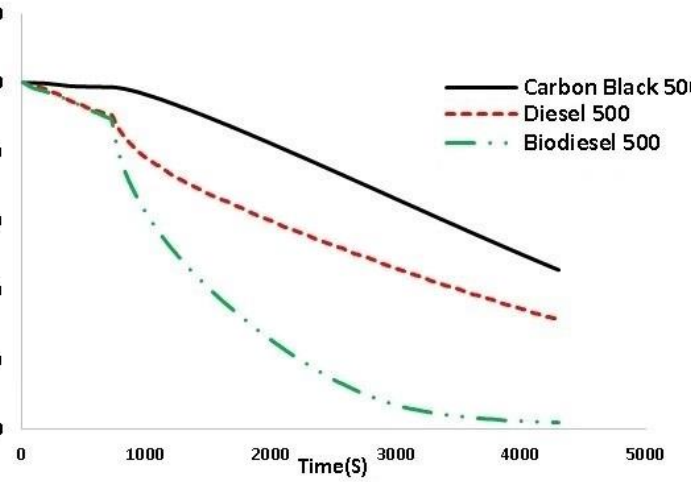

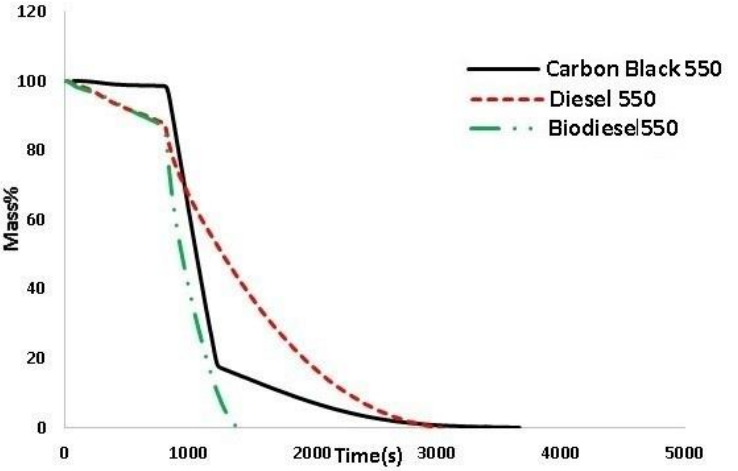

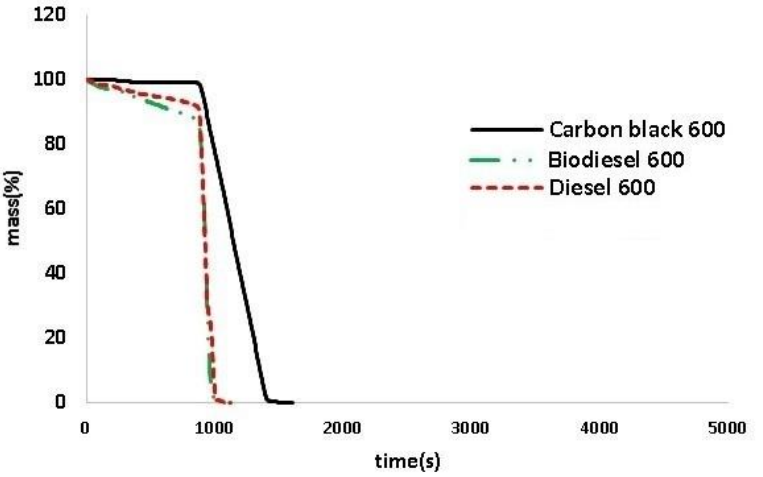

Figure 51.The comparison of engine soot with carbon black in TGA with Oxygen

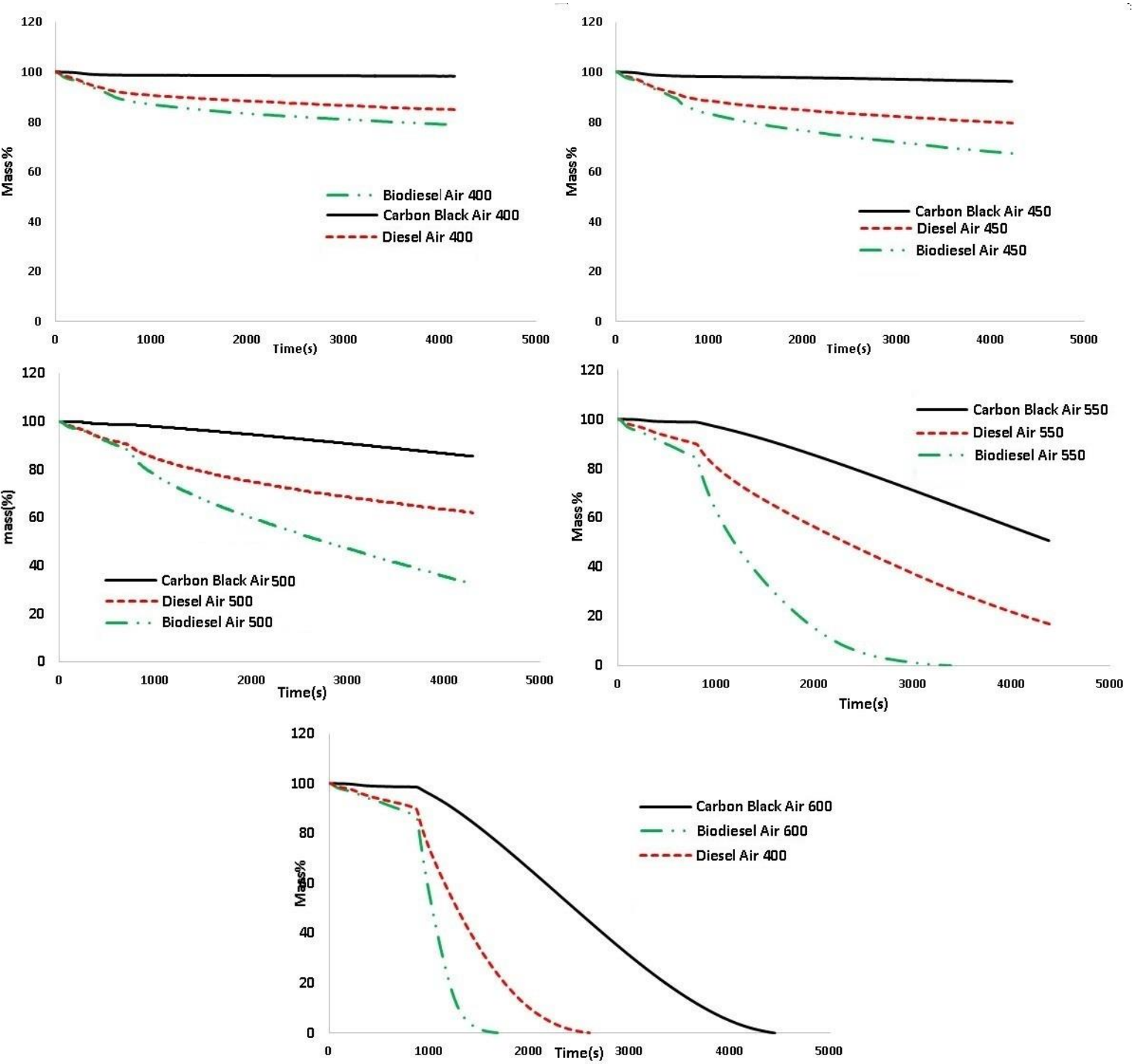

Figure 52. The comparison of engine soot with carbon black in TGA

As seen in figure 51 and 52, in all temperatures, carbon back has the lowers reactivity and biodiesel has the fastest and highest trend. It clearly illustrates that VOF and SOF of diesel engine PM affects the oxidation and improves it while for pure carbon the oxidation trend is slower. The effect of temperature on the rate of oxidation of a carbon may be expressed by an overall activation energy, which is, in fact, a weighted average of the activation energies of several elementary reactions. The activation energy of the reactions are discussed in next section. The figure 51 and 52 showed that the chemical reactions, which governs the carbon oxidation will be altered by VOF and SOF compositions, therefore the activation energy of the soot will be affected by its chemical component. Calculation of activation energy is discussed in next section.

4.2.1. Reaction Order of Carbon, n, and Activation Energy

Then Chemical kinetics of TGA results were analyzed by relations below:

$$PM+O_2 \rightarrow CO_2 \qquad (1)$$

The chemical reaction rate in eq.1 can calculate from the TGA curve based on the chemical kinetic in eq.2.

$$-\frac{d[PM]}{dt} = k[PM]^n[O_2]^m \qquad (2)$$

Where PM is particulate matter mass, t is time, k is specific rate constant, m, n are the reaction order. The dependence of the specific rate constant k is expressed by eq.3.

$$K = A\, e^{-Ea/RT} \qquad (3)$$

Where A is the frequency factor, Ea. is the activation energy, R is the gas constant. The apparent activation energy can be calculated by eq.4.

$$\ln\left[\frac{-1}{[PM]^n}\frac{d[PM]}{dt}\right] = -\frac{E_a}{RT} + (\ln A + m\ln[O_2]) \qquad (4)$$

Reaction order, *n*

The reaction order of carbon varies between different experiments and samples. Neeft et al [21] found a range of 0.65-0.80 for reaction order of Printex-U. In their research they have also mentioned that the water can affect the order of reaction and in absence of water the reaction order of carbon for diesel soot 0.56 while the value was 0.69 in presence of water. In order to calculate the order of reaction for carbon, the natural logarithm of the rate formula (eq.2) is used and the results are shown in Figure 53 and the results are presented in table 5.

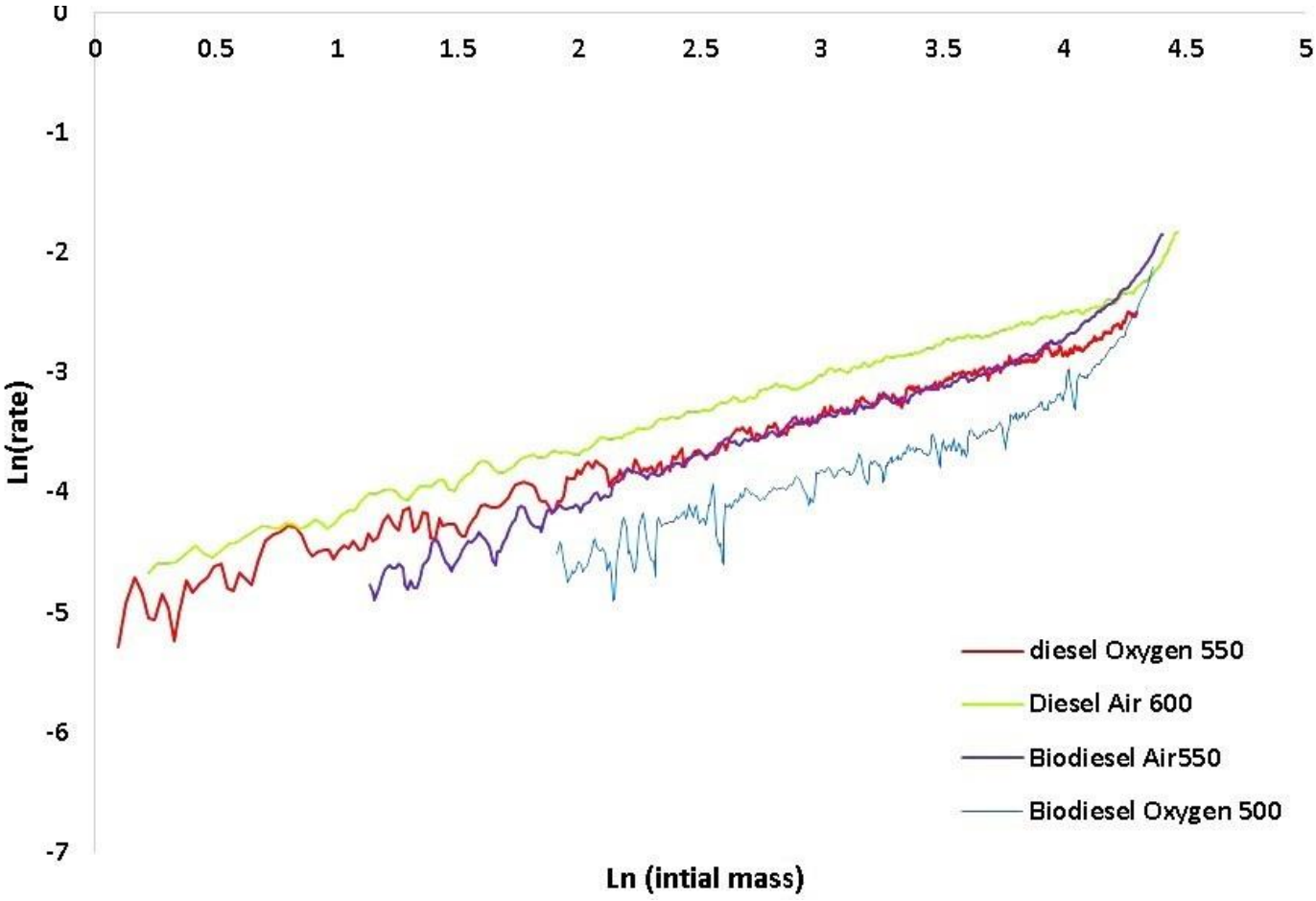

Figure 53. Carbon reaction order, n for diesel and biodiesel soot in air and oxygen TGA.

Table 5. The results of carbon reaction order.

Soot sample	n value
Biodiesel Oxygen 500	0.76
Biodiesel Air 550	0.74
Diesel Air 600	0.57
Diesel Oxygen 550	0.56

According to table 5, for both TGA condition biodiesel has higher n value in comparison with diesel soot and thus it shows better reactivity. None of the samples meet the shrinking core value (2/3) and it can be claimed that the soot particles do not have a complete spherical shape.

Activation Energy (Ea)

Activation energy (Ea) is the minimum energy which is required to initiate and complete a chemical reaction. The lower Ea, the better reactivity. At this study the, it's tried to divide the soot mass conversion in three main groups and then the Ea for each division is calculated. This can clarify the different compositions of soot, VOF, SOF and SOL, by difference of Ea value. The soot conversion of all samples is divided to three parts, based on equal percentages of conversion rate of the samples including (80-60%), (60-40%) and (40-20%). The activation energy of soot samples at each division is calculated from Arrhenius graphs which are depicted in figure 54, for oxygen, and figure 55 for air. The overall Arrhenius and the results of Ea for each division are presented in figure 56 and 57.

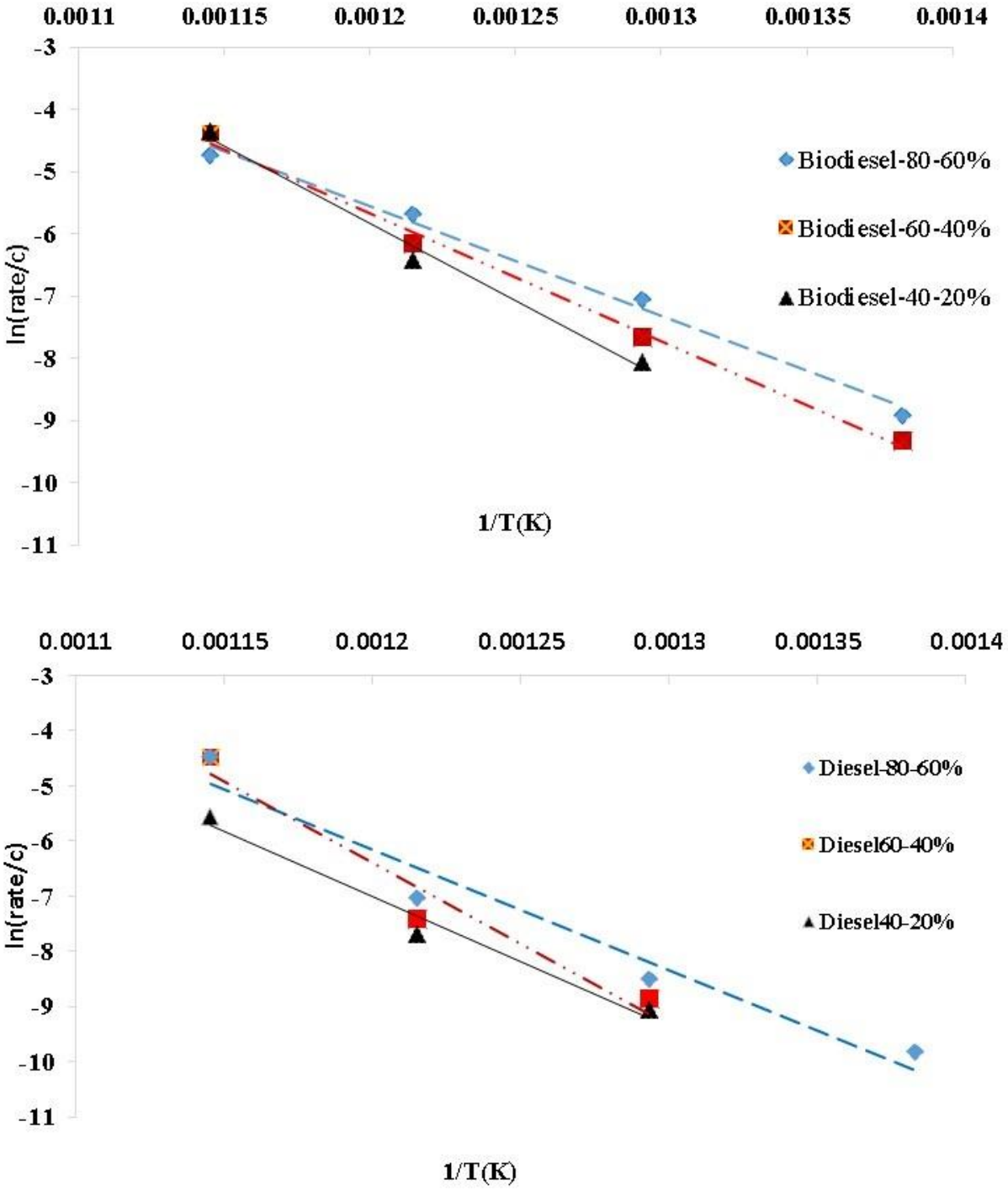

Figure 54. Arrhenius plot of three fractions of PM of Diesel and Biodiesel PM with oxygen.

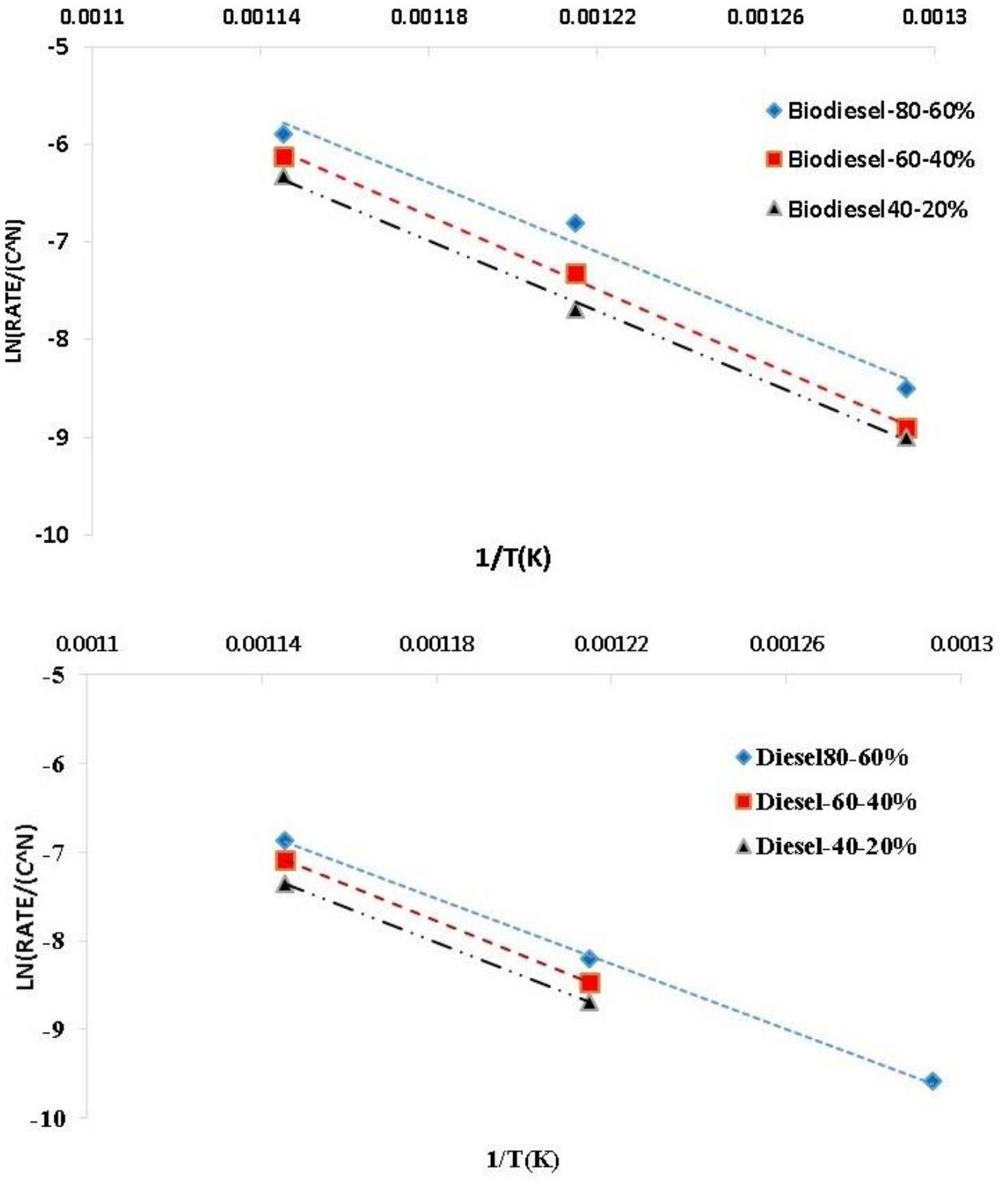

Figure 55. Arrhenius plot of three fractions of PM of Diesel and Biodiesel PM with air.

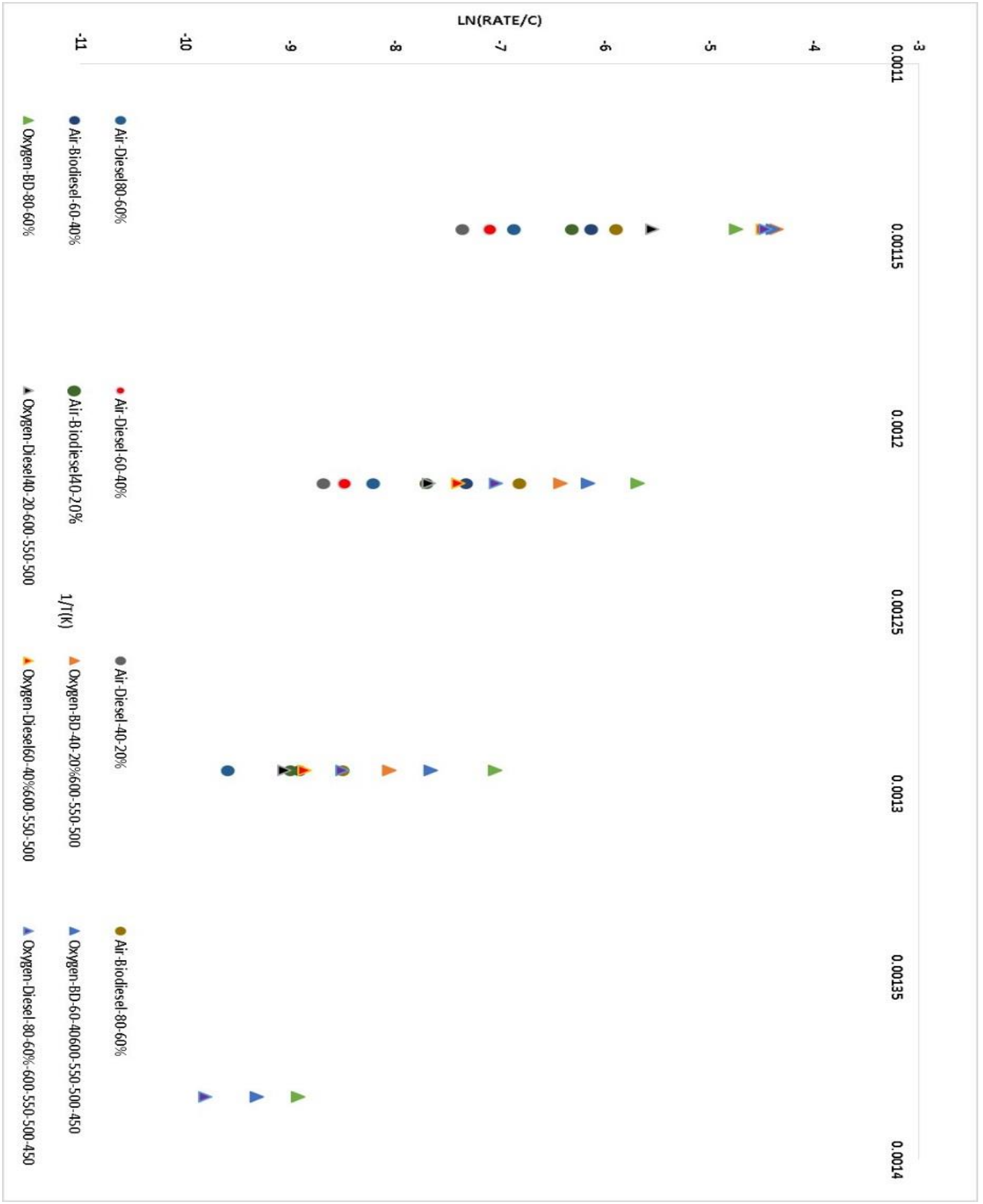

Figure 56. The overall activation energy of soot samples.

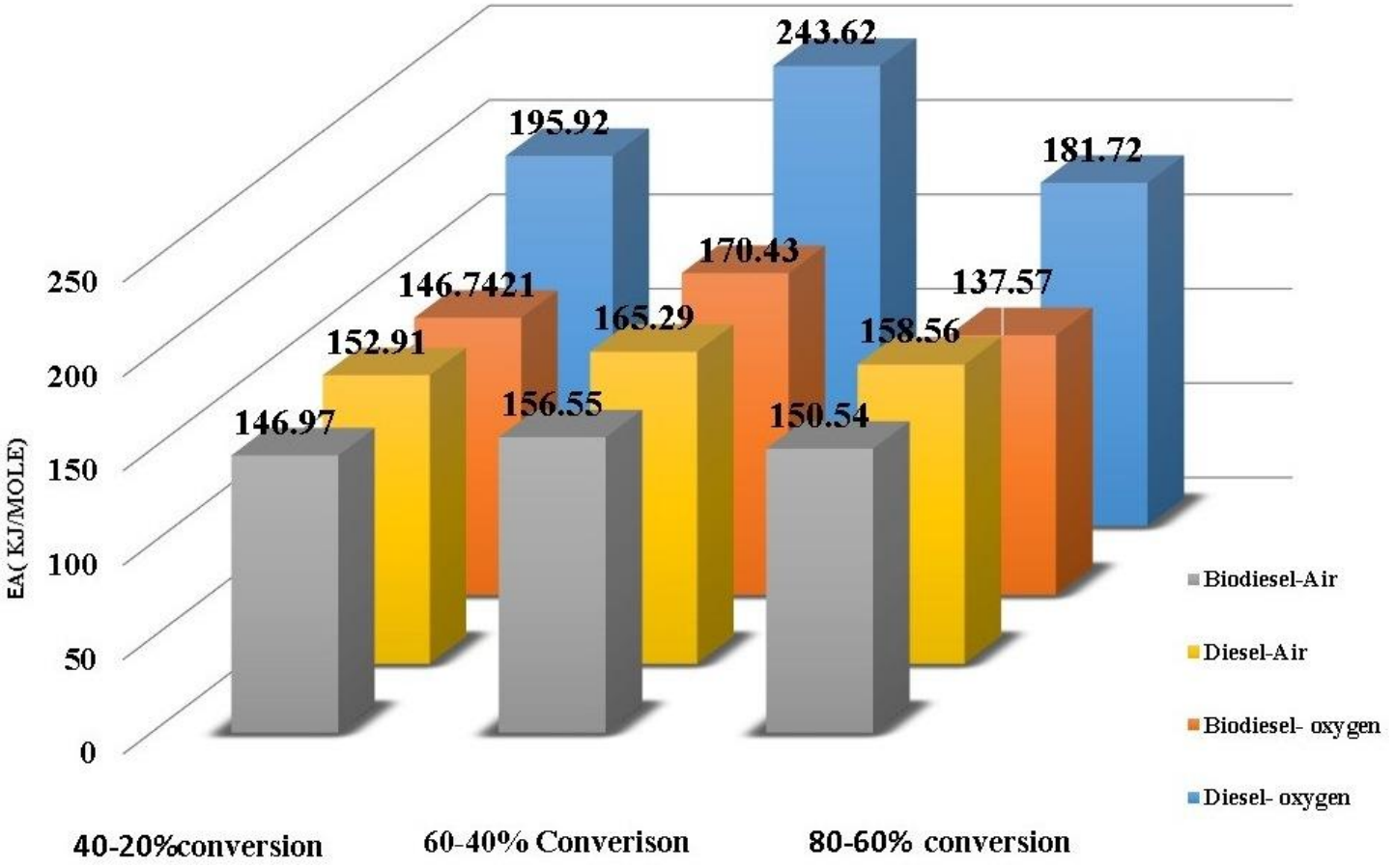

Figure 57.The results of activation energy of soot samples from air and oxidation TGA.

The elemental composition of soot sample is one of the factors which affects the Ea and thus soot reactivity. The results of elemental analyze of PM samples shows that the PM of biodiesel is made of 1.1% H and 74.1% C while for diesel PM its consists of 1.1% H and 81% C. The Ea corresponds to the energy barrier to be overcome during the reaction. Its maximum value corresponds to the bond energies in the molecule the Ea [5].

The H/C ratio can be correlated to the oxidative reactivity of soot particles. The higher H content per unit C atom increases the possibility of H abstraction by O_2 or the radicals present in the

combustion environment such as H, OH, CH_3 and C_3H_3 to create a radical site on soot to facilitate O_2 addition on it, which can enhance soot oxidation rate [31]. The diesel fuel is mainly consists of aromatic components and poly aromatic hydrocarbons, PAHS, generally have lower H/C ratios and thus lower reactivity but in biodiesel the presence of saturated components chains in the soot can increase its H/C ratio as well as its oxidative reactivity[30]. In the literature the published values of activation energy of unanalyzed soot oxidation is found to cover a range between 140 and 210 kJ/mole [32]. For TGA with air, the Ea of first division (20-40%) is lower in comparison with the two remaining divisions and is 146.97 kJ/mole for biodiesel in air and 146.74 kJ/mole in oxygen and for diesel 195.92 kJ/mole in oxygen and 152.91 kJ/mole in air. This can be due to presence of more VOF and SOF in the first stage of conversion ,while in later stages most of SOF and VOF are consumed and most of the composition is SOL or carbonaceous ,especially at last stage and therefore the higher values for Ea can be seen in figure 56. In comparison between diesel and biodiesel soot samples, the Ea of biodiesel is lower in all divisions and thus it can be a good reason for better reactivity of the biodiesel soot hence lower Ea is indication of easier oxidation at lower temperature. In other word, the bigger the Ea, the harder the soot oxidize. However, the exact and precise reason for difference of Ea can’t be obtained and needs more detailed experiments.

4.3. Morphology and Image Processing

In order to know the micro scale and Nano scale of the PM and the pores of DPF, image processing was done on obtained SEM and TEM images from DPF and soot samples. At first step the SEM image of DPF sample was subjected to analyze by changing the gray scale to binary (black & white) format. The open architecture image processing program, ImageJ, was used for image processing.

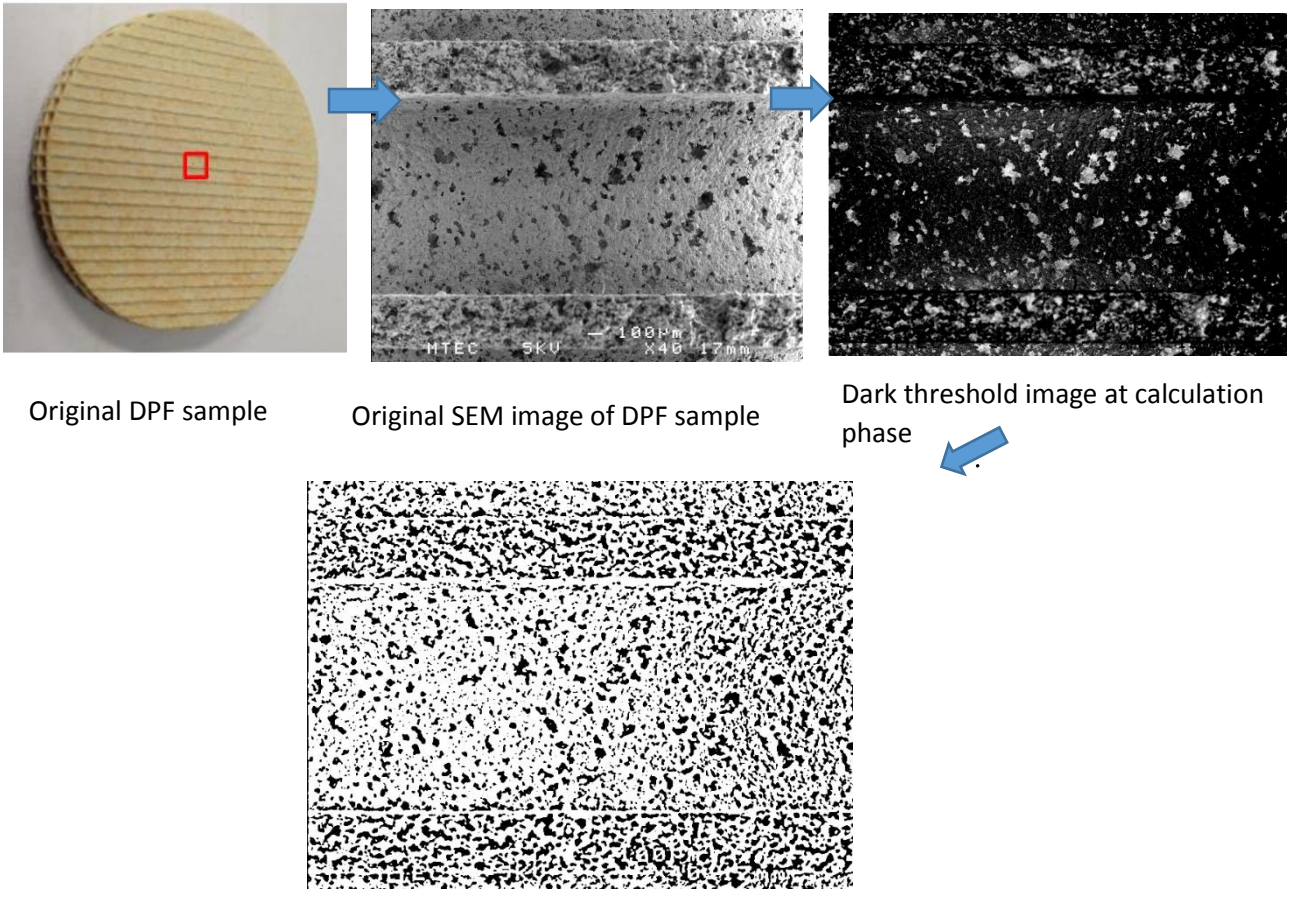

Figure 58. Image processing for pore size measurement of DPF from SEM image.

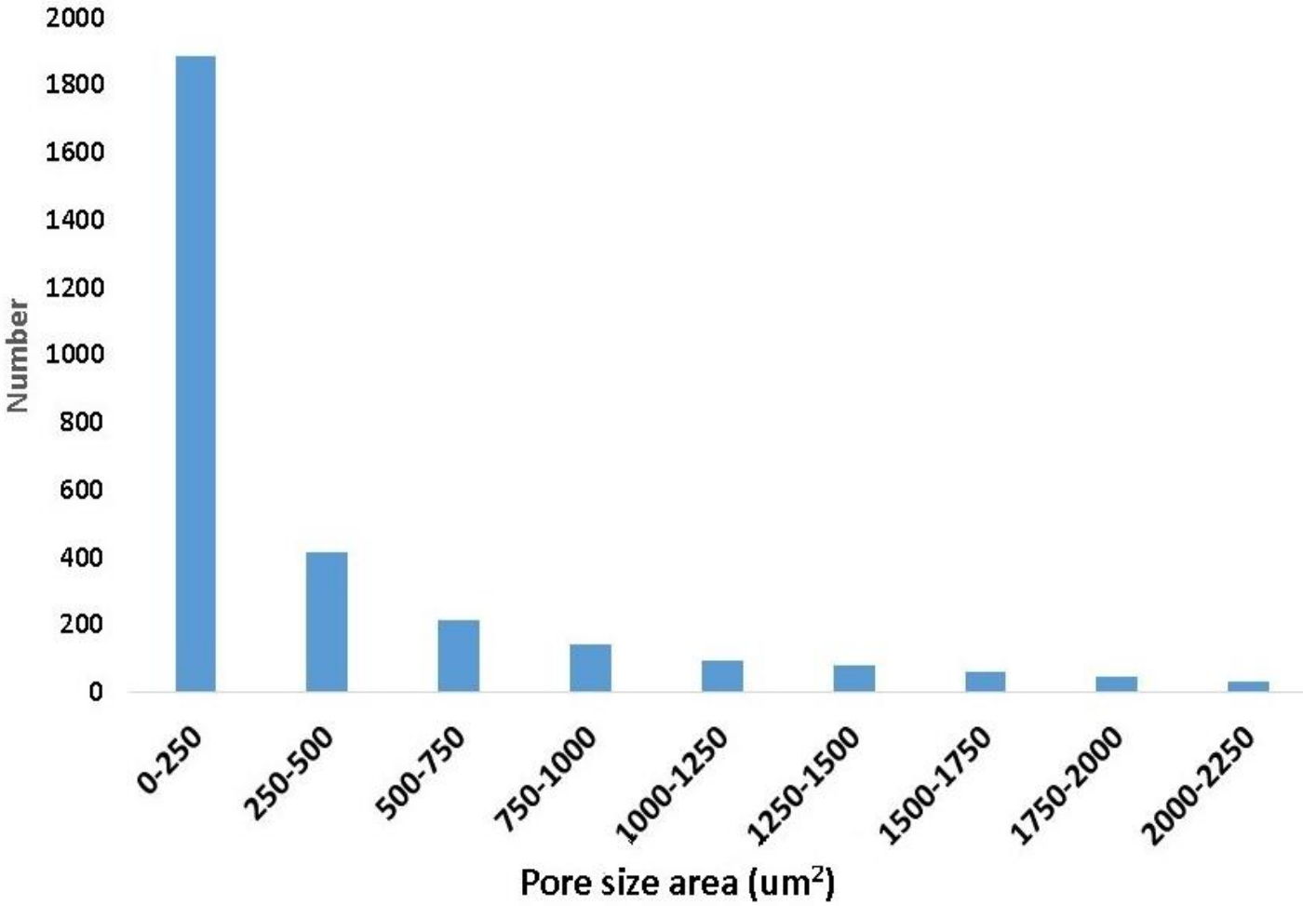

Figure 59.Pore size distribution of DPF sample.

For DPF SEM image efforts were concentrated on measuring the pore size of the DPF. The stages of this process is shown in figure 58. The results of the calculation and size distribution is plotted in figure 59.

As seen in figure 59, most of the pores of DPF sample are placed within the range of 1-1000 μm which consists of up to 250 while the rest of the size range covers only a few numbers which at most reaches to 13 number.

Macrostructure & Microstructure:

Similar process was done for TEM images from diesel and biodiesel soot samples. The TEM images were subjected to image processing and the PM surface area was measured. Two TEM image with equal resolution and scale were used for image processing for diesel and biodiesel soot samples. The TEM pictures of diesel and biodiesel soot samples and an example of the process is illustrated at figure 60 and 61.

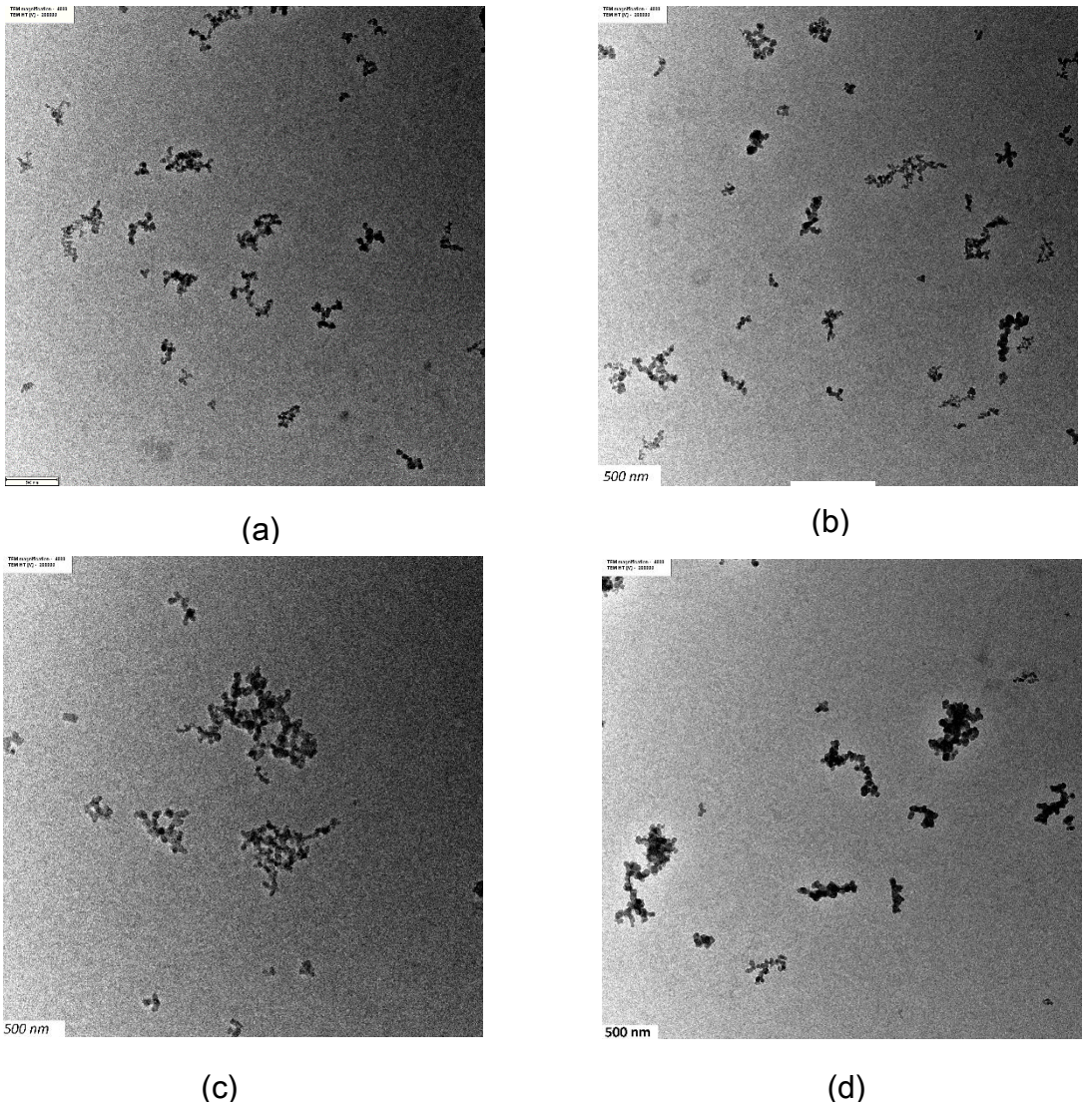

(a) (b)

(c) (d)

Figure 60. TEM images of soot samples in agglomerate mode (a) & (b) biodiesel PM, (c) & (d) diesel PM

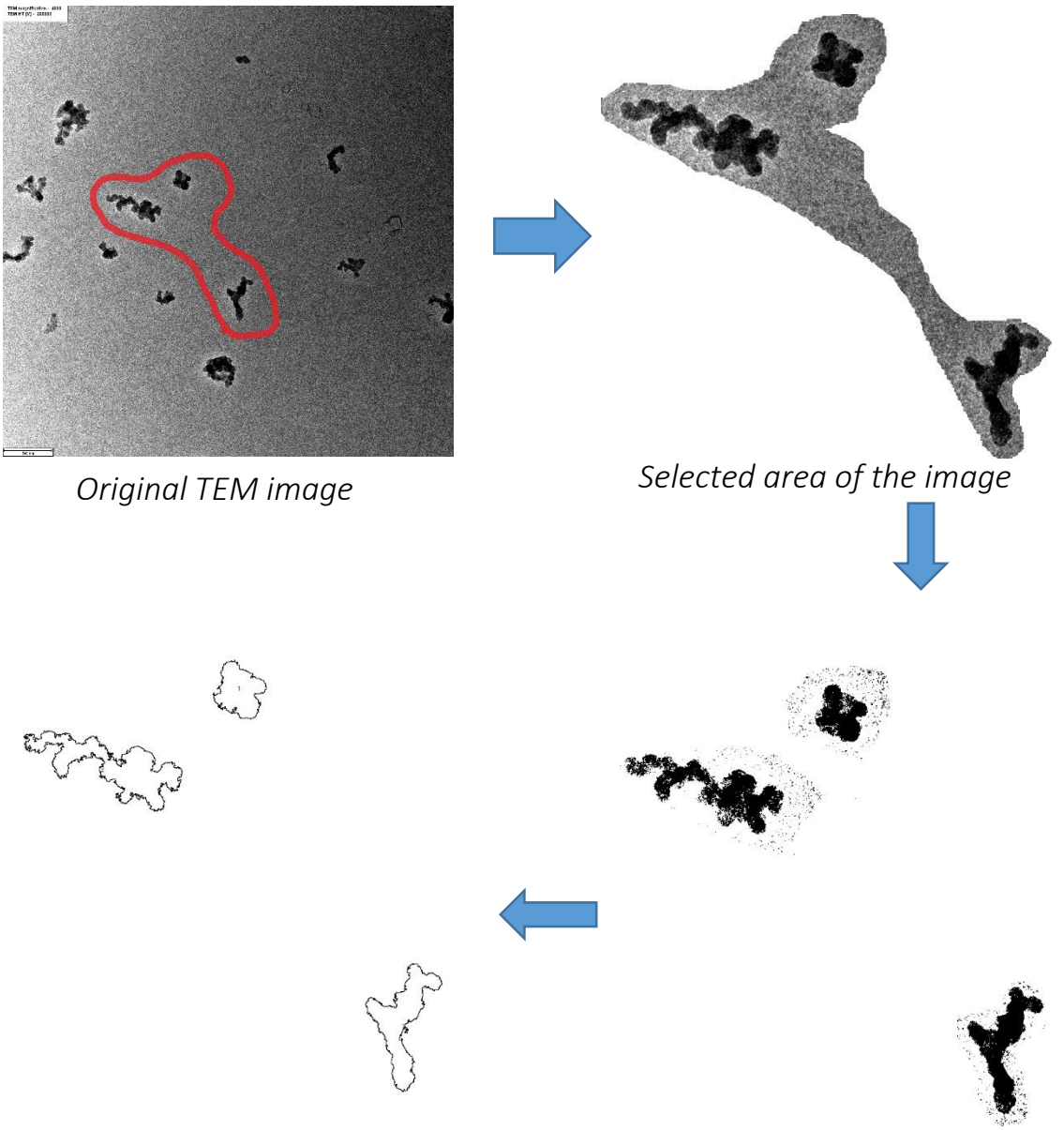

Figure 61. The overall process of image processing for measurement of PM surface area.

the results of image processing which are depicted in figure 62 shows that the surface area of agglomerated PM from biodiesel are mostly within the range of 2~44 (μm^2) and more concentrated while for diesel PM the range is wider and reaches up to 186 (μm^2) and size distribution is more dispersed. Although TEM image does not allow for the three-dimensional nature of agglomerates, and will generally underestimate the true maximum values of length of the agglomerate but the measurement of 2D area still gives a good picture for better illustration of size difference between two PM samples. Similar approach was done to determine the PM length in nano scale. The measurements process and the size distribution results are shown in figure 63 and 64. As seen in figure 64, the range

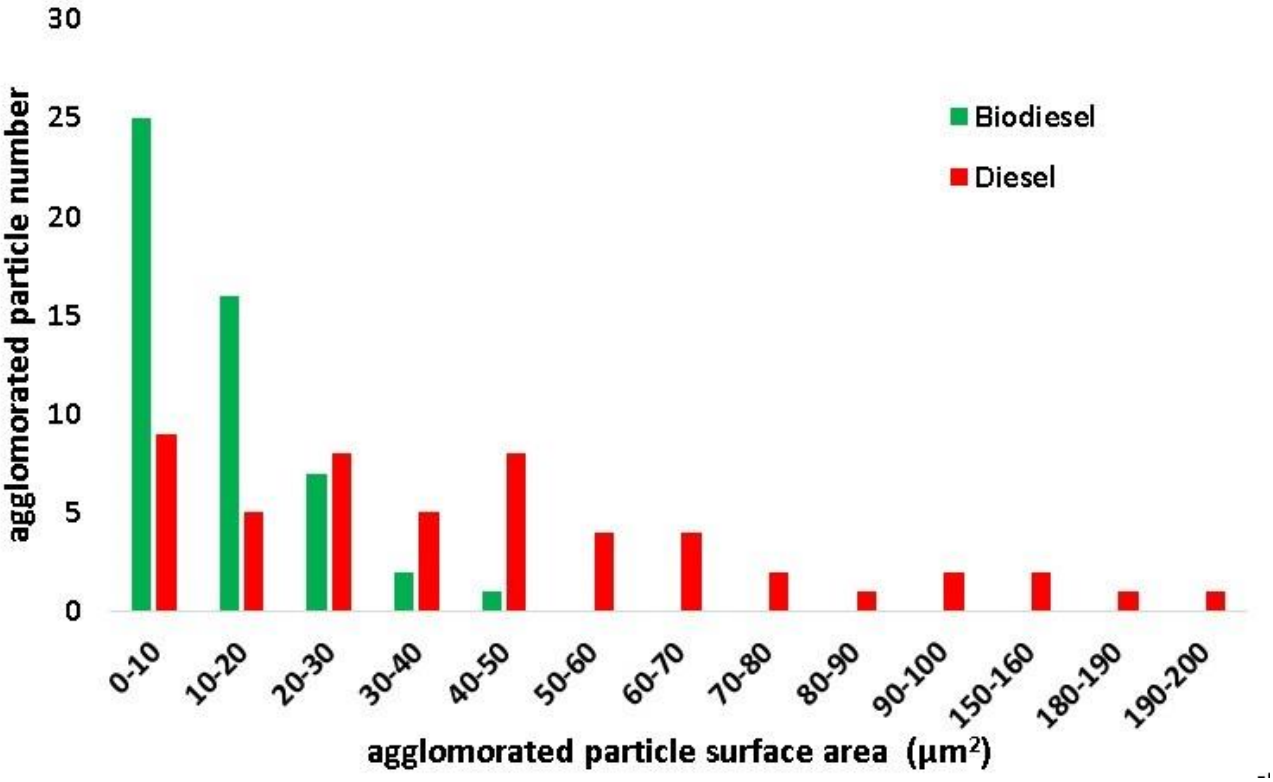

Figure 62. The surface area of agglomerated particles

of agglomerate length of biodiesel PM is within the range of 40~650 nm while the range of diesel agglomerate length is between

100~200k nm. The size distribution of diesel soot is much more scattered in comparison with biodiesel soot sample in which most of particles are within a close range. The number of counted particles for biodiesel PM is more than diesel while this trend is invers for the length of agglomerate particles. In figure 65 and 66 also, the combined graph of length and cross section area of diesel and biodiesel PM and the normalized size distribution of them is illustrated. Agglomerate surface area and length of biodiesel PM are smaller than diesel and this can result in better oxidation trend in comparison with diesel PM. The size of PM samples and their belonging parts can be related to each other and studies shows the amount of volatile matter is a function of particle size. Most of the material in the accumulation mode above about 100 nm is nonvolatile, presumably mainly elemental carbon [5, 34].

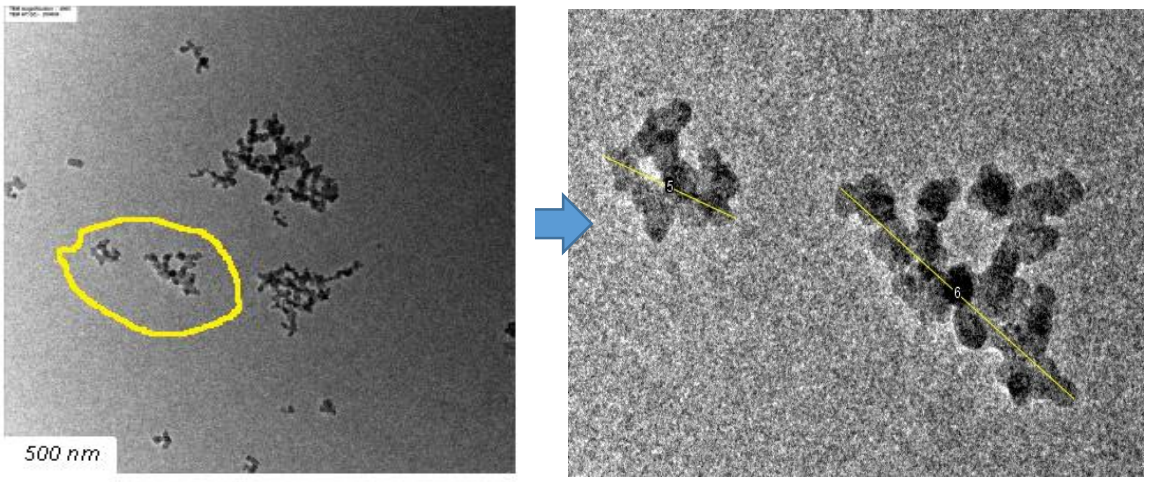

Figure 63. Measurement of length of agglomerated particles with image processing

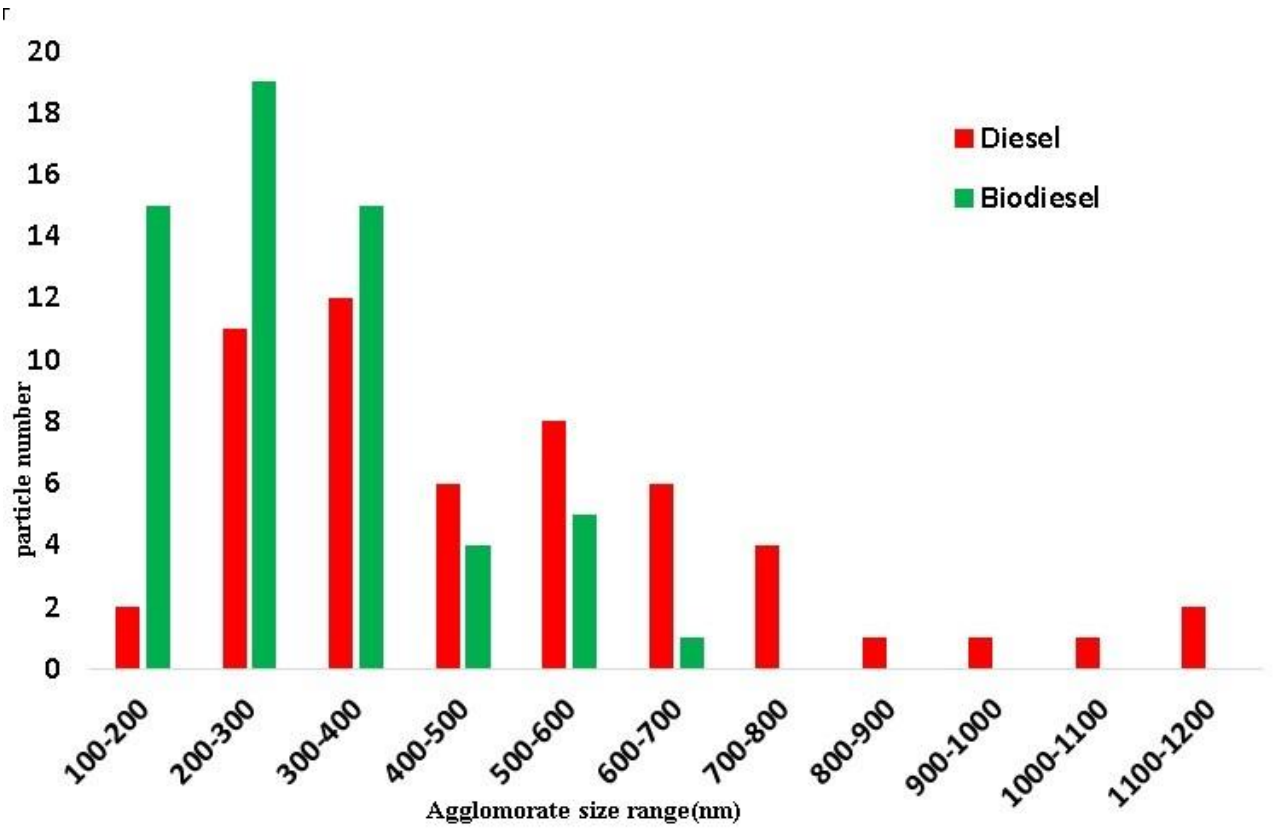

Figure 64. Measurement of length of agglomerated particles from diesel and biodiesel with image processing.

The oxygenate components of biodiesel can end up in more complete combustion resulting in the smaller size of agglomerate and single particle of PMs and it's also possible that the remnants of these oxygenated agent affect the PM surface oxidation [9].

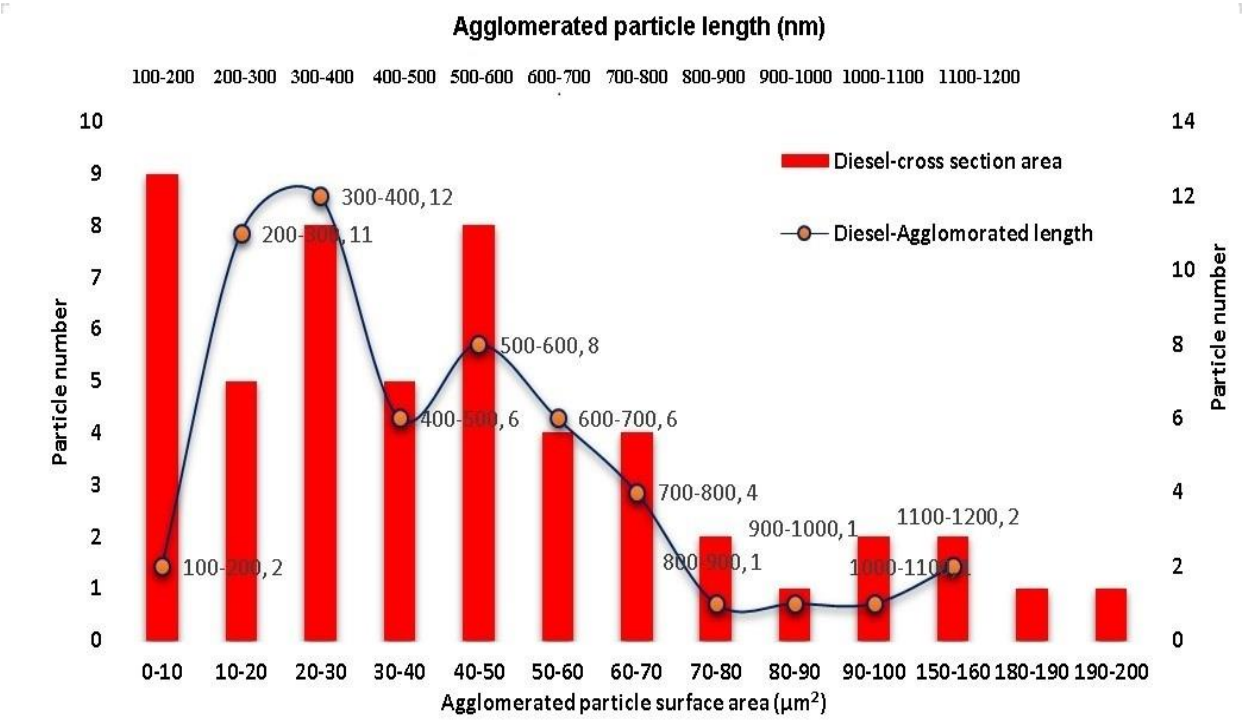

(a)

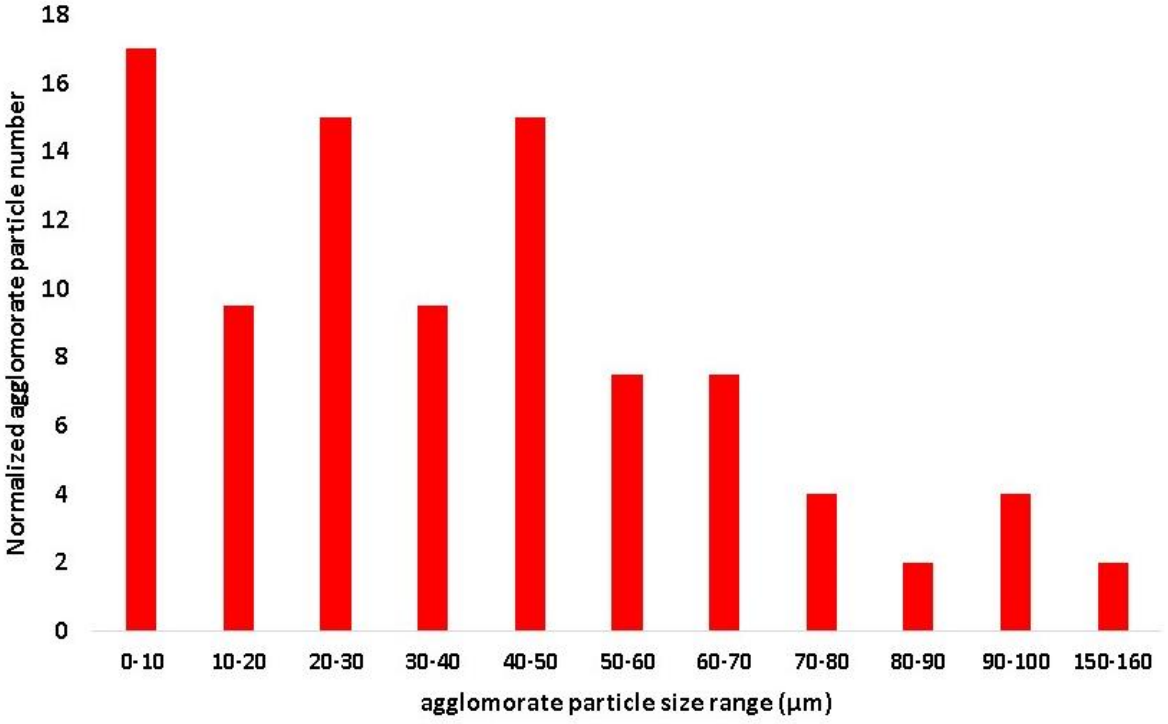

(b)

Figure 65. (a) The combined graph of length and cross sectional area (b) normalized chart of agglomerated PM size distribution.

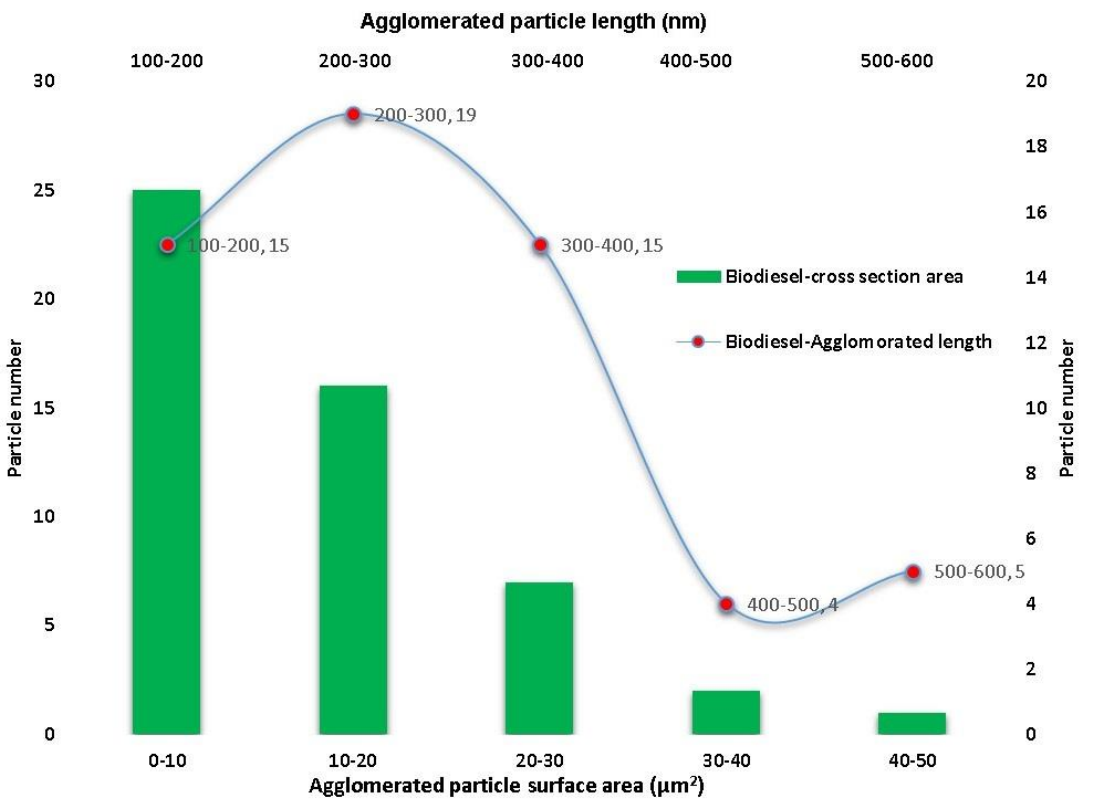

(a)

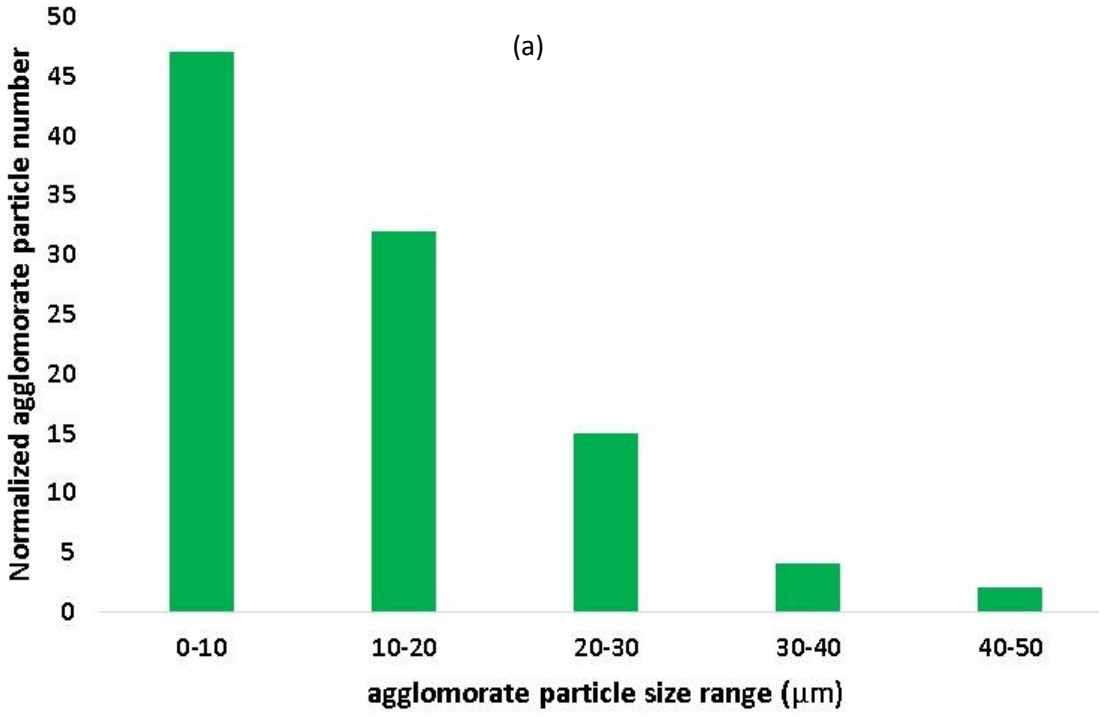

(b)

Figure 66. (a) The combined graph of length and cross sectional area (b) normalized chart of agglomerated PM size distribution of

The size of agglomerated particles can also be contributed to their compactness and the more compact particle, the smaller size of agglomerate particles. Based on this theory the compactness can be categorized in two main types. The first type is reaction limited cluster aggregation (RLCA) and the second type is diffusion-limited cluster aggregation (DLCA). A schematic of RLCA and DLCA is shown in figure 67.

This phenomenon is depended on rate of soot aggregation. If the rate is fast then the DLCA regime is governing and the particle is lesser packed and ramified, leading to open, branching fractal aggregates , while in slower rate RLCA is occurring and the agglomerate is more compact.

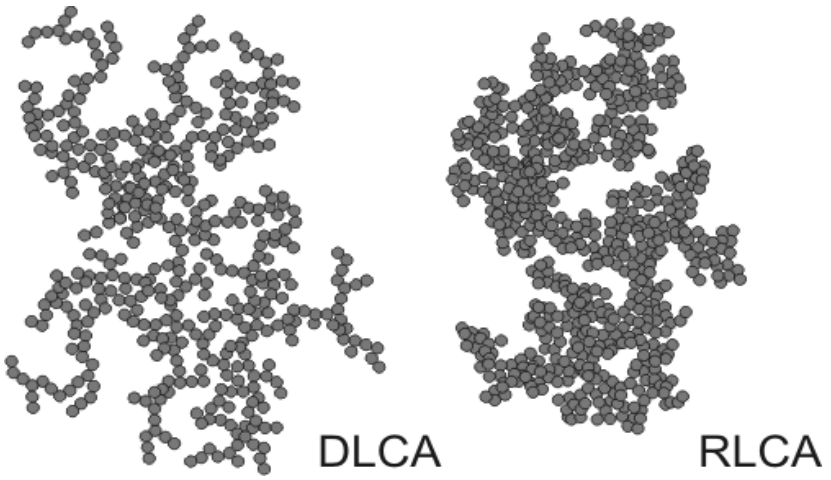

Figure 67.The schematic of DLCA and RLCA [33].

As seen in TEM images in figure 60 and size Distribution graph in figures 62, 64 and 65 and 66, the diesel PM seems lesser compact and has bigger size in comparison with biodiesel. The fuel composition can alter this trend. Fast pyrolysis allows less time for mixing prior to particle formation and thus RLCA will be dominant and amount of oxygen can is accelerate the pyrolysis. Hence

biodiesel is oxygenated fuel it has faster pyrolysis and therefore an RLCA. At next step, the size of primary particles (single particles) is measured. Two images at 50 nm scale were selected for each soot samples and then they were subjected to image processing with different color them in order to visualize single particles and then area and the diameter of PM samples were calculated and the chosen images are depicted in figure 68. One image processing procedure is shown in figure 69 as an example of method. The results of size distribution of single particle area is plotted in figures 70.In this method particles were selected randomly and procedure was done manually. As seen in figure 70, the area of single particles of biodiesel is smaller than the ones from diesel soot samples.

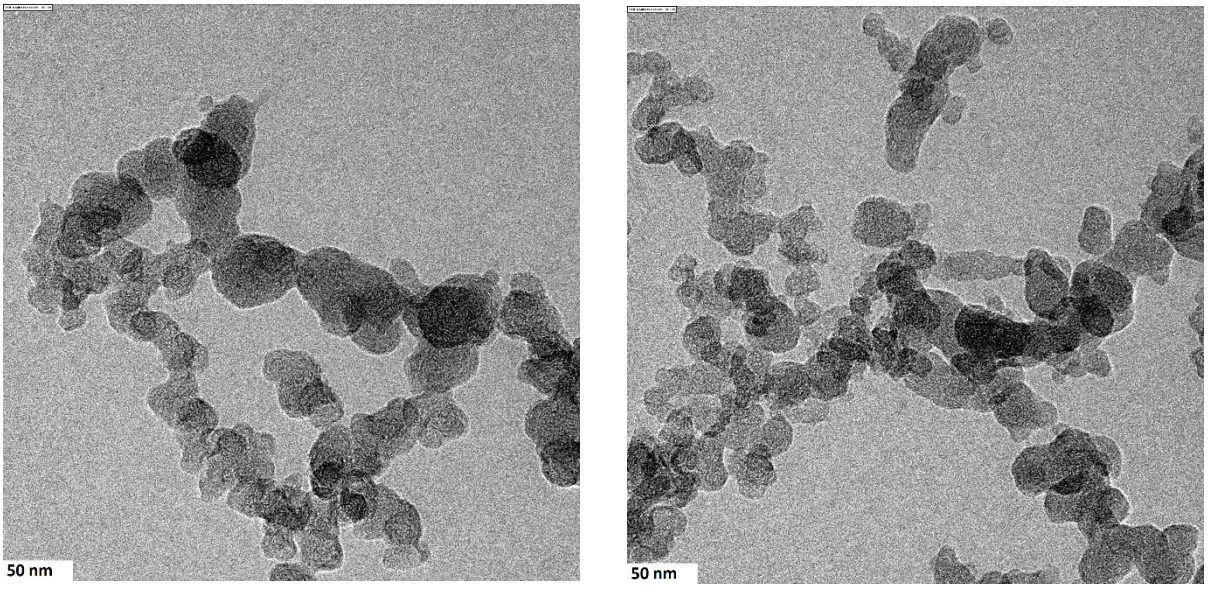

Figure 68. TEM images of soot samples (a) diesel PM, (b) biodiesel PM

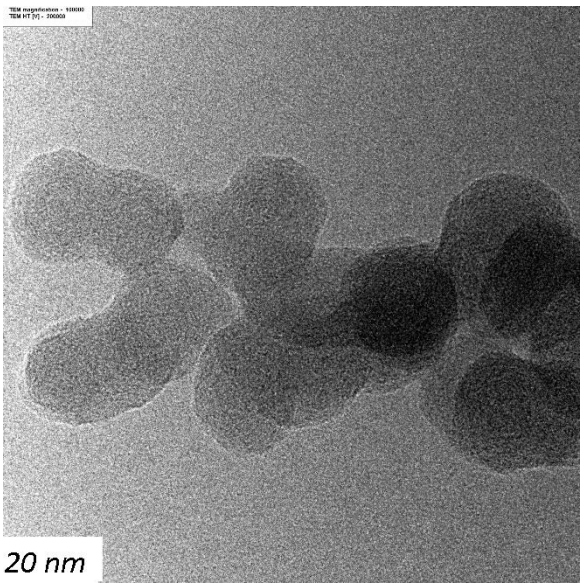

Selected TEM image.

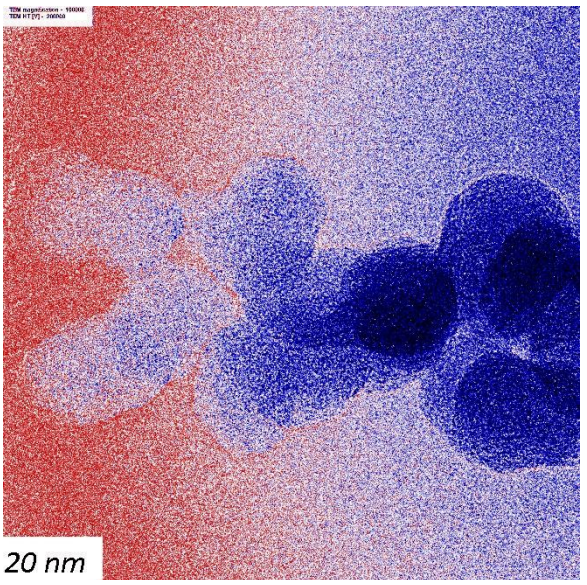

The LUT (look up table) processed image.

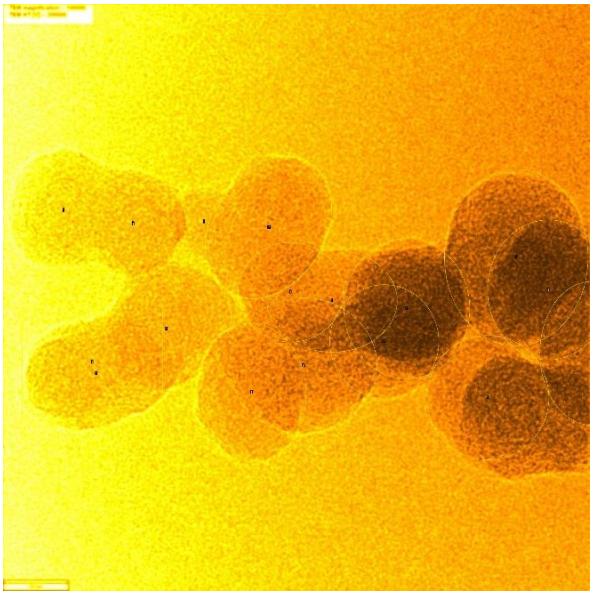

Choosing the single particles after modifying the color them.

Figure 69. The single particle area measurement method. Hand chosen method

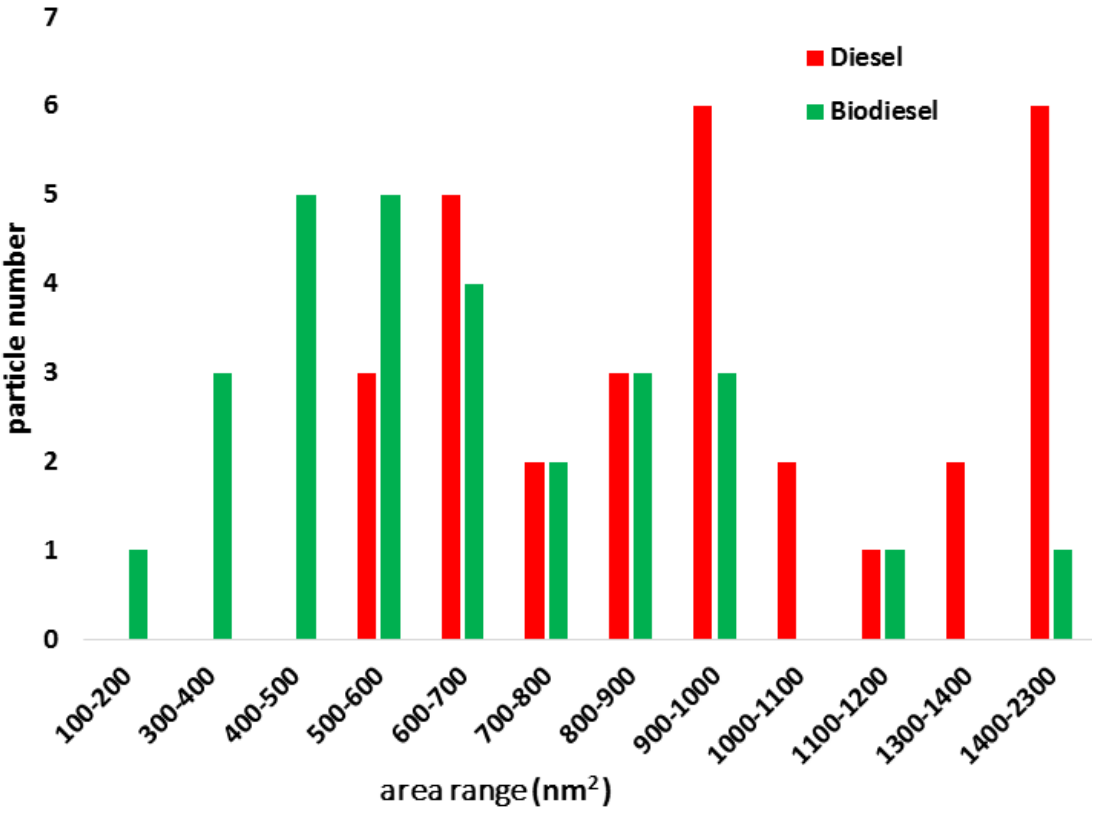

Figure 70. The single particle area size distribution with manual drawing method.

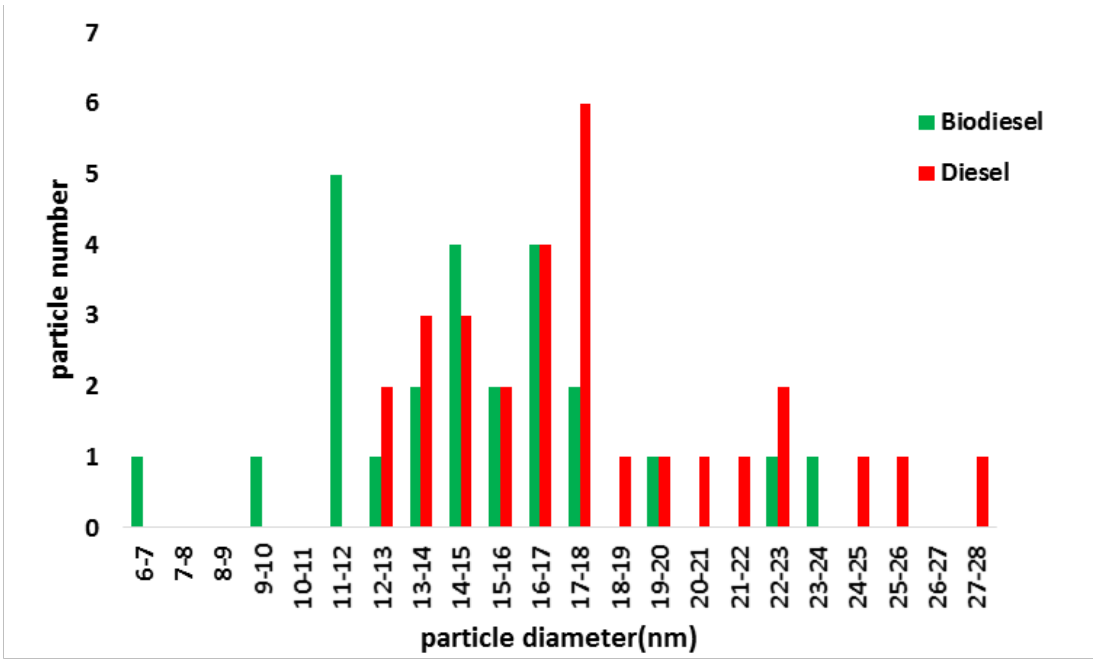

Figure 71. The size distribution of particles diameter.

At this procedure the selected particles were assumed as complete sphere and the diameter of the particles were measured by this assumption and the results were showed in figure 71. Similar to area size distribution, biodiesel PM has lower diameter size. This trend is similar to previous study in our lab [9] but with a different size range. The manual process with ImageJ software could give a general overview about the size of single and agglomerated PM but for better and more precise results another software, Icy, were applied and more details of PM size and shape were obtained Image processing with Icy software is shown in figure 72. Hence the single particles are not real spherical, the assumption of full shpericity, which were applied to ease the calculation may be far from reality. For more exact results it's better to refer to minor and major 2D diameter, X&Y length, max Feret diameter and Chord length. Feret diameter is used to measure the size of a particle or object in an especial direction. Generally it's defined as the distance between two parallel planes restricting the object perpendicular to that direction. This measure is used in study of particle sizes, in microscopic scale, where it is applied to projections of a three-dimensional (3D) object on a 2D plane. This is not a diameter in its actual sense but the common basis of a group of diameters. A chord length is defined by the distance of two points of the contour, measured exactly across the center of gravity of the projection area. This is why all methods of evaluating the chord length imply an evaluation of the center of gravity of the projection area.

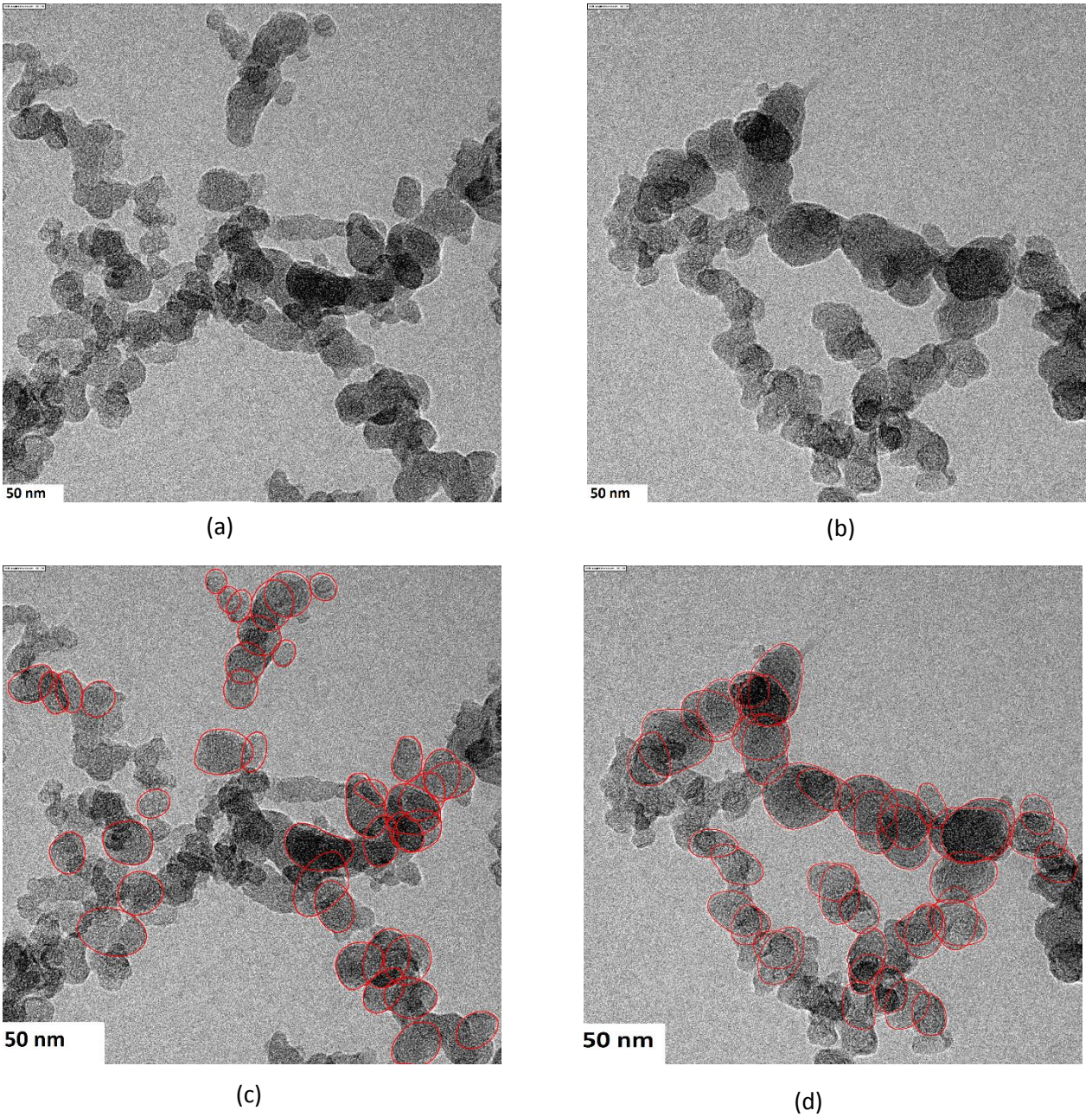

Figure 72. Image processing with ICY software (a) diesel PM, (b) biodiesel PM original TEM image (c) processed image of diesel (d) processed image of biodiesel.

Schematic of chord length and Feret diameter is depicted in figure 73. These results are compared with the average size of selected particles, obtained with Icy software.

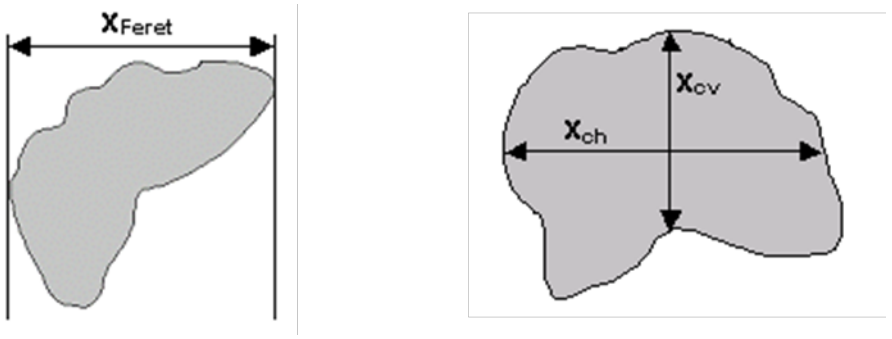

Figure 73. The schematics of (a) Feret diameter (b) chord length.

The particle size in X and Y direction and the average of them was acquired and compared between diesel and biodiesel. The results are shown in figure 74. For X direction biodiesel PM shows increasing trend in size in comparison with diesel but the trend is vice versa in Y direction and diesel PM length overweight the system.

The Feret diameter, chord length and major diameter is compared with each other for each soot sample. The result of this comparison is illustrated in figure 75. Each of the mentioned parameters also is compared with each other between different PM samples. The trend for Feret diameter and major diameter is similar for both samples but for diesel PM more fluctuations between the two mentioned parameter is seen while for biodiesel the trend is much closer to each other. In figure 76 the average of the mentioned parameters for both soot samples is illustrated.

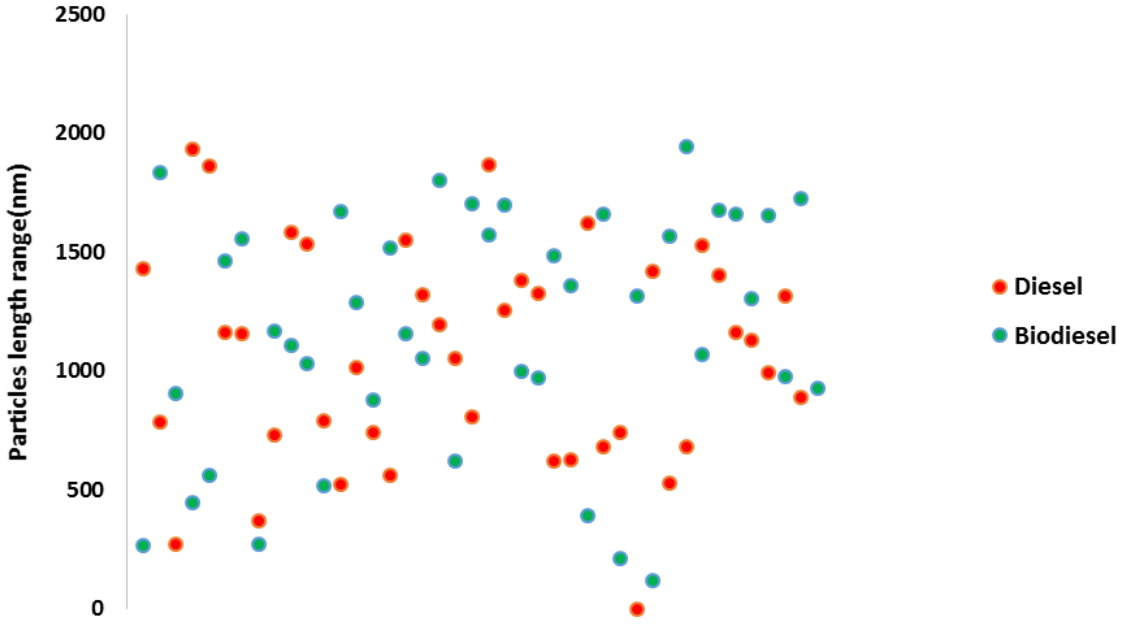
2500
2000
1500
1000
500
0
Particles length range(nm)
Diesel
Biodiesel

(a)

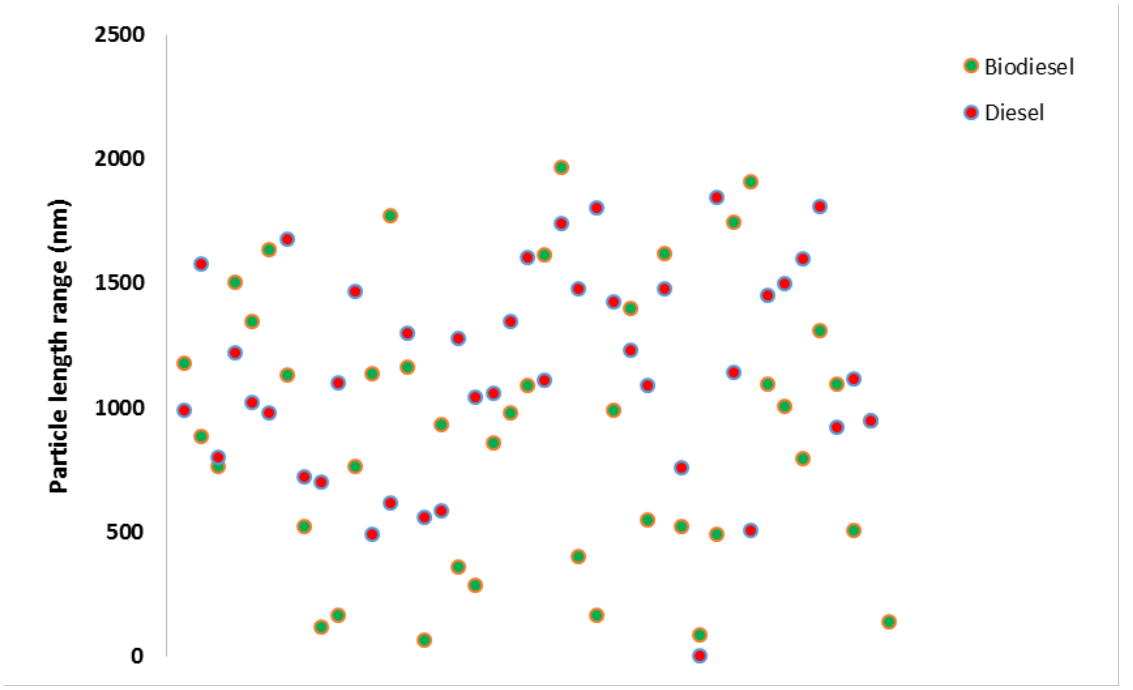
2500
2000
1500
1000
500
0
Particle length range (nm)
Biodiesel
Diesel

(b)

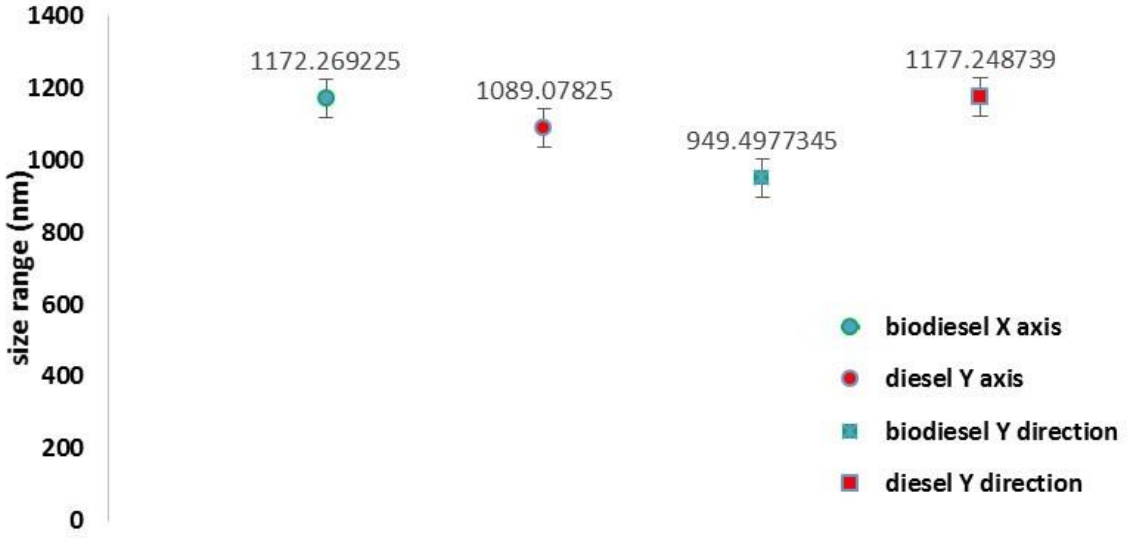

(c)

Figure 74. Size of PM in (a) X direction (b) Y direction.(c) average value.

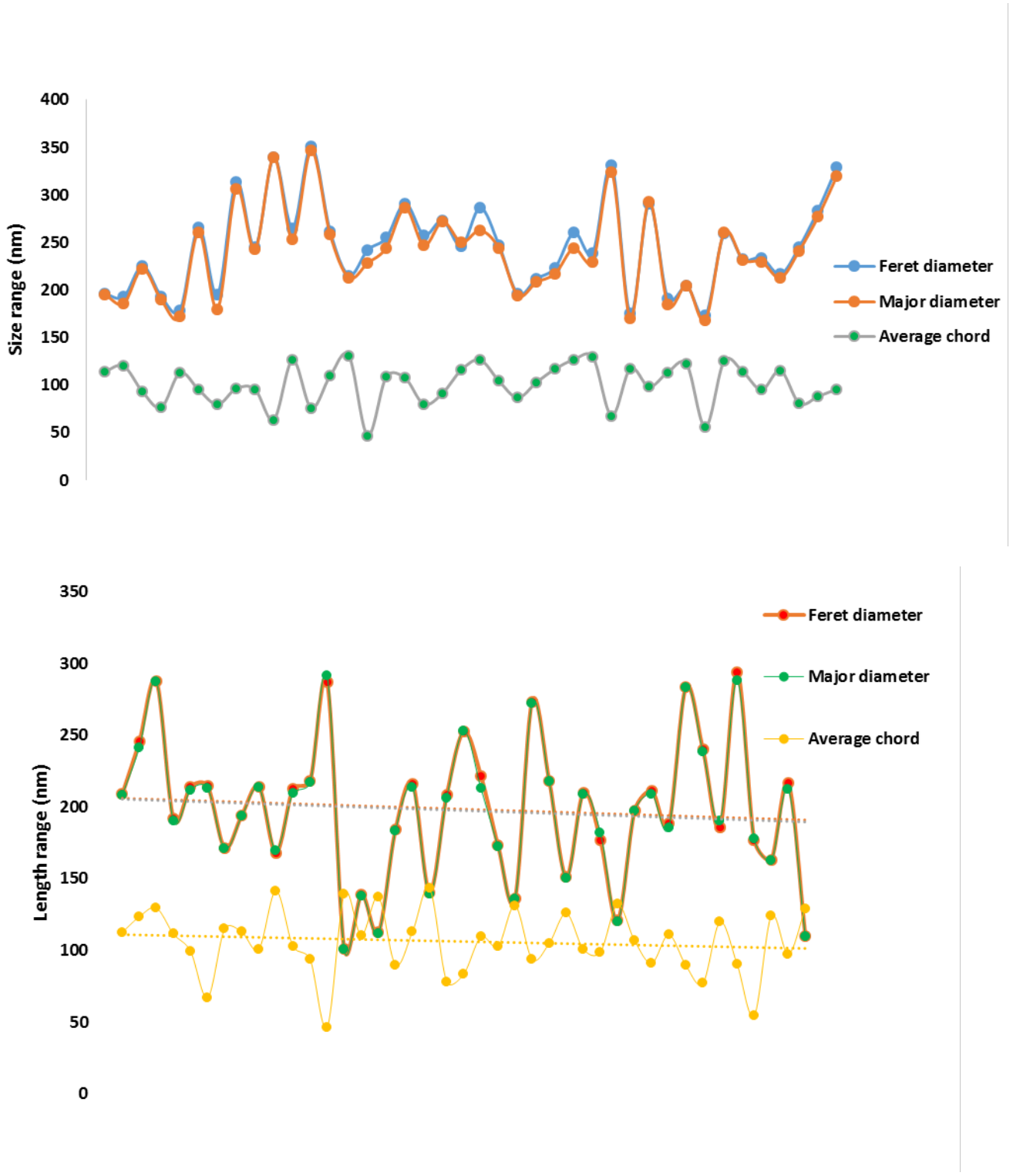

Figure 75. Feret diameter, Major diameter and Average chord length (a) diesel (b) biodiesel

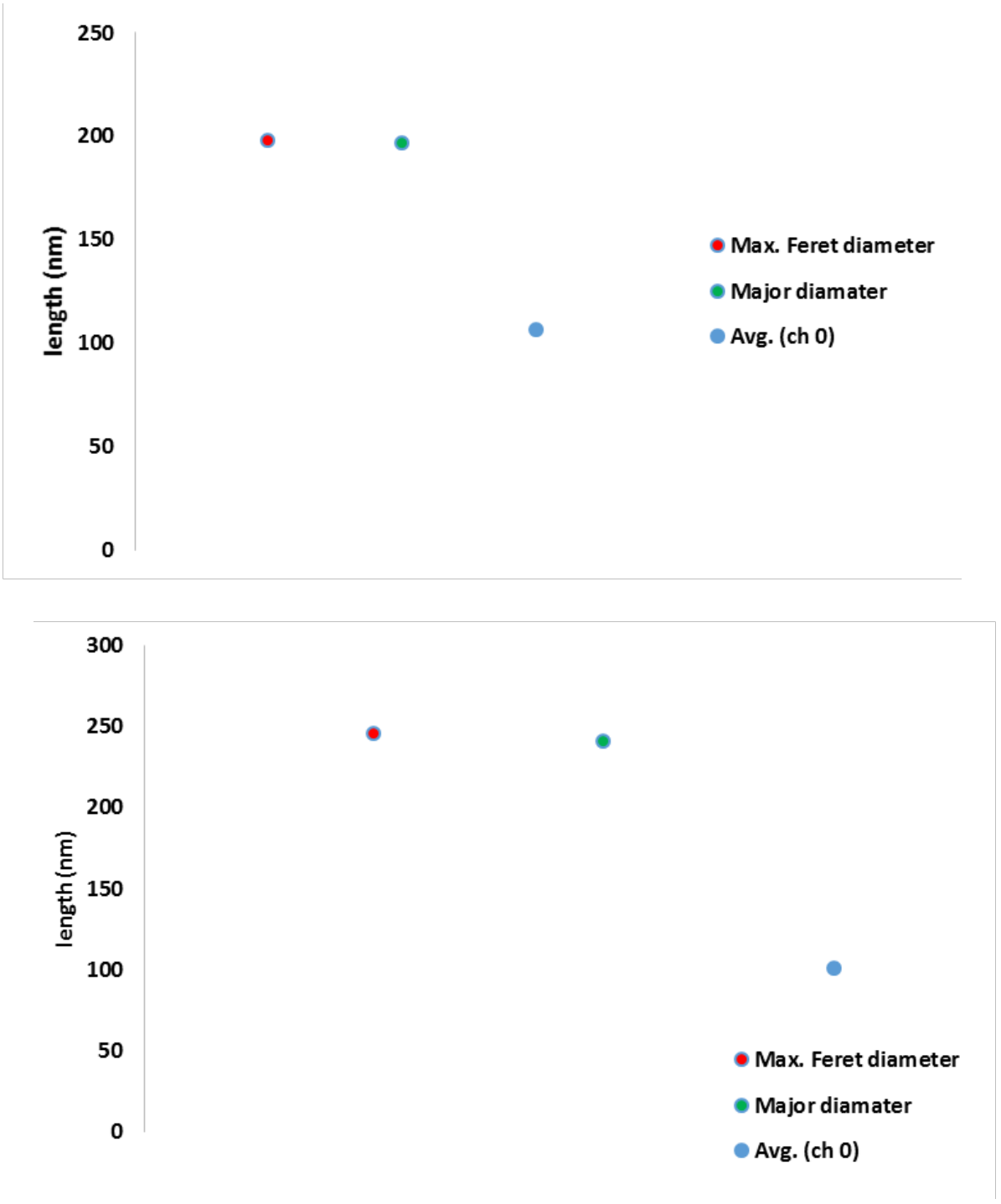

Figure 76. Average of Feret diameter, Major diameter and chord length (a) biodiesel (b) diesel.

The trend of size distribution of primary particles are also alike the agglomerated type and similar reasons can be affecting too. Pyrolysis reactions are generally endothermic resulting in the fact

that their rates are often highly temperature dependent. The rate of pyrolysis of fuel is a function of concentration. One possible reason can be the pyrolysis of fuel. Fuel pyrolysis results in the production of some species which are precursors or building blocks for soot. Soot precursor formation is a competition between the rate of pure fuel pyrolysis and the rate of fuel and precursor oxidation by the hydroxyl radical, OH. Both pyrolysis and oxidation rates increase with temperature, but the oxidation rate increases faster. As biodiesel have more oxygenate component they have faster pyrolysis. It is expected that small amounts of O, O_2 and OH might accelerate pyrolysis since many of the reactions take place by means of a free radical mechanism [34]. Temperature has the greatest effect of any parameter on the soot forming process by increasing all of the reaction rates involved in soot formation and oxidation and the higher load of engine (higher rate of combustion) and higher amount of oxygen of biodiesel can results in more complete combustion and thus higher temperature and faster oxidation and pyrolysis, which results in smaller PM size. Petroleum based diesel is a mixture of many types of hydrocarbons and normally contains no oxygenate composition and a small amount of sulfur so the trend of soot formation, which governs the biodiesel soot formation is not present in formation of diesel soot. Studies shows that sulfur involves in soot indirectly but alters PM mass by oxidizing and attaching to soot particles, which ends in increase of PM size and mass [34]. The diesel fuel is consists of sulfuric components and thus this can be a reason for larger size of diesel PM hence sulfur in the fuel is oxidized to SO_2, which can combine with unburned hydrocarbon and become absorbed by neighboring

soot particles. Therefore, the PM from biodiesel, which is smaller, can oxidize faster than diesel PM. However, in order to be sure about the effect of these elements especial experiments and investigations is needed which is out of scope of this research and can be investigated in future projects.

Chemical and Physical relation and PM shape

The chemical characteristics, which were discussed earlier are dominant at lower temperatures, however at higher temperature most of the impurities oxidize or vaporize and the carbonaceous part of PM remains, thus the chemical features lose their importance and physical characteristics of PM will play a key rule. At this study it's tried to relate the chemical parameters of soot oxidation to the physical shape of soot particle. The reaction order of the carbon and shrinking core model have impact on each other and the spherical shape of the soot particle. As the reaction order, n, increases the importance of that element in reaction and as its higher the reactivity.

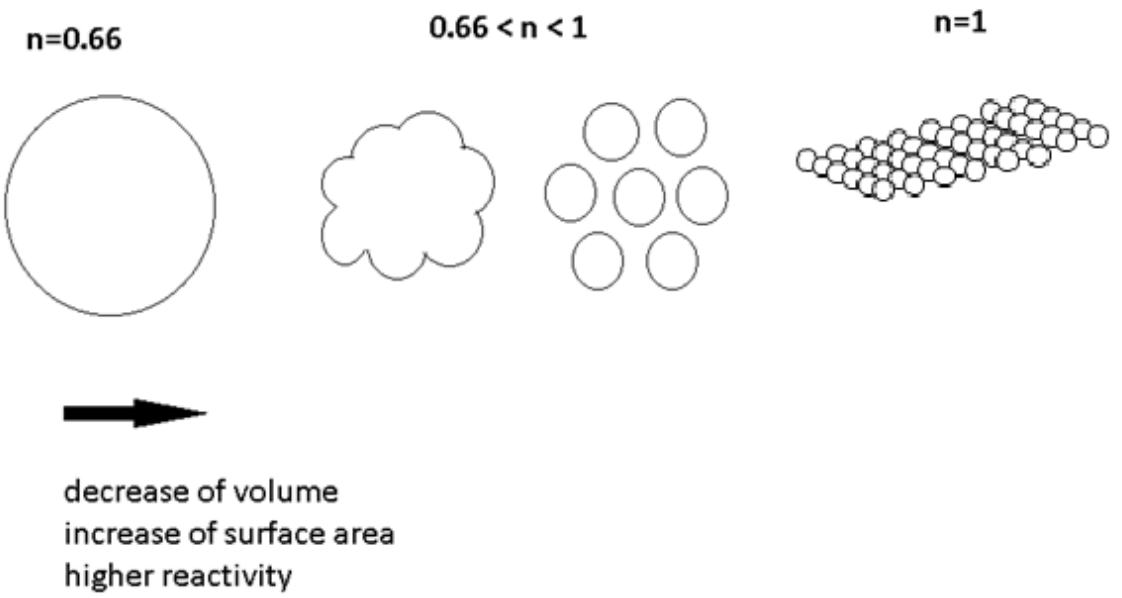

Figure 77. Schematic picture of reaction order and PM reactivity.

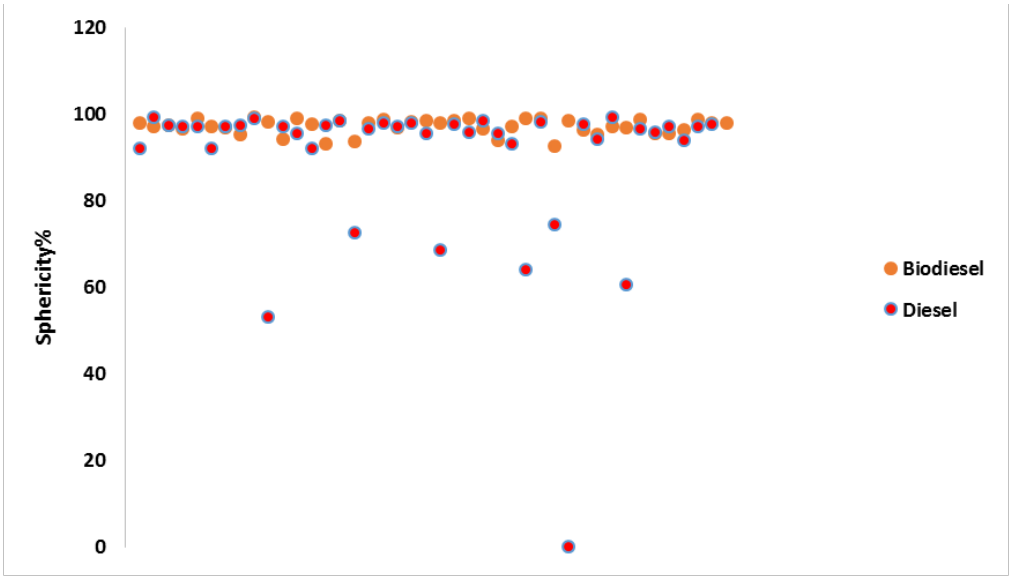

(a)

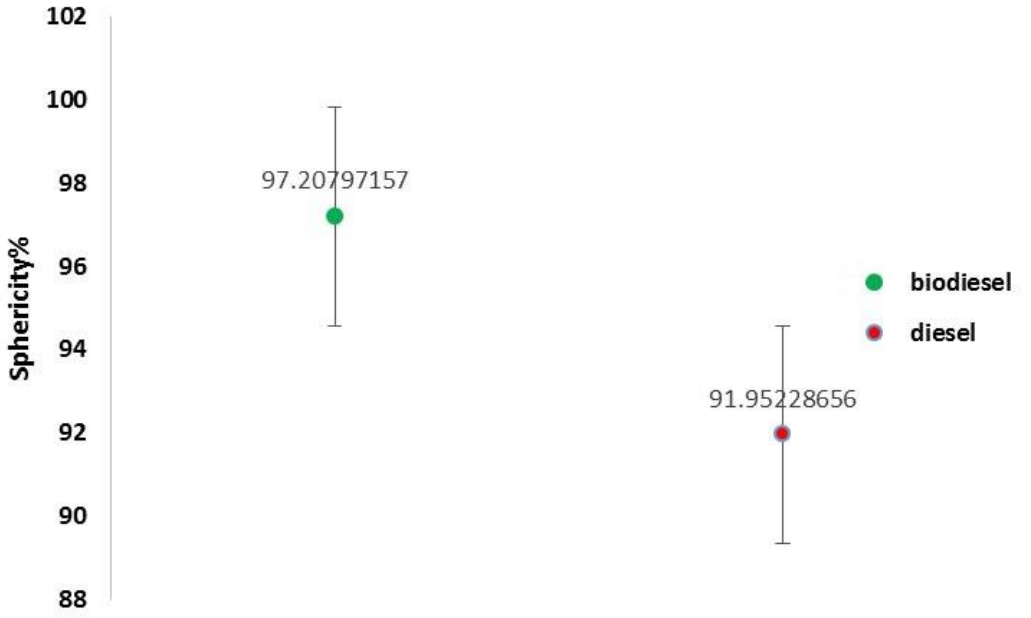

(b)

Figure 78. (a)Results of sphericity of particles.(b) Average of sphericity.

The *n* value is between 0 ~1 and as it's closer to 1, it means higher reactivity is possible, and in unity, all the element (here carbon) will be consumed. As mentioned in previous section, the *n* value for biodiesel soot is 0.74~0.76 and for diesel is 0.56~0.57 , while the shrinking core model value is about 0.63 and values higher and lower than this can indicated an incomplete spherical shape of soot. This trend is schematically depicted in figure 77. It's also tried to measure the sphericity of particles with Icy software and the results were exhibited in figure 78. Sphericity of particles is defined as ratio of the sphere surface to the real surface of the particle which means for complete spherical PM the sphericity is equal to 1 and lower for other different shapes. In other words The sphericity, S, is the ratio of the perimeter of the equivalent circle, P_{EQPC}, to the real perimeter, P_{real} and is defined by formula below with regard to figure 79:

$$S = \frac{P_{EQPC}}{P_{real}} = \frac{2\sqrt{\pi \cdot A}}{P_{real}}$$

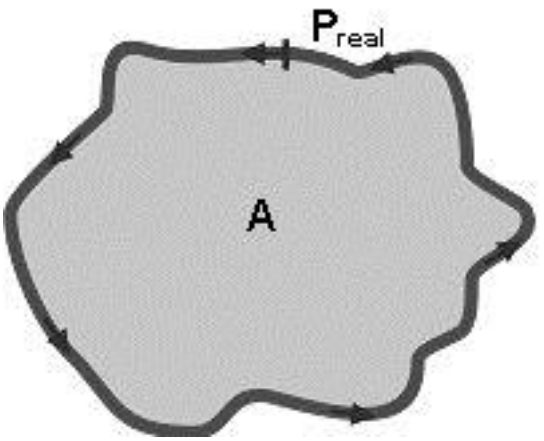

Figure 79.Schematic of a real PM and its perimeter.

As seen in figure 78, sphericity of biodiesel selected particles have a constant trend and most of the particles have similar sphericity and closer to 1 but diesel PM shows lesser sphericity for some of particles and the sphericity of some particles (about 25% of

particles) are far below 1.

This trend seems to be parallel with the reaction order, *n*, but yet it may need more investigation for repeatability. The average sohericity of biodiesel is 97% while for diesel it's about 92%.

Nano structure carbon platelet

For investigation of carbon platelet of the soot samples in nano scale, the image processing was done, with ImageJ, to obtain the skeletonized images of TEM images and then the length of the carbon platelets (fringe length) and the size distribution of them was acquired. The example of image processing and the results are shown in figure 80, 81 and 82. The carbon platelet of biodiesel is shorter and has more unique shape and they more twisted in comparison with diesel, as can be understood from figures 81 and 82. This trend is match with the compactness trend of the PM samples. As seen in figure 82, the platelet of biodiesel are closer to each other and thus the PM is more compact in comparison with the diesel PM and the order of platelet formation is more erratic for biodiesel PM while for diesel PM its seems more uniformed shape. Size distribution also has similar trend with our previous study [9] in which a Matlab image processing code was used to calculate the fringe length.

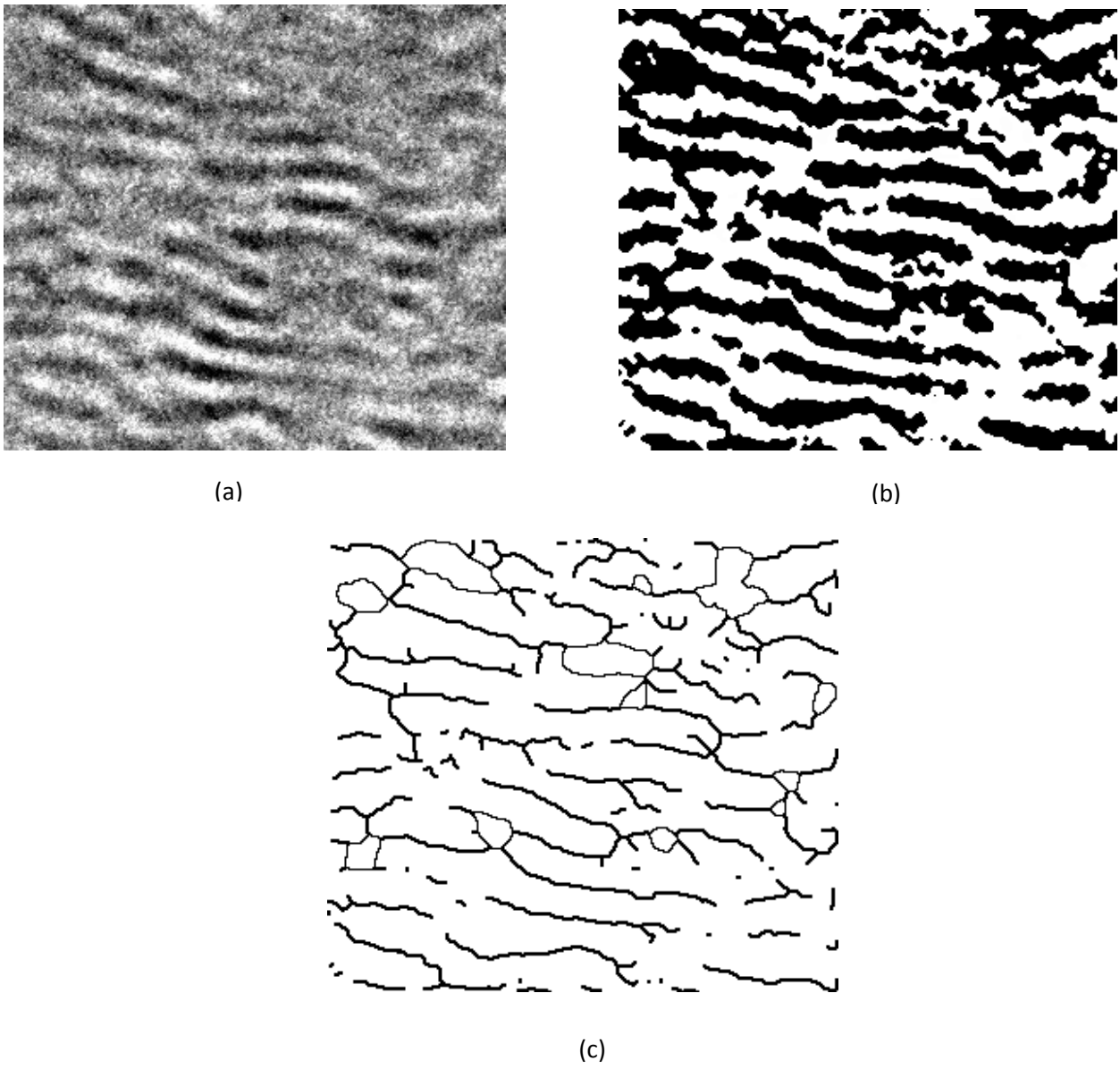

(a) (b)

(c)

Figure 80.The image processing of skeletonizing images for study of carbon platelets (a) selected TEM image area (b) Binary image of selected image (c) The skeletonized image.

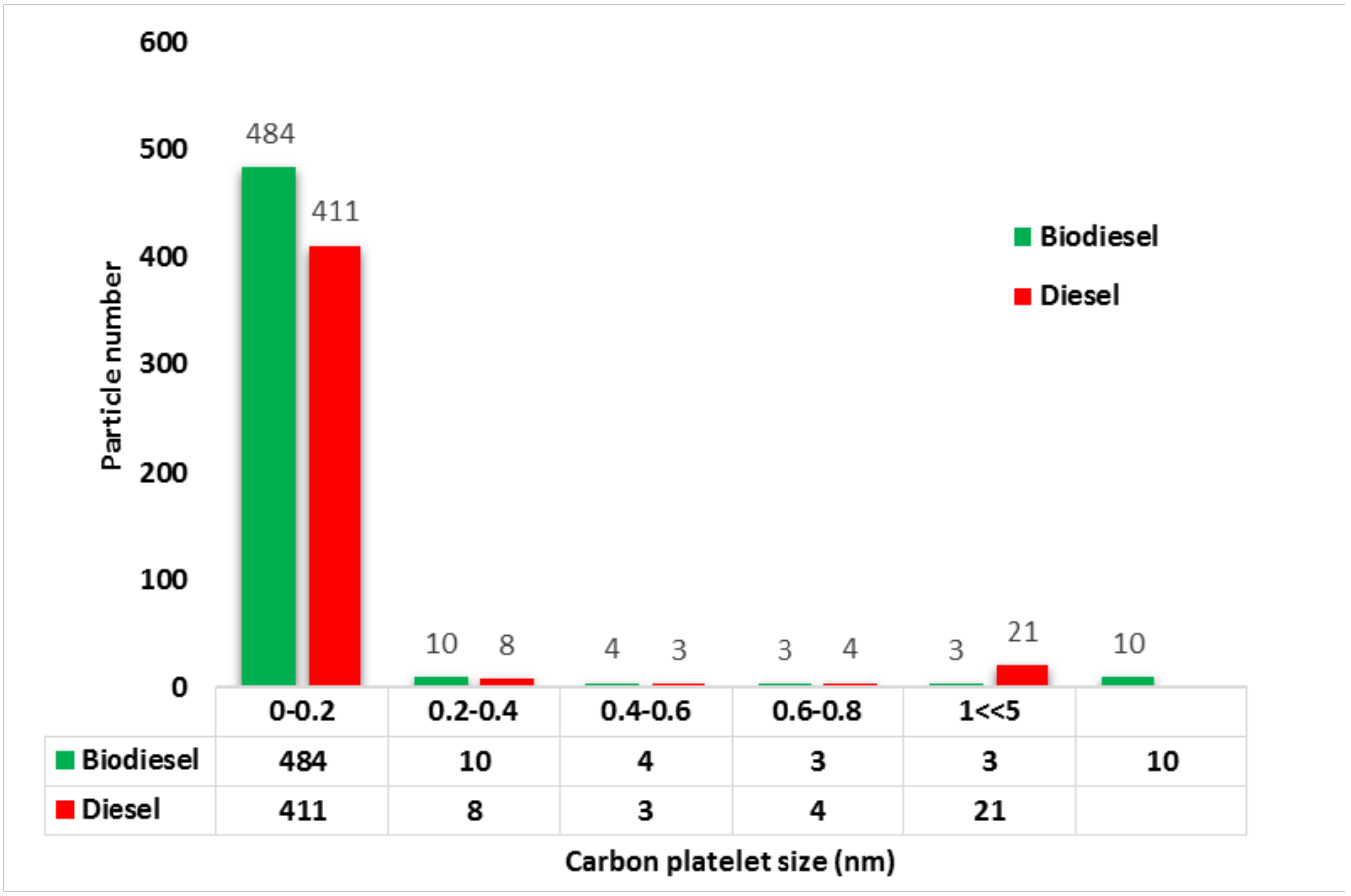

Figure 81.The size distribution of carbon platelet length.

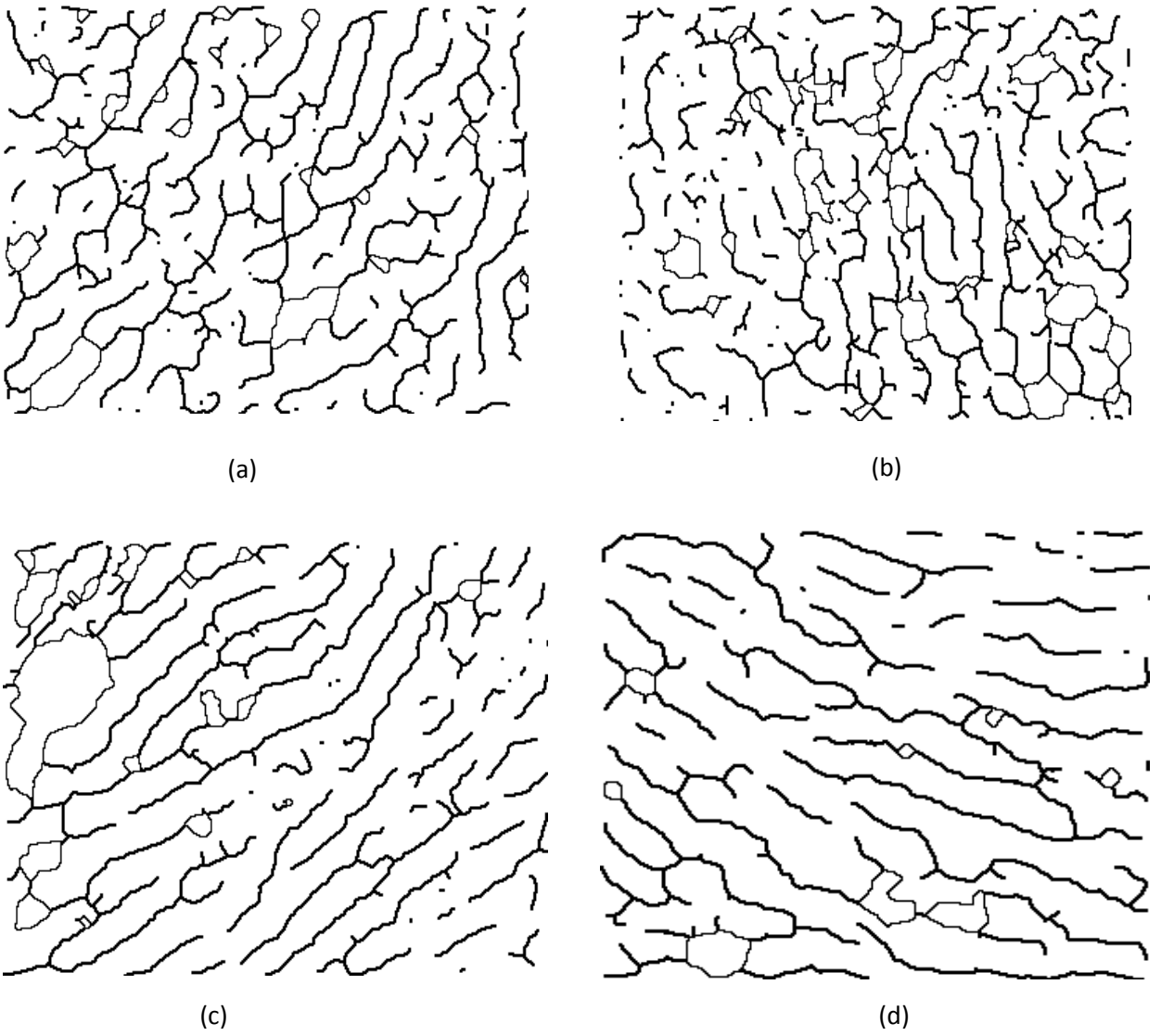

Figure 82.The skeletonized image samples from image processing,(a) ,(b) biodiesel carbon platelet (c)and (d) diesel carbon platelet.

In order to have a better idea about the Nano particles, the inner shell of single particles from diesel and biodiesel were subjected to image processing. The inner core of particles were approximately studied and skeletonize image of fringes of carbons of both diesel and biodiesel soot were obtained. In figure 83 and 86 the procedure

of this measurements is pictured. The inner core diameter of diesel soot is 11.02 nm in X direction and 13.93 nm in Y direction.

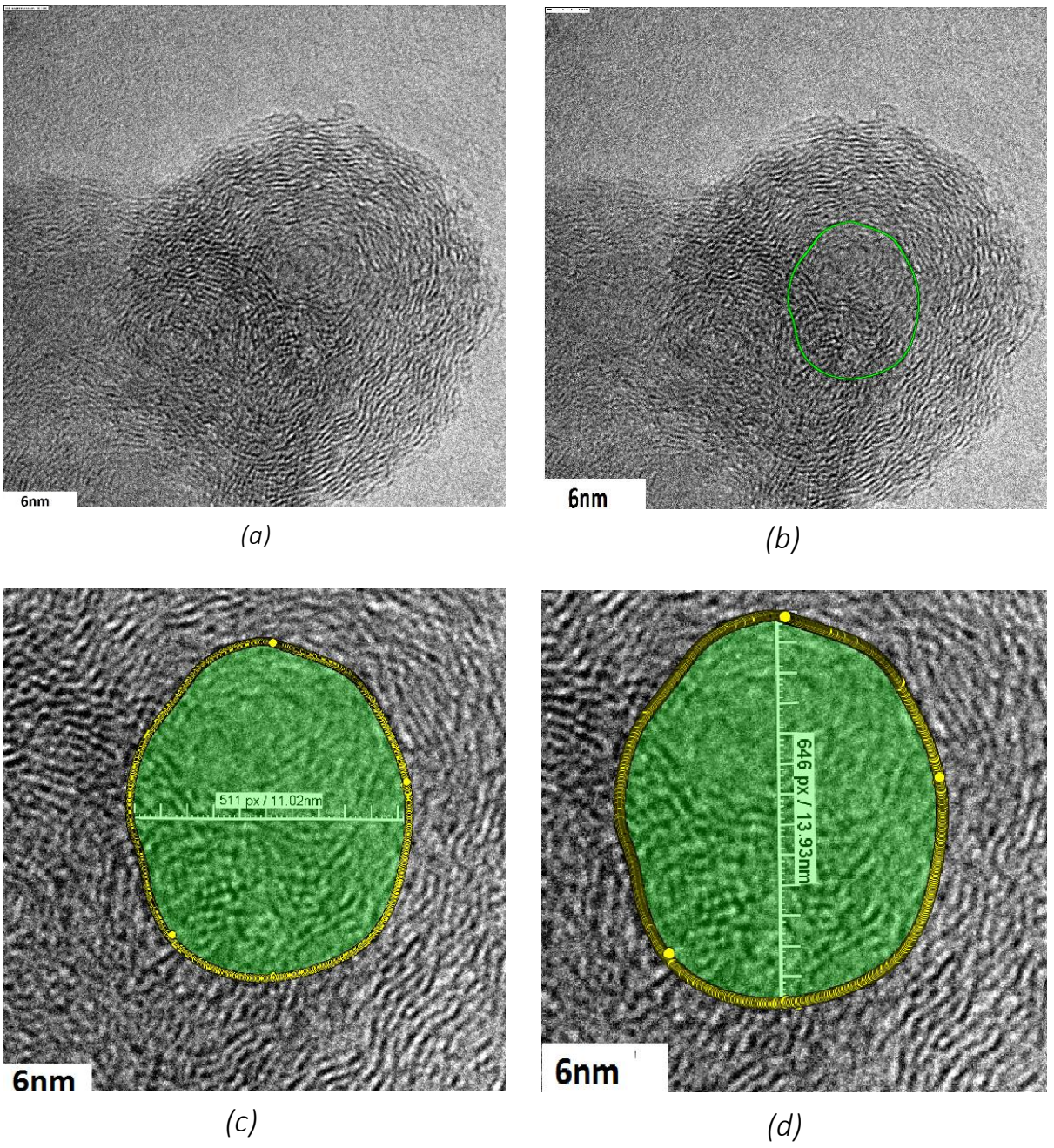

(a) (b)

(c) (d)

Figure 83. Inner shell of diesel PM. (a) original TEM (b) selected inner core area (c) length in X direction (d) Length in Y direction.

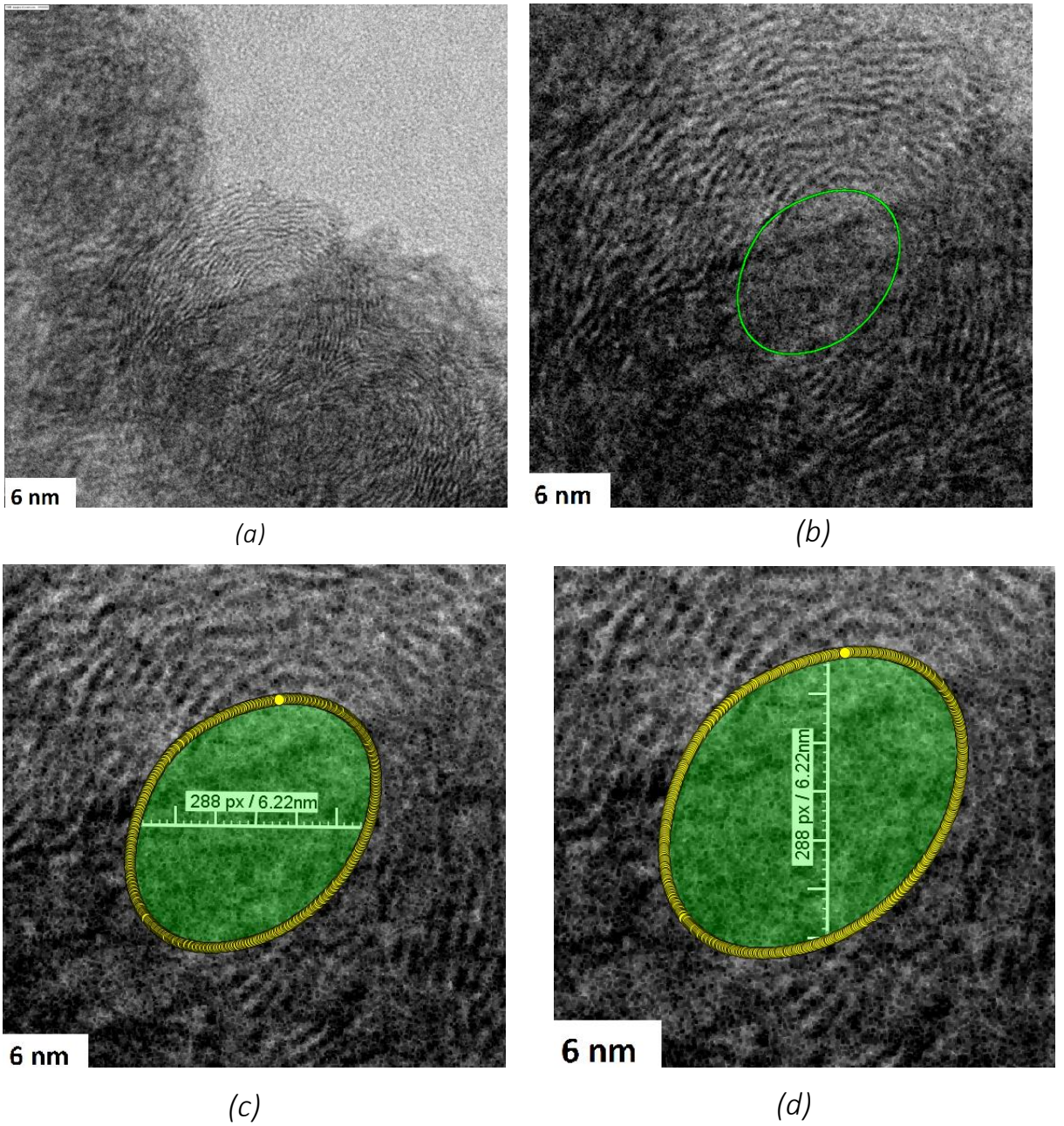

Figure 84. Inner shell of diesel PM. (a) original TEM (b) selected inner core area (c) length in X direction (d) Length in Y direction.

For biodiesel, the size in both directions is equal and almost half of diesel. The size in both direction 6.22 nm. The skeletonized images of the inner cores of both samples were also obtained and illustrated in figure 85 and figure 86.

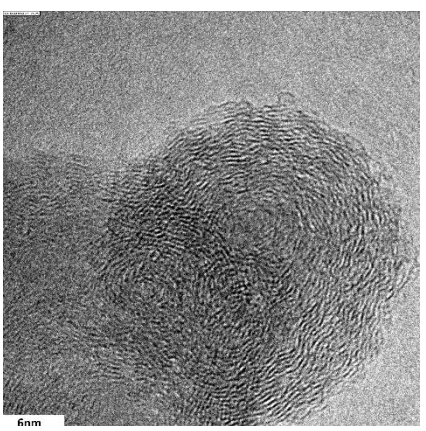

(a)The diesel PM single

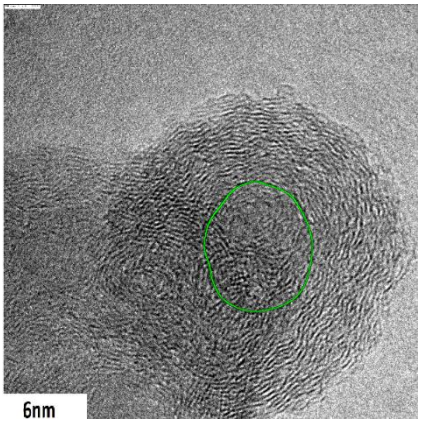

(b) Approximate inner core particle

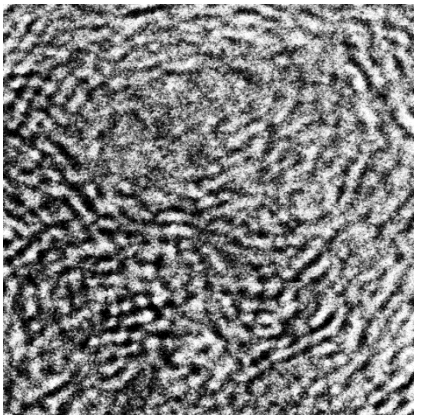

(c) Zoomed and separated of selected

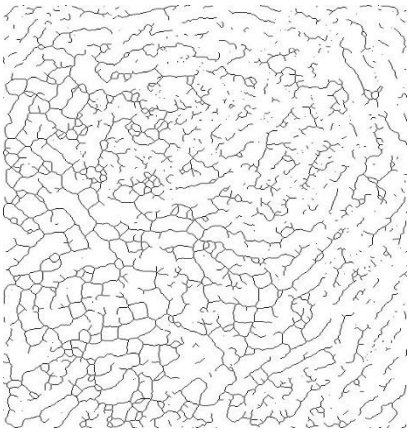

(d) Skeletonized image of selected part

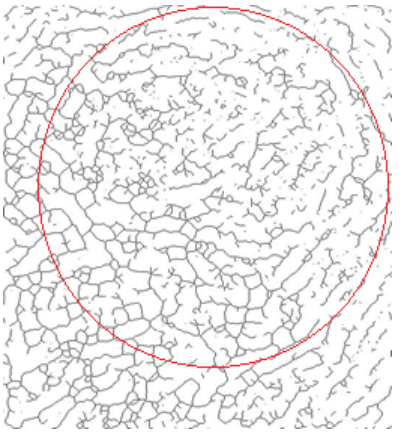

(e) Approximate fine particle

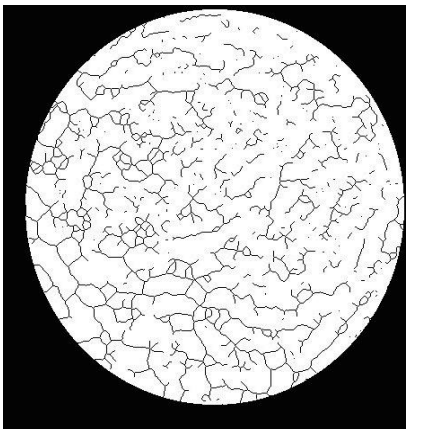

(f) Skeletonized image of selected part fine particle

Figure 85. The procedure of making skeletonized image of inner core of diesel PM.

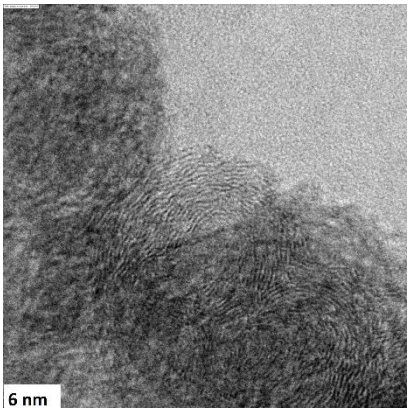

(a)The diesel PM single

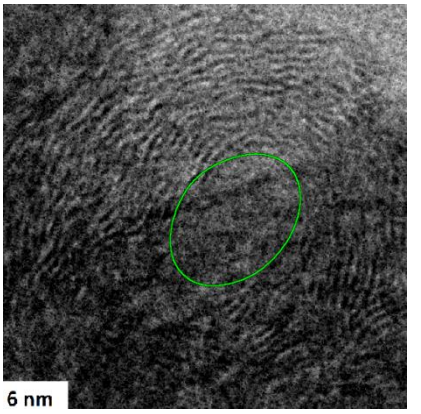

(b) Approximate inner core particle

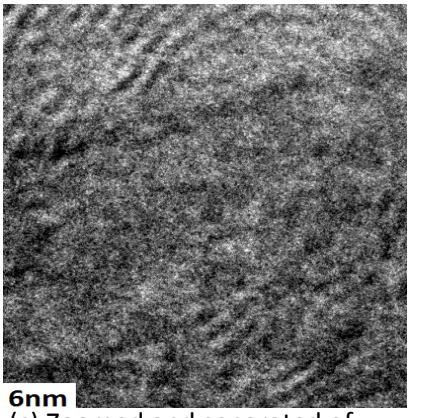

(c) Zoomed and separated of selected zone

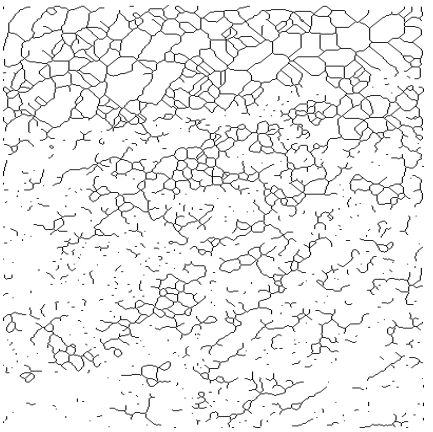

(d) Skeletonized image of selected part

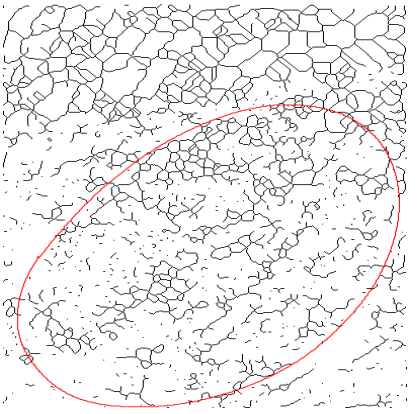

(e) Approximate fine particle

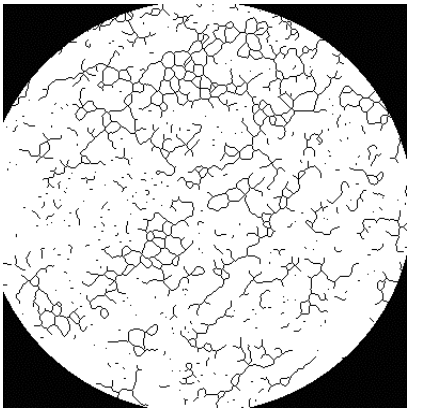

(f) Skeletonized image of selected part fine particle

Figure 86.The procedure of making skeletonized image of inner core of biodiesel PM.

The peripheral region of particle (surface layer) is made of crystalline structure of carbon. The inner structure consist of a nuclei particle, at the chosen pictures, which consists of several small carbon platelet (fringes), formed in a compact condition. In core structure of both diesel and biodiesel PM, carbon platelets have turbostratic formation. The diesel PM inner core shows more uniformed and compact structure in comparison with biodiesel but hence none of the PM samples have a pure single particle, this

compactness level can't be compared correctly. This inner nuclei or fine particle, is covered by the inner core, which consists of several carbon chain, in a better ordered form, but still not well arranged and can be considered as amorphous structure. The bending structure of these fringes may indicate that they may not made of 6 carbons ,C_6 , but also a five carbon structure [35] and development of this inner core stops the growth of nuclei fine particle. The outer core, is made up well organized carbon fringes and has crystallites structure and has a uniform pattern and it can be seen in figures 82, 83 and 84. This is can be due to surface reaction and condensation of small chemical species. The pyrolysis can play a key role in the difference of the structure of these parts. The chemical elements, which are responsible for generation of inner and outer shell would be different due duration of fuel pyrolysis. The inner core is formed by nucleation of none planar molecules and the growth, while for outer shell, the formation is governed by molecules, radicals or ions, consists of two to four carbon atoms, which leads to surface reaction boost up and promotes the polycyclic growth of the graphitic crystallites.

A more amorphous structure is seen in biodiesel core in comparison with diesel soot. As the amorphous structure increase the reactivity trend also increases [31] and therefore this can be another possible reason for better oxidation of biodiesel PM. At lower temperatures, soot oxidation begins from the inner core towards the outer surface, possibly due to the higher reactivity and higher active surface area of the amorphous part rather than the graphitic part therefore, by increasing the amorphous content of soot through the reduction of crystallite thickness, its reactivity can be increased [31].So this may enable the biodiesel soot to oxidize easier and faster, in lower

temperature in comparison with diesel soot but it shall be considered that the reasons which were mentioned above each one need specific and independent study to be sure whether they are affecting in this case or not.

4.4 Filtration and regeneration behavior

Soot production rate

The rate of soot production has a key role in DPF filtration trend and this feature is also the main outcome of diesel and biodiesel difference in emission. The measurement of soot production rate usually requires high tech and high precision devices which was not available for this project, thus it was tried to design a system based on the available facilities which is able to provide us an overview about the soot production rate of both fuel samples. A system based on filtration system was designed with air filter material. This filtrations system was attached at the end of the exhaust pipe and every 60 seconds the filter was changed. The filters were weighted before and after test and the difference of the weight was accepted as the rate of soot production per minute. The average rate of soot production for diesel is 0.224 (g/min) and for biodiesel this rate was 0.131 (g/min) which is almost twice lower than diesel. The pictures of filters for both fuel samples is shown in figure 87.

In picture (a) and (b) it's clearly seen that diesel has higher soot production and in picture (c) also the both graphs apparently show the difference of soot production rate which is dominated by diesel within 1000 seconds.

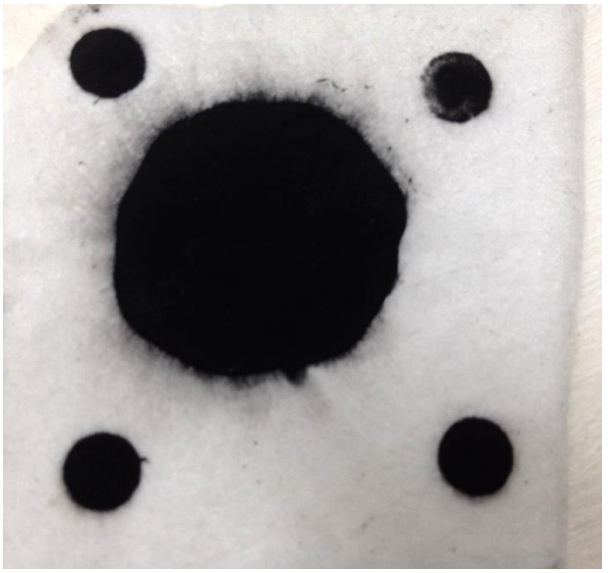

(a)

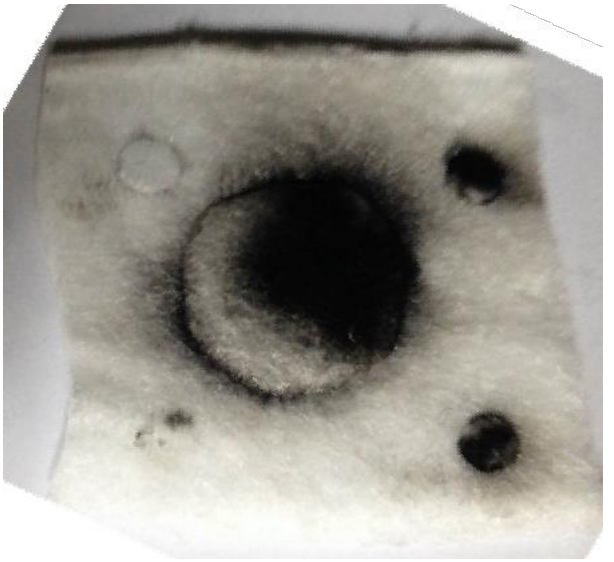

(b)

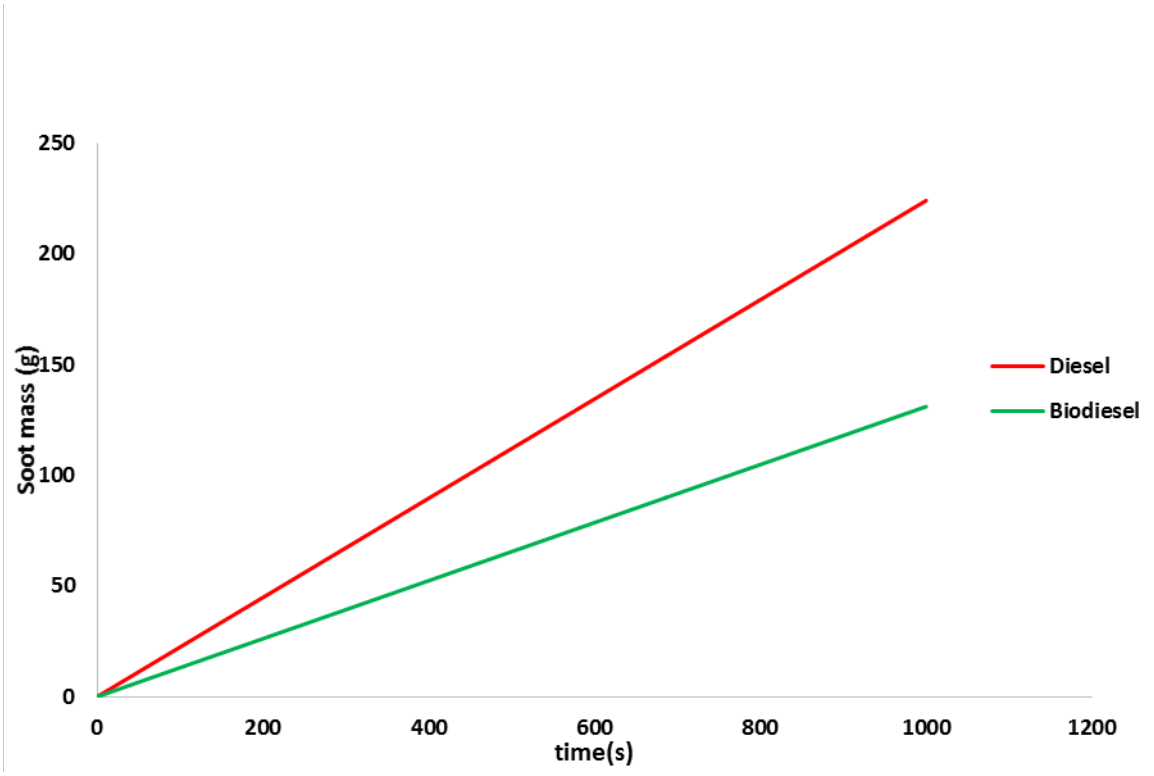

(c)

Figure 87 .The results of soot production rate measurement (a) diesel (b) biodiesel (c) comparison of soot production in an equal time.

Filtration

In order to investigate the filtration, the permeability of the DPF was tested by a vacuum pumps, 50 (lit/min). The test tube temperature was set to be 200 ◦ C and the pressure drop was measured. The results are shown in figure 88.

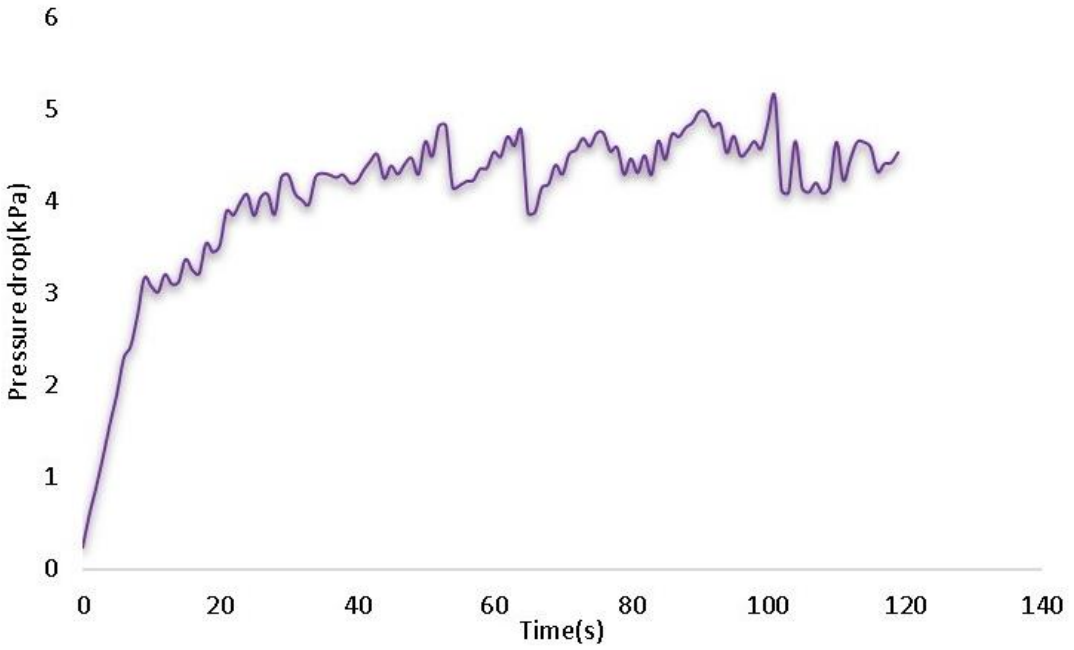

Figure 88. The permeability of the DPF vacuum pump.

The graph shows that the pressure drop without engine run is within the range of 3 to 5 kPa. The superficial velocity of the pump in front of DPF is 6.41(m/s). The diesel and biodiesel were tested in similar condition, as mentioned in methodology chapter. It shall be considered that the controlling parameters at this experiment are pressure drop, time, and temperature and soot mass accumulation. The soot mass and the pressure drop can't be kept constant at same time so at first phase the equal pressure drop was set as the reference of comparison. So the fuels were burnt until pressure drop, caused by diesel PM and biodiesel PM reaches almost the same level and then comparison and regeneration were done.

For diesel fuel the test of trapping was done three times to ensure repeatability and results were shown in figure 89 but for biodiesel, due to lack of fuel, only one time trapping was done and the result of filtration trend of DPF is depicted in figure 90. Figure 89 shows that the filtration trend of diesel fuel is not significantly different in all three conditions. As depicted in figure 90, the trapping time for biodiesel is much longer than the one with diesel fuel about 6 times in order to reach same level of pressure drop as diesel. This is an indication of better filtration behavior and enables the system to work for a longer period of time when biodiesel is applied. This can be due to faster soot production rate of diesel fuel and in figure 91 it's tried to show the pressure drop trend with regard to soot accumulation rate. Due to more aromatic content and absence of oxygenated components in diesel fuel, the combustion produces higher amount of soot in comparison with biodiesel, in an equal period of time. While for biodiesel, cleaner combustion, which can be the result of oxygenate molecules of biodiesel and thus more complete combustion. So it needs a longer time for trapping due to lesser soot production rate of biodiesel. Although at the end of filtration more amount of trapped soot from biodiesel is trapped, with regard to longer filtration time, pressure drop level is still same as diesel filtration test. This trend may be an indication of more porosity of biodiesel PM too but more investigations is needed for obtaining accurate results about porosity.

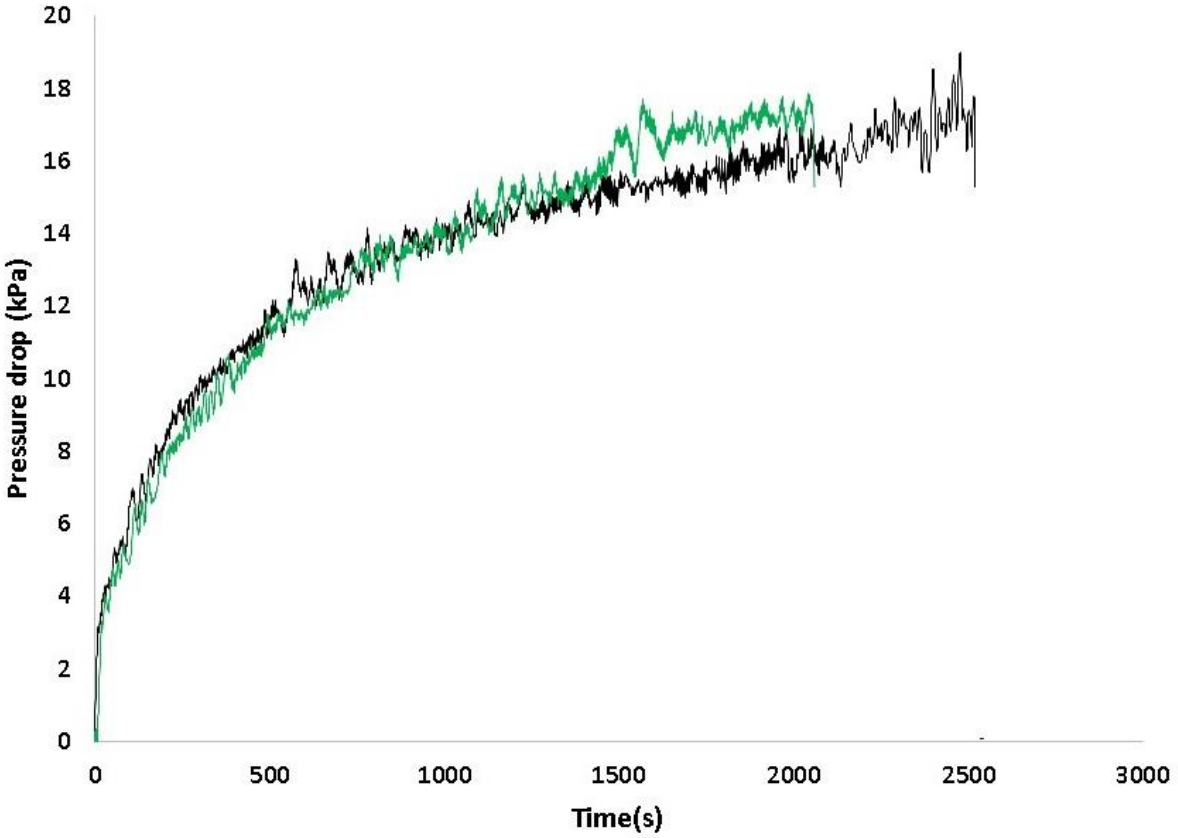

Figure 89. Repeatability of diesel filtration trend.

Smaller size of biodiesel PM may enable it to settle in the deeper pores of DPF and thus surface filtration becomes slower which can lead to longer filtration time and absorption of higher amount of PM. Due to bigger size of diesel PM, as discussed before, the soot aggregation of the surface of DPF porous media has a higher rate and this may lead to faster surface filtration which can prevent PM to be trapped in the inner pores and block the air flow(exhaust flow) path faster and thus ends in higher pressure drop level in a shorter time with lesser amount of trapped soot. Meanwhile, the oxidation of trapped PM inside the DPF by exhaust temperature is more probable for biodiesel PM due to higher reactivity of biodiesel PM, which is already discussed in earlier sections.

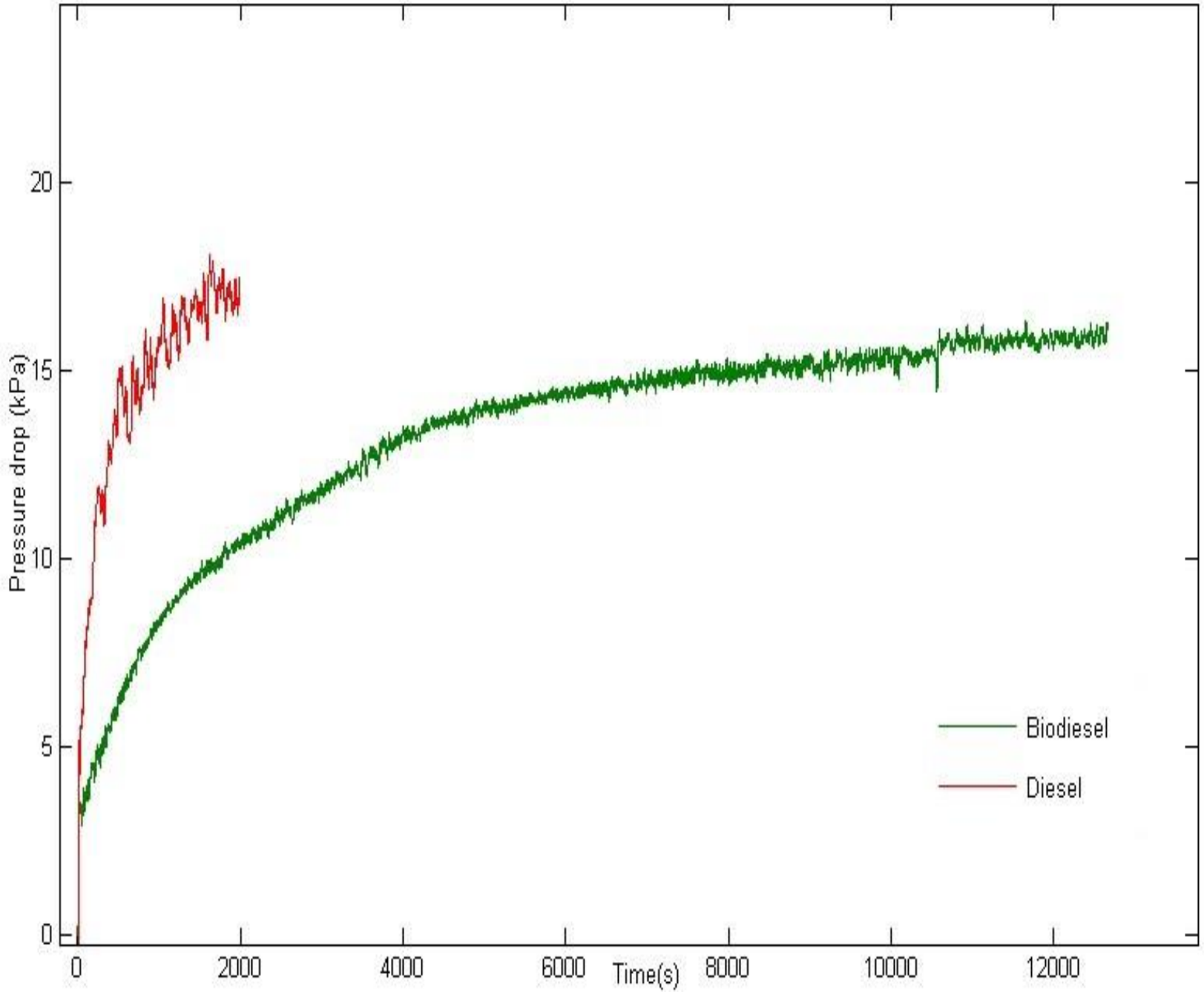

Figure 90. Regeneration of DPF for both diesel and Biodiesel PM.

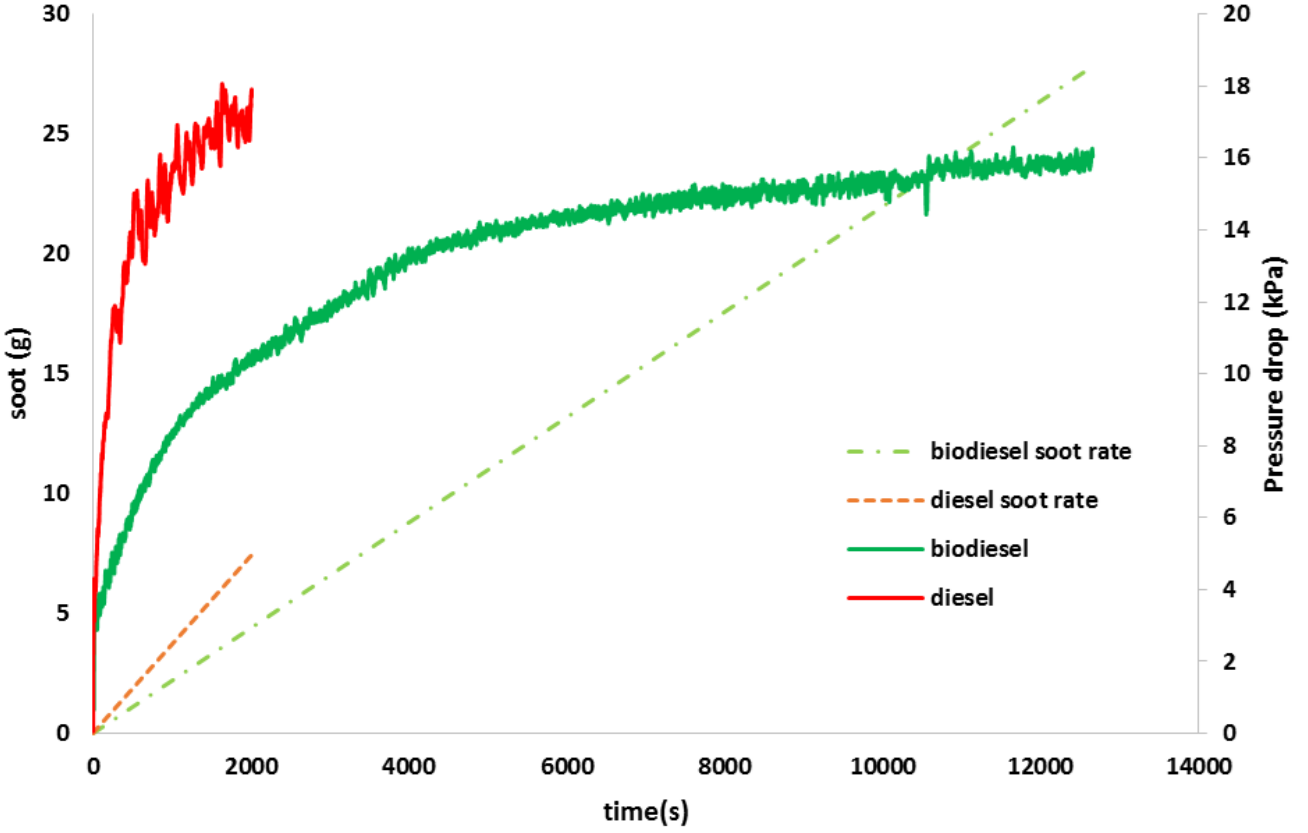

Figure 91. The comparison of pressure drop and soot accumulation.

In order to have a general view about the soot accumulation in DPF ,it's been tried to estimate the different phases of filtration based on soot generation and pressure drop and then the results were shown in figure 92 for diesel and in figure 93 for biodiesel. As seen in the figures, the slopes of different parts of the graph indicates the rate of soot accumulation. For biodiesel, the trend of soot accumulation is much slower, thus the longer time and more fuel is needed to be used and therefore the slop of the graph, which is indicator of soot accumulation rate has a slower trend.

But for diesel, as seen in figure 93, the trend is much faster and the graph moves turns to linearity and at the end of soot cake layer formation phase about 7.44 grams of diesel soot is trapped while for

biodiesel the final estimated amount of soot mass 27.88 grams, which is about 3.75 times more than diesel. For better understanding, both of the graphs were depicted in one picture and illustrated in figure 94. The trend lines in the graphs show the rate of soot accumulation inside the DPF.

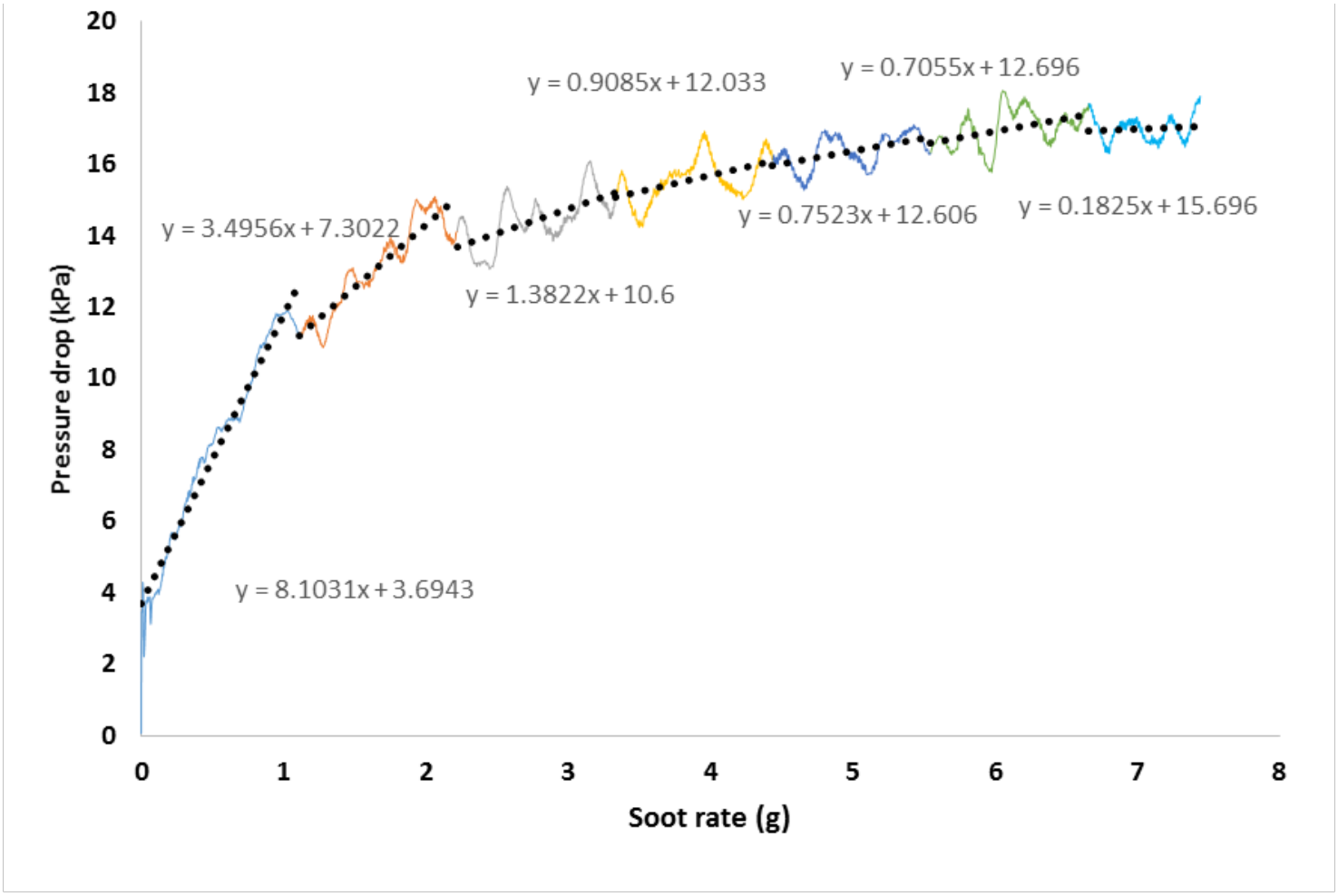

Figure 92 .Filtration estimation of diesel fuel.

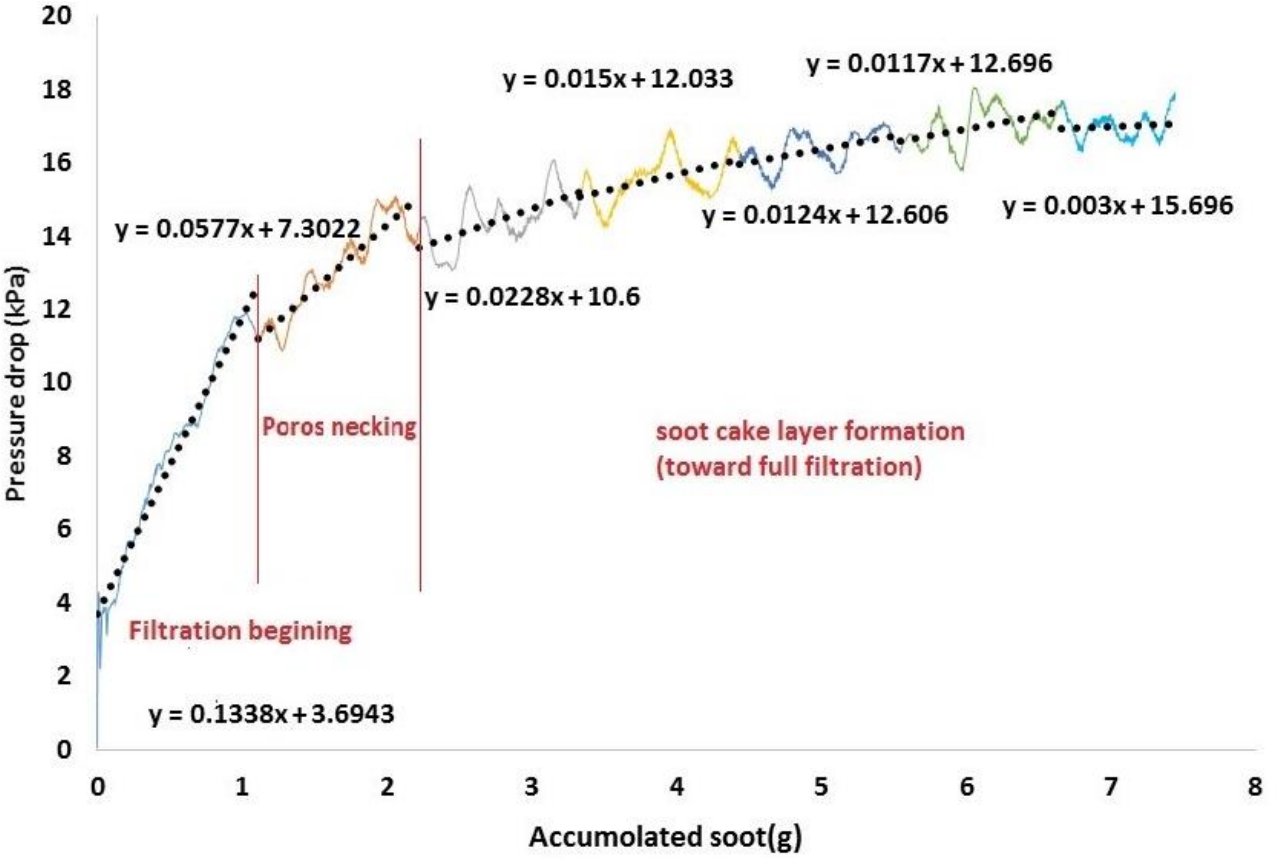

Figure 93 .Filtration estimation of biodiesel fuel.

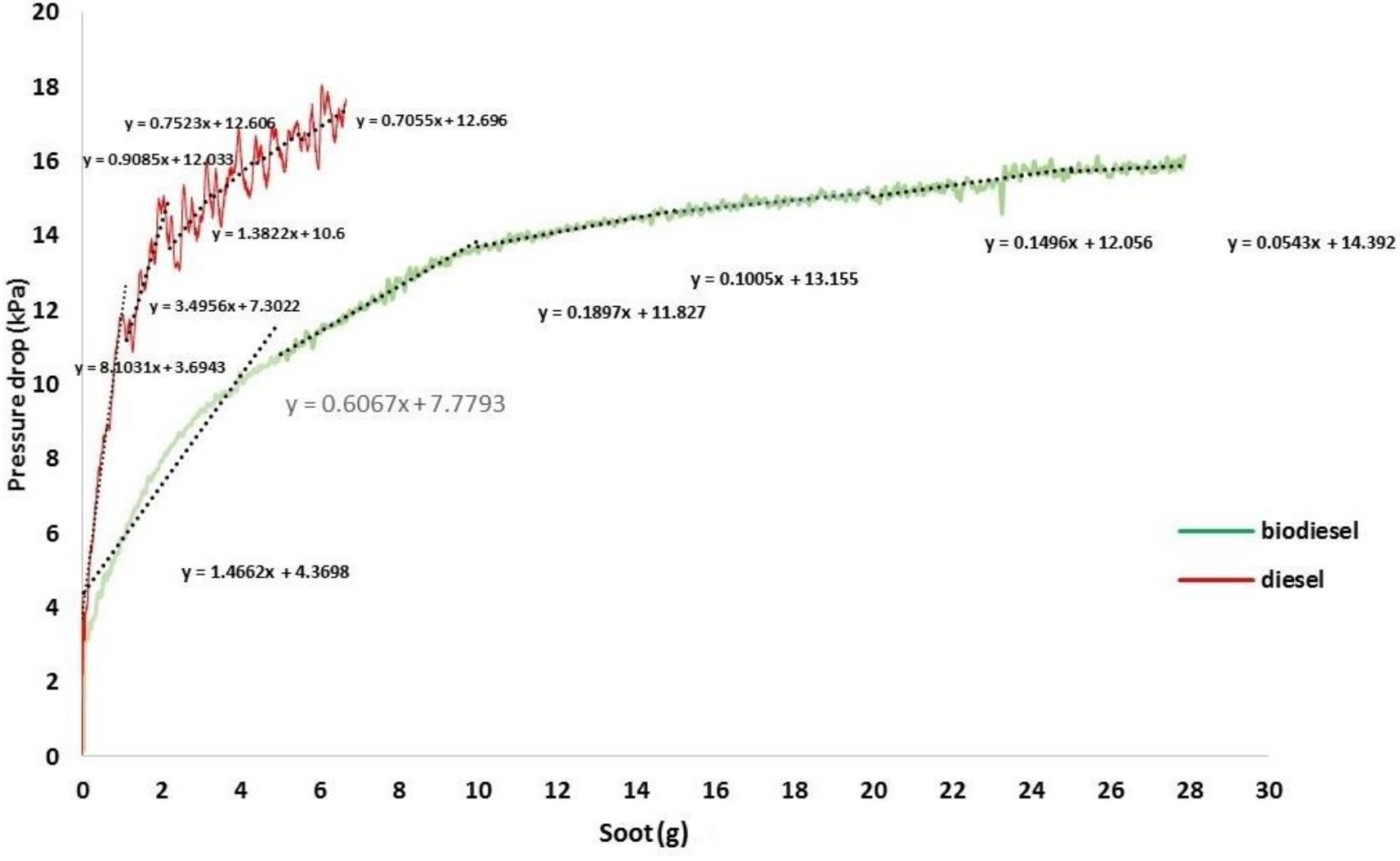

Figure 94.The comparison of diesel and biodiesel filtration with regard to soot formation rate.

Regeneration

The regeneration phase is done with the high temperature tube furnace. As temperature increase up to 600 ºC, the pressure drop falls and regeneration begins. The result of regeneration graph is pictured in figure 95. As seen, regeneration trend of biodiesel is faster than diesel with regard to more amount of biodiesel PM. Also, the regeneration duration of biodiesel is also shorter than diesel about one hour. This allows an easier regeneration and thus faster operability. The reason for this trend is related to the reactivity of soot samples and their activation energy. As discussed in previous section, the biodiesel has higher and faster reactivity due to difference of fuel composition, PM size, soot composition and VOF and SOF ratio. This results in lower resistance to oxidation which enables the DPF regeneration becomes easier at lower temperatures and thiserefore results in faster oxidation and regenration behavior. As showed in previous part,the diesel fuel makes more soot,about twice more than biodiesel, and this also can be one reason for slower oxidation of diesel soot.

The regenration trend of DPF is similar to oxidation trend of PM samples in TGA. For better explanation, a combined graph of TGA and regeneration is depicted in figure 96. Although its not possible to conect TGA and regenration graphs mathematically ,the regeneration trend of soot samples show a similar trend to their TGA reaction results with air and for both conditions, the diesel soot has slower reaction trend and longer duration.

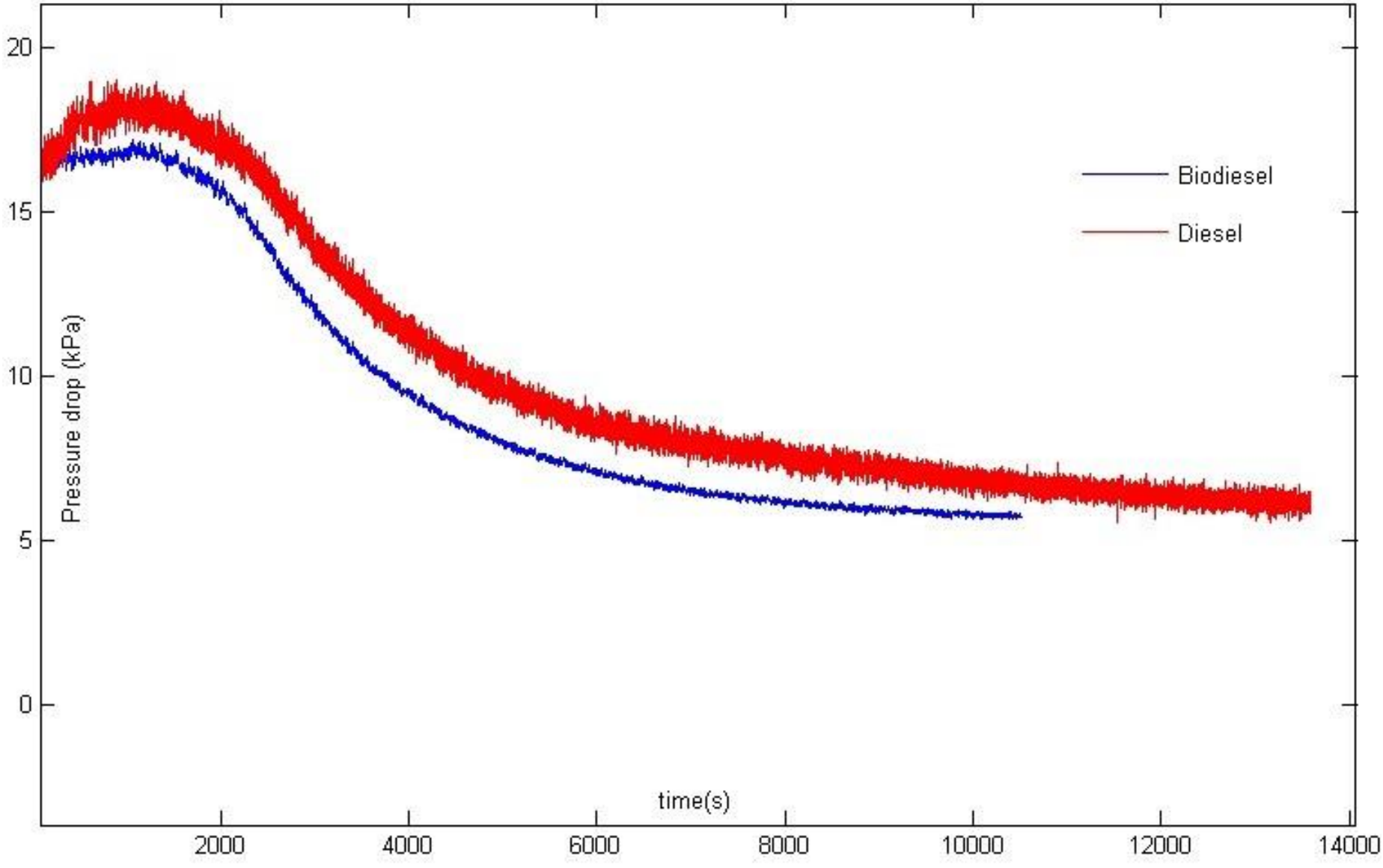

Figure 95.Regeneration of DPF for both diesel and Biodiesel PM.

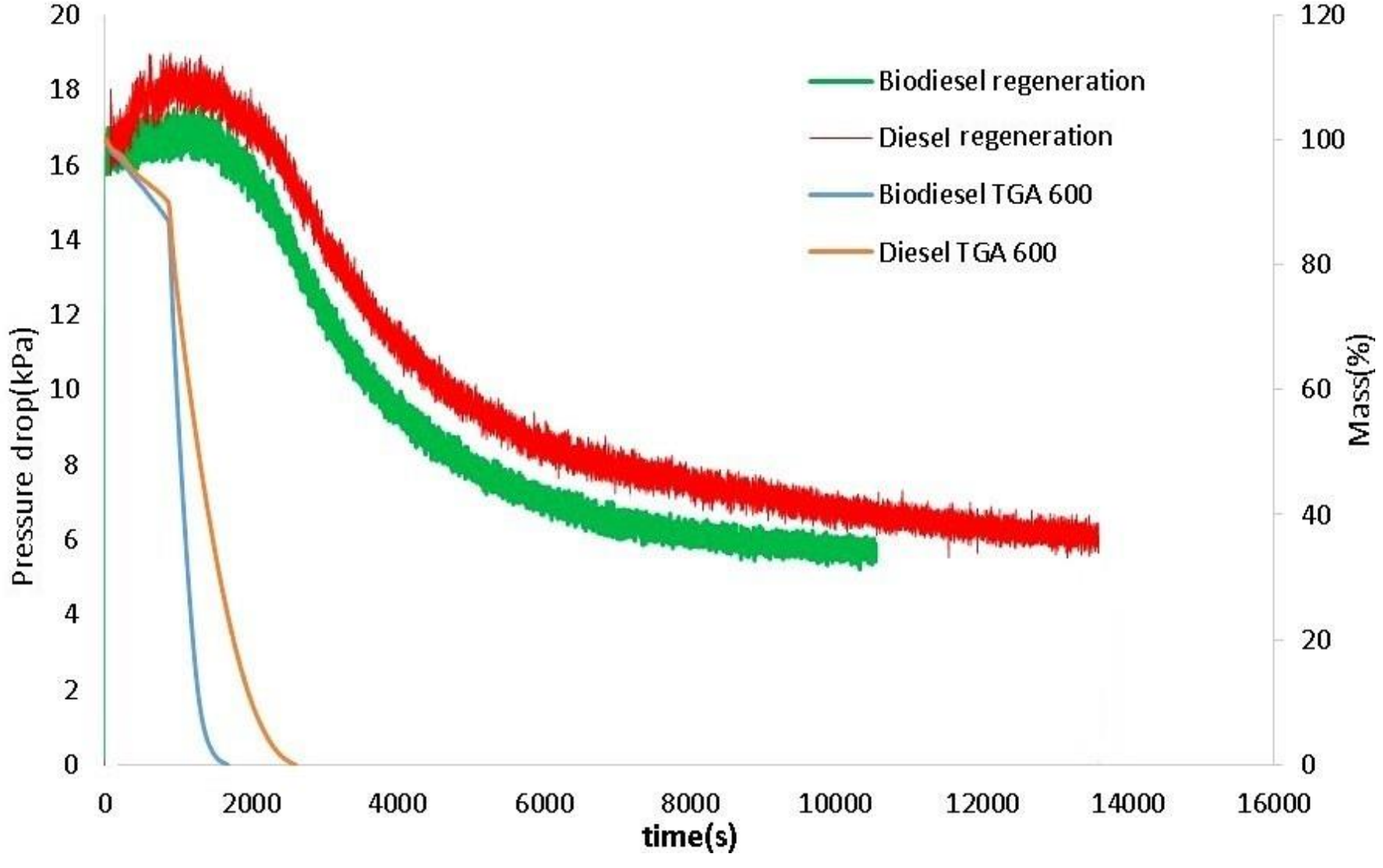

Figure 96.combined graph of TGA and regeneration.

CHAPTER 5

SUMMARY AND CONCLUSIONS

At this study the chemical and physical features of diesel and biodiesel fuel and their soot was investigated. The chemical characteristics of soot generated by diesel and biodiesel combustion were subjected to study by TGA and CHN. The physical features and morphologies of soot samples also analyzed by image processing. At the later phase of project, the filtration and regeneration trend of a sample of DPF while utilizing diesel and biodiesel by means of engine back pressure drop. The regeneration trend of DPF also, was tested by high temperature tube furnace.

5.1. Fuel properties:

- The molecular structure of both fuel is significantly different and biodiesel is mainly made of several fatty acids which can alter fuel physical and chemical properties such as viscosity and density and oxidation stability.
- Blending with commercial diesel can improve the physical and chemical properties of fuels and makes it more convenient for using in conventional and agricultural engines.
- Calorific value of biodiesel is lower than commercial diesel, however, blending with commercial diesel improves it. Lower calorific value is due to higher percentage of oxygen in biodiesel but this also leads to cleaner combustion due to more complete combustion, although more fuel shall be used.

- Higher kinematic viscosity and lower boiling point which make fuel atomization and evaporation more difficult under cold start conditions. Pure biodiesel can't be used in low temperature due to poor cold flow trend which is related to higher cloud point and pour point.

- Elemental analyzes shows that biodiesel has higher oxygen content which improves more complete combustion and lesser soot production but adverse oxidation stability and rancidity.

5.2. Oxidation kinetics and chemical features

- The carbon black N330, as a reference, and soot, obtained from combustion of diesel and biodiesel fuel in a single cylinder engine, at 2400 rpm and 80% load, were subjected to TGA and CHN analyze. TGA test was done in six different temperatures (400 ^{o} C, 450 ^{o} C, 500 ^{o} C, 550 ^{o} C and 600 ^{o} C) in isothermal condition. The nitrogen gas was used as the inert gas for heat up phase and then in active phase, oxygen at first test and air at second test were done.
- The acquired results shows that in all temperatures and in both testing conditions (oxygen and air), the biodiesel PM shows higher reactivity and has higher rate of conversion/oxidation in comparison with diesel and carbon black. This is indication of higher amount of VOF and lesser carbonaceous compositions of biodiesel PM in comparison with diesel. As temperature increases, the reactions becomes

more complete and at 550 and 600 (◦ C) all amount of samples oxidizes but still the biodiesel PM has faster rate of conversion in comparison with diesel. This trend is due to different chemical composition of PM samples. Higher amount oxygenated agents and lesser carbonaceous parts and higher H/C ratio can be possible reasons for better oxidation.

- The Activation energy of soot samples were calculated. At this study it is tried to separate the conversion zones in three main divisions including 80-60%, 60-40% and 40-20% of total mass conversion and activation energy of each division was obtained. In all conditions, biodiesel PM has lower activation energy in comparison with diesel and this will result in lesser resistance against oxidation and thus better reactivity regardless to other factors.
- Reaction order of carbon, *n*, was calculated for both fuel samples. Biodiesel has higher value, 0.74~0.76 while for diesel its lower, 0.56~0.57. This can indicate that none of the soot samples have complete spherical form which is match with shrinking core value, 0.66. However higher value of *n* is indication of more participation in reaction and as its closer to unity this trend be more but this assumption is not so clear yet and needs more investigations.

5.3. Morphology and Image Processing

Morphology of soot samples was studied by manual image processing of TEM images of the soot samples. Macro and micro structures features such as agglomerate particle area, Feret diameter, chord length, cross sectional area and PM compactness was studied and results were plotted and compared. In Nano scale, carbon platelet length (fringe length), inner core structure was investigated.

- Image processing of TEM pictures shows that agglomerate PM form biodiesel combustion has smaller length and cross sectional area in comparison with diesel PM. Such trend can be contributed to presence of more oxygen in biodiesel molecules which leads to more oxidation and more complete combustion.
- The Feret diameter, Chord length and cross sectional area of biodiesel is lower in than diesel. All these elements prove the smaller size of biodiesel PM which can be the main physical reason of better oxidative trend of biodiesel PM.
- One probable reason for better oxidative trend of biodiesel can be related to oxygen molecules of biodiesel which promote the rate of oxidation in combustion and reduce the pyrolysis duration in comparison with diesel. This provides the suitable condition for reaction limited cluster aggregation (RLCA) of PM and aggregation is slower and better ordered while for diesel it seems diffusion limit cluster aggregation (DLCA) is more prevalent and agglomerate PM shape is lesser packed and thus bigger size of PM can be observed however this

hypothesis needs precise study and modeling and cannot be concluded only by the experiments of this project.

- The fringe length of carbon structure in biodiesel is shorter than which can make oxidation easier. The inner core of diesel PM is slightly larger than biodiesel but this result may not be free from errors.
- For biodiesel a more amorphous structure is seen in the core and thus higher reactivity while for diesel the core has more crystallite structure and therefore higher resistance for oxidation. But in general the outer core has more crystallite structure in comparison with inner core for both PM samples, based on observations from image processing.
- The sphericty of biodiesel PM is higher than diesel PM. This is parallel with higher *n* value of biodiesel PM and the more the Pm is close to complete sphere the more participation in reaction is expected but more mathematical modeling and study is needed for this assumption.

5.4 Filtration and regeneration behavior

Filtration and regeneration trend of diesel and biodiesel fuels were studied by application of a sample of DPF and high temperature tube furnace and a single cylinder agricultural engine at high load (80%) and 2400rpm. The soot production rate of both fuels were also measured.

- The diesel soot production rate, based on the measurement method of this project, was 0.224 (g/min) while for biodiesel the rate was 0.131 (g/min).
- The base of experiment was set according to equal level of pressure drop. Filtration trend of diesel fuel is much faster than biodiesel and engine back pressure drop peaks much faster than biodiesel and then becomes linear. This is due to more PM production of diesel fuel (in an equal time period) and bigger agglomerate size of diesel PM in comparison with biodiesel. Bigger PM size increases the rate of soot cake layer formation on the porous media of DPF. On the other hand, due to higher reactivity of biodiesel PM, some trapped PM can oxidize by engine exhaust temperature during filtration and longer time and much more biodiesel is needed to burn to reach pressure drop level same as diesel .

- Higher amount of biodiesel trapped PM (to reach the equal level of diesel pressure drop) may be indication of more porosity of biodiesel PM which can enable the air flow passes throw the filter easier and thus slower filtration trend can be seen ,however this can only be considered as an assumption.

- Although the soot production rate of biodiesel is lower than diesel, but due to longer time of engine run(to reach equal level of pressure drop same as diesel) more amount of PM is trapped at the end of filtration test(about 4 times more).

- The biodiesel PM oxidizes faster in comparison with diesel and the filter can be clean faster with regard to this important parameter that the amount of biodiesel trapped PM is about 4 times more than diesel. This trend, along with filtration trend, makes biodiesel more convenient for application in DPF and provides a longer filtration duration and shorter regeneration period.
- This is basically related to chemical and physical features of fuels and consequently their soot. Although more PM from biodiesel is trapped, the regeneration is faster and it’s alike to the oxidation rate of PM samples in TGA. The smaller size of and higher reactivity of the biodiesel PM can be the main reasons for better oxidation but for more accurate results more investigation is required.

- Slower filtration and faster regeneration of biodiesel PM (with regard to more amount of trapped soot from biodiesel) makes biodiesel a promising fuel for wide usage and helps environmental protection.

REFERENCES

1. Deciding the Future: Energy Policy Scenarios to 2050 Executive Summary World Energy Council 2007. Published 2007 by: World Energy Council Regency House 1-4 Warwick Street London W1B 5LT United Kingdom ISBN: 0 946121 29 X.
2. Deploying Renewables in Southeast Asia Trends and potentials. © OECD/IEA, 2010 International Energy Agency 9 rue de la Fédération 75739 Paris Cedex 15, France.
3. Adrian Zhou, Elspeth Thomson, The development of biofuels in Asia0306-2619/$ - see front matter 2009 Elsevier Ltd. All rights reserved. doi:10.1016/j.apenergy.2009.04.028.
4. Morteza Borhanipour, Preechar Karin, Chinda Charoenphonphanich, Nuwong Chollacoop, Katsunori Hanamura: Investigation of diesel and biodiesel soot oxidation in presence of pure oxygen, Presented at the JSAE Annual Congress on May, 23, 2014.
5. Morteza Borhanipour, Preechar Karin, Chinda Charoenphonphanich, Nuwong Chollacoop, Katsunori Hanamura: Investigation of diesel and biodiesel soot oxidation in presence of pure oxygen, Presented at the JSAE Annual Congress on May, 23, 2014.
6. Preechar Karin, Yutthana Songsaengchan, Songtam Laosuwan, ChindaCharoenphonphanich, Nuwong Chollacoop and Hanamura Katsunori. Chemical Characterization of Biodiesel Particle Emission . Regional Conference on Mechanical and Aerospace Technology Bangkok, February 12 – 13, 2013.

7. Preechar Karin, Hiroshi Oki, Katsunori Hanamura and Chinda Charoenphonphanich, Nanostructures and Oxidation Kinetics of Diesel Particulate Matters. Journal of Research and Applications in Mechanical Engineering (JRAME) Vol.1 No. 2.
8. Preechar Karin et al, Nanostructure of Renewable Oxygenated Fuels Particulate Matter, ASEAN Engineering Journal Part A Volume 3, Number 1 March 2013.
9. Preechar Karin, Yutthana Songsaengchan,Songtam Laosuwan, Chinda Charoenphonphanich, Nuwong Chollacoop and Katsunori Hanamura, Nanostructure Investigation of Particle Emission by Using TEM Image Processing Method, Energy Procedia 34 (2013) 757 – 766. 10th Eco-Energy and Materials Science and Engineering (EMSES2012).
10. Michael C. Madden,Judy H. Richards, Lisa A. Dailey, Gary E. Hatch, and Andrew J. Ghio, Effect of Ozone on Diesel Exhaust Particle Toxicity in Rat Lung. Toxicology and Applied Pharmacology 168, 140–148 (2000)doi:10.1006/taap.2000.9024, available online at http://www.idealibrary.com on.
11. Joellen Lewtas , Air pollution combustion emissions: Characterization of causative agents and mechanisms associated with cancer, reproductive,and cardiovascular effects. 1383-5742/$ – see front matter # 2007 Elsevier B.V. All rights reserved.doi:10.1016/j.mrrev.2007.08.003.
12. Naveena Yanamala et al, Biodiesel versus diesel exposure: Enhanced pulmonary inflammation, oxidative stress, and differential morphological changes in the mouse lung. 0041-

008X/$ – see front matter. Published by Elsevier Inc.http://dx.doi.org/10.1016/j.taap.2013.07.006.

13. Khalid Al-Qurashi, André L. Boehman , Impact of exhaust gas recirculation (EGR) on the oxidative reactivity of diesel engine soot0010-2180/$ – see front matter © 2008 The Combustion Institute. Published by Elsevier Inc. All rights reserved.doi:10.1016/j.combustflame.2008.06.002.
14. Magín Lapuerta et al, Effect of fuel on the soot nanostructure and consequences on loading and regeneration of diesel particulate filters, 0010-2180/$ - see front matter. The Combustion Institute. Published by Elsevier Inc. All rights reserved.doi:10.1016/j.combustflame.2011.09.003.
15. Dongke Zhang , Yu Ma, Mingming Zhu. Nanostructure and oxidative properties of soot from a compression ignition engine: The effectof a homogeneous combustion catalyst. 1540-7489/$ - see front matter 2012 The Combustion Institute. Published by Elsevier Inc. All rights reserved.http://dx.doi.org/10.1016/j.proci.2012.05.096.
16. Aleksey Yezerets et al, Differential kinetic analysis of diesel particulate matter (soot) oxidation by oxygen using a step–response technique. 0926-3373/$ – see front matter # 2005 Elsevier B.V. All rights reserved.doi:10.1016/j.apcatb.2005.04.014.
17. J. Jung Et Al, Measurement Of Soot Oxidation With No2-O2-H2o In A Flow Reactor Simulating Diesel Engine Dpf, International Journal of Automotive Technology, Vol. 9, No. 4, pp. 423−428 (2008)DOI 10.1007/s12239−008−0051−4.

18. Kuen Yehliu,et al, Impact of fuel formulation on the nanostructure and reactivity of diesel soot, 0010-2180/$ 2012 The Combustion Institute. Published by Elsevier Inc. All rights reserved.http://dx.doi.org/10.1016/j.combustflame.2012.07.004.
19. C.J. Tighe et al, The kinetics of oxidation of Diesel soots by NO2, 0010-2180/$ - 2011 The Combustion Institute. Published by Elsevier Inc. All rights reserved.doi:10.1016/j.combustflame.2011.06.009.
20. Robert L. Mccormick,Michael S. Graboski,Teresa L. Alleman, ANDANDREW M. HERRING Impact of Biodiesel Source Material and Chemical Structure on Emissions of Criteria Pollutants from a Heavy-Duty Engine. 10.1021/es001636t CCC: $20.00 · 2001 American Chemical Society Published on Web 03/30/2001
21. John P.A. Neeft, T.Xander Nijhuis, Erik Smakman, Michiel Makkee, Jacob A. Moulijn, Kinetics of the oxidation of diesel soot, doi:10.1016/S0016-2361(97)00119-1
22. B.R. Stanmore , J.F. Brilhac, P. Gilot, The oxidation of soot: a review of experiments, mechanisms and models, 0008-6223/01/$ – see front matter · 2001 Elsevier Science Ltd. All rights reserved. PII: S0008-6223(01)00109-9.
23. Pierre Darcy et al , Kinetics of catalyzed and non-catalyzed oxidation of soot from a diesel engine0920-5861/$ – see front matter # 2006 Elsevier B.V. All rights reserved.doi:10.1016/j.cattod.2006.08.056.
24. Diesel-Engine Management:An Overview. The Bosch Yellow Jackets Edition 2003 Expert Know-How on Automotive TechnologyDiesel-Engine Management. Published by:© Robert Bosch GmbH, 2003Postfach 1129,D-73201

Plochingen.Automotive Aftermarket Business Sector,Department of Product Marketing Diagnostics &Test Equipment (AA/PDT5).

25. Diesel Fuels Technical Review. © 2007 Chevron Corporation. All rights reserved.
26. Particulate Emissions from Vehicles. ISBN 978-0-470-72455-2 (cloth)1. Automobiles—Motors—Exhaust gas. I. Title.TD886.5.E205 2008629.25 28—dc22 2007044839
27. Victor Fernandez-Alos, Justin K. Watson, Randy vander Wal, Jonathan P. Mathews, Soot and char molecular representations generated directly from HRTEM lattice fringe images using Fringe3D. 0010-2180/$ - see front matter 2011 The Combustion Institute. Published by Elsevier Inc. All rights reserved. doi:10.1016/j.combustflame.2011.01.003
28. W. Addy Majewski . Diesel Particulate Filters. www.DieselNet.com. Copyright © Ecopoint Inc. Revision 2001.07b.
29. Microscopic Visualization and Characterization of Particulate Matter Trapping and Oxidation In Diesel Particulate Filters And Membrane Filters. Phd Thesis. Preechar Karin.
30. Wirojsakunchai, E., Schroeder, E., Kolodziej, C., Foster, D. et al., "Detailed Diesel Exhaust Particulate Characterization and Real-Time DPF Filtration Efficiency Measurements During PM Filling Process," SAE Technical Paper 2007-01-0320, 2007, doi:10.4271/2007-01-0320.

31. Abhijeet Raj et al, tructural effects on the oxidation of soot particles by O2: Experimental and theoretical study. A. Raj et al., Combust. Flame (2013), http://dx.doi.org/10.1016/j.combustflame.2013.03.010
32. G.A. Stratakis,A.M. Stamatelos. Thermogravimetric analysis of soot emitted by a modern diesel engine run on catalyst-doped fuel. Combustion and Flame 132 (2003) 157–169.
33. Wikipedia .
34. Dale R. Tree, Kenth I. Svensson , Soot processes in compression ignition engines. 0360-1285/$ - see front matter r 2006 Elsevier Ltd. All rights reserved.doi:10.1016/j.pecs.2006.03.002
35. Ishiguro,T.Takatori,Y.andAkihama,K.(1997). Microstructure of Diesel Soot Particles Probed by Electron Microscopy: First Observation of Inner Core and Outer Shell, Combustion and Flame, 108, pp.231-234.
36. Heejung Jung: Characteristics of SME Biodiesel-Fueled Diesel Particle missions and the Kinetics of Oxidation Environ. Sci. Technol. 2006, 40, 4949 4955.

APPENDIX

Publications

1. Comparison Study on Fuel Properties of Biodiesel from Jatropha and Palm and Petroleum Based Diesel Fuel-The 10th International Conference on Automotive Engineering.
2. Oxidation Kinetics of Small CI Engine's Biodiesel Particulate Matter, International Journal of Automotive Technology, paper no: 220140181. P. Karin,M.Borhanipour et al.
3. Investigation of diesel and biodiesel soot oxidation in presence of pure oxygen, Presented at the JSAE Annual Congress on May, 23, 2014. : Morteza Borhanipour, Preechar Karin, Chinda Charoenphonphanich, Nuwong Chollacoop, Katsunori Hanamura.

4. Investigation of Diesel and Biodiesel Soot Oxidation Burapha University International Conference 2014 Burapha University, Thailand July 3-4, 2014. Morteza Borhanipour, Preechar Karin et al.

5. Investigation of Diesel and Biodiesel Soot Oxidation inside a Sample of Conventional DPF: Morteza Borhanipour, Preechar Karin, Chinda Charoenphonphanich, Nuwong Chollacoop, Katsunori Hanamura.

Comparison Study on Fuel Properties of Biodiesel from Jatropha, Palm and Petroleum Based Diesel Fuel

2014-01-2017
TSAE-14IC-2017
Published 03/24/2014

Morteza Borhanipour
King Mongkut's Inst of Tech Ladkrabang

Preechar Karin
King Mongkut's Inst. of Tech Ladkrabang

Manida Tongroon and Nuwong Chollacoop
National Metal and Materials Technology

Katsunori Hanamura
Tokyo Institute of Technology

CITATION: Borhanipour, M., Karin, P., Tongroon, M., Chollacoop, N. et al., "Comparison Study on Fuel Properties of Biodiesel from Jatropha, Palm and Petroleum Based Diesel Fuel," SAE Technical Paper 2014-01-2017, 2014, doi:10.4271/2014-01-2017.

Abstract

The increase of air pollution and global warming is a threat for human life. Besides, the price of petroleum is increasing rapidly and the resources are diminishing. This obliged scientists and engineers to look for alternative sources of energy, which are cleaner and more sustainable. Biodiesel, defined as mono-alkyls of esters from vegetable oils and animals fat, is a cleaner renewable fuel and has been considered as the best alternative for petroleum based diesel fuel hence it can be used in any compression ignition engines without any significant modification. The main advantages of using biodiesel are its renewability and better quality of exhaust gas emissions due to their higher content of oxygen. The produce less soot and hence the feed stuck is plant it will regenerate the CO2 by the photosynthesis which ensures the renewability and reduces global warming. But these alternative fuels have faced some obstacles while utilizing in CI engines which are due to some of their physical and chemical characteristics. At this study the fuel properties of jatropha biodiesel and its blends (a non-edible feedstock) were compared with the properties of Palm biodiesel (an edible feedstock) and petroleum based diesel. The viscosity, density, oxidation stability, acid value, water content, iodine value, flash point, pour point, cloud point and calorific value of the samples were analyzed an discussed. The physical properties of the biodiesels are controlled by their chemical properties such as unsaturation level of fatty acids and oxidation stability. Results show that the viscosity of jatropha is higher than palm biodiesel although the density of palm biodiesel is higher. Oxidation stability of the biodiesel has impact on several chemical and physical properties and improvement of oxidation stability can make betterment in these properties. The results of this study will be used as a data backup for another research project.

Introduction

The pollution of the air, price and dependability of industries and transportation to fossil fuels has obliged countries to find an alternative source of energy to fulfill their energy demands. Among several alternatives, biodiesel is known as a good and promising substitute for petroleum diesel fuels. Crude petroleum resources are not widely available around the world and their high price is another problem for importer countries. Meanwhile, the petroleum based diesel fuels produce more pollution. On the other hand, biodiesel is cleaner, renewable and domestic which can reduce the dependency to importing the fossil fuels. The first application of biodiesel dates back to 1900, when Rudolf Diesel, inventor of diesel engine, in his first demonstration of first diesel engine at World Exhibition at Paris used peanut oil as a fuel [1]. But due to abundance of fossil fuels at that time the researches about biodiesel were not persuaded seriously. Only after knowing that fossil fuel sources are limited and the air pollution became more important, the

researchers began to investigate about biofuels. Biodiesels, defined as mono-alkyl esters of long chain fatty acids derived from renewable feedstock such as vegetable oils and animal fats, for using in CI engines. They are commonly composed of fatty acid methyl esters that can be prepared from triglycerides, by transesterification with methanol. The biodiesels are more environmental friendly due to cleaner combustion, biodegradability, being non-toxic and lower emission profile as compared to petroleum based diesels [2]. However, there are some critical obstacles in widely usage of biodiesels. The reduction in engine power for biodiesel as well as the increase of fuel consumption is one concern [3]. Biofuels generally have lower energy content in comparison to petroleum diesel fuels. Oxidation of biodiesels is another drawback. Auto oxidation occurs in biodiesels due to higher sensitivity to reaction with fuel-bound oxygen and hot air [4]. Higher viscosity and density are two other disadvantages of biodiesel. It can cause poor fuel atomization, advanced injection, incomplete combustion and injector clogging [3], [5]. Therefore, these parameters shall be investigated in order to make betterment for utilization of biofuels.

Methodology

At this study, jatropha biodiesel (JB100), palm biodiesel (PB100), blends of 10 %(JB10, PB10) and 20 % (JB20, PB20) of these two with commercial diesel and commercial diesel fuels. The commercial diesel is produced by PTT Company, the jatropha biodiesel is provided by Renewable energy Lab of MTECH and palm biodiesel is provided by Phatum Company. The viscosity, density, pour point, cloud point, flash point, oxidation stability, acid value, water content and calorific value of all samples were tested. Gas chromatography test and iodine value test for biodiesels and CHN test for all pure samples is done in order to make the relation between physical and chemical properties of fuel more clear.

The viscosity test is done by Cannon mini Av viscose meter at 40 °C. The density test is done by using density meter Anton paar DMA 4500 and each test is done 3 times for each sample. Acid value test is done by typical titration method with KOH solvent and Metro-ohm acid value meter device was used to determine the acid value and each test is done thrice for each sample. The gas chromatography test is done with Shimadzu GC-2010. Flash point test is done with Pensky-Martens (Tanaka) APM-7 and each sample is tested two times. Calorific value test is done by application of bomb calorimeter Leco-AC-350 each test is done thrice for each sample. Oxidation stability test is done by Ranciment device model Metro-ohm 743 ranciment, each test is done twice for each sample. Cloud point and pour point tests were done twice for each sample with CPP 5GSCH Chemical device. The study is divided in two parts. First part is fuel chemical properties and second part is about physical properties of the fuels.

Results and Discussion

Chemical Properties

Fatty Acid Composition

The fatty acid composition of biodiesel has a key role in the physical and chemical properties of fuel. The performance of an ester (biodiesel) as diesel fuel depends on the chemical composition of the ester, particularly on the length of carbon chain and the degree of saturation (and unsaturation) of fatty acid molecules [6]. Studies show that properties such as cetane number, cold flow characteristics and oxidation stability are affected by the composition [1], [7]. There are three main types of fatty acids including saturated, unsaturated and polyunsaturated. Vegetable oils with higher degree of unsaturation tend to have higher freezing point, poor flow characteristic and can become solid [7]. The composition of jatropha biodiesel and palm biodiesel were analyzed by gas chromatography. The results of JB100 and PB100 are shown in the table 1 and 2. The dominant components in JB100 are Oleic acid (69.3 %), which is an unsaturated acid, Palmitic acid (14.58%) and Stearic acid (11.7%), which are saturated type. For the PB100 the results are different and Palmitic acid, which is a saturated acid, is more (38.77%) and Oleic acid percentage is lesser in comparison with jatropha biodiesel (37.612%) and it can be said that JB100 is more unsaturated.

Table 1. fatty acid composition of jatropha biodiesel

Lauric acid methyl ester C12:0	0.049676
Myristic acid methyl ester C14:0	0.020036
Palmitic acid methyl ester C16:0	14.58014
Palmitoleic acid methyl ester C16:1	0.766552
Stearic acid methyl ester C18:0	11.69947
Oleic acid methyl ester C18:1mono	69.2841
Linoleic acid methyl ester C18:2	3.310399
Linolenic acid methyl ester C18:3	0.035092
Arachidic acid methyl ester C20:0	0.185798
Eicosenoic acid methyl ester C20:1	0.068739
Molecular weight	277

Table 2. fatty acid composition of palm biodiesel

Lauric acid methyl ester C12:0	0.8735
Myristic acid methyl ester C14:0	0.036
Palmitic acid methyl ester C16:0	38.7725
Stearic acid methyl ester C18:0	3.158
Oleic acid methyl ester C18:1	37.612
Linoleic acid methyl ester C18:2	8.783
Linolenic acid methyl ester C18:3	0.1625
Arachidic acid methyl ester C20:0	0.2125
Eicosenoic acid methyl ester C20:1	0.092
Molecular weight	240

Oxidation Stability

The oxidation stability of fuels is an important element which can help to determine the quality of fuel and it can also affect some of fuel physical and chemical properties such as density, viscosity and water content. Biodiesels usually have 10% more oxygen in their structure which can increase the risk of oxidation. The fuel composition can also affect the oxidation stability. Studies show the vegetable oils which are rich in poly

unsaturated acids tend to give methyl ester fuels poor oxidation stability [7], [8], [9]. Oxidation occurs in the forms of aldehydes, alcohols, carboxylic acids, insoluble gum and sediments in biodiesel [4]. The temperature also has a great impact on oxidation rate. The thermal oxidation is determined by the rate of oxidation reaction at high temperature when the fuel is exposed to air and as the temperature increase the rate of oxidation increases [4].

The fuel samples were tested by Ranciment instrument method by heating up to 110 °C. The results of the test are shown in Fig. 1. The results show the induction period (IP) of PB100 (22.86 h) is more than JB100 (9.63h) about 2.37 times and for commercial diesel is (158.21h) which is significantly higher than the rest. Among the blends also we can see the stability of palm biodiesel blends are more than jatropha biodiesel although the difference is not as much as pure biodiesels. This can be due to various percentages of saturated fatty acids in biodiesel [4]. Jatropha biodiesel has higher amount of Oleic acid, which is an unsaturated fatty acid, in comparison with palm biodiesel and therefore it shows lesser oxidation stability. The induction period decreases by increase of unsaturated fatty acids [4]. As amount of diesel increases in the blends the stability shows better results. This can be due to reduction of unsaturated components and amount of oxygen. Oxidation of biofuels is also affected by storage time and condition, pressure of the air, heat, trace of metal and exposure of light [8], [7]. Oxidation stability cannot be prevented entirely but can be delayed by application antioxidant [4].

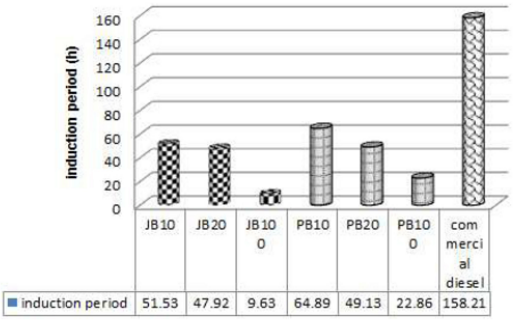

Figure 1. Comparison of induction period of different fuel samples.

Iodine Value

The iodine value is a measure of unsaturation of fats and oils [7]. Iodine value is expressed in terms of number of centigrams of iodine absorbed per gram sample of biodiesel. The iodine is introduced in biodiesel reacts with the double bonds within the fatty acid structure. Therefore, higher the percentage of unsaturation, the larger will be the iodine value [6]. The iodine numbers can influence oxidation stability and the polymerization of glycerides. This can lead to the formation of deposits formed in diesel engines injectors [8], [10]. The results of iodine value test are shown in table 3. This can be a good indication of unsaturation of jatropha biodiesel in comparison with palm biodiesel. The unsaturation of fuel can have significant effects on several chemical and physical properties of fuels. Based on the results of Iodine value test, the JB100 has higher Iodine value in comparison with PB100 and it can be indication of higher unsaturation of JB100.

Table 3. iodine value of jatropha and palm biodiesel.

Fuel sample	Jatropha biodiesel	Palm biodiesel
Iodine value(g I2/100 g)	90.56	51.5

Calorific Value

Defined as the energy contained in a fuel, determined by measuring the heat produced by the complete combustion of a specified quantity of it. Calorific value is an important parameter in the selection of a fuel. The fuel elements of primary interest to diesel engine combustion are carbon, hydrogen, oxygen, and sulfur and the calorific value of a fuel is directly related to its elemental composition [6]. Calorific value of fuel increase with chain length of molecule [11]. The heating value is experimentally obtained by using an oxygen bomb calorimeter under defined conditions. As seen in Fig.2, the highest calorific value belongs to the commercial diesel (45.8 MJ/kg). As percentage of biofuel in the blends increases the calorific value decreases. The calorific value of pure biofuels, JB100 &PB100, is the lowest among the rest. The calorific value of JB100 (40.475 MJ/kg) is higher than PB100 (39.900 MJ/kg) but the difference is not so significant. This can be due to higher amount of carbon of JB100 in comparison with PB100. Such trend is also seen among the blend of jatropha and palm. The main reason for these phenomena is related to the elemental composition of the fuels. The lower calorific value of biofuels in comparison with commercial diesel is due to the higher oxygen content of the biofuels [1], [5]. The diesel fuel is mad up a mixture of various hydrocarbon molecules and contains very little oxygen percentage (0.3%) but for the biofuels the amount of oxygen is about 10% of the fuel composition. The increase of oxygen in fuel structure results in reduction of carbon and hydrogen in the fuel and this will result in lower energy content [6]. Oxygen is ballast in fuel and carbon and hydrogen are source of thermal energy [6]. The results of elemental analyze test is shown in the table 4. It can also verify this explanation that biofuels have higher concentration of oxygen and lower concentration of carbon in comparison with commercial diesel. Presence of more oxygen can also cause lower stoichiometric air/fuel ratio. This can ensure improvement of combustion [1], [6].

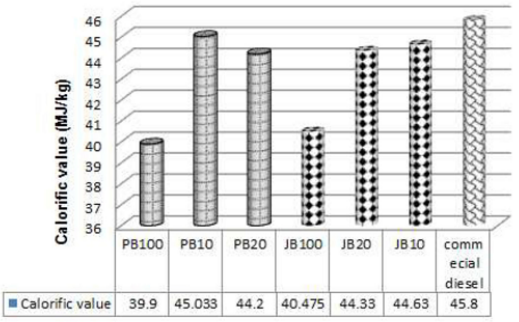

Figure 2. Results of calorific value of each fuel sample from calorimeter bomb.

Table 4. results of elemental analyze of JB100, PB100 and Commercial diesel.

Fuel sample mass	C%	H%	O%	Molecular formula
JB100	76.5735	12.209	11.217	C17.658H33.787O1.94
PB100	78.322	13.281	8.3749	C15.2635H29.479O1.706
Commercial diesel	85.177	14.047	-----	C16.165 H32.006

Acid Value

Acid value is defined as the number of milligrams of potassium hydroxide required to neutralize the free fatty acid presents in 1 gram of the sample. The main acid component could possibly be found in biodiesel are: 1-residual mineral acids from production process. 2-residual free fatty acids from hydrolysis process or post-hydrolysis process of esters. 3-oxidation byproducts in forms of other organic acids [12]. Acid value can also be an indication of lubricity degradation [13]. Higher acid value can cause fuel system deposits and reduces the lifelong of fuel pump [8]. The test was done in typical titration method with a potassium hydroxide (KOH) solvent with known concentration. Phenolphthalein is used as a color indicator. The results are shown in Fig.3. As the concentration of biodiesel increases in the fuel samples the acid value increases. The acid value of JB100 is the highest (0.2 mg of KOH) and PB100 stands next (0.115 mg of KOH). The lowest value is for commercial diesel. The main reason for this trend can be due to unsaturation level of the biofuels, as the jatropha has higher unsaturation level in comparison with palm can show higher acidity hence the fuels containing unsaturated fatty acid with double bonded long chain hydrocarbons have more susceptibility to oxidation and oxidation has an inverse relation with acid value [4]. Increase of acid value can be considered as a result of oxidation of the fuel which may lead to gum and sludge formation besides corrosion [1]. Temperature can also affect the acid value. If fuel is exposed to high temperature oxidation occurs due to higher rate of reaction of fuel molecules with oxygen in the air, resulting in increase of acid value [4].

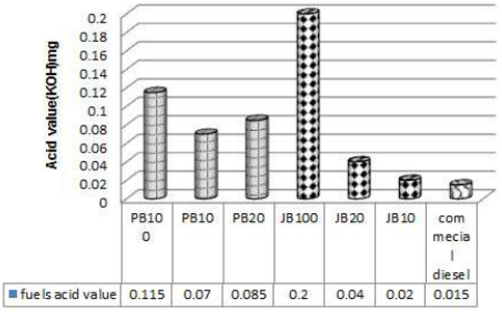

Figure 3. Results of acid value test of the biodiesel fuels, blends of biodiesel fuels and commercial diesel.

Water Content

Water content is a purity indicator of biodiesels. The moisture accumulated in biodiesel leads to the increase of free fatty acid concentration which can result in corrosion of metallic parts of engine and fuel system [12]. Biodiesel fuels are much more hygroscopic than diesel oil fuels which absorbs more moist [10], [12]. This can also cause troubles in handling the fuel and storage [12]. Water in biodiesel can also facilitate the growth of microbiological components and formation of sediments [12], [14]. Water and sediments can shorten the fuel filter life or plug fuel filter, which lead to engine fuel starvation [14]. The results of water content test are shown in Fig.4. Among the all samples, JB100 has the highest value (467.1ppm) and the PB100 stands after it with (297.66ppm), such trend is also seen for blends of these two biodiesel. By decreasing the content of biodiesel in blends the level of water content decrease. Storage time and condition and oxidation stability

can be one of the affecting factors for this trend. The water content generally increases with storage time and initiation of oxidation instability which is governed by peroxide chain mechanism [10]. Another reason can be related to the fatty acid composition of biodiesels. Decomposition of unsaturated fatty acids can extend formation of primary oxidation products such as hydro-peroxide which results in increase of water content [12]. The production process and feed stock of biodiesels also can be considered as an affecting factor. Studies shows biodiesel samples with lower M/H (methanol/ hydrogen) ratio have higher water content [10].

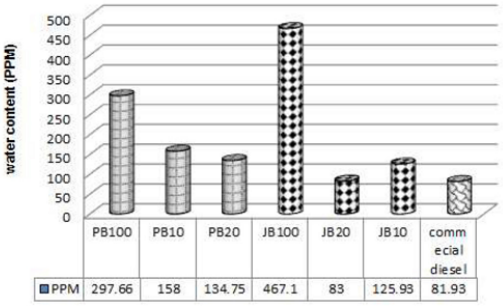

Figure 4. Results of water content analyze of biodiesel fuels, blends of biodiesel fuels and commercial diesel.

Physical Properties

Density

The density of biofuels is one of the main concerns in widely utilization of them. Density is defined as the ratio of mass per unit of volume of an object. The higher density, the tighter particles are packed in the substance. Fuel injection devices work on a volumetric system, hence a higher density for biodiesels results in delivery of slightly greater mass of fuel into combustion chamber higher density of biodiesels can also cause more pm production due to deterioration of fuel atomization [2], [3], [6]. The results of density test are shown in the Fig.5. The highest value is for PB100 (0.8748 g/cm3) and JB100 stands next with (0.8648 g/cm3) but the difference is not so significant. This trend can be connected to saturation level of fatty acids. Saturation of fatty acids can increase the density. Since the fuels containing shorter chain length of hydrocarbon and more saturated fatty acid have more prone to be crystalized, therefore cause of reduction of its volume and consequently increase of density [4]. Palm biodiesel is more saturated and this can be a reason of having higher density. As the amount of biodiesel decrease in fuel samples by blending with commercial diesel, the density decreases. The density of vegetable oil based methyl esters from different source, reported in many studies is very close to each other [2], [7]. The density also is affected by oxidation of fuel. The density has direct relation with fuels molecular weight, thus oxidation of fuels can increase the mass of fuel by producing by products and sediment, and therefore it results in increase of density [4]. The higher density can cause more fuel consumption due to advance of injection [3]. In comparison between PB100, JB100 and commercial diesel we can refer to molecular weight of the fuels. As molecular weight of biodiesels is higher in comparison with commercial diesel and therefore their density should be higher.

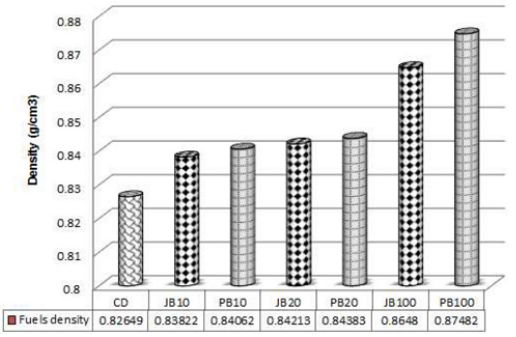

Figure 5. Density of biodiesel fuels, blends of biodiesel fuels and commercial diesel.

Viscosity

Viscosity is defined as the resistance of a liquid to flow. Viscosity can be considered as one of the main obstacles in widely usages of biodiesel fuels. In the fuels with higher viscosity, engine durability is the main concern. Fuel with higher viscosity can cause soot deposit formation on injectors (injector clogging), certain components of piston (rings), inlet and outlet valves and fuel filter plugging [9], [3]. The higher amount of biodiesel concentration partly dissolves the lubricant, resulting in increased friction of engine moving parts [3]. Fuel atomization and volatility is also affected by viscosity. Higher viscosity results in poorer fuel atomization which leads to combustion deterioration [3], [4], [6], [15, 16, 17, 18, 19]. The higher viscosity can also make low temperature flow problems and cold engine start up and ignition delay [8], [13]. The results of viscosity test are shown in Fig.6. The viscosity values of pure biodiesels are higher than the blends and commercial diesel. By blending with the commercial diesel and decrease of biodiesel percentage the viscosity value decreases. In comparison between two pure biodiesel samples, JB100 has higher viscosity (5.110 (mm2/s)) than palm biodiesel (4.452 (mm2/s)). Such trend is also seen among the blends too and the blends of jatropha have higher viscosity than palm biodiesel blends. This can be due to the difference of molecular composition of the samples and the level of unsaturation. As the proportion of saturated fatty acids with longer carbon chain increases, it can increase the viscosity [2], [8]. Thus, for jatropha with higher percentage of unsaturated components (about 70%) can show higher viscosity in comparison with palm biodiesel with lower unsaturation (about 46.56%). Blending with commercial diesel can decrease the unsaturation level and results in reduction of viscosity. Oxidation stability of fuels is another important parameter. Oxidation of fuel can increase the viscosity hence it leads to formation of free fatty acids, double bounds isomerization, saturation and production of higher molecular weight [2]. Since jatropha biodiesel show poorer oxidation stability in comparison with palm biodiesel, it can be referred to having higher viscosity. The same reason can be contributed to reduction of viscosity by blending with

commercial diesel. Hence biofuels are more oxygenated; blending can reduce the amount of oxygen and consequently improvement of oxidation stability and viscosity.

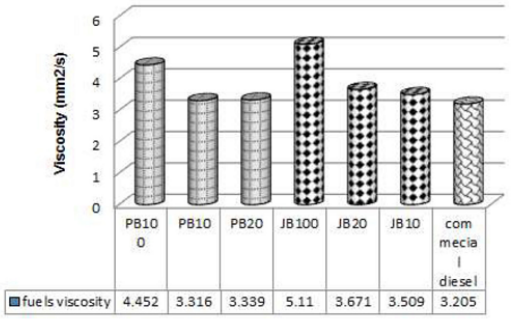

Figure 6. Results of viscosity test at 40 °C biodiesel fuels, blends of biodiesel fuels and commercial diesel.

Flash Point

Flash point is another important property of any fuel. It is defined as the temperature at which a fuel can provide a combustible mixture with air while exposed to flame or spark. Flash point has an inverse relation with fuel's volatility [12], [13]. Flash point is an important factor to consider in handling, storage and safety of fuels [16]. The results of flash point test are shown in Fig.7. As amount of biofuel increase in the blends the flash point increase too. The lowest flash point is for commercial diesel (65.5 °C) and highest belong to JB100 and PB100 (198.5 & 198 °C) which are more than 3 times. This ensures the safety of biofuels. The reason for this trend can be related to fuel composition of the samples. Diesel consists of hundreds of different hydro carbon components but biofuels are usually consisting of 4 to 5 major components that will boil at the same temperature [4]. Flash point can also decrease by oxidation and storage time [4].

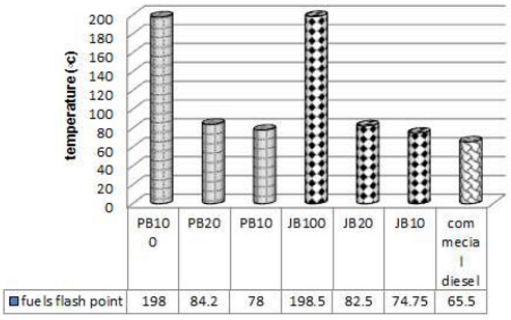

Figure 7. Flash point of biodiesel fuels, blends of biodiesel fuels and commercial diesel.

Cloud Point

The cloud point is an important feature of fuels in winter application. The cloud point is defined as the temperature at which crystals first starts to form in the fuel. The saturation of fatty acids increases the cloud point [1], [8]. The cloud point is most commonly used as a measure of low-temperature operability of the fuels [12]. The cloud point of biofuels typically higher than the cloud point of conventional diesel [12]. The results of cloud point test are shown in Fig. 8. Among the samples, PB100 has the highest cloud point (15.2 °C) and JB100 stand after it with temperature of (12.8°C). This could be due to higher saturation level of palm biodiesel in comparison with jatropha. As amount of biofuel decreases in the samples the cloud point becomes lower and closer to the commercial diesel which make the application of the biodiesel blends easier especially in cold climates.

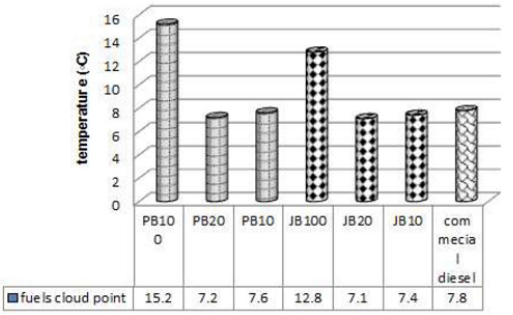

Figure 8. Results of cloud point test biodiesel fuels, blends of biodiesel fuels and commercial diesel.

Pour Point

Pour point is the lowest temperature that the fuel is observed to flow. Pour point is an important property in winter use. Biodiesel exhibits poor flow properties at low temperature [14]. The structural properties of biodiesel that can affect the pour point are degree of unsaturation, chain length and degree of branching [14]. The results of the pour point test are shown in Fig.9. The highest pour point belongs to PB100 (12.1 °C) and the JB100 (10 °C) stands in the second. By blending with commercial diesel the pour point falls drastically. The commercial diesel has the lowest value (−11.2 °C) which can cope with cold climate flow problems. The blends also show betterment in pour point. Fuels with higher pour point will face difficulty in cold climates [14]. The higher level of saturation increases the pour point [14], [15]. As palm biodiesel has higher level of saturation it shows higher pour point.

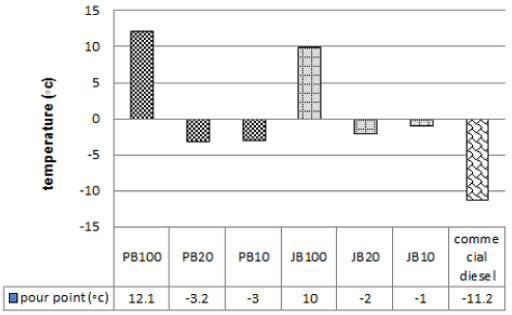

Figure 9. Results of pour point test for biodiesel fuels, blends of biodiesel fuels and commercial diesel.

Conclusions

Jatropha biodiesel, palm biodiesel, commercial diesel and blends of 10 % and 20 % of jatropha and palm biodiesel with commercial diesel were tested. The conclusions can be summarized as below:

- Both of pure biodiesel samples (JB100&PB100) meet the ASTM D6751 standards for all tested parameters.
- All blends of the biodiesels (JB10, JB20, PB10 and PB20) meet ASTM standards for biodiesel blends ASTM D7467 specification.
- The fatty acid structure of biodiesel can impact the oxidation stability of the fuels. This is mainly due to the level of saturation of the biodiesels.
- The density of PB100 is higher than JB100. This can be due to higher saturation of PB100. It seems saturation has more significant effect on density in comparison with chain length of molecular formula.
- The viscosity of JB100 is higher than PB100. This is due to higher level of unsaturation of JB100 in comparison with PB100 regardless of higher density of PB100.
- Blending with commercial diesel can improve the physical and chemical properties of fuels and makes it more convenient for using in conventional and agricultural engines.
- Oxidation stability can affect other fuel properties such as acid value, viscosity, flash point and water content due to creation of sediments and oxidation by-products. Storage condition of fuels is very important for oxidation stability especially for long term storage.
- Calorific value of biodiesels are lower than commercial diesel, however, blending with commercial diesel improves it. Lower calorific value is due to higher percentage of oxygen in biodiesels but this also leads to cleaner combustion due to more complete combustion.
- Flash point of both biodiesel samples is much higher than commercial diesel, which make it safer in handling and storage.
- None of the pure biodiesel samples are suitable for cold climates due to high cloud point and pour point. These elements can cause engine malfunctions such as fuel gelling and cold start.
- Blending with commercial diesel improves the cloud point and pour point of the fuels and therefor problems due to cold flow characteristics will be moderate.

References

1. Sahoo P.K., Das L.M., “Process optimization for biodiesel production from Jatropha, Karanja,” Fuel 88 (2009) 1588-1594.
2. Altun Şehmus, Yaşar Fevzi and Öner Cengiz, “The fuel properties of methyl esters produced from canola oilanimal tallow blends by base-catalyzed transesterification,” International Journal of Engineering Research and Development, Vol.2, No.2, June 2010.
3. Xuea Jinlin, Grift Tony E., Hansen Alan C., “Effect of biodiesel on engine performances and emissions,” Renewable and Sustainable Energy Reviews 15 (2011) 1098-1116.
4. Shahabuddin M., Kalam M.A.*, Masjuki H.H., Bhuiya M.M.K., Mofijur M., “An experimental investigation into biodiesel stability by means of oxidation and property determination,” Energy xxx (2012) 1e7.
5. “Diesel Fuel tech Review.2007-Chevron Corporation,” 2007 Chevron Corporation. All rights reserved.
6. Rao P. V., “Experimental Investigations on the Influence of Properties of Jatropha Biodiesel on Performance, Combustion, and Emission Characteristics of a DI-CI Engine,” World Academy of Science, Engineering and Technology 51 2011.
7. Akbar Emil, Yaakob Zahira, Kamarudin Siti Kartom, Ismail Manal, Salimon Jumat, “Characteristic and - composition of Jatropha Curacas oil seed from Malaysia and its Potential as Biodiesel feedstock,” European Journal of Scientific Research ISSN 1450-216X Vol.29 No.3 (2009), pp.396-403 © EuroJournals Publishing, Inc. 2009.
8. Ong H.C., Silitonga A.S., Masjuki H.H., IMahlia T.M., Chong W.T., Boosroh M.H., “Production and comparative fuel properties of biodiesel from non-edible oils: Jatropha curcas, Sterculia foetida and Ceiba pentandra,” Energy Conversion and Management 73 (2013) 245-255.
9. Pramanik K., “Properties and use of jatropha curcas oil and diesel fuel blends in compression ignition engine,” published in Renewable Energy, 2003, Vol 28, Iss 2, 239-248.
10. Lin Cherng-Yuan* and Lin Yi-Wei, “Fuel Characteristics of Biodiesel Produced from a High-Acid Oil from soybean Soap stock by Supercritical-Methanol Transesterification,” Energies 2012, 5, 2370-2380; doi:10.3390/en5072370.
11. Knothe Gerhard, “Dependence of biodiesel fuel properties on the structure of fatty acid alkyl esters,” Fuel Processing Technology 86 (2005) 1059-1070.

12. Barabás István, “Biodiesel Quality, Standards and Properties,” ISBN: 978-953-307-784-0, InTech.
13. Atabani A.E., Badruddin Irfan Anjum, Masjuki H.H., Chong W.T., “Investigation of physical and chemical properties of potential edible and non-edible feedstock for biodiesel production, a comparative analysis,” Renewable and Sustainable Energy Reviews 21 (2013) 749-755.
14. Barua Pranab K., “Biodiesel from Seeds of Jatropha Found in Assam, India,” International Journal of Energy, Information and Communications Vol. 2, Issue 1, February 2011.
15. Ong H.C., Mahlia T.M.I., Masjuk H.H., Norhasyima R.S., “Comparison of palm oil, Jatropha curcas and Calophyllum inophyllum for biodiesel: A review,” Renewable and Sustainable Energy Reviews 15 (2011) 3501-3515.
16. Yoon Seung Hyun, Park Su Han, Lee Chang Sik, “Experimental Investigation on the Fuel Properties of Biodiesel and Its Blends at Various Temperatures,” Energy & Fuels 2008, 22, 652-656.
17. Tesfa, Belachew, Mishra, Rakesh, Gu, Fengshou and Powels, Nicholas (2010)., “Prediction Models for Density and Viscosity of Biodiesel and their Effects on Fuel Supply System in CI Engines”. Renewable Energy, ISSN 0960-1481 (In Press).
18. Chen Lu-Yen, Chen Yi-Hung, Chiang Tsung-Han, Tsai Cheng-Hsien, “Fuel properties and combustion characteristics of jatropha oil biodiesel-diesel blends,” Journal of the Taiwan Institute of Chemical Engineers 44 (2013) 214-220.
19. Chauhan Bhupendra Singh, “Performance and emission study of preheated Jatropha oil on medium capacity diesel engine,” Energy 35 (2010) 2484e2492.

Acknowledgments

The author thanks for Kind Corporation and assistance of Co-authors and staffs of fuel testing lab and Renewable energy lab in National metal and material technology center (MTEC), National Science and Technology Development Agency (NSTDA) Thailand.

The Engineering Meetings Board has approved this paper for publication. It has successfully completed SAE’s peer review process under the supervision of the session organizer. The process requires a minimum of three (3) reviews by industry experts.

ISSN 0148-7191

http://papers.sae.org/2014-01-2017

20145250

453-20145250 Investigation of diesel and biodiesel soot oxidation in presence of pure oxygen

Morteza Borhanipour [1)] Preechar Karin [2)] Chinda Charoenphonphanich [3)] Nuwong Chollacoop [4)]

Katsunori Hanamura [5)]

1, 2) King Mongkut's Institute of Technology Ladkrabang, International College, Bangkok, 10520, Thailand
(E-mail: mortezaborhanipour@gmail.com)
3) King Mongkut's Institute of Technology Ladkrabang, Faculty of Engineering, Bangkok, 10520, Thailand
4) National Metal and Materials Technology (MTECH) NSTDA, Phatumthani, Thailand
5) Tokyo Institute of Technology, Department of Mechanical and Control Engineering
2-12-1-I1-24 O-okayama, Meguro-ku, Tokyo, 152-8552, Japan

Presented at the JSAE Annual Congress on May, 23, 2014

ABSTRACT: At this article, soot oxidation kinetics diesel PM and palm biodiesel PM from a single cylinder engine at 80% load is investigated by conventional TGA analyze in the isothermal condition. Nitrogen is used as the inert gas and then pure oxygen is introduced for soot oxidation. Mass conversion and apparent activation energy of all samples were analyzed at different fractions of conversion and order of reaction is calculated for each sample. The soot sample from biodiesel shows better oxidation behavior.

KEY WORDS: **Soot oxidation, Diesel PM, TGA, Biodiesel PM, Isothermal, carbon black**

1. INTRODUCTION

Application of CI engines are common around the world due to their high efficiency and power. However, particulate matter (PM) of diesel engine exhaust is one of the adverse feature of the diesel engines due to environmental hazards. This trend has led countries to use tougher limitation and emission regulation. To meet the new emission requirements it's common to make improvements in fuels and after treatment systems.

For fuel improvement, application of biodiesels is one of the prevalent remedies for this problem among many countries. The biodiesels are more environmental friendly due to cleaner combustion, biodegradability, being non-toxic and lower emission profile as compared to petroleum based diesels[(1)]. The composition of PMs from a diesel engine may vary widely depending on the operating conditions and fuel composition. PM is traditionally divided into three main fractions: solid fraction (SOL), soluble organic fraction (SOF), and sulfate particulates (SO4) that consist of sulfuric acid and water. The SOL of diesel PMs is composed primarily of elemental carbon, sometimes referred to as inorganic carbon. This carbon, which does not chemically bound with other elements, is the finely dispersed carbon black or soot substance responsible for black smoke emission. Hydrocarbons (HCs) adsorbed on the surface of the carbon particles are present in the form of fine droplets from the SOF of diesel particulates. In some researches, this fraction is also referred to as the volatile organic fraction (VOF) [(2)]. For after treatment, diesel particulate filter (DPF) is a common and effective control of PM emission and development of DPF is an ideal way for soot emission control. Understanding of soot oxidation kinetics is a common way for DPF betterment. Several conducted experiments to define the kinetics of characteristics associated with soot oxidation [(3)]. The common methods are a flow reactor with the flatbed or thermo gravimeter analyzer (TGA) [(3)]. Thermo-analytical (TA) techniques have certain advantages and disadvantages in comparison with the more traditional flow-reactor techniques which are also widely employed. An important advantage of TA techniques is their convenience, as small sample sizes can be used and the analyses are usually rather fast compared with flow-reactor experiments. The main disadvantage of ta techniques is that the sample is enclosed in a small crucible. As a result, the gas feed flows around the sample, instead of through the sample as is the case in most flow-reactor samples. The sample is more or less isolated from its surroundings. Therefore, heat and mass-transfer limitations between the sample and the surroundings can easily occur when the chemical or physical processes in the sample are fast [(4)].

At this study, the soot oxidation kinetics of palm biodiesel (PB100) and diesel is investigated on the presence of pure oxygen with isothermal TGA, under four different temperatures including (450, 500, 550, 600 (C)). Mass-conversion, apparent activation energy and order of carbon, *n*, of each sample is calculated and discussed. Hence the composition of the PM of diesel and biodiesel is different the CHN analyze is done in order to find out the composition of PM for each sample. The results of this study will help us for further researches about DPF soot trapping and DPF regeneration.

2. EXPERIMENTAL SETUP AND PROCEDURE

2.1. Fuels

The fuels which were used for soot trapping at this project were conventional diesel and palm biodiesel (PB100). The characteristics and technical data of fuels which were used at this project for soot trapping are discussed at an earlier published technical paper [1].

2.2. The engine

The small single cylinder diesel engine, Yanmar, is used for soot generation with PB100 and diesel. The technical data of engine is mentioned at table 1.

Table 1 engine technical data

Type	Direct injection (D.I)
No. of cylinder	1
Bore × Stroke (mm)	92 × 96
Displacement (Lit)	0.638
Compression ratio	16.1:1
Injection pressure (Kg/cm^2)	200
Injection timing (degree)	BTDC 19.0
Max.Output (Kw/rpm)	8.8/2400

The engine was set at 80 % load with 2400 rpm on the Eddy current engine dynamometer (Tokyo plant ED-60kw-LC at KMITL). Metallic filter were used to collect PM and for each fuel new filter were used for collection. Then samples were collected and kept at sealed containers and sent for TGA.

2.3. TGA

Isothermal TGA test was done for all PM samples. Each sample was tested at four different temperature including 450, 500, 550 and 600 ºC). For non-isothermal part nitrogen was used to heat up the sample to desired temperature then pure oxygen is introduced for soot oxidation for one hour. Then Chemical kinetics of TGA results were analyzed by relations below:

$$PM+O_2 \rightarrow CO_2 \qquad (1)$$

The chemical reaction rate in eq.1 can calculate from the TGA curve based on the chemical kinetic in eq.2

$$-\frac{d[PM]}{dt} = k[PM]^n[O_2]^m \qquad (2)$$

Where PM is particulate matter mass, *t* is time, *k* is specific rate constant, m, *n* are the reaction order. The dependence of the specific rate constant k is expressed by eq.3.

$$k=Ae^{-E_a/RT} \qquad (3)$$

Where A is the frequency factor, Ea. is the activation energy, R is the gas constant. The apparent activation energy can be calculated by eq.4 [5].

$$\ln\left[\frac{-1}{[PM]^n}\frac{d[PM]}{dt}\right] = -\frac{E_a}{RT} + (\ln A + m\ln[O_2]) \qquad (4)$$

3. RESULUTS AND DISSCUSION

3.1. Mass conversion at high temperatures

The result of isothermal TGA at higher temperatures including 500,550 and 600 º(C) is plotted at Fig 1. (a) and (b). The increase of temperature will results to faster and higher conversion rate as shown in figures. The conversion rate of all samples including diesel and biodiesel increases by increase of temperature. At 500 º(C) the PM from biodiesel converts and oxidizes faster than diesel about 1.5 times at initial point of isothermal part while at non-isothermal part before 500 º(C) both fuels have similar trends. At 550 º (C) the conversion trend lines change. At non-isothermal part, where there is no oxygen, the conversion rate of biodiesel and diesel is almost the same while after introduction of oxygen at desired temperature the PM sample from biodiesel shows a relatively faster conversion rate in comparison with the diesel. At this temperature diesel PM shows the slower conversion rate than biodiesel PM again. At 600 º(C) the samples from diesel and biodiesel have almost similar trends of conversion and oxidation. The main reason for all these behaviors is due to difference in composition of PM from diesel and biodiesel. The PM from biodiesel consist of more unburned hydrocarbon (HC) in comparison with diesel. This is due to fuel characteristics of biodiesel which is studied at earlier paper [1]. Due to more incomplete combustion at higher combustion rate and load, more fuel consumption due to lower calorific value of biodiesel and longer evaporation time and ignition delay due to higher viscosity and density the unburned HC will be more in the exhaust PM in comparison with diesel. The percentage of volatile fraction (VOF) in the particulate emitted by a diesel engine depends on the engine

design characteristics (DI, IDI, turbocharged), the fuel injection system (injection principle, injection pressure and timing, nozzles characteristics), the exhaust gas recirculation (EGR) rate, and engine operation point (speed and load, exhaust temperature) and high-boiling point components contained in fuel, such as higher boiling point pagans or aromatics adsorbed from particulates emitted by the engine, are reported to increase VOF content [6]. As biofuels are oxygenated fuels, they may have more oxygen content in the PM and this can boost oxidation and thus biodiesel shows faster oxidation rate in comparison with diesel. The increase in temperature is also responsible for increase in rate of conversion. In order to have a general overview about the conversion range of PM samples we can refer to earlier study [7] at our lab, the PM of biodiesel consists of 4% moisture, 40% HC and 56% C while composition of diesel PM is made of 4% moisture, 29% HC and 67 % C at 80% load from non-isothermal TGA curves. At the same study, the conversion range of moistures and VOF is from 25-100 °(C), soluble fraction (SOF) parts which mainly consists of HC oxidizes from 100-500 °(C) and carbonaceous part of PM or solid (SOL) oxidizes at higher peak of temperature between 500-600 °(C). This can also be used to describe the difference of conversion rate of samples. The difference of composition of PM will result in difference of energy of activation, Ea.

3.2. The reaction order of carbon, *n*, at different temperatures

The reaction order of carbon varies between different experiments and samples. Neeft et al [8] found a range of 0.65-0.80 for reaction order of Printex-U. They have also mentioned that the water can affect the order of reaction and in absence of water the reaction order of carbon for diesel soot 0.56 while the value was 0.69 in presence of water. In order to calculate the order of reaction for carbon, the natural logarithm of the rate formula (eq.2) is used and the results are shown in Fig2. The results shows that the *n* value for diesel is *n*= 0.58 and *n*=0.42 for biodiesel. The *n*, reaction order, for diesel PM is higher than biodiesel PM. This also shows the importance of carbon reaction order in estimation of Ea. and can vary the Ea .

3.3. Activation energy

In order to explain the different part of PM (VOF, SOF and SOL) and have a better picture of conversion of PM samples, for each sample, after normalizing, the soot conversion of all samples is divided to three parts , based on equal percentages of conversion rate of the samples including (80-60%),(60-40%)and (40-20%). In all temperatures also, the VOF and SOF parts of biodiesel has higher oxidation rate. Based on the composition of the PM from diesel and biodiesel, as mentioned before, amount of unburned HC in biodiesel is more than diesel PM about 1.93 times and biodiesel PM also have more oxygenated content which can enhance the conversion rate and oxidation. In order to have a better description about the conversion of the sample it's necessary to know the activation energy of the PM samples. To do so, the Arrhenius plot of the samples are plotted at Fig.3 and the activation energy of three fraction parts of PM samples are plotted at table 2. At the carbonaceous part the Ea. for each sample for each level is calculated and the results are shown at table 2.

Table 2. The calculated results of Ea for diesel and biodiesel PM with different reaction order, *n*

Mass fraction %	Ea (kJ/mole) with Calculated n=0.42	Mass fraction %	Ea(kJ/mole) with Calculated n= 0.58
Biodiesel 80-60%	146.74	Diesel 80-60%	181.70
Biodiesel 60-40%	180.63	Diesel 60-40%	244.74
Biodiesel 40-20%	206.42	Diesel 40-20%	235.74

The difference of PM composition in biodiesel PM and diesel PM also has noticeable effect on Ea. The difference of Ea at (80-60%) and (60-40%) fraction can be referred to difference in amount and type of HC and elemental composition while at (40-20%) stage the results get closer and can be an indication of more pure carbonaceous part and more similar composition. This can be due to difference in bond energy of PM remaining SOL parts and carbonaceous parts. Generally the VOF and SOL parts of PM vaporize and oxidize at earlier fractions and usually the later fractions are consists of more carbonaceous parts and ash. In determination of Ea, the weight factor influences the results of the fit of Arrhenius equation and therefore the magnitude of the determined activation energy [8].

The CHN analyze of PM samples shows that the PM of biodiesel is made of 1.1% H and 74.1% C while for diesel PM its consists of 1.1% H and 81% C . The Ea corresponds to the energy barrier to be overcome during the reaction. Its maximum value corresponds to the bond energies in the molecule the Ea is approximately equal to the bond energy of, which is split [9] and bonding energy between C and O and H are different and these differences can alter the Ea . The H/C ratio can be correlated to

the oxidative reactivity of soot particles. The higher H content per unit C atom increases the possibility of H abstraction by O_2 or the radicals present in the combustion environment such as H, OH, CH_3 and C_3H_3 to create a radical site on soot to facilitate O_2 addition on it, which can enhance soot oxidation rate [10]. The diesel fuel is mainly consists of aromatic components and poly aromatic hydrocarbons ,PAHS, generally have lower H/C ratios and thus lower reactivity but in biodiesel the presence of saturated components chains in the soot can increase its H/C ratio as well as its oxidative reactivity [10] . For more clarification the conversion test at 600^0(C) is done again and compared with conversion rate of carbon black. This comparison can clearly show the difference of conversion rate of engine PM and pure carbon and thus effect of impurities such as VOF and SOF parts.

3.4. Size distribution

Some earlier studies shows that when diesel particles are heated to temperatures as high as 300-400 °C, they may be classified into two types, ‘‘less volatile” ones that shrink only slightly, and ‘‘more volatile” ones that almost completely disappear. The “more volatile” ones were identified to be mainly heavy hydrocarbons and some sulfate, the “less volatile” ones were identified as carbonaceous agglomerates, although most of the volatile materials associated with PM are usually found adsorbed on these agglomerates [11]. The size of PM samples and their belonging parts can be related to each other and studies shows the amount of volatile matter is a function of particle size [11]. Therefore, the size distribution of PM samples is shown at an earlier study from our lab [12] and TEM pictures are shown in Fig 4. The surface to volume ration of PM has invers relation with PM size and thus lower *n* value, however for diesel PM, higher *n* and larger size in comparison with biodiesel can be seen. This can be due to presences of lesser intersectional points in diesel PM in comparison with biodiesel and this can cause decrease in value of *n* for biodiesel PM. Most of the material in the accumulation mode above about 100 nm is nonvolatile, presumably mainly elemental carbon [11]. As shown in [12], higher numbers of diesel PM are in range of 80- 120 (nm) and can be contributed to be lesser volatility. The size of biodiesel PM is smaller than diesel and this trend might be due to more complete combustion due to higher oxygen content of biodiesel. Other impurities such as trace of metals and engine lubricant oil can also affect the results [11]. The soot generated by oxygenated fuel has a nanostructure with more reactive sites for oxidation, which makes it burn much faster compared to soot made by their reference fuel [11] [13]. Boehm an et al. compared reactivity and nanostructure of both diesel soot and biodiesel soot. They found biodiesel soot has higher reactivity and more amorphous nanostructure, which inconsistent with VanderWal and Tomasek’s finding [11] [14]. But further analyze in nano structure is needed to discuss it more clearly.

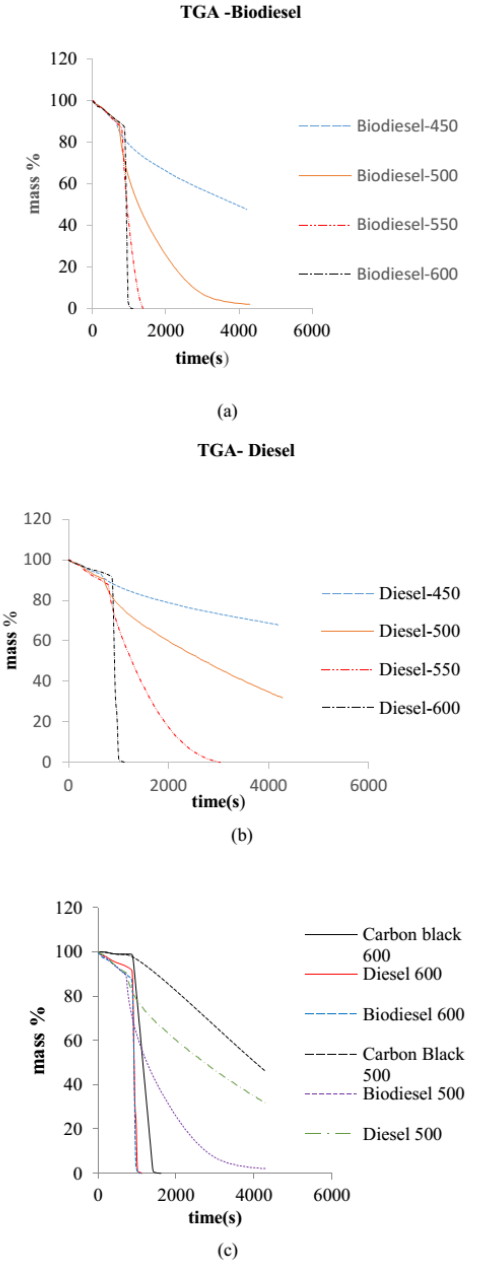

Fig 1. The conversion rate of samples (a) Biodiesel (b) Diesel PM (c) comparison with carbon black

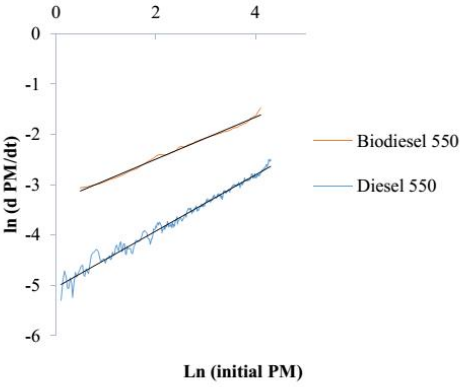

Fig2. The reaction order of soot samples 550º(C)

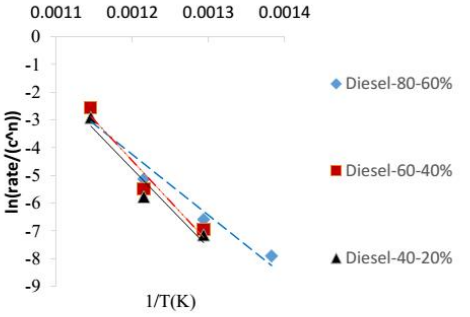

(a)

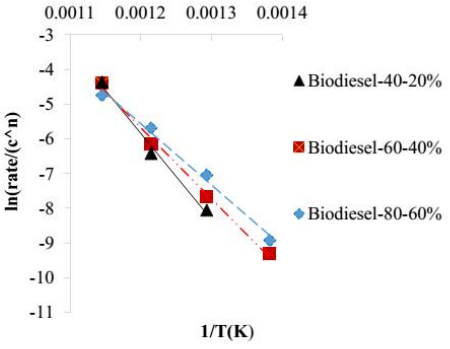

(b)

Fig 3. Arrhenius plot of three fractions of PM of (a) Diesel (b) Biodiesel PM

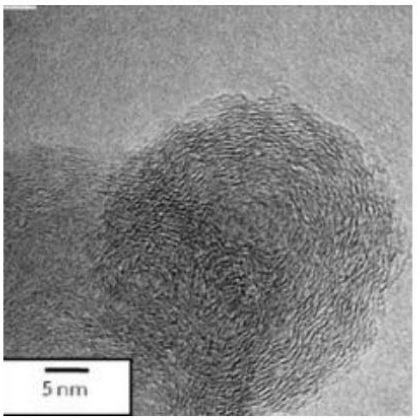

(a)

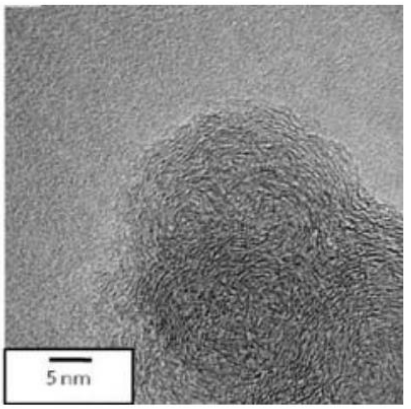

(b)

Fig 4. The TEM pictures of (a) Diesel (b) Biodiesel PM

4. CONCLUSION

- The conversion of diesel and biodiesel PM were investigated and compared with carbon black and among the samples the biodiesel PM showed faster conversion and oxidation rate and initial mass of conversion can affect the conversion trend.
- The Ea of the soot samples were calculated for each fraction of mass conversion and at the 80-60% and 60-40% fractions diesel shows higher Ea in comparison with biodiesel. This can be due to higher amount of HC in biodiesel PM.

- The difference of Ea between biodiesel and diesel PM at 60-40% fraction is the highest. This part is believed to be controlled mainly by effect of PM SOL composition part of diesel PM and biodiesel PM. Oxygenated contents in biodiesel PM might have affected the easiness of oxidation and thus it may require lesser Ea.
- Higher values for Ea at 40-20 % fraction in biodiesel PM can be an indication of higher percentage of carbonaceous part . At this fraction, although the Ea of diesel PM is still higher than biodiesel PM but the difference is lesser and it can be contributed to higher similarity of composition of the both PMs.
- The fuel composition such as elemental composition, H/C ration and type of hydrocarbon such as PAHs can affect the conversion rate, Ea and probably order of reaction.
- The size of PM also can have a significant role and smaller size of biodiesel PM can be a sign of different volatile part and therefore different conversion trend.
- The order of carbon in reaction for diesel is higher than biodiesel and this can also be an affecting factor on Ea. The higher value of the *n* can be referred to better oxidation trend. However this factor can't be considered solely as an indication of better oxidation and several other factors are engaged at oxidation process.

ACKNOWLEDGEMENTS

The authors gratefully acknowledge the financial support from Thailand Research Fund (TRF), ministry of Science and Technology, Thailand and TAIST Tokyo Tech program and MTEC for their support.

REFERENCES

(1) Morteza Borhanipour: Comparison Study on Fuel Properties of Biodiesel from Jatropha, Palm and Petroleum Based Diesel Fuel. SAE Technical Paper 2014-01-2017, 2014, doi: 10.4271/2014-01-2017.

(2) Preechar Karin, Yutthana Songsaengchan: Physical Characterization of Biodiesel Particle Emission by Electron Microscopy. JSAE 20139150 / SAE 2013-32-9150.

(3) Kyeong o. Lee: DETAILED analysis of kinetic reactions in soot oxidation by simulated diesel exhaust emissions proceedings of the combustion institute 34 (2013) 3057–3065.

(4) John P.A. Neeft, The effects of heat and mass transfer in thermo gravimetrical analysis. A case study towards the catalytic oxidation of soot Thermochemical Acta 287 (1996) 261-278.

(5) Preechar Karin et al: Nanostructure of renewable oxygenated fuels particulate matter g.a. ASEAN Engineering Journal Part A Volume 3, Number 1 March 2013.

(6) Stratakis: Thermogravimetric analysis of soot emitted by a modern diesel engine run on catalyst-doped fuel Combustion and Flame 132 (2003) 157–169.

(7) Yuttana Songsaengchan: nanostructures investigation of biodiesel particulate matter presented at the JSAE Annual Congress on May, 24, 2012.

(8) John P. A. Neeft :kinetics of soot oxidation S0016-2361(97)00119-1.

(9) Soot Formation Modeling during Hydrocarbon Pyrolysis and Oxidation behind Shock Waves. Ruprecht-Karls-Universit¨atHeidelberg terdisziplin¨ares Zentrum f¨ur Wissenschaftliches Rechnen2007.

(10) Abhijeet Raj: structural effects on the oxidation of soot particles by O2: Experimental and theoretical study Combustion and Flame xxx (2013) xxx–xxx.

(11) Heejung Jung: Characteristics of SME Biodiesel-Fueled Diesel Particle Emissions and the Kinetics of Oxidation. Environ. Sci. Technol. 2006, 40, 4949 4955.

(12) Yuttana Songsaengchan:Investigation of Biodiesel particulate matter in Nanostructure, The 2nd International Conference on automotive technology, engine and alternative fuels ,HCMUT,VNUHCM, December 4-5 , 2012.

(13) Vander Wal,Tomasek: Soot nanostructure ,Definition, quantification and implicationAAR: Atlanta, GA, 2004

(14) Nagle,J.,Strickland-Constable: Oxidation of carbon between 1000 and 2000 °C. In Fifth Carbon Conference;Pergamon: Oxford, 1962; pp 154-164.

Burapha University International Conference 2014
Burapha University, Thailand
July 3-4, 2014

Investigation of Diesel and Biodiesel Soot Oxidation

Morteza Borhanipour [1], Preechar Karin [2], Chinda Charoenphonphanich [3], Nuwong Chollacoop [4], Manida Tngroon[4], Katsunori Hanamura [5]

1, 2) King Mongkut's Institute of Technology Ladkrabang, International College, Bangkok, 10520, Thailand
3) King Mongkut's Institute of Technology Ladkrabang, Faculty of Engineering, Bangkok, 10520, Thailand
4) National Metal and Materials Technology (MTEC) National Science and Technology Development Agency, Phatumthani, Thailand
5) Tokyo Institute of Technology, Department of Mechanical and Control Engineering
2-12-1-I1-24 O-okayama, Meguro-ku, Tokyo, 152-8552, Japan
E-mail: mortezaborhanipour@gmail.com

ABSTRACT

At this study, soot oxidation kinetics diesel PM and palm biodiesel Particulate Matter (PM) from a single cylinder engine at 80% load is investigated by conventional Thermal gravimetric analysis (TGA) in the isothermal condition. Nitrogen is used as the inert gas and then air is introduced for soot oxidation. Carbon black is used as the reference material. Mass conversion, order of carbon in reaction, apparent activation energy and conversion rate of all samples were analyzed at different fractions of conversion for each sample. The soot sample from biodiesel shows better oxidation behavior.

Keywords: soot oxidation kinetics, activation energy, TGA isothermal.

1. INTRODUCTION

Higher efficiency of diesel engines has made them to be used widely around the world. But particulate matter (PM) of diesel engine exhaust is one of the disadvantages of the diesel and causes environmental hazards. To overcome this problem countries have legislated higher emission standards and to meet the new emission requirements and betterment in fuels and after treatment systems is two common solutions. Common way for fuel improvement is application of biodiesels or blending petroleum based diesel with biodiesels. Biodiesels are more environmental friendly due to cleaner combustion, biodegradability, being non-toxic and lower emission profile as compared to petroleum based diesels (Morteza Borhanipour et al. SAE 2014). The composition of PMs from a diesel engine may vary widely depending on the operating conditions and fuel composition. PM is traditionally divided into three main fractions: solid fraction (SOL), soluble organic fraction (SOF), and sulfate particulates (SO4) that consist of sulfuric acid and water. The SOL of diesel PMs is composed primarily of elemental carbon, sometimes referred to as inorganic carbon. This carbon, which does not chemically bound with other elements, is the finely dispersed carbon black or soot substance responsible for black smoke emission. Hydrocarbons (HCs) adsorbed on the surface of the carbon particles are present in the form of fine droplets from the SOF of diesel particulates. In some researches, this fraction is also referred to as the volatile organic fraction (VOF) (Preechar Karin et al SAE 2013). Diesel particulate filter (DPF) is a prevalent device for filtration of diesel exhaust PM. Understanding of soot oxidation kinetics is a common way for DPF improvement. Several conducted experiments to define the kinetics of characteristics associated with soot oxidation. The common methods are a flow reactor with the flatbed or thermo gravimeter analyzer (TGA) (Kyeong o. Lee, 2013). The TGA technique offers the advantage that only a small amount of sample is needed, typically less than 20 mg, and the

kinetic parameters are determined by a limited number of experiments (I. C. Jaramillo et al 2013). At this study, the soot oxidation kinetics of palm biodiesel (PB100) and diesel is investigated on the presence of air with isothermal TGA, under three different temperatures including (500, 550, 600^{o}(C)). Mass-conversion, apparent activation energy and order of carbon, *n*, of each sample is calculated and discussed. Hence the composition of the PM of diesel and biodiesel is different the CHN analyze is done in order to find out the composition of PM for each sample. The results of this study will help us for further researches about DPF soot trapping and DPF regeneration.

2. MATERIALS AND METHODS

2.1. Fuels

Technical date of fuels which were used at this study is shown at earlier technical paper (M.Borhanipour et al. SAE 2014).

2.2. The engine

The small single cylinder diesel engine, Yanmar, is used for soot generation with PB100 and diesel. The technical data of engine is mentioned at table 1. The engine was set at 80 % load with 2400 rpm on the Eddy current engine dynamometer (Tokyo plant ED-60kw-LC at KMITL). Metallic filter were used to collect PM and for each fuel new filter were used for collection. Then samples were collected and kept at sealed containers and sent for TGA.

2.3. Sample Preparation

Isothermal TGA test was done for all PM samples. Each sample was tested at four different temperature including 500, 550 and 600 ^{o}(C). For non-isothermal part nitrogen was used to heat up the sample to desired temperature then pure oxygen is introduced for soot oxidation for one hour. Same process is done with air at isothermal part. In order to have a good reference, carbon black N330 is used for TGA test at 600 ^{o}(C). Then Chemical kinetics of TGA results were analyzed by relations below:

$$PM+O_2 \rightarrow CO_2 \qquad (1)$$

The chemical reaction rate in eq.1 can calculate from the TGA curve based on the chemical kinetic in eq.2.

$$-\frac{d[PM]}{dt} = k[PM]^{n}[O_2]^{m} \qquad (2)$$

Where PM is particulate matter mass, *t* is time, *k* is specific rate constant, m, *n* are the reaction order. The dependence of the specific rate constant k is expressed by eq.3.

$$K = A\, e^{-Ea/RT} \qquad (3)$$

Where A is the frequency factor, Ea. is the activation energy, R is the gas constant. The apparent activation energy can be calculated by eq.4 (Preechar Karin et al: ASEAN Engineering Journal 2013).

$$\ln\left[\frac{-1}{[PM]^{n}}\frac{d[PM]}{dt}\right] = -\frac{E_a}{RT} + (\ln A + m\ln[O_2]) \qquad (4)$$

The value of *m*, is considered as unity, m=1 at this study for simplicity of calculation.

3. RESULTS & DISCUSSION

3.1. Mass conversion at high temperatures

The result of TGA is shown in Fig.1. As seen in graph, as the temperature increases the rate of mass conversion and oxidation increases too because higher amount of energy for reaction is available. For all samples, the highest rate of conversion belongs to 600^{o}(C) graph. In comparison between the soot samples, biodiesel shows faster and higher percentage of conversion in comparison with diesel in all temperatures. This can be contributed to composition of PM of diesel and biodiesel. The PM samples from biodiesel has higher amount of hydrocarbon (HC) in comparison with diesel and this is due to biodiesel features, which is discussed at earlier technical paper (M.Borhanipour et al. SAE 2014). At higher engine load the rate of fuel injection is higher and ignition delay is lower and more incomplete combustion can be seen. Besides, more fuel consumption due to lower calorific value of biodiesel and longer evaporation time due to higher viscosity and density the unburned HC will be more in the exhaust PM in comparison with diesel. The composition of HC in biodiesel PM is also different from diesel PM. Biodiesels also have higher oxygenated components in their PM in comparison with diesel hence they are consists of higher amount of oxygen. In previous study at our lab (Yuttana Songsaengchan:JSAE 2012), the composition of diesel and biodiesel PM is determined by non-isothermal TGA test and results shows that the PM of biodiesel consists of 4% moisture, 40% HC and 56% C while composition of diesel PM is made of 4% moisture, 29% HC and 67 % C at 80% load. Therefore, the diesel PM has higher carbonaceous components and lower percentage of HC, thus slower conversion rate in comparison with biodiesel. The apparent activation energy of the samples plays a key role in the oxidation and it is discussed at next chapter.

3.2. Reaction order of carbon, *n*, at different temperatures for soot samples

Variety of *n* value is common among the studies. Earlier studies (John P. A. Neeft 1996), the range of n was 0.65-0.80 for reaction order of Printex-U. They have also mentioned that the water can affect the order of reaction and in absence of water the reaction order of carbon for diesel soot 0.56 while the value was 0.69 in presence of water. At this study, for calculation of *n*, the natural logarithm of the rate formula (eq.2) is used and the results are shown in Fig 2. The calculated results show that the *n* value for biodiesel is 0.72 at 550 ^{o}(C) and 0.57 at 600 ^{o}(C) for diesel. The reason for choosing these two temperatures is the more uniform trend of conversion.

3.3. Activation energy

For better explanation of the different part of PM (VOF, SOF and SOL) and have a better picture of conversion of PM samples, for each sample, after normalizing, the soot conversion of all samples is divided to three parts , based on equal percentages of conversion rate of the samples including (80-60%),(60-40%) and (40-20%). The results of Ea. is shown in table 2 and Arrhenius plots are shown in Fig 3. In comparison between the soot samples, diesel PM has higher Ea in all fractions. Among three different fractions, the (60-40%) fraction has highest value of Ea. Based on the composition of the PM from diesel and biodiesel, as mentioned before, amount of unburned HC in biodiesel is more than diesel PM about 1.93 times and biodiesel PM also have more oxygenated content which can enhance the conversion rate and

oxidation. The CHN analyze of PM samples shows that the PM of biodiesel is made of 1.1% H and 74.1% C while for diesel PM its consists of 1.1% H and 81% C. The H/C ratio is indication of oxidation reactivity and higher H/C value increases the possibility of H abstraction by O_2 or the radicals present in the combustion such as H, OH, CH_3 and C_3H_3 to create a radical site on soot to facilitate O_2 addition on it, which can enhance soot oxidation rate. The diesel fuel is mainly consists of aromatic and poly aromatic hydrocarbons and generally have lower H/C ratios and thus lower reactivity. But in biodiesel the presence of saturated components chains in the soot can increase its H/C ratio and its oxidative reactivity (Morteza Borhanipour, JSAE 2014).

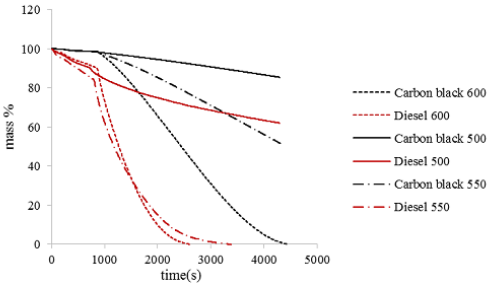

(a)

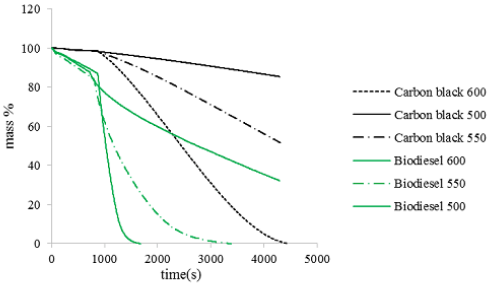

(b)

Fig 1. Results of TGA (a) Diesel vs. Carbon black (b) Biodiesel vs. Carbon black

Table 1 engine technical data

Type	Direct injection (D.I)
No. of cylinder	1
Bore × Stroke (mm)	92 × 96
Displacement (Lit)	0.638
Compression ratio	16.1:1
Injection pressure (Kg/cm^2)	200
Injection timing (degree)	BTDC 19.0
Max.Output (Kw/rpm)	8.8/2400

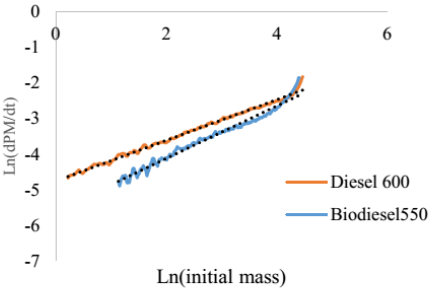

Fig2.The reaction order of Carbon, *n*.

The difference of Ea in fractions can be also due to different PM components percentages. Generally the VOF and SOF parts of PM vaporize and oxidize at earlier fractions and usually the later fractions are consists of more carbonaceous parts and ash. In determination of Ea, the weight factor influences the results of the fit of Arrhenius equation and therefore the magnitude of the determined activation energy (John P. A. Neeft S0016-2361(97)00119-1).

Table 2. The calculated results of Ea

Mass fraction	**Ea (kJ/mole)**	**Mass fraction**	**Ea (kJ/mole)**
Diesel 80-60%	152.91	Biodiesel 80-60%	146.97
Diesel 60-40%	165.29	Biodiesel 60-40%	156.55
Diesel 40-20%	158.56	Biodiesel 40-20%	150.54

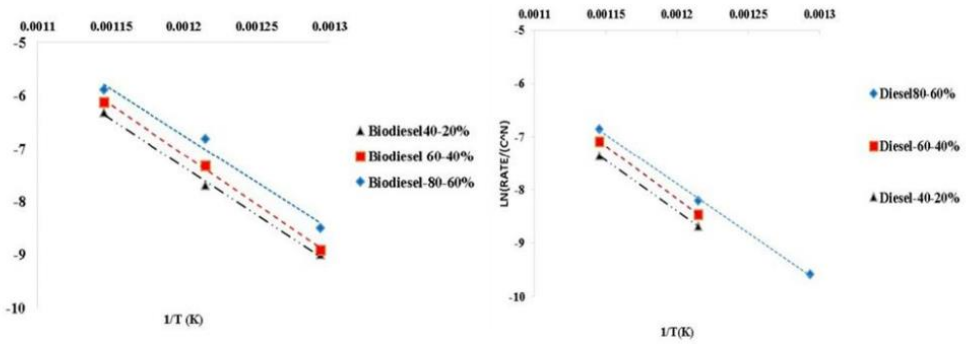

(a) (b)

Fig 3. Arrhenius plot of three fractions of PM of (a) Biodiesel (b) Diesel PM

3.4. Rate of conversion

The rate of conversion of the soot samples were measured and shown in Fig 4. This results also shows higher rate of conversion of biodiesel soot in comparison with the diesel. The first small Peak (non-isothermal part) can be contributed to the VOF and second (main and isothermal part) peak is the point of introduction of air and oxidation begins. As temperature increase the slop of the graph becomes sharper, especially for biodiesel at 600º (C). Carbon black shows more constant rate and slower due to higher amount of carbonaceous component (about 93%) while soot samples consist of unburnt hydrocarbons and other impurities. At 600º (C) the graphs are so smooth due to faster rate of conversion and we see lesser fluctuations.

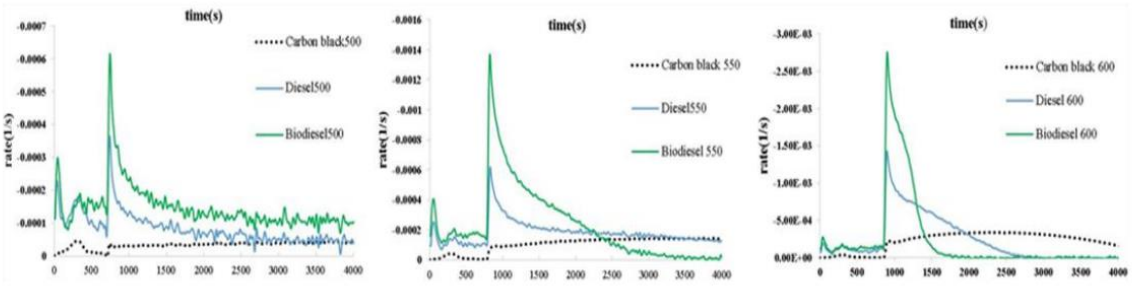

(a) (b) (c)

Fig 4. The rate of conversion (a) rate at 500 º (C) (b) rate at 550 º (C) (c) rate at 600 º (C).

4. CONCLUSION

- The conversion rate of biodiesel is higher than diesel and carbon black. This is due to difference of PM compositions and amount of them. The biodiesel fuel characteristics can alter the composition of HC parts of PM significantly by direct impact or by changing the engine working condition (injection rate, ignition delay…).
- The order of reaction on biodiesel is higher and it may be indication of an incomplete spherical shape of PM and shape is not match with value from the shrinking core model which is (2/3).
- The different H/C ratio, elemental compositions, activation energy of PM can impact the rate of oxidation.
- The rate per time graphs shows rapid oxidation of soot, especially for biodiesel while carbon black shows a relatively more constant rate and this clearly shows the impact of different SOF and VOF parts of PM soot.

ACKNOWLEDGEMENTS

The author would show his gratitude to King Mongkut's Institute of Technology Ladkrabang engine lab, Thailand Research Fund (TRF), ministry of Science and Technology, Thailand and TAIST Tokyo Tech program and MTEC for their financial and technical support.

REFERENCES

Morteza Borhanipour: Comparison Study on Fuel Properties of Biodiesel from Jatropha, Palm and Petroleum Based Diesel Fuel. SAE Technical Paper 2014-01-2017, 2014, doi: 10.4271/2014-01-2017.

Morteza Borhanipour, Preechar Karin, Chinda Charoenphonphanich, Nuwong Chollacoop, Katsunori Hanamura: Investigation of diesel and biodiesel soot oxidation in presence of pure oxygen, Presented at the JSAE Annual Congress on May, 23, 2014.

I.C. Jaramillo, J. Levinthal and J. S. Lighty: Oxidation Kinetics and Nanostructure of Model Carbons Based On TGA Data. May 19-22, 2013

Preechar Karin et al: Nanostructure of renewable oxygenated fuels particulate matter g.a. ASEAN Engineering Journal Part A Volume 3, Number 1 March 2013.

Preechar Karin, Yutthana Songsaengchan: Physical Characterization of Biodiesel Particle Emission by Electron Microscopy. JSAE 20139150 / SAE 2013-32-9150.

Kyeong o. Lee: Detailed analysis of kinetic reactions in soot oxidation by simulated diesel exhaust emissions proceedings of the combustion institute 34 (2013) 3057–3065.

John P.A. Neeft, The effects of heat and mass transfer in thermo gravimetrical analysis. A case study towards the catalytic oxidation of soot Thermochemical Acta 287 (1996) 261-278.

Yuttana Songsaengchan: nanostructures investigation of biodiesel particulate matter presented at the JSAE Annual Congress on May, 24, 2012.

The 5th TSME International Conference on Mechanical Engineering
17-19th December 2014, The Empress, Chiang Mai
TSME-ICoME 2014 ASEAN AND BEYOND

AEC161

Investigation of Diesel and Biodiesel Soot Oxidation inside a Sample of Conventional DPF

Morteza Borhanipour[1], Preechar Karin [2], Chinda Charoenphonphanich [3]Nuwong Chollacoop [4]
Manida Tongroon[4] and Katsunori Hanamura [5]

[1 & 2] King Mongkut's Institute of Technology Ladkrabang, International College, Bangkok, 10520, Thailand
[3] King Mongkut's Institute of Technology Ladkrabang, Faculty of Engineering, Bangkok, 10520, Thailand
[4] National Metal and Materials Technology (MTEC) NSTDA, Phatumthani, Thailand
[5] Tokyo Institute of Technology, Department of Mechanical and Control Engineering
2-12-1-I1-24 O-okayama, Meguro-ku, Tokyo, 152-8552, Japan
*Corresponding Author: motezaborhanipour@gmail.com

Abstract

Higher demands of fossil fuels and increase of air pollution due to widely usage of diesel engines has made countries to enhance the after treatment systems. At this study, the soot oxidation of Diesel and Biodiesel is studied with isothermal Thermo gravimetric analyze (TGA) and Mass conversion, apparent activation energy of all samples were analyzed at different temperatures of conversion for each sample. Carbon black N330 was used as a reference material of oxidation. Then a sample of Diesel Particulate Filter (DPF) was used to trap Particle Matter (PM) from engine exhaust from diesel and bio diesel combustion. After trapping the DPF was regenerated by heating up the filter with tube furnace .The results of the tests show significant impact of the fuel properties on soot oxidation. Soot from Biodiesel shows better oxidation behavior and faster regeneration.

Keywords: Soot oxidation, Diesel & Biodiesel soot, DPF regeneration, TGA.

1. Introduction

Diesel engines are widely in use in all over the world due to their higher efficiency in different fields of transport and industry. However the increase in fossil fuel demands and new emission regulations has obliged the countries to legislate new policies and restriction to cope with these two main disadvantages of diesel engines. Increase of fossil fuels price and air pollution has made companies and scientists to look for alternative fuels to compensate the energy demands and emission regulations and meet the new global standards. To do so a dual policy is required to reduce the dependency to fossil fuels and air pollution at a relatively parallel action. For fuel improvement, application of biodiesels is one of the prevalent remedies for this problem among many countries. The biodiesels are more environmental friendly due to cleaner combustion, biodegradability, being non-toxic and lower emission profile as compared to petroleum based diesels [1]. Diesel particulate matter is part of a complex mixture of combustion of diesel engines product which is consists of carbonaceous, unburnt Hydrocarbons and other impurities. The

composition of PMs from a diesel engine may vary widely depending on the operating conditions and fuel composition. PM is traditionally divided into three main fractions: solid fraction (SOL), soluble organic fraction (SOF), and sulfate particulates (SO4) that consist of sulfuric acid and water. The SOL of diesel PMs is composed primarily of elemental carbon, sometimes referred to as inorganic carbon. This carbon, which does not chemically bound with other elements, is the finely dispersed carbon black or soot substance responsible for black smoke emission. Hydrocarbons (HCs) adsorbed on the surface of the carbon particles are present in the form of fine droplets from the SOF of diesel particulates. In some researches, this fraction is also referred to as the volatile organic fraction (VOF) [2-7]. Diesel particulate filter (DPF) is a prevalent device for filtration of diesel exhaust PM. The mechanism of DPF is based on entrapment of exhaust PM by the porous material of DPF. After compiling the PM inside DPF, the filter will be regenerated in two main method, active and passive method. In active method, the heat of engine exhaust is responsible for DPF regeneration and the trapped PM will be oxidized by engine exhaust while in passive form, the DPF will be regenerated by the heating up the DPF with a high temperature system separately after removal from the vehicle. At this study, at first step the PM samples were collected from single cylinder engine by application of diesel and biodiesel and TGA and CHN test were done on them. Then a round sample of conventional DPF was used to investigate the trapping behavior of DPF and pressure drop of soot trapping, which is described in methodology section. Finally the DPF was regenerated by high temperature furnace and the results were collected and compared in order to study the affecting elements of DPF soot filtration and regeneration.

2. Preparation

2.1. Fuels

The main characteristics of applied fuels is shown in table 1. More technical data of fuels which were used at this study is shown at earlier technical paper [1].

Table.1 fuel properties.

Fuel properties	Diesel	Biodiesel
Viscosity(mm2/s)	3.205	4.452
Density(g/cm3)	0.82649	0.87482
Calorific value(MJ/kg)	45.8	39.9
Oxidation stability (hr)	158.21	22.86
Flash point (^{o}C)	65.5	198

2.2. The engine, TGA and CHN

The small single cylinder diesel engine, Yanmar, is used for soot generation with PB100 and diesel. The engine was set at 80 % load with 2400 rpm on the Eddy current engine dynamometer (Tokyo plant ED-60kw-LC at KMITL). Metallic filter were used to collect PM and for each fuel new filter were used for collection. Then samples were collected and kept at sealed containers and sent for TGA. CHN test and Isothermal TGA test was done for all PM samples. Each sample was tested at four different temperature including 500, 550 and 600 ^{o}(C). For non-isothermal part nitrogen was used to heat up

the sample to desired temperature then air was introduced for soot oxidation for one hour. In order to have a good reference, carbon black N330 is used for TGA test at 600 °(C). The more detailed discussion about TGA test is presented at [4].

2.3 The DPF sample and apparatus

The DPF apparatus and system structure schematic is shown in Fig.1.

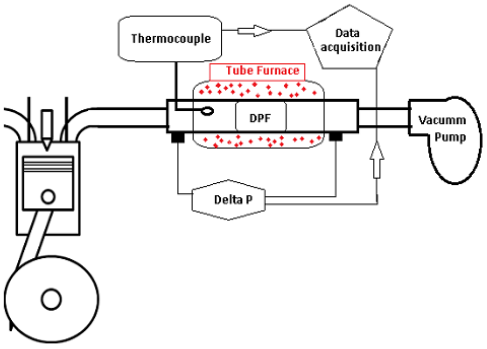

Fig. 1 DPF trapping apparatus and heating system

A sample of DPF is held in the middle of a ceramic tube. Two pressure sensors and one thermocouple are connected to the pipe and to a data acquisition card. The inlet is connected to the engine exhaust and the outlet is connected to the vacuum pump. The pressures sensors will measures the pressure drop of the system after soot trapping and at 200 °(c), which is almost close to the engine exhaust temperature. All the collected data were gathered by Lab View program and plotted in excel. At first step the diesel fuel was used and the soot were trapped and after pressure drop got to a constant condition, the trapping phase was stopped and then the filter was heated up to 600 °(c) to regenerate the filter. The same process is done for biodiesel.

3. Results and discussion

The result of TGA isothermal is shown in Fig.2. “(a)” and “(b)” for diesel and biodiesel and both samples are compared with carbon black N330.

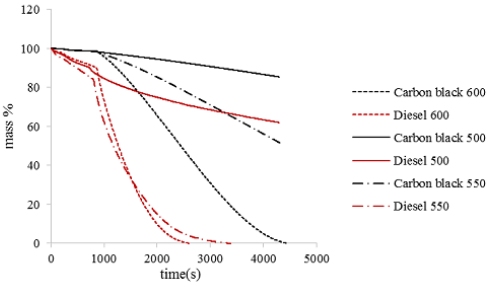

“(a)”

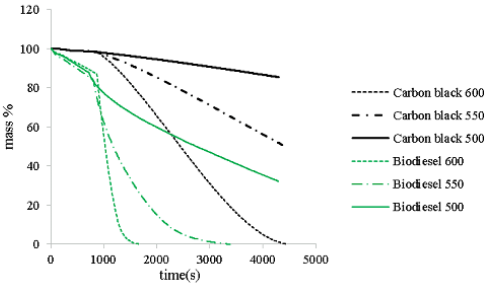

“(b)”

Fig. 2 Soot conversion of “(a)”diesel and “(b)” biodiesel soot in TGA isothermal condition.

As seen in figures, in all temperatures for both samples the biodiesel soot sample shows a faster conversion and oxidation trend in comparison with diesel. This is mainly due to elemental compositions of the soot samples and difference of fuel properties which can alter the soot oxidation kinetics and activation energy of the sot samples. More detailed investigation on the soot

oxidation kinetics of these two samples are provided at [6]. This can be clear indication of better oxidation behavior of biodiesel PM in comparison with diesel and also impact of fuel properties on PM composition. The general stages of trapping includes 4 phases. At first stage the DPF is clean and pores are empty and ready to trap the PM. At second stage initial trapping begins and soot deposits fill the pores of DPF wall. From second to third stage, the pressure drop starts to rise and at third stage the trapped soot covers the pores. In the final stage the soot cake layer forms on the surface of the wall and pressure drop shows a constant trend.

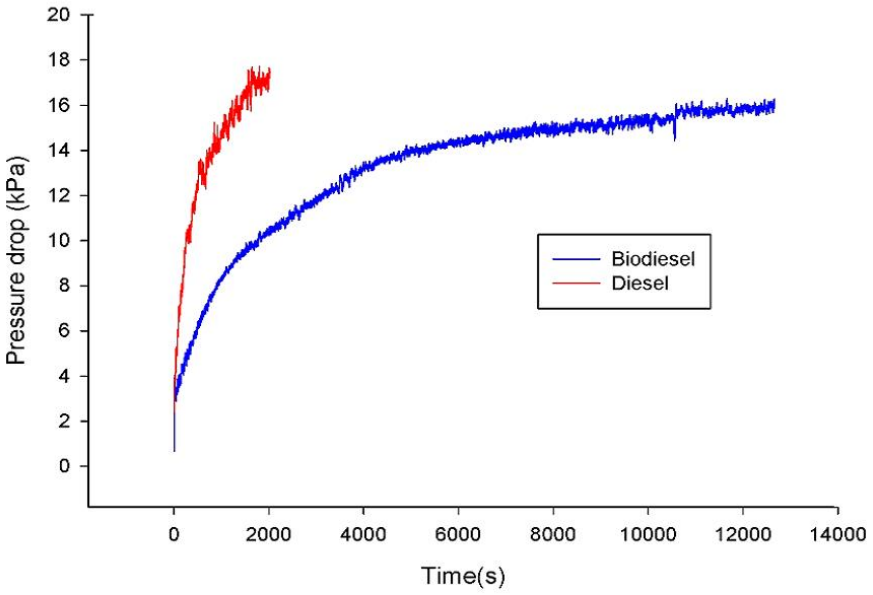

Fig. 3 trapping trend of both fuels samples.

As seen in Fig.3 the trapping time for diesel is much faster than biodiesel and it takes longer time for biodiesel soot to rise the pressure drop to a level which is equal to diesel pressure drop (more than 6 times longer). This can be contributed to several factors including chemical and physical. Based on previous studies [5, 7] the PM size made by biodiesel combustion is smaller than diesel due to different chemical composition of biodiesel and presence of more oxygen in biodiesel fuel results in more complete combustion and provides higher chance for carbon molecules to be oxidized. The density and viscosity of biodiesel is higher than diesel and this will cause advance in injection and also ignition delay so more fuel will be consumed. Besides, Biodiesel has lower calorific value in comparison with diesel and thus more amount of fuel is required. This will lead to longer trapping time in Comparison with diesel and hence the trapping Trend is slower the graph of biodiesel is lesser fluctuated and smoother in comparison with diesel. Figure 4 shows regeneration behavior of both

soot samples. The DPF is heated up to 600^0 (C) and to start regeneration of DPF. Regeneration of biodiesel is faster in comparison with diesel (about one hour). This is can be related to soot oxidation kinetics of biodiesel. The lower

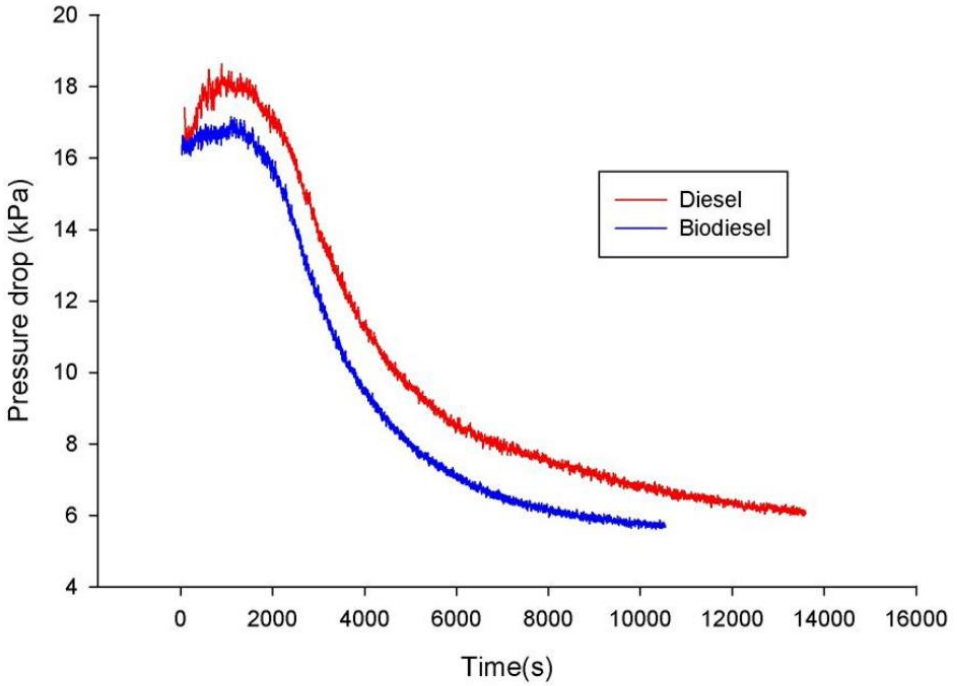

Fig. 4 Regeneration of DPF for both diesel and Biodiesel PM.

Activation energy of biodiesel makes it easier to oxidize and according to previous study at our lab [4, 7] biodiesel PM has much more volatile organic fraction (VOF) and soluble organic fraction (SOF) compositions while for diesel more solid fraction (SOL) and Carbonaceous is seen which makes diesel PM lesser oxidative and the activation energy. In the Same study the PM TGA conversion from both fraction including 80-60 % 60-40% and 40-20% of diesel and biodiesel were divided to three main conversion rate. For initial stage which is mainly VOF and SOF composition the activation energy is 152.91(kJ/mole) and for second and third fraction of conversion is 165.29 (kJ/mole) and for the latest fraction which Usually carbonaceous part is 158.56 (kJ/mole). For biodiesel the activation energy of first fraction Of PM is 146.97 (kJ/mole) and for second and third fraction 156.55 (kJ/mole) and 150.54 (kJ/mole).The Arrhenius plots of the study is Shown in Fig.5 and detailed explanation is discussed in [6]. In the same recent study on soot Oxidation results show the order of reaction for carbon in biodiesel PMs higher than diesel pm and it's 0.74 for biodiesel PM while 0.57 for diesel PM [6]. This indicates that the PM shapes are not completely spherical and doesn't meet shrinking

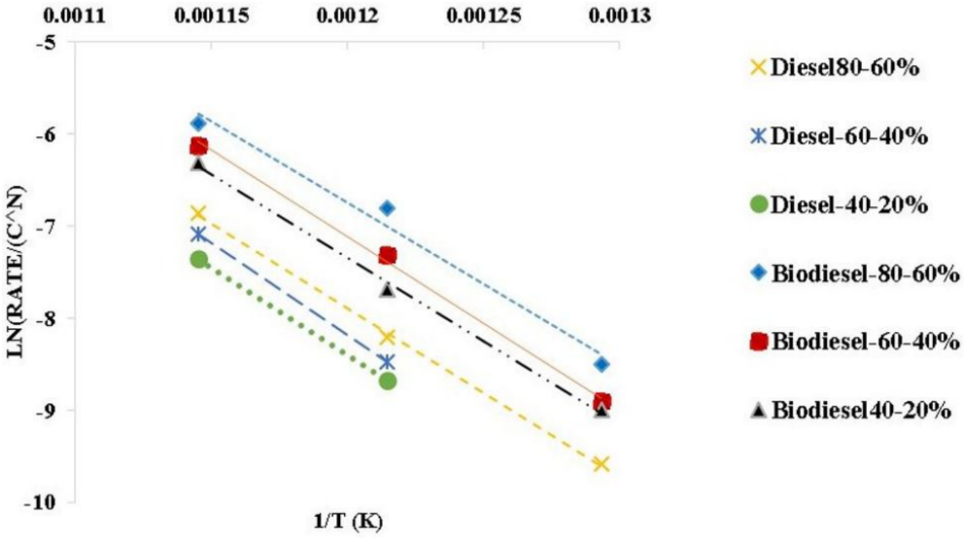

Fig.5 Arrhenius plot of three fractions of PM of Biodiesel and Diesel PM

core model and more active sites for reaction with Oxygen available for biodiesel. The CHN test results shows that diesel PM has higher amount of carbonaceous elements (1.1% H and 81% C) in comparison with biodiesel PM (1.1% H and 74.1% C). This can alter the soot oxidation behavior hence the bonding energy of carbon related molecules are much higher the higher activation energy is required for breaking the old bonds and starting of oxidation. So lower activation energy and lesser carbonaceous components, smaller PM size, higher amount of unburnt hydrocarbon and higher carbon reaction order, *n*, can be the affecting factors which lead to faster regeneration trend. The pump and suction speed and rate might have impact on regeneration but hence the pump for both fuel was same this factor can be omitted. This enables the DPF to work for a longer time when biodiesel is utilized and regeneration.

4. Conclusions

The soot trapping and regeneration behavior of diesel and biodiesel is investigated at this study and results can be summarized as below:

- The trapping time for biodiesel is longer than diesel and this can be related to chemical composition of biodiesel fuel and biodiesel PM and physical characteristics of the biodiesel which can affect engine function.
- The regeneration process for biodiesel PM is faster than diesel due to better oxidative trend of biodiesel PM in comparison with diesel.
- The factors which affect the soot oxidation kinetics such as PM elemental composition, PM size, PM carbonaceous composition and reaction order of carbon can be responsible for different oxidation trend of diesel and biodiesel PM.

- Biodiesel can reduce regeneration time and postpone the trapping duration which makes the DPF working period longer.

Acknowledgement

The author would show his gratitude to King Mongkut's Institute of Technology Ladkrabang engine lab, Thailand Research Fund (TRF), ministry of Science and Technology, Thailand and TAIST Tokyo Tech program and MTEC for their financial and technical support.

7. References

[1] Borhanipour, M., Karin, P., Tongroon, M., Chollacoop, N. et al., "Comparison Study on Fuel Properties of Biodiesel from Jatropha, Palm and Petroleum Based Diesel Fuel," SAE Technical Paper 2014-01-2017, 2014, doi: 10.4271/2014-01-2017.

[2] Preechar Karin et al: Nanostructure of renewable oxygenated fuels particulate matter g.a. ASEAN Engineering Journal Part A Volume 3, Number 1 March 2013.

[3] P. Karin, M. Borhanipour et al, Oxidation Kinetics of Small CI Engine's Biodiesel Particulate Matter, International Journal of Automotive Technology, paper no: 220140181.

[4] Preechar Karin, Yutthana Songsaengchan, Songtam Laosuwan, Chinda Charoenphonphanich, Nuwong Chollacoop and Katsunori Hanamura, Nanostructure Investigation of Particle Emission by Using TEM Image Processing Method, Energy Procedia 34 (2013) 757 – 766. 10th Eco-Energy and Materials Science and Engineering.

[5] Yuttana Songsaengchan: Investigation of Biodiesel particulate matter in Nanostructure,The2ndnternational Conference on automotive technology,ngine and alternative fuels ,HCMUT,VNUHCM, December 4-5 , 2012.

[6] Morteza Borhanipour, Preechar Karin et al, Investigation of Diesel and Biodiesel Soot Oxidation Burapha University International Conference 2014 Burapha University, Thailand July 3-4, 2014.

[7] Morteza Borhanipour, Preechar Karin, Chinda Charoenphonphanich, Nuwong Chollacoop, Katsunori Hanamura: Investigation of diesel and biodiesel soot oxidation in presence of pure oxygen, Presented at the JSAE Annual Congress on May, 23, 2014.

Technical data

1-Engine

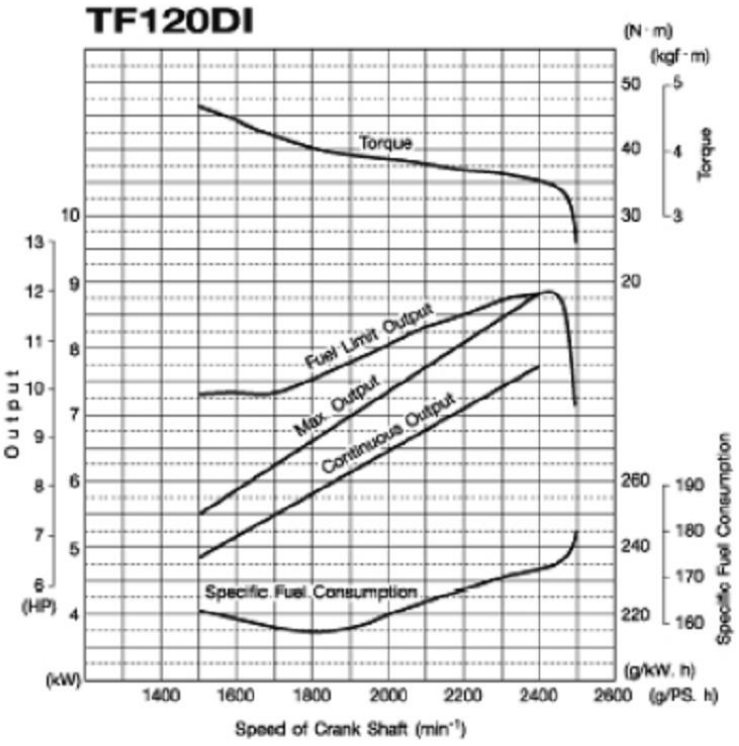

SPECIFICATION

Model		Unit	TF80DI-L	TF80DI-H	TF90DI-L	TF90DI-H	TF110DI-L	TF110DI-Y	TF110DI-H	TF120DI-L	TF120DI-Y	TF120DI-H
Type			Horizontal water cooled diesel engine									
Combustion system			Direct Injection (D.I.)									
Number of cylinder			1									
Bore x stroke		mm.	80 x 87	80 x 87	85 x 87	85 x 87	88 x 96	88 x 96	88 x 96	92 x 96	92 x 96	92 x 96
Displacement		lit.	0.437	0.437	0.493	0.493	0.583	0.583	0.583	0.638	0.638	0.638
Cont. rating output		hp / rpm.	7.0 / 2400	7.0 / 2400	8.0 / 2400	8.0 / 2400	9.8 / 2400	9.8 / 2400	9.8 / 2400	10.5 / 2400	10.5 / 2400	10.5 / 2400
		kW / rpm.	5.1 / 2400	5.1 / 2400	5.9 / 2400	5.9 / 2400	7.2 / 2400	7.2 / 2400	7.2 / 2400	7.7 / 2400	7.7 / 2400	7.7 / 2400
Max. output		hp / rpm.	8.0 / 2400	8.0 / 2400	9.0 / 2400	9.0 / 2400	11.0 / 2400	11.0 / 2400	11.0 / 2400	12.0 / 2400	12.0 / 2400	12.0 / 2400
		kW / rpm.	5.9 / 2400	5.9 / 2400	6.6 / 2400	6.6 / 2400	8.1 / 2400	8.1 / 2400	8.1 / 2400	8.8 / 2400	8.8 / 2400	8.8 / 2400
Specific fuel consumption		g. / hp-h.	177									
Compression ratio			16.8 : 1	16.8 : 1	16.6 : 1	16.6 : 1	16.3 : 1	16.3 : 1	16.3 : 1	16.1 : 1	16.1 : 1	16.1 : 1
Applicable fuel oil			Diesel									
Fuel injection pump			Bosch type									
Injection timing		deg.	bTDC 20.0				bTDC 19.0					
Injection pressure		kg. / cm.^{2}	200									
F.O. tank capacity		lit.	10.6				11.0					
Lubrication system			Fully sealed forced lubrication with trochoid pump & hydraulic regulator valve									
Lubrication oil			SAE NO. 40 / API GRADE CD / SF									
Lubricating oil capacity (oil pan)		lit.	2.2				2.8					
Cooling system			Radiator	Hopper	Radiator	Hopper	Radiator	Radiator	Hopper	Radiator	Radiator	Hopper
Cooling water capacity		lit.	1.6	9.4	1.6	9.4	2.1	2.1	11.8	2.1	2.1	11.8
Starting System			Hand starting									
Dimension	Lenght	mm.	676.5				704.0					
	Width	mm.	339.5				355.5					
	Height	mm.	524.0				549.0					
Engine Dry Weight		kgs.	87.5	84.0	88.5	85.0	104.5	104.5	101.5	105.5	105.5	102.5

2-LAB view program

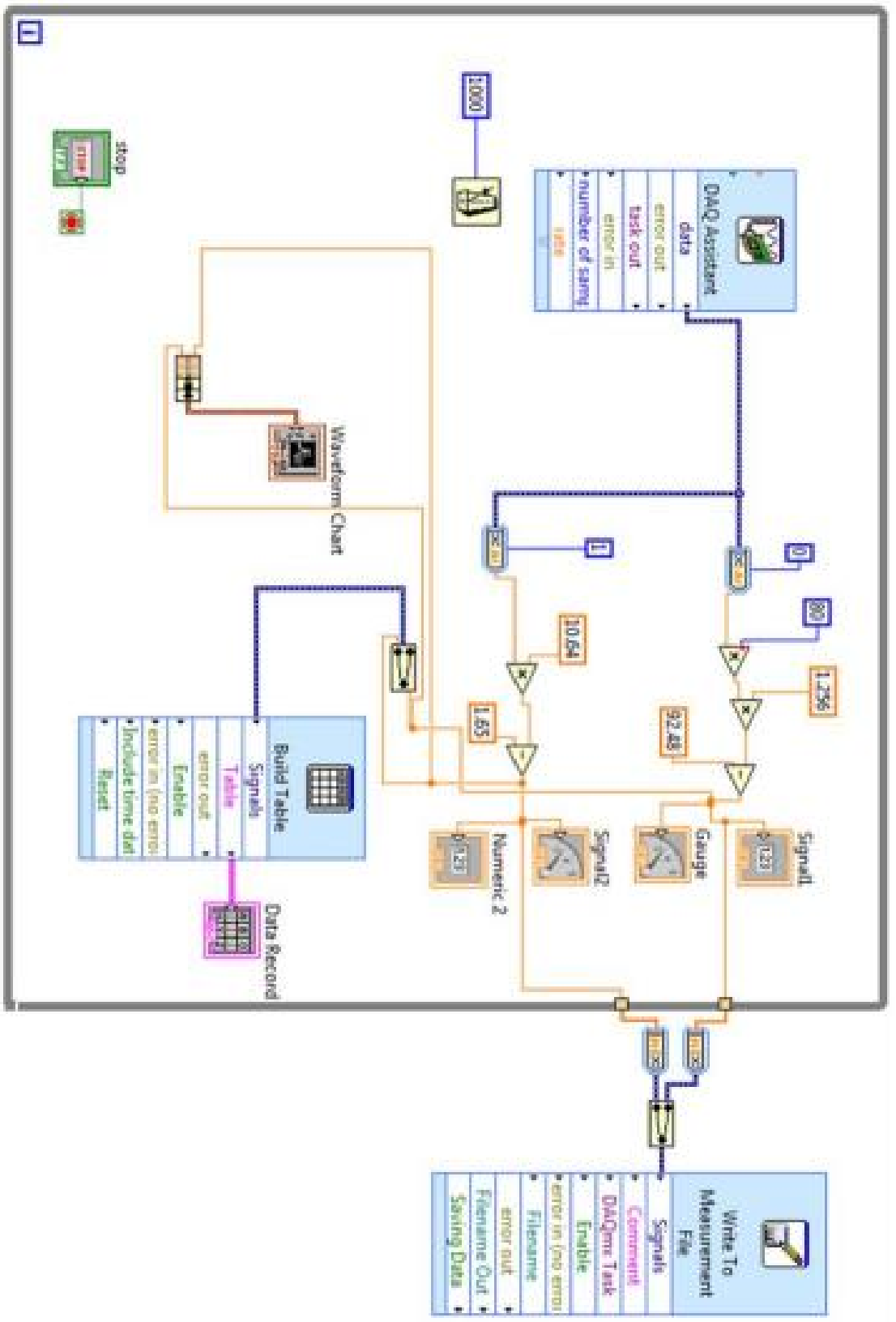

3-DAQ card

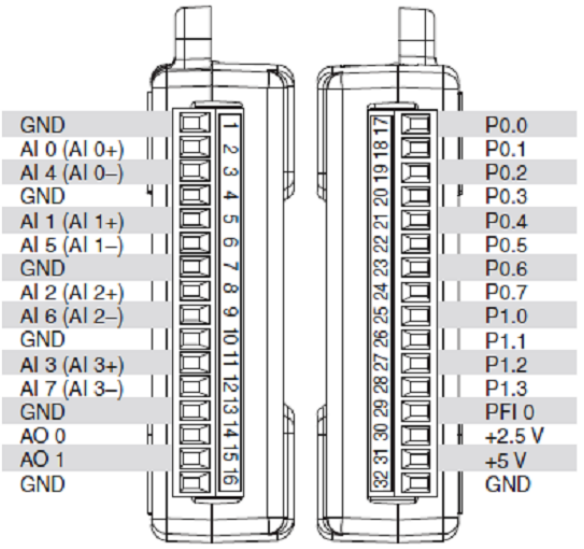

Signal Name	Reference	Direction	Description
GND	—	—	**Ground**—The reference point for the single-ended analog input measurements, analog output voltages, digital signals, +5 VDC supply, and +2.5 VDC at the I/O connector, and the bias current return point for differential mode measurements.
AI <0..7>	Varies	Input	**Analog Input Channels 0 to 7**—For single-ended measurements, each signal is an analog input voltage channel. For differential measurements, AI 0 and AI 4 are the positive and negative inputs of differential analog input channel 0. The following signal pairs also form differential input channels: AI<1, 5>, AI<2, 6>, and AI<3, 7>. Refer to the *Analog Input* section for more information.
AO <0, 1>	GND	Output	**Analog Output Channels 0 and 1**—Supplies the voltage output of AO channel 0 or AO channel 1. Refer to the *Analog Output* section for more information.
P0.<0..7>	GND	Input or Output	**Port 0 Digital I/O Channels 0 to 7**—You can individually configure each signal as an input or output. Refer to the *Digital I/O* section for more information.
P1.<0..3>	GND	Input or Output	**Port 1 Digital I/O Channels 0 to 3**—You can individually configure each signal as an input or output. Refer to the *Digital I/O* section for more information.
PFI 0	GND	Input	**PFI 0**—This pin is configurable as either a digital trigger or an event counter input. Refer to the *PFI 0* section for more information.
+2.5 V	GND	Output	**+2.5 V External Reference**—Provides a reference for wrap-back testing. Refer to the *+2.5 V External Reference* section for more information.
+5 V	GND	Output	**+5 V Power Source**—Provides +5 V power up to 200 mA. Refer to the *+5 V Power Source* section for more information.

4-pressure sensor

Operating Characteristics

Table 1. Operating Characteristics (V_S = 5.0 Vdc, T_A = 25°C unless otherwise noted, P1 > P2. Decoupling circuit shown in Figure 4 required to meet electrical specifications.)

Characteristic		Symbol	Min	Typ	Max	Unit
Pressure Range[1]		P_{OP}	0	—	50	kPa
Supply Voltage[2]		V_S	4.75	5.0	5.25	Vdc
Supply Current		I_o	—	7.0	10	mAdc
Minimum Pressure Offset[3] @ V_S = 5.0 Volts	(0 to 85°C)	V_{off}	0.088	0.2	0.313	Vdc
Full Scale Output[4] @ V_S = 5.0 Volts	(0 to 85°C)	V_{FSO}	4.587	4.7	4.813	Vdc
Full Scale Span[5] @ V_S = 5.0 Volts	(0 to 85°C)	V_{FSS}	—	4.5	—	Vdc
Accuracy[6]	(0 to 85°C)	—	—	—	±2.5	$\%V_{FSS}$
Sensitivity		V/P	—	90	—	mV/kPa
Response Time[7]		t_R	—	1.0	—	ms
Output Source Current at Full Scale Output		I_{o+}	—	0.1	—	mAdc
Warm-Up Time[8]		—	—	20	—	ms
Offset Stability[9]		—	—	±0.5	—	$\%V_{FSS}$

1. 1.0 kPa (kiloPascal) equals 0.145 psi.
2. Device is ratiometric within this specified excitation range.
3. Offset (V_{off}) is defined as the output voltage at the minimum rated pressure.
4. Full Scale Output (V_{FSO}) is defined as the output voltage at the maximum or full rated pressure.
5. Full Scale Span (V_{FSS}) is defined as the algebraic difference between the output voltage at full rated pressure and the output voltage at the minimum rated pressure.
6. Accuracy (error budget) consists of the following:
   Linearity: Output deviation from a straight line relationship with pressure over the specified pressure range.
   Temperature Hysteresis: Output deviation at any temperature within the operating temperature range, after the temperature is cycled to and from the minimum or maximum operating temperature points, with zero differential pressure applied.
   Pressure Hysteresis: Output deviation at any pressure within the specified range, when this pressure is cycled to and from the minimum or maximum rated pressure at 25°C.
   TcSpan: Output deviation over the temperature range of 0° to 85°C, relative to 25°C.
   TcOffset: Output deviation with minimum pressure applied, over the temperature range of 0° to 85°C, relative to 25°C.
   Variation from Nominal: The variation from nominal values, for Offset or Full Scale Span, as a percent of V_{FSS} at 25°C.
7. Response Time is defined as the time for the incremental change in the output to go from 10% to 90% of its final value when subjected to a specified step change in pressure.
8. Warm-up Time is defined as the time required for the product to meet the specified output voltage after the Pressure has been stabilized.
9. Offset Stability is the product's output deviation when subjected to 1000 hours of Pulsed Pressure, Temperature Cycling with Bias Test.

5-Temperature control

- Indication Accuracy
  Thermocouple input: ±0.3% of PV (previous models: ±0.5%)
  Pt input: ±0.2% of PV (previous models: ±0.5%)
  Analog input: ±0.2% FS (previous models: ±0.5%)
- New E5CN-U Models (Plug-in Models) with analog inputs and current outputs.
- A PV/SV-status display function can be set to automatically alternate between displaying the status of the Temperature Controller (auto/manual, RUN/STOP, and alarms) and the PV or SV.
- Preventive maintenance for relays in the Temperature Controller using a Control Output ON/OFF Counter.

Specifications

Ratings

Power supply voltage		No D in model number: 100 to 240 VAC, 50/60 Hz D in model number: 24 VAC, 50/60 Hz; 24 VDC	
Operating voltage range		85% to 110% of rated supply voltage	
Power consumption	E5CN	100 to 240 VAC: 7.5 VA (max.) (E5CN-R2T at 100 VAC: 3.0 VA) 24 VAC/VDC: 5 VA/3 W (max.) (E5CN-R2TD at 24 VAC: 2.7 VA)	
	E5CN-U	100 to 240 VAC: 6 VA (max.) 24 VAC/VDC: 3 VA/2 W (max.) (models with current output: 4 VA/2 W)	
Sensor input		Models with temperature inputs Thermocouple: K, J, T, E, L, U, N, R, S, B, W, or PL II Platinum resistance thermometer: Pt100 or JPt100 Infrared temperature sensor: 10 to 70°C, 60 to 120°C, 115 to 165°C, or 140 to 260°C Voltage input: 0 to 50 mV	
		Models with analog inputs Current input: 4 to 20 mA or 0 to 20 mA Voltage input: 1 to 5 V, 0 to 5 V, or 0 to 10 V	
Input impedance		Current input: 150 Ω max., Voltage input: 1 MΩ min. (Use a 1:1 connection when connecting the ES2-HB.)	
Control method		ON/OFF control or 2-PID control (with auto-tuning)	
Control outputs	Relay output	E5CN	SPST-NO, 250 VAC, 3 A (resistive load), electrical life: 100,000 operations, minimum applicable load: 5 V, 10 mA
		E5CN-U	SPDT, 250 VAC, 3 A (resistive load), electrical life: 100,000 operations, minimum applicable load: 5 V, 10 mA
	Voltage output (for driving SSR)	E5CN E5CN-U	Output voltage: 12 VDC ±15% (PNP), max. load current: 21 mA, with short-circuit protection circuit
	Current output	E5CN	4 to 20 mA DC/0 to 20 mA DC, load: 600 Ω max., resolution: approx. 10,000
	Long-life relay output	E5CN	SPST-NO, 250 VAC, 3 A (resistive load), electrical life: 1,000,000 operations, load power supply voltage: 75 to 250 VAC (DC loads cannot be connected.), minimum applicable load: 5 V, 10 mA, leakage current: 5 mA max. (250 VAC, 60 Hz)
Auxiliary outputs	Number of outputs	1 or 2 max. (Depends on the model.)	
	Output specifications	Relay output: SPST-NO, 250 VAC, 3 A (resistive load), electrical life: 100,000 operations, minimum applicable load: 5 V, 10 mA	
Event inputs	Number of inputs	2	
	External contact input specifications	Contact input: ON: 1 kΩ max., OFF: 100 kΩ min.	
		Non-contact input: ON: Residual voltage: 1.5 V max., OFF: Leakage current: 0.1 mA max.	
		Current flow: Approx. 7 mA per contact	
External power supply for ES1B		12 VDC ±10%, 20 mA, short-circuit protection circuit provided	
Setting method		Digital setting using front panel keys	
Indication method		11-segment digital display and individual indicators (7-segment display also possible) Character height: PV: 11 mm, SV: 6.5 mm	
Multi SP		Up to four set points (SP0 to SP3) can be saved and selected using event inputs, key operations, or serial communications.	
Bank switching		Not supported	
Other functions		Manual output, heating/cooling control, loop burnout alarm, SP ramp, other alarm functions, heater burnout detection, 40% AT, 100% AT, MV limiter, input digital filter, self-tuning, temperature input shift, run/stop, protection functions, control output ON/OFF counter, extraction of square root, MV change rate limit, logic operations, PV/SV status display, simple program, automatic cooling coefficient adjustment	
Ambient operating temperature		−10 to 55°C (with no condensation or icing), for 3-year warranty: −10 to 50°C	
Ambient operating humidity		25% to 85%	
Storage temperature		−25 to 65°C (with no condensation or icing)	

6- Fuel and emission standards in Thailand

6-1-diesel

รายละเอียดแนบท้ายประกาศกรมธุรกิจพลังงาน
เรื่อง กำหนดลักษณะและคุณภาพของน้ำมันดีเซล (ฉบับที่ ๕)
พ.ศ. ๒๕๕๔

รายการ	ข้อกำหนด	อัตราสูงต่ำ	น้ำมันดีเซล		วิธีทดสอบ[๔]
			หมุนเร็ว	หมุนช้า	
1	ความถ่วงจำเพาะ ณ อุณหภูมิ 15.6/15.6 *องศาเซลเซียส* (Specific Gravity at 15.6/15.6 °C)	ไม่ต่ำกว่า และ ไม่สูงกว่า	0.81 0.87	- 0.920	ASTM D 1298
2	จำนวนซีเทน (Cetane Number) หรือ				ASTM D 613
	ดัชนีซีเทน (Calculated Cetane Index)				ASTM D 976
	ก่อนวันที่ 1 มกราคม พ.ศ. 2555	ไม่ต่ำกว่า	47	45	
	ตั้งแต่วันที่ 1 มกราคม พ.ศ. 2555 เป็นต้นไป	ไม่ต่ำกว่า	50	45	
3	ความหนืด (Viscosity, *เซนติสโตกส์ cSt*)				ASTM D 445
	3.1 ณ อุณหภูมิ 40 *องศาเซลเซียส* (at 40 °C)	ไม่ต่ำกว่า และ	1.8	-	
		ไม่สูงกว่า	4.1	8.0	
	หรือ				
	3.2 ณ อุณหภูมิ 50 *องศาเซลเซียส* (at 50 °C)	ไม่สูงกว่า	-	6.0	
4	จุดไหลเท (Pour Point, *องศาเซลเซียส °C*)	ไม่สูงกว่า	10	16	ASTM D 97
5	กำมะถัน (Sulphur, *ร้อยละโดยน้ำหนัก %wt.*)				
	ก่อนวันที่ 1 มกราคม พ.ศ. 2555	ไม่สูงกว่า	0.035	1.5	ASTM D 4294
	ตั้งแต่วันที่ 1 มกราคม พ.ศ. 2555 เป็นต้นไป	ไม่สูงกว่า	0.005	1.5	ASTM D 2622
6	การกัดกร่อนแผ่นทองแดง (Copper Strip Corrosion)	ไม่สูงกว่า	หมายเลข 1	-	ASTM D 130
7	เสถียรภาพต่อการเกิดปฏิกิริยาออกซิเดชัน (Oxidation Stability, *กรัม/ลูกบาศก์เมตร g/m³*)	ไม่สูงกว่า	25	-	ASTM D 2274
8	กากถ่าน (Carbon Residue, *ร้อยละโดยน้ำหนัก %wt.*)	ไม่สูงกว่า	0.05	-	ASTM D 189
9	น้ำและตะกอน (Water and Sediment, *ร้อยละโดยปริมาตร %vol.*)	ไม่สูงกว่า	0.05	0.3	ASTM D 2709
10	เถ้า (Ash, *ร้อยละโดยน้ำหนัก %wt.*)	ไม่สูงกว่า	0.01	0.02	ASTM D 482

รายการ	ข้อกำหนด		อัตราสูงต่ำ	น้ำมันดีเซล		วิธีทดสอบ[1/]
				หมุนเร็ว	หมุนช้า	
11	จุดวาบไฟ (Flash Point,	*องศาเซลเซียส* *°C)*	ไม่ต่ำกว่า	52	52	ASTM D 93
12	การกลั่น (Distillation,	*องศาเซลเซียส* *°C)*				ASTM D 86
	อุณหภูมิของส่วนที่กลั่นได้โดยปริมาตรในอัตราร้อยละเก้าสิบ (90% recovered)		ไม่สูงกว่า	357	-	
13	โพลีไซคลิก อะโรมาติก ไฮโดรคาร์บอน (Polycyclic Aromatic Hydrocarbon,	*ร้อยละโดยน้ำหนัก* *% wt.)*				ASTM D 2425
	ก่อนวันที่ 1 มกราคม พ.ศ. 2555		-	-	-	
	ตั้งแต่วันที่ 1 มกราคม พ.ศ. 2555 เป็นต้นไป		ไม่สูงกว่า	11	-	
14	สี (Colour)			-		
	14.1 ชนิดของสี (Hue)			เหลือง	น้ำตาล	
	14.2 ความเข้มของสี (Intensity)		ไม่ต่ำกว่า และ	-	4.5	ASTM D 1500
			ไม่สูงกว่า	4.0	7.5	
15	ไบโอดีเซลประเภทเมทิลเอสเตอร์ของกรดไขมัน (Methyl Ester of Fatty Acid,	ร้อยละโดยปริมาตร *%vol.)*	ไม่ต่ำกว่า และ	3	-	EN 14078
			ไม่สูงกว่า	5	-	
16	คุณสมบัติการหล่อลื่น รอยขีดข่วน (Lubricity , Wear Scar	*ไมโครเมตร* *μm)*	ไม่สูงกว่า	460	-	CEC F – 06 - 96
17	สารเติมแต่ง (ถ้ามี) (Additive)		ให้เป็นไปตามที่ได้รับความเห็นชอบจากอธิบดีกรมธุรกิจพลังงาน			

หมายเหตุ 1/ วิธีทดสอบอาจใช้วิธีอื่นที่เทียบเท่าก็ได้ แต่ในกรณีที่มีข้อโต้แย้งให้ใช้วิธีที่กำหนดในรายละเอียดแนบท้ายนี้

6-2-Biodiesel

รายละเอียดแนบท้ายประกาศกรมธุรกิจพลังงาน
เรื่อง กำหนดลักษณะและคุณภาพของไบโอดีเซลประเภทเมทิลเอสเตอร์ของกรดไขมัน
พ.ศ. ๒๕๕๒

รายการ	ข้อกำหนด		อัตราสูง-ต่ำ		วิธีทดสอบ [1]
1	เมทิลเอสเตอร์ (Methyl Ester,	*ร้อยละโดยน้ำหนัก* *% wt.)*	ไม่ต่ำกว่า	96.5	EN 14103
2	ความหนาแน่น ณ อุณหภูมิ 15 °ซ (Density at 15 °C,	*กิโลกรัม/ลูกบาศก์เมตร* *kg/m ^{3})*	ไม่ต่ำกว่า และ ไม่สูงกว่า	860 900	ASTM D 1298
3	ความหนืด ณ อุณหภูมิ 40 °ซ (Viscosity at 40 °C,	*เซนติสโตกส์* *cSt)*	ไม่ต่ำกว่า และ ไม่สูงกว่า	3.5 5.0	ASTM D 445
4	จุดวาบไฟ (Flash Point,	*องศาเซลเซียส* *°C)*	ไม่ต่ำกว่า	120	ASTM D 93
5	กำมะถัน (Sulphur,	*ร้อยละโดยน้ำหนัก* *%wt.)*	ไม่สูงกว่า	0.0010	ASTM D 2622
6	กากถ่าน (ร้อยละ 10 ของกากที่เหลือจากการกลั่น) (Carbon Residue , on 10 % distillation residue,	*ร้อยละโดยน้ำหนัก* *%wt)*	ไม่สูงกว่า	0.30	ASTM D 4530
7	จำนวนซีเทน (Cetane Number)		ไม่ต่ำกว่า	51	ASTM D 613
8	เถ้าซัลเฟต (Sulphated Ash,	*ร้อยละโดยน้ำหนัก* *%wt.)*	ไม่สูงกว่า	0.02	ASTM D 874
9	น้ำ (Water,	*ร้อยละโดยน้ำหนัก* *wt.)*	ไม่สูงกว่า	0.050	EN ISO 12937
10	สิ่งปนเปื้อนทั้งหมด (Total Contaminate,	*ร้อยละโดยน้ำหนัก* *%wt.)*	ไม่สูงกว่า	0.0024	EN 12662
11	การกัดกร่อนแผ่นทองแดง (Copper Strip Corrosion)		ไม่สูงกว่า	หมายเลข 1	ASTM D 130
12	เสถียรภาพต่อการเกิดปฏิกิริยา ออกซิเดชั่น ณ อุณหภูมิ 110 องศาเซลเซียส (Oxidation Stability at 110 °C,	*ชั่วโมง* *hours)*	ไม่ต่ำกว่า	10	EN 14112

(ต่อ-2-)

รายการ	ข้อกำหนด		อัตราสูง-ต่ำ		วิธีทดสอบ 1/
13	ค่าความเป็นกรด (Acid Value ,	*มิลลิกรัมโปตัสเซียมไฮดรอกไซด์/กรัม mg KOH/g)*	ไม่สูงกว่า	0.50	ASTM D 664
14	ค่าไอโอดีน (Iodine Value ,	*กรัมไอโอดีน/ 100 กรัม g Iodine / 100 g)*	ไม่สูงกว่า	120	EN 14111
15	กรดลิโนเลนิกเมทิลเอสเตอร์ (Linolenic Acid Methyl Ester ,	*ร้อยละโดยน้ำหนัก %wt.)*	ไม่สูงกว่า	12.0	EN 14103
16	เมทานอล (Methanol,	*ร้อยละโดยน้ำหนัก %wt.)*	ไม่สูงกว่า	0.20	EN 14110
17	โมโนกลีเซอไรด์ (Monoglyceride	*ร้อยละโดยน้ำหนัก %wt.)*	ไม่สูงกว่า	0.80	EN 14105
18	ไดกลีเซอไรด์ (Diglyceride ,	*ร้อยละโดยน้ำหนัก %wt)*	ไม่สูงกว่า	0.20	EN 14105
19	ไตรกลีเซอไรด์ (Triglyceride ,	*ร้อยละโดยน้ำหนัก %wt)*	ไม่สูงกว่า	0.20	EN 14105
20	กลีเซอรีนอิสระ (Free glycerin ,	*ร้อยละโดยน้ำหนัก %wt.)*	ไม่สูงกว่า	0.02	EN 14105
21	กลีเซอรีนทั้งหมด (Total glycerin,	*ร้อยละโดยน้ำหนัก %wt.)*	ไม่สูงกว่า	0.25	EN 14105
22	โลหะกลุ่ม 1 (โซเดียมและโปแตสเซียม) (Group I metals (Na+K),	*มิลลิกรัม/กิโลกรัม mg/kg)*	ไม่สูงกว่า	5.0	EN 14108 และ EN 14109
	โลหะกลุ่ม 2 (แคลเซียมและแมกนีเซียม) (Group II metals (Ca+Mg),	*มิลลิกรัม/กิโลกรัม mg/kg)*	ไม่สูงกว่า	5.0	pr EN 14538
23	ฟอสฟอรัส (Phosphorus,	*ร้อยละโดยน้ำหนัก %wt.)*	ไม่สูงกว่า	0.0010	ASTM D 4951
24	สารเติมแต่ง (ถ้ามี) (Additive)		ให้เป็นไปตามที่ได้รับความเห็นชอบจากอธิบดีกรมธุรกิจพลังงาน		

หมายเหตุ 1/ วิธีทดสอบอาจใช้วิธีอื่นที่เทียบเท่าก็ได้ แต่ในกรณีที่มีข้อโต้แย้งให้ใช้วิธีที่กำหนดในรายละเอียดแนบท้ายนี้

6-3- Emission standards

ประกาศกระทรวงอุตสาหกรรม

ฉบับที่ ๔๓๕๔ (พ.ศ. ๒๕๕๔)

ออกตามความในพระราชบัญญัติมาตรฐานผลิตภัณฑ์อุตสาหกรรม

พ.ศ. ๒๕๓๓

เรื่อง กำหนดมาตรฐานผลิตภัณฑ์อุตสาหกรรม

รถยนต์ขนาดเล็กที่ใช้เครื่องยนต์แบบจุดระเบิดด้วยการอัด เฉพาะด้านความปลอดภัย : สารมลพิษจากเครื่องยนต์ ระดับที่ 7

หน่วยเป็น g/km

ประเภทรถยนต์	มวลอ้างอิง (kg)	คาร์บอนมอนอกไซด์	ออกไซด์ของไนโตรเจน	ไฮโดรคาร์บอนรวมกับออกไซด์ของไนโตรเจน	สารมลพิษอนุภาค
รถยนต์นั่ง มวลเต็มอัตราบรรทุกไม่เกิน 2 500 kg	-	0.50	0.25	0.30	0.025
รถยนต์นั่งมวลเต็มอัตราบรรทุกเกิน 2 500 kg หรือรถยนต์บรรทุกและรถยนต์นั่งที่ดัดแปลงมาจากรถยนต์บรรทุกที่มีมวลเต็มอัตราบรรทุกไม่เกิน 3 500 kg	ไม่เกิน 1 305	0.50	0.25	0.30	0.025
	เกิน 1 305 แต่ไม่เกิน 1 760	0.63	0.33	0.39	0.04
	เกิน 1 760	0.74	0.39	0.46	0.06